MONITORING HONEY & COMPLEX LIQUIDS BY OPTICAL CHROMATICITY

UNIVERSITY OF LIVERPOOL

Thesis submitted in accordance with the requirements of University of Liverpool for the degree of Doctor in Philosophy
by

Amr Towfick Sufian

February 2014

Abstract

The potential of optically monitoring complex composite liquids such as honey has been demonstrated using optical light properties. The novel approach has the potential for distinguishing between various honey samples to quantify and discriminate for deviations from the norm and for early warning of contamination/adulteration in honey using readily available, cost effective and portable instrumentation that can be used robustly on the field, which replaces individual absolute measuring instruments.

The novel approach was developed based upon chromatically processing test data with three different optical methods simultaneously (transmission, polarization and fluorescence) for use as primary, secondary chromatic maps and an assessment flow chart to provide a rapid decision capability on the condition of the honey according to quality attributes. As such it can provide insight into conditions important to the food industry.

Novel methods for compensation, calibration, normalization and ambient light rejection procedures have been developed to allow operation in a range of lightening conditions such as in the field and factory.

The chromatic approach sensitivity for identifying the correct classification of high quality honey samples was 91% and the sensitivity for identifying very poor quality samples was 75%.

The portable honey monitoring system was tested for field trials at various locations across Yemen for monitoring the condition of honey samples. The sensitivity for correct classifications of the high quality honey sample samples was 88% and the sensitivity for identifying very poor quality honey samples was 63%. Chromatic methodology provided robustness for field use.

Acknowledgment

"Lord, inspire me to thank you for Your favours to me and to my parents and to act righteously so as to please You. Admit me by Your mercy into the company of Your righteous servants"

I would like express my grateful thanks to Allah for lightning the path for me to do this work submitted for the degree of Doctorate of Philosophy. For Him I mostly dedicate this effort and for Him I call mankind to follow His path.

I would like to express my deepest thanks to my parents for their continued support and encouragement through out life, for their prayers and patience at times I was away and mostly I thank them for their endless love.

I dedicate this work to my father "Professor. Towfick Sufian" to be honoured and proud and to his eternal love for honey. To my mother "Mrs Dorah Abduljabar" to be honoured and proud and to her endless love for knowledge. To my brother " Mohammed" whom I seek support at hard times, to my three dearest sisters "Kawther, Sarah an Alaa' whom are always their for me and to my beloved wife "Safa" whom was waiting to see this day. To my grandfather "Mr. Sufian" and to all my family members who believed and supported me all the way.

I would like to express my extreme thanks to both of my supervisors "Professor Gordon Jones " and "Professor Joseph Spencer" whom guided, supported, encouraged and advised me through out this research work. I would also like to thank "Dr. Anthony Deakin " for his continued assistance.

I would like to thank the "Yemen Ministry of Higher Education and Scientific Research " for their financial support and the " British Yemeni Society" for their assistant grant supporting the field test that was constructed in Yemen. Finally I would like to thanks the University of Liverpool for the great opportunity it gave me to be one of its students.

Contents

List Of Figures

List Of Tables

Chapter 1

Introduction

1.1 Research objectives

The objective of this research was to study the monitoring of complex liquids with regards to the different conditions to which the liquid has been subjected using different optical properties of light (Transmission/Reflection, Polarization and Fluorescence) and the developed chromatic techniques to quantify and alert/discriminate for deviations from the norm using an integrated monitoring device that replaces individual absolute measuring instruments.

Calibration, normalization and ambient light rejection procedures have been developed to allow operation in a range of lightening conditions such as in the field (sunlight) and factory. Methods for compensating for variation in the ambient light, varying illumination conditions in the field and variations in the VDU illumination or camera characteristics from the supplier or time have also been developed.

The thesis describes in particular the application of the monitoring techniques to honey samples (which are a particular form of complex liquids) to classify samples regarding their quality/ authenticity using readily available, portable and cost effective instruments that could be used on site.

The aim was to provide an insight into the different conditions of such honeys. The three properties of light (Transmission, polarization and Fluorescence) are integrated into the system and monitored simultaneously to quantify the complex composition of honey and alert for deviations from required quality/ authenticity and to give early warning indications of contamination/ adulteration rather than precise analysis.

A rapid decision capability flow chart on the condition/quality of the honey is developed which shows the philosophy for relating optical properties of light and visually observed properties of honey in one single graphs analysis.

The developed chromatic procedures can also be adapted for use with mobile phone technology using daylight or artificial light illumination with the mobile phone camera.

1.2 Complexity And Monitoring

Complex systems are nonlinear and subject to unpredictability (Jones G. R, Deakin A. G et al. 2008), therefore, evaluating the state of health of the complex system from instantaneous values of a number of parameters is too numerous to consider and systems do not operate in isolation. The increasing complexity and unpredictability in complex systems require intelligent monitoring systems to asses and assure the overall system behavior (Jones G. R, Deakin A. G et al. 2008).

Figure 1.1 illustrates the difference between measurement, diagnosis and monitoring. Measurement is the comparison with a fixed scale/ unit while diagnosis is the determination of such condition from symptoms. However, monitoring is concerned with observation to indicate the likelihood of a condition evolving. Thus, it offers the possibility of addressing the emergent nature of complexity, which involves the interactions of several events, often with the outcomes not anticipated. Monitoring and diagnosis maybe regarded as bridging the gap between measurements and the production of relevant information that emerges from the complexity of various situations (Jones G. R, Deakin A. G et al. 2008).

A typical example of the difference between monitoring and measurement is the traffic light system, the three traffic light colours (Red, Amber, Green) are used as indicators to indicate/alert of a conditions evolving at the junction crossing. For example, when "Red" light is on, it gives an early warning indication that the junction crossing is busy, therefore the driver must stop at the junction to avoid clash. The three traffic light colours (Red, Amber, Green) can be seen as monitoring indicators of the traffic condition at the junction crossing. It would be unnecessary and irrelevant to measure the intensity of "Red" light in order to stop at the junction crossing.

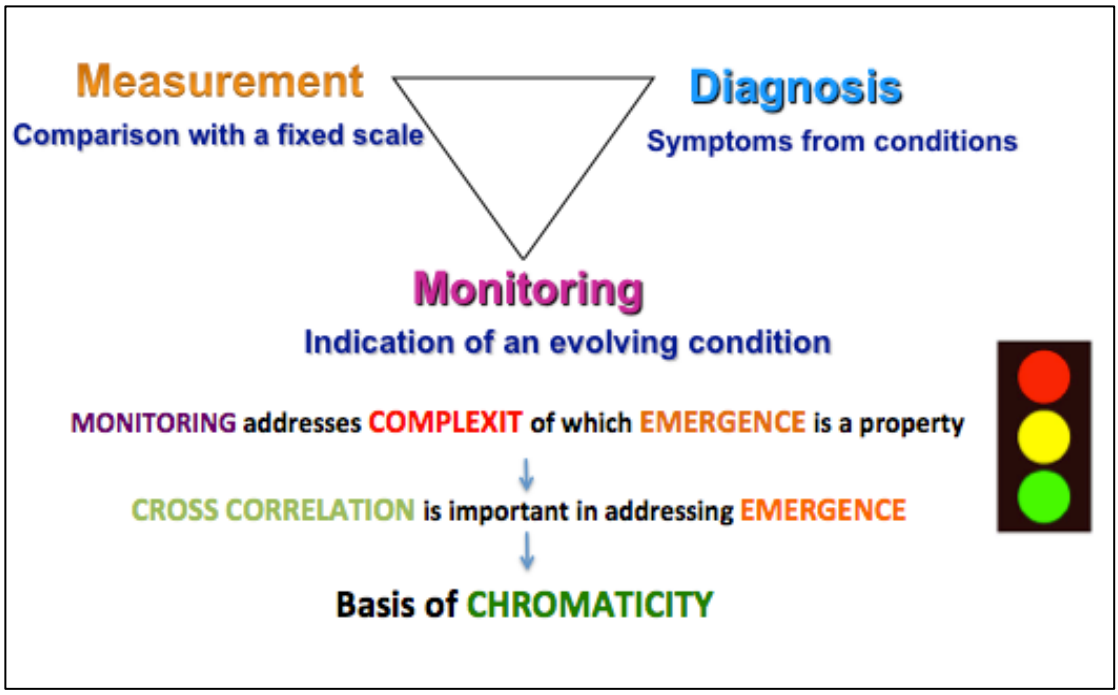

Figure 1.1: Illustration of the difference between monitoring, measurement and diagnosis

Complex liquids are an example of a complex system. Their complexity arises from the dynamical combination of molecules (Deshpande, Murali Krishnan et al. 2010) and non-linear rheological behavior (Gelbart, Ben-Shaul 1996), which necessarily plays a key role in determining the properties and the behavior of the liquid.

The dynamics of their structure is dominated by the particles redistribution between different regions in their dynamic mixture. The relative motions and correlations between molecules in liquids are a direct consequence of the intermolecular potential, which can be related to the fluctuation and dissipation processes that govern the physical behavior of the liquid as well as dictate the course of reactions (Torre 2007).

Optical methods have been applied to the study of complex liquids to provide a window on the motion of molecules that distinguish the dynamics of the liquid state (Torre 2007).

Complex liquids such as honey are composed of different chemical/biological compounds, which can vary in a regular manner with its composition content (White 1975). Understanding the behavior of such complex liquid and how the properties of light can address such complexity are very important, therefore improved methods capable to quantifying complex changes in optical spectra is needed for monitoring.

Various methods have been used to make fraudulent honey and many methods continue to evolve. For example, the original honey is blended with other less expensive components including inverted sugar. Alternatively, bees are intentionally fed sweeteners to increase its production in order to seek a quick profit. These honeys are deceptively marketed on the basis that they are pure and natural. These fraudulent practices have lead to the increasing occurrence of adulterated honey, which affects the reputation of the honey market in many countries such as "Yemen" (Al-Muraqab 2012, Hassan 2012) and also may have a negative effect on consumers' nutrition and health (Pilizota V, Nedic Tiban N 2009).

Unfortunately, traditional methods currently used to examine honey to ensure quality through taste or smell is no longer feasible and visual assessment methods (e.g. colour index) is also not reliable with the development of the new means and ways to produce fraudulent honey (Martin, Bogdanov 2002).

Although other methods are available to test the quality of the honey (e.g. using different chemical procedures, optical spectroscopy, etc.) can be expensive (lab infrastructure/ high cost of equipment/ precise optics) and time consuming (multiple tests) because of the complexity of the composition of such liquid. It is difficult to obtain a rapid decision capability and an overall evaluation of the condition of such honey sample from individual tests and multiple test impact on the cost.

Application of chromatic techniques for monitoring complex biological/chemical liquids based upon optical light properties and polychromatic light source was shown to be efficient. It allows essential information to be extracted about the different condition to which the liquid has been subjected (Jones G. R, Deakin A. G et al. 2008).

The three properties of light (Transmission, Polarization and Fluorescence) integrated into the system and monitored simultaneously to provide a rapid decision capability on the condition and quality of honey samples using readily available, portable and cost effective instruments that could be used on robustly site. The developed novel chromatic techniques quantify the complex composition of honey and discriminate for deviations from the norm and alert/ early warring indication of honey adulteration (i.e. honey fraud) rather than precise analysis. The methods for compensating for ambient or varying illumination conditions in the field and variations in the VDU and webcam characteristics are also original aspects of the research.

1.3 Thesis layout

Chapter 1 outlines the motivations and context of this work.

Chapter 2 describes the fundamentals light properties relevant to addressing liquids of complex composition. The principles of chromatic monitoring are also introduced that utilizes polychromatic light to monitor the changes in light properties.

Chapter 3 provides a literature review on complex liquids. It starts by giving some examples of complex liquids and their classification aspects. Then it focuses on a very complex liquid (honey), detailing some background knowledge and classification aspects. It also describes different conventional optical measuring techniques used in complex liquids and in particular honey. Finally it outlines some chromatic techniques applied in complex liquids and the potential for such technique in addressing honey.

Chapter 4 presents the different experimental optical setup (transmission, scattering, polarization and fluorescence) and the procedures adopted. An overview of the complete system is presented containing information about the portable system utilizing a camera and a laptop screen for producing light, followed by more detailed information on the major components used and the experimental procedures described for the different types of experiment. The method used for computational data processing is also described.

Chapter 5 describes the procedures for analyzing the test data and manner in which referencing used for measuring test to test aberrations followed by the procedures for normalizing the signal parameters leading to production of primary and secondary chromatic maps.

Chapter 6 presents the raw RGB results of the experimental tests with some examples of visual images taken by such monitoring system. The raw results for the calibrations test are presented first followed by the real honey tests.

Chapter 7 presents the chromatically processed RGB outputs that are used for compensating any aberrations in the experimental test results followed by the chromatically normalized RGB output for the calibration tests and the real honey test before they are combined for chromatic transformation.

Chapter 8 describes the application of the primary and secondary chromatic procedures for analyzing the test data. It fist describes how the primary chromatic maps are applied for the calibration tests to provided calibration measures, followed by application to the real honey samples. Finally it descries how the secondary chromatic procedures applied to the chromaticities for the three types of optical signals (transmission, polarization and fluorescence) on a single chromatic map to form the basis upon which the condition/composition of various honeys may found.

Chapter 9 summarizes the chromatic classification of the honey samples and compares the results with the conventional grading of the samples. It also presents the decision flow chart produced for chromatically classifying honey samples.

Chapter 10 describes the application of the chromatic honey monitoring system developed that was used for field-testing at various locations across Yemen.

Chapter 11 contains the main conclusions of this work, the future applications and the recommended work for further research.

Chapter 2

Properties Of Light

2.1 Introduction

This chapter describes the fundamentals of properties of light relevant to addressing liquids of a complex composition. These include the transmission and absorption of light along with reflection, refraction, scattering, fluorescence and polarization. One method for monitoring changes in such properties is with chromatic techniques, which utilizes polychromatic light. Fundamental aspects of chromatic techniques are described which are relevant to addressing liquids containing complex components.

2.2 Properties of Light

Light can give visual information about the surrounding environment, which can be sensed by eye or an optical instrument. In addition it can be used in critical applications such as monitoring or transmitting information.

Electromagnetic waves are transverse waves, consisting of oscillating electric and magnetic fields (figure 2.1). They have a wide range of frequencies and can travel through many media, including vacuum. These different waves are distinguished by their wavelength (λ) and travel at a velocity of 3.10^6km/sec (Stockley, Oxlade et al. 2007).

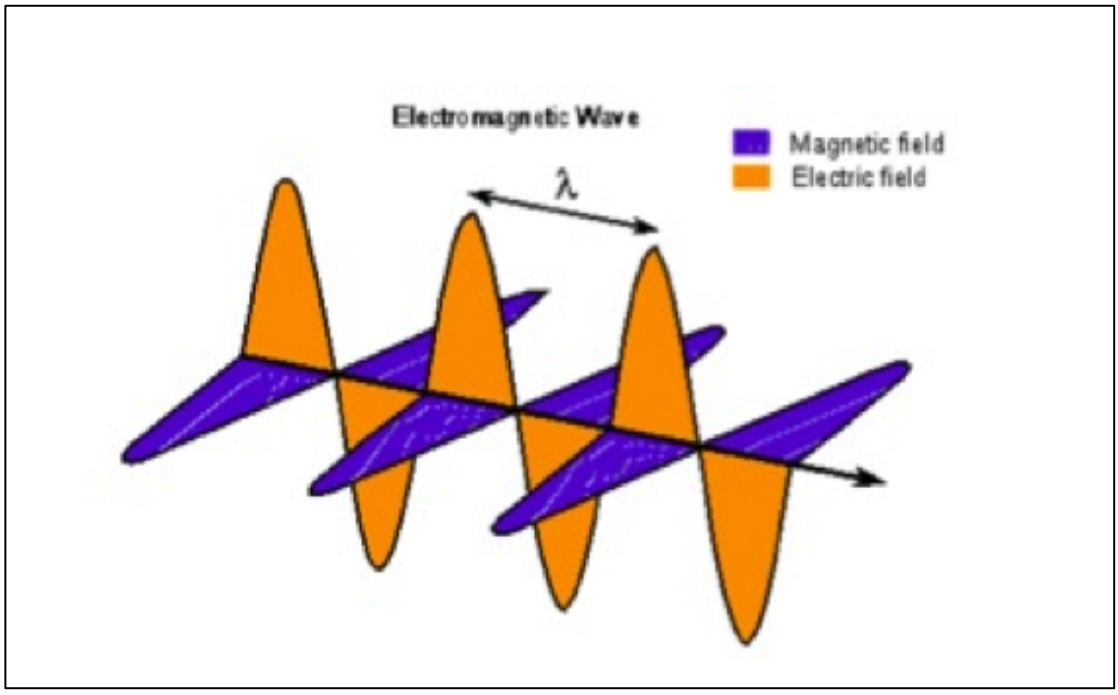

Figure 2.1: Electromagnetic wave (Magnetic and Electrical fields perpendicular to each other) (Strobel 2001)

2.2.1 Polychromatic Light

Light consists of electromagnetic waves of particular frequencies and wavelengths (e.g. Ultraviolet, Visible light, Infrared) (figure 2.2). Visible light consist of electromagnetic waves exists in the wavelength range $4.0–7.0x10^{-7}$ m and is usually quoted in nanometers (400–700nm) (Stockley, Oxlade et al. 2007).

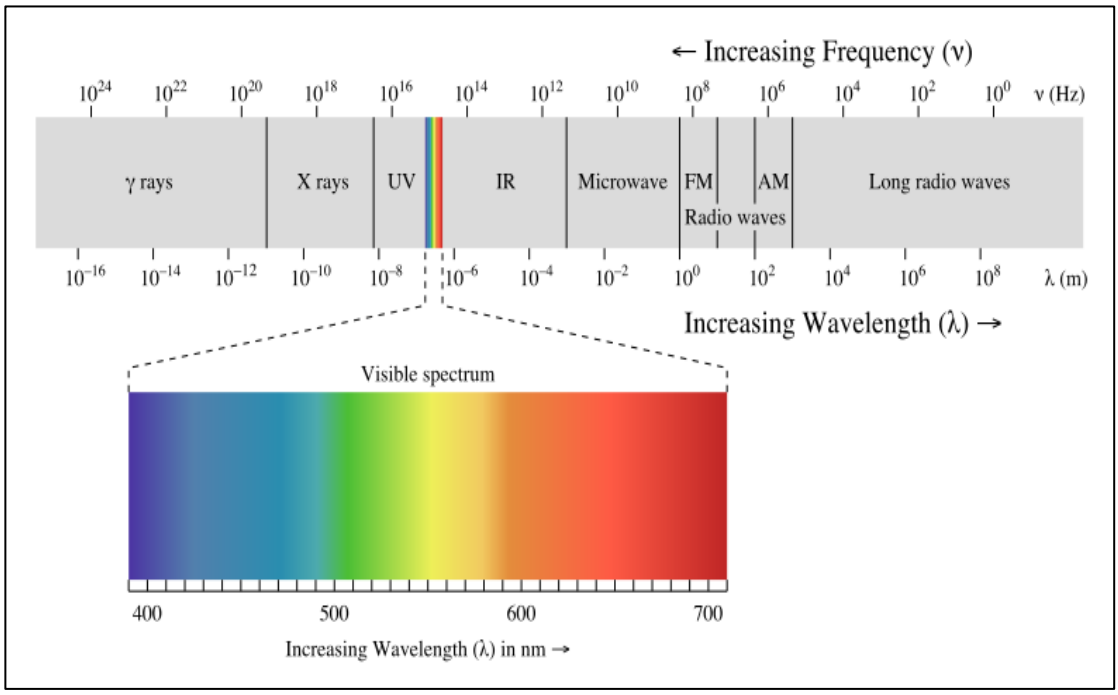

Figure 2.2: The Electromagnetic Spectrum (Ronan 2007)

In atomic physics, the Bohr Atomic Model explained how electrons could change from one orbit to another only by emitting or absorbing energy of a fixed value (Kragh 2012). For example, if an electron changes to one orbit closer to the nucleus, it must emit energy equal to the difference between the energies of the two orbits. Conversely, when the electron changes to a higher orbit, it must absorb a quantum of light equal in energy to the difference between the orbits.

The quantized orbits of the electrons provides for a simple explanation of the origin of photons, and the spectrum of light (figure 2.3) (Schneider, Arny 2007). Photons are produced by the transition of electrons in their orbits. A descending transition releases potential energy in the form of a light particle, a photon. Likewise, electrons could absorb photons, so that they move ascending in their

orbits. Figure 2.3(a) shows an example of polychromatic light incident on the atom of a material. The atom may absorb particular wavelengths (e.g. “orange”) and emit at a different wavelengths (e.g. “yellow”). As such the spectrum of light is changed from having components at all wavelengths to having some wavelengths weakened (orange) and others strengthened (yellow) (figure 2.3(b)).

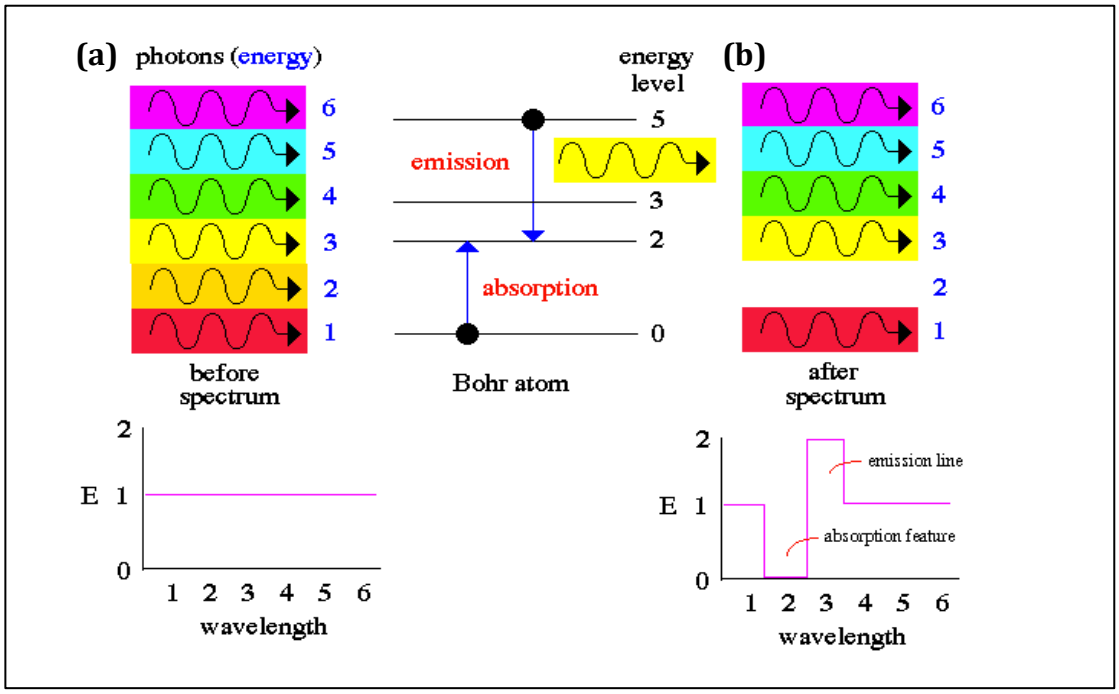

Figure 2.3: Photons and spectrum of light (Schneider, Arny 2007)

The energy of visible light received from an object depends upon the wavelength incident on the object and the extent to which it is reflected, scattered or transmitted. So if light interacts with atoms in a material that has an atomic energy level lower than the light energy, the light will be absorbed. The detected colour is actually the colour of the light, which has been affected by the energy absorbed by the atoms. Once colour has been detected from the light transmitted through an object, it may be considered as being the colour of the light rather than the colour of the object (Schneider, Arny 2007).

2.3 Fundamental Properties Of Light

Light behaves in different ways depending upon the medium through which it travels. The behavior of light may be described in term of the following attributes:

- Transmission
- Absorption
- Reflection
- Refraction
- Diffusion (scattering)
- Fluorescence
- Polarization

Reflection and refraction can be regarded as forms of coherent scattering, while diffusion is a form of incoherent scattering.

The links between the optical parameters being measures and the properties of the liquids being evaluated is discussed on Chapter 3.

2.3.1 Transmission & Absorption Of Light

An electromagnetic wave incident upon an object will affect the atoms of the object (Bohren, Huffman 2008). In the case of transmission (figure 2.4) the vibrating atoms will resonate for a short period of time with small amplitude before re-emitting a light wave. If the object is optically clear then the light will pass through the object with only very small amplitude changes. On the other hand, if the object is not clear and contains particles, then some of the light energy is absorbed by the atoms of the materials and converted into thermal energy. This may be manifested as a change of wavelength, which can be observed with a spectrum analyzer (Bohren, Huffman 2008). Uniformity of the transmitted light is considered as an advantage.

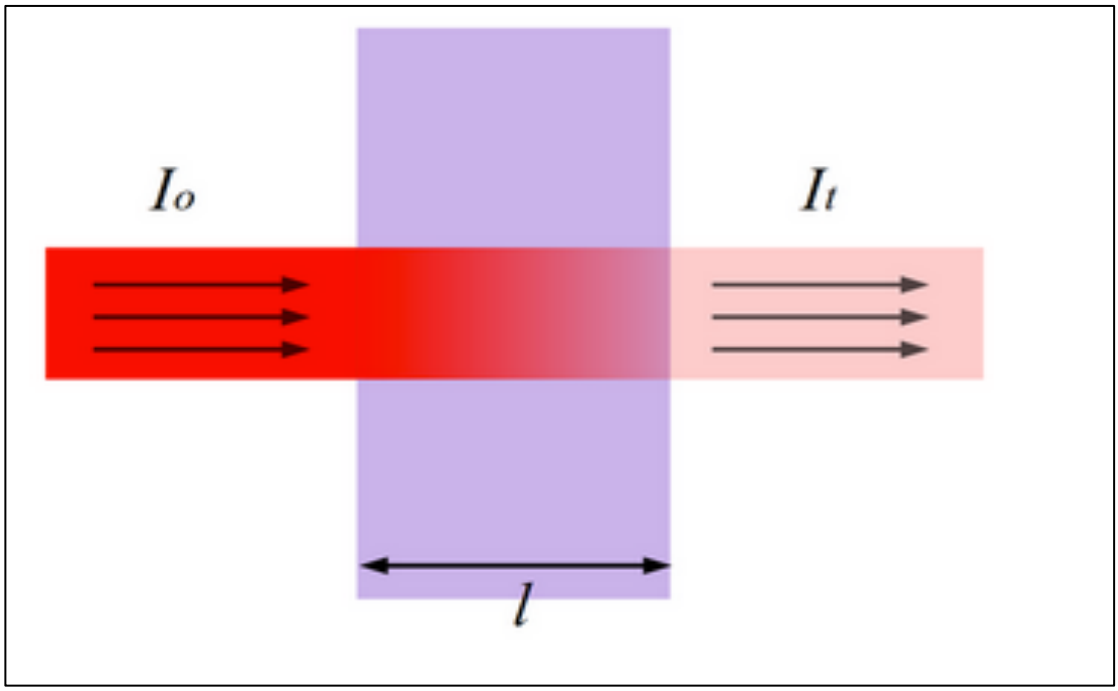

Figure 2.4: Transmission of light through a material (Shim). (Io = incident light intensity, It = transmitted light intensity, l= thickness /path length)

The number of photons that passes through the material (figure 2.4) is dependent on the thickness of the material and the concentration of the sample. Once the intensity of light is known after it passes through the material, I(t) the transmittance can be calculated.

Transmittance (the fraction of light that passes through a sample) is defined by

$$Transmittance\ I(t) = \frac{I_t}{I_o} \tag{2.1}$$

Transmittance is related to absorption by the expression below

$$Absorbance\ (A) = -\log(T) = -\log\left(\frac{I_t}{I_o}\right) \tag{2.2}$$

Where the absorbance stands for the number of photos that are absorbed. The amount of absorption can vary from one material to another (e.g. glass, plastic, etc). The variation will depend on the shift in the wavelength and the thickness of the materials (figure 2.5). The relationship between the internal transmission τ_i (λ) at a given wavelength and the path length is given by Bouger's law (equation 2.3) (Ryer 1997).

$$\tau_i(\lambda) = \frac{I(\lambda)}{P_d} \tag{2.3}$$

I(λ) is the transmittances of the sample at a wavelength (λ) and P_d is the reflection coefficient factor of the material.

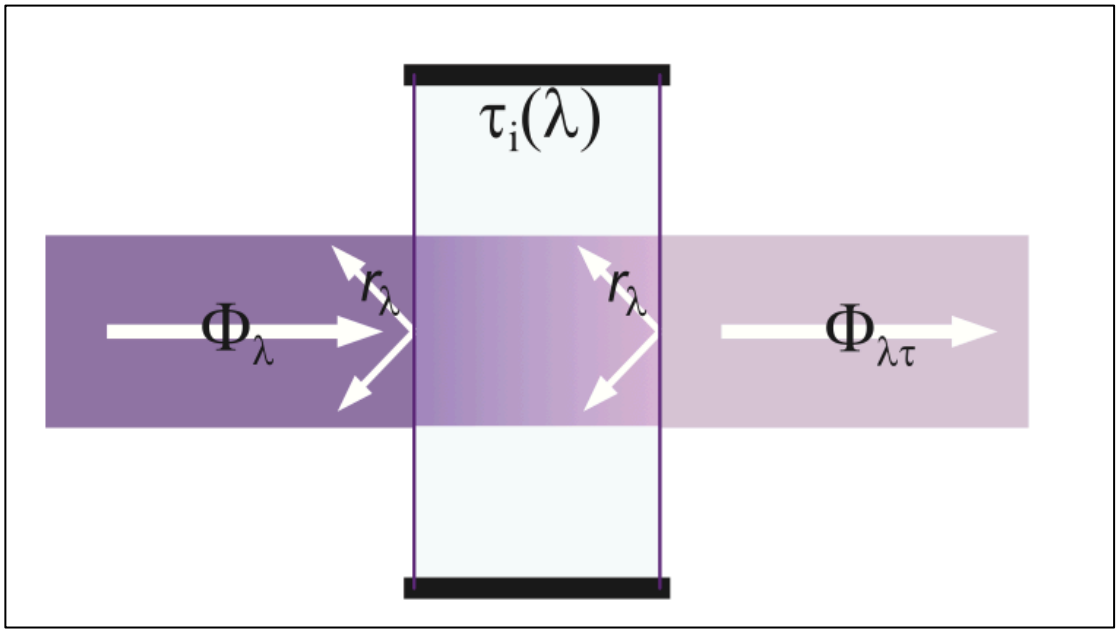

Figure 2.5: External Vs. Internal transmittance (Ryer 1997). (Φλ = incident light, Φλτ = transmitted light , τi(λ) = internal transmission, rλ= external reflected light)

2.3.2 Reflection Of Light

Light reflecting of a surface obeys the law of reflection: the angle between the incident ray (θ_i) and the normal to the surface is equal to the angle between the reflected ray (θ_r) and the normal (Ryer 1997). When light obeys the law of reflection (equation 2.4), it is termed a *specular* reflection.

$$\theta i = \theta r \tag{2.4}$$

2.3.3 Refraction Of Light

The velocity of propagation of light in a material is defined by the materials refractive index, which is defined by (N) (equation 2.5).

$$Refractive\ index\ (N) = \frac{C}{V} \tag{2.5}$$

Where C is the speed of light in vacuum and V is the speed of light in the material.

The refractive index is defined by the measure of light refraction when passing from one medium into another. It usually changes when a medium is changed from liquid to gas to solid. So any increase in electron density within the materials also increases the reflective index (Stockley, Oxlade et al. 2007). A change in the phase velocity of a beam of light can be caused by a change in the density of the medium through which it travels (Ryer 1997) causing the light to be refracted.

When light passes between dissimilar materials, the rays bend and change velocity slightly. Refraction is dependent on two factors: the incident angle (θ1) and the refractive indices of the two materials (n1 and n2), as given by Snell's law of refraction (equation 2.6) (Ryer 1997).

$$n_1 . \sin(\theta_1) = n_2 . \sin(\theta_2) \tag{2.6}$$

2.3.4 Diffusion (Incoherent Scattering)

Diffused (incoherent scattered) light can be defined as follows: Whenever light is incident on a rough surface or material its interaction with atoms that form the medium causes the light to be scattered in many directions i.e. light is deviated from its original incident beam (Bohren, Huffman 2008). As a result most objects observed in daily light is due to scattered light.

Furthermore, the wavelength and the interaction of the scattered light are controlled by the light atoms distribution on the surface of an object. For instance, when the atomic particles are small, such as in clear crystal (less than 250nm diameter), the scattering of the light is uniform over all wavelengths and only the propagation speed of the incident wave is changed. On the other hand, if the particles are larger than 250nm (e.g gas and liquid), the fluctuations of the atoms can cause extraordinary scattering depending on the interaction of wavelength with these. Based on this interaction, light can be scattered elastically or in-elastically (Bohren, Huffman 2008). Elastic and inelastic light scattering can be used to measure shape, size and index of micro particles. Usually most of the scattered light is elastic, where the wavelength of the scattering is the same as that of the incident light due to the molecules not changing their energy state (Bohren, Huffman 2008). In the case of the in-elastic scattering, the emitted light has a wavelength different from the incident light i.e. due to the molecules changing their energy state (Smith, Dent 2005).

2.3.4.1 Rayleigh & Mie Theory

Rayleigh scattering is the elastic scattering of light or other electromagnetic radiation by particles much smaller than he wavelength of light (Bohren, Huffman 2008). The oscillating electric field of a light wave acts on the charges within a particle, causing them to move at the same frequency. The particle therefore becomes a small radiating dipole whose radiation we see as scattered light. Mie theory describes the scattering and absorption of electromagnetic radiation by spherical particles similar to or larger than the wavelength of light through solving Maxwell equations.

2.3.5 Fluorescence

Luminescence is the emission of light from a substance and occurs from electronically excited states, formally divided into two categories (fluorescence and phosphorescence) depending on the nature of the excited state (Lakowicz 2006).

Some molecules are capable of being excited, via absorption of light energy, to a higher energy state " excited state". The energy of the excited state which cannot be sustained for long "decays" or decreases, resulting in the emission of light energy. The three-stage process of excitation, excited lifetime, and emission is called fluorescence (Lakowicz 2006).

Fluorescence typically occurs from aromatic molecules. Some typical fluorescent substances (fluorophores) are given on figure 2.6(a) and the optical emission from them is shown on figure 2.6(b).

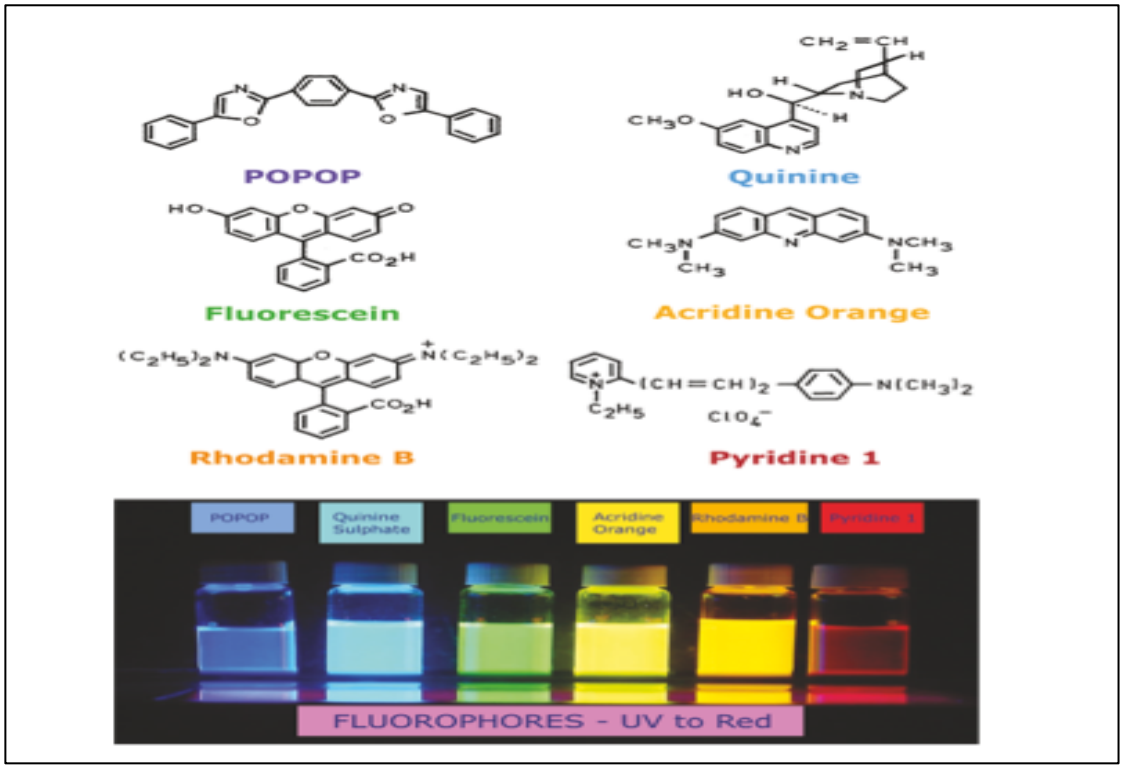

Figure 2.6: Fluorescence:(a) Chemical structure of some fluorescent material, (b) Fluorocsent light from each flourecent material (POPOP, Quinine, Fluorescein, Acridine Orange, Rhodamine B, Pyridine 1). (Lakowicz 2006)

Fluorophores absorb a range of wavelengths of light energy and also emit a range of wavelengths. Within these ranges are the excitation maximum and the emission maximum. The energy of the emission is typically less than that of absorption, therefore fluorescence typically occurs at lower energies or longer wavelengths. This energy difference is the Stokes shift (figure 2.7) (Gispert 2008). Because the excitation and emission wavelengths are different, the absorbed and emitted lights are detectable as different colours or areas on the visible spectrum (figure 2.8) (Lakowicz 2006).

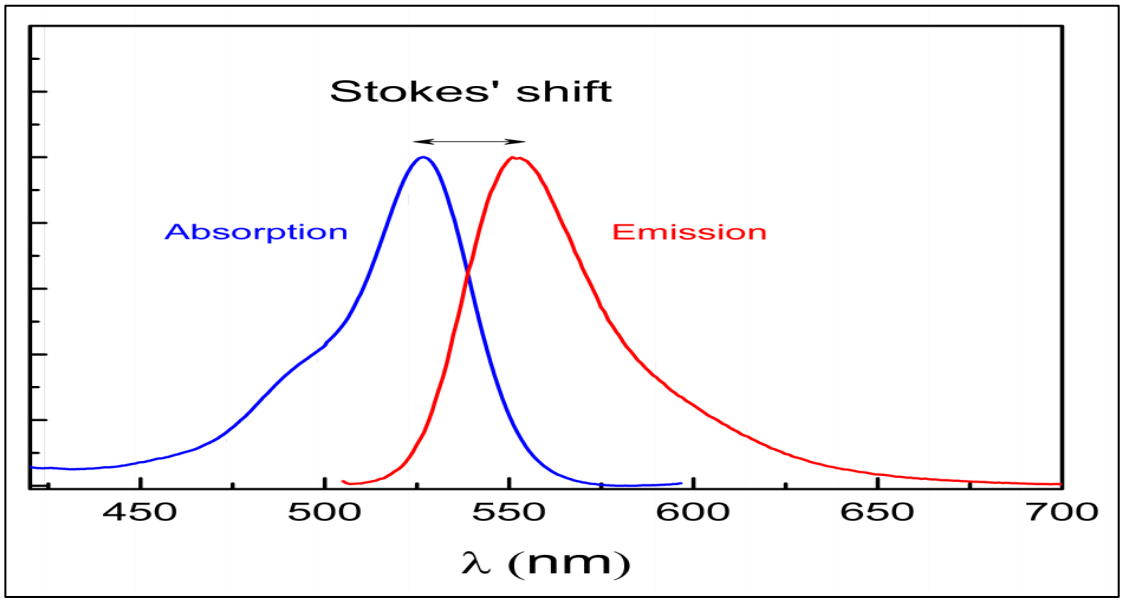

Figure 2.7: Stoke shift of abortion and emission spectra (Sobarwiki 2013).

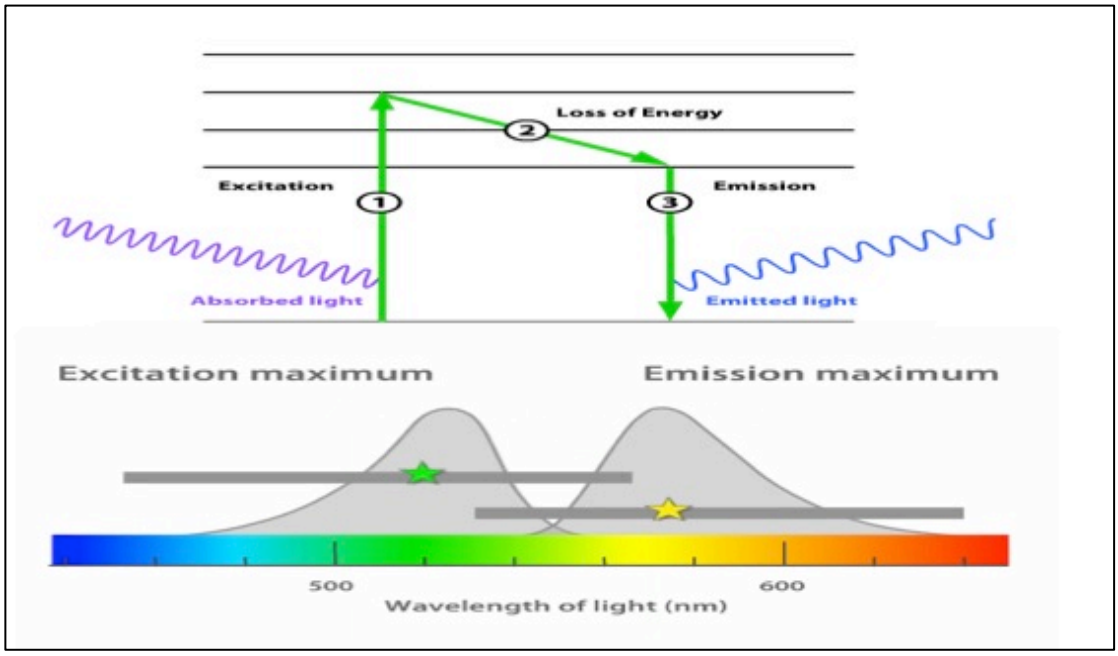

Figure 2.8: Fluorescence excitation and emission spectrum(Fisher Scientific 2014).

2.3.6 Polarization of Light

2.3.6.1 Nature of polarized light

Polarized light can be considered as a transverse electromagnetic wave (Jenkins, White 1976) propagating in the *z* direction with the **E** field in the *x,y* plane and **B** field orthogonal to it. If the **E** vector of the wave is stationary in space then it may be said to be a plane or linearly polarized light ray.

In optically active materials, the asymmetry of the structure or molecules results in what is termed "specific optical activity' also known as "rotatory power", which is a property of the optically active chemical (Jenkins, White 1976, Swindell 1975).

This was first addressed by Fresnel were he considered the linearly polarized wave be broken into two circularly polarized components and that these would experience different reactive indexes (i.e. for right and left handed circular polarization components as different index of refraction is seen) (Smith, March 2007).

For linearly polarized light, the **E** oscillating field maybe split into two components, right and left handed circularly polarized waves E_r and E_l. Since these components encounter differing refractive indices within an optically active material a phase shift will result and a rotation of the plane of polarization is observed (Jenkins, White 1976, Egan 2006, Swindell 1975).

2.3.6.2 Transmission of light through a polarizer

Light normally consists of multiple random polarization states. For some waves the **E** field is vibrating in the horizontal axis, for others the vertical axis and any angle in between. Interactions with materials can cause a change in this polarization (Jenkins, White 1976). An example of this type of material is a polarizer.

There are different configurations of polarizers. Some are made from special glass others from plastic. An example un-polarized light is light that contains one horizontal component and one vertical component of equal magnitude (Jenkins, White 1976). A polarizer that selectively blocks one of these components, allowing the other to pass are knows as a linear polarizer. Light incident on a linear polarizer will, in theory only be transmitted if it is in the correct polarization state (i.e. the direction of oscillation is parallel to the polarization or transmission axis of the polarizer).

When the polarizer is at a fixed position (vertical) (figure 2.9), light with a polarization angle close to this will pass. Altering the polarizer angle will not change the intensity of the signal because of the symmetrical nature of the un-polarized light resulting in a similar number of waves and intensity at any given angle (E_1). However introducing a second polarizer (analyzer polarizer) at an angle (θ=45), only one component will pass through ($E_1.\cos\theta$). This is known as Malus's law (equation 2.7) (Swindell 1975). The intensity of the signal will vary according to $\cos^2$ as the angle of the polarizer is changed.

$$E(\theta) = E(1)\cos^2\theta \quad (2.7)$$

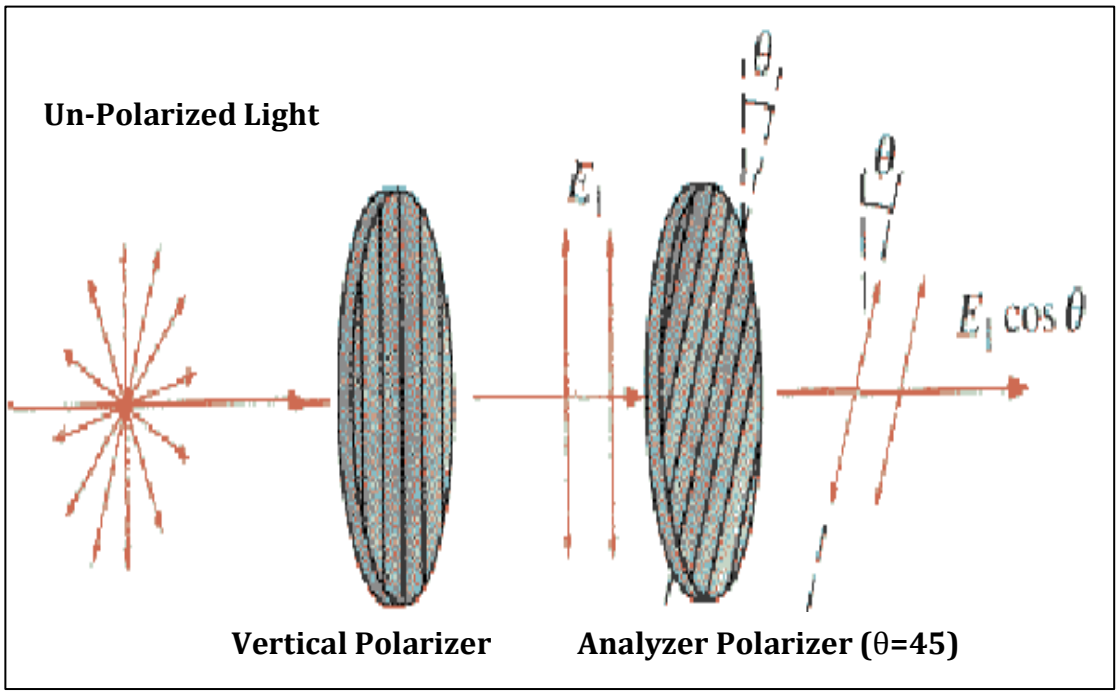

Figure 2.9: A linear polarizer – Malus Law (Sanny, Moebs 1996)

2.3.6.3 Optical Rotatory Dispersion

The refractive index of a substance is usually wavelength-dependent, and so is the optical rotation (Swindell 1975). The wavelength dependence of the optical rotation is called optical rotatory dispersion. Optical rotatory dispersion an affect related to polarimetry. In polarimetry, it is assumed that only one wavelength is present (i.e. monochromatic light), therefore if the wavelength is changed, the optical rotation will change (Egan 2006). With optical rotatory dispersion, the light is polychromatic. The specific rotation of each wavelengths of the polychromatic light is given by (equation 2.8) (Jirgensons 1973).

$$Specific\ Rotation\ [\alpha] = \frac{A}{(\lambda^2 - \lambda_c^2)} \quad (2.8)$$

Where λ_c is the wavelength associated with the dominant molecular interaction in the material and A is a constant of proportionality depending upon the molecular weight of the optically active compound. Consequently, polarized light of different wavelengths will have their plane of polarization rotated by different amounts, the longer the wavelengths being rotated more than the shorter ones (rotary dispersion).

When a monochromatic light source is replaced by a broad polychromatic source in a polarimeter setup, varying the angle of rotation of the analyzer polarizer will vary the colour spectrum due to the polychromatic signal being spread over a varying range of angles (figure 2.10). The analyzer-polarizer combination acts to selective narrow bands of light to pass. Hence a particular colour can be seen at a particular angle of rotation, corresponding to a shift in the dominant wavelength of the signal (Jones G. R, Deakin A. G et al. 2008, Egan 2006).

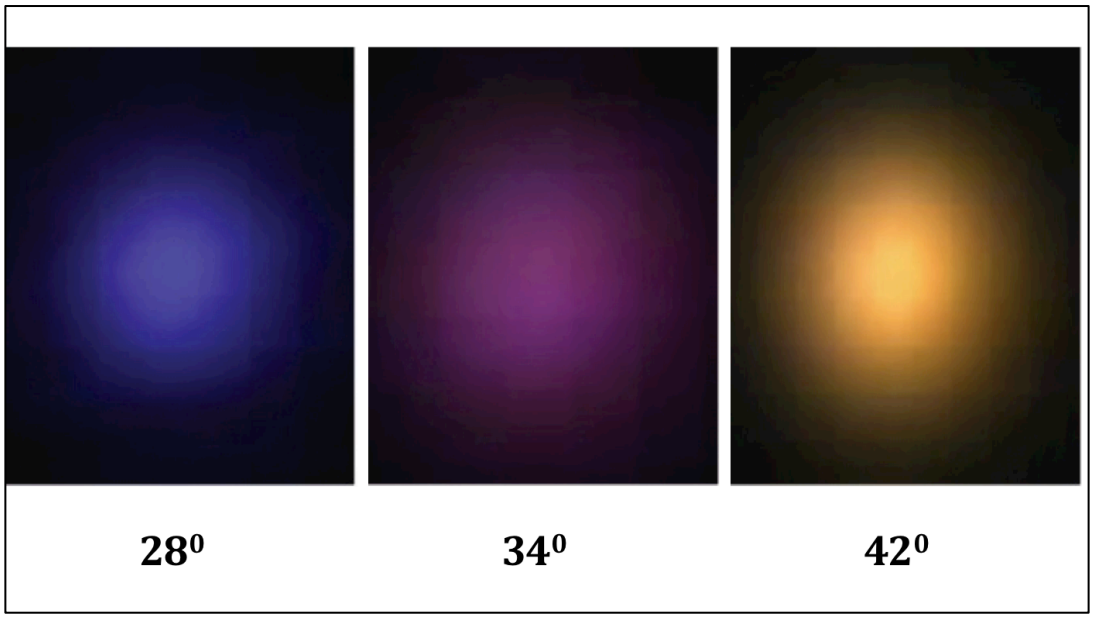

Figure 2.10: Chromatic images as a function of polarization angle (Jones G. R, Deakin A. G et al. 2008).

2.4 Fundamentals Of Chromatic Monitoring

2.4.1 Complexity, Monitoring & Chromaticity

It is important to recognize the difference between measurement, diagnosis and monitoring to appreciate the problem of monitoring complex conditions. Measurement is mainly concerned with the quantification of extent by comparison with a standard. As such it is reductionalist in nature being based on addressing isolated and specific parameters to high accuracy (Jones G. R, Deakin A. G et al. 2008). Diagnosis is concerned with the determination of a condition from symptoms and thus requires relevant information. Monitoring is concerned with observation to indicate the likelihood of a condition evolving.

Monitoring and diagnosis may be regarded as bridging the gab between measurement and production of relevant information that emerges from the complexity of various situations (Jones G. R, Deakin A. G et al. 2008).

The chromatic methodology is based upon comparisons, which are translated into mathematic cross correlation, enabling numerical scales of judgment to be established (Jones G. R, Deakin A. G et al. 2008). This technique has been demonstrated for extracting data from a number of different sources for various applications.

Complex colour problems are an area that is vital to researchers as colour may be used for many different applications such as monitoring (Jones G. R, Deakin A. G et al. 2008). Complexities associated with colour maybe addressed by improving contrast or separation, which leads to the introduction of mathematical algorithms, which promote colour classification.

Chromaticity is a monitoring technique concerned with addressing different signals detected by different detector processors with at least three overlapping filters. As such colour is a special case of chromaticity, these chromatic filters can distinguish between complex spectral data. The complex spectral data are simplified to at least three parameters, (R,G,B) which will have a high level of traceability and contain sufficient information (Jones G. R, Deakin A. G et al. 2008).

2.4.2 Colour

Colour is one of the most useful properties for identifying a substance without any additional chemical or physical tests (such as determining the physical conditions of liquids) (Manahan 2000). For many years, colour has been used for image identification, playing an important role in identifying an image or object for visual perception (Storozhuk 2010).

Colour identification maybe regarded as a measure of the chromaticity of the light spectrum in the visible region using the response of the detectors of the human eye. Whereas spectrometry is concerned with analyzing the fundamental wavelength components of light, colour is a manifestation of the mixture of various components superimposed upon each other (Storozhuk 2010).

Colour vision by the human eye is associated with the reflection of light from a coloured object. The spectral reflection depends on the intrinsic condition of the reflected surface and the illumination level (Wolff, Shafe et al. 1992). Human vision interprets light as a colour in the brain using information transmitted from the receptors in the eye in order to derive representation.

Colour may be regarded as being represented by three properties hue, lightness and saturation. These properties are psychological aspects of the optical spectrum. Hue is referred to as the effective dominant wavelength of light that is detected by the human eye (retina) causing the sensation of colour as red, green or blue etc. Saturation indicates how widely hue is spread. The lower the saturation the closer the colour is to grey whilst high saturation is close to a pure (single wavelength) colour. The range between the high and low saturation represents the hue concentration. Lightness is the strength (energy) of the colour (brightness) ranging from zero (black, no light) to one (white, maximum red, green and blue) (Glomon 2003).

Although hue, brightness and saturation describe the psychological aspects of the optical spectrum, the physical aspects are defined only by hue and saturation. The ability of classifying colour psychologically and physically is an important requirement for many applications. To address this issue, the CIE (Comission Internationale de liEclairage) (CIE 2004) suggested a set of defined colour matching functions to form tri stimulus model.

2.4.3 Human Perception System

Humans have five main highly complex sensing systems (hearing, smell, taste, touch, colour) that monitor the surroundings. Each one of these systems is important, but each one has its own function, which distinguishes it from the other senses.

Light enables a human to visually monitor surrounding objects. Similar to a camera that can capture images, the eye has its own image processor, which consists of millions of processor units.

The light contains different wavelengths, which can be affected by factors such as absorption, reflection, refraction, scattering or diffraction in transmission to the human eye pupil through a lens (Oyster 1999).

The cross section of the human eye and the schematic view of the retina are shown on figure 2.11. At the rear of the eye is a photosensitive structure of cells called the Retina. This consists of primary sensory neurons (Rods and Cones), having a main purpose that is to convert the received light into neural impulses (Oyster 1999). Rods are photosensitive cells which can operate at low level illumination and are able to sense black and white and different grey shades i.e. rods do not provide colour sensation. Cones are cells which wavelength sensitive to provide colour discrimination. Cones are separated into three different types: *Red* (high sensitivity at long wavelengths of visible light), *Green* (high sensitivity at middle wavelength of visible light) and *Blu*e (high sensitivity at short wavelength of visible light). The sensitivity curves for these three receptors in the human eye are observed in the visual spectrum (figure 2.12). The observation of colour by the eye is determined by the combination of the three RGB receptors (King 2005).

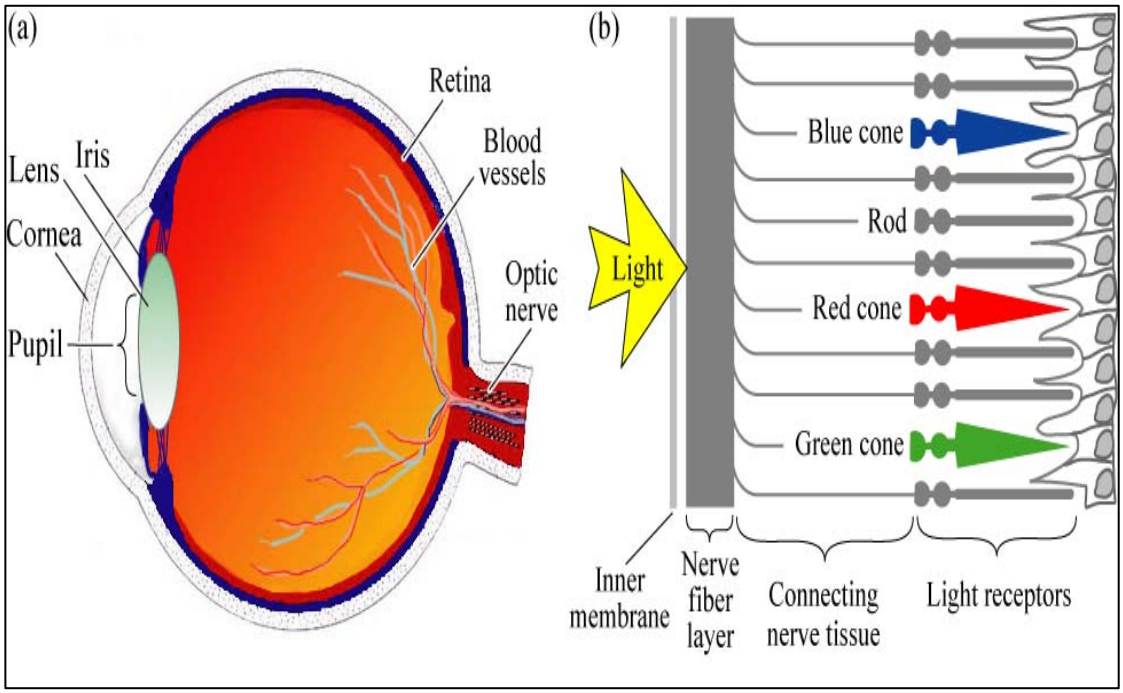

Figure 2.11: The Human eye: (a) cross section through human eye, (b) schematic view of the retina including rod and con light receptors (Encyclopedia Britannica, 1994).

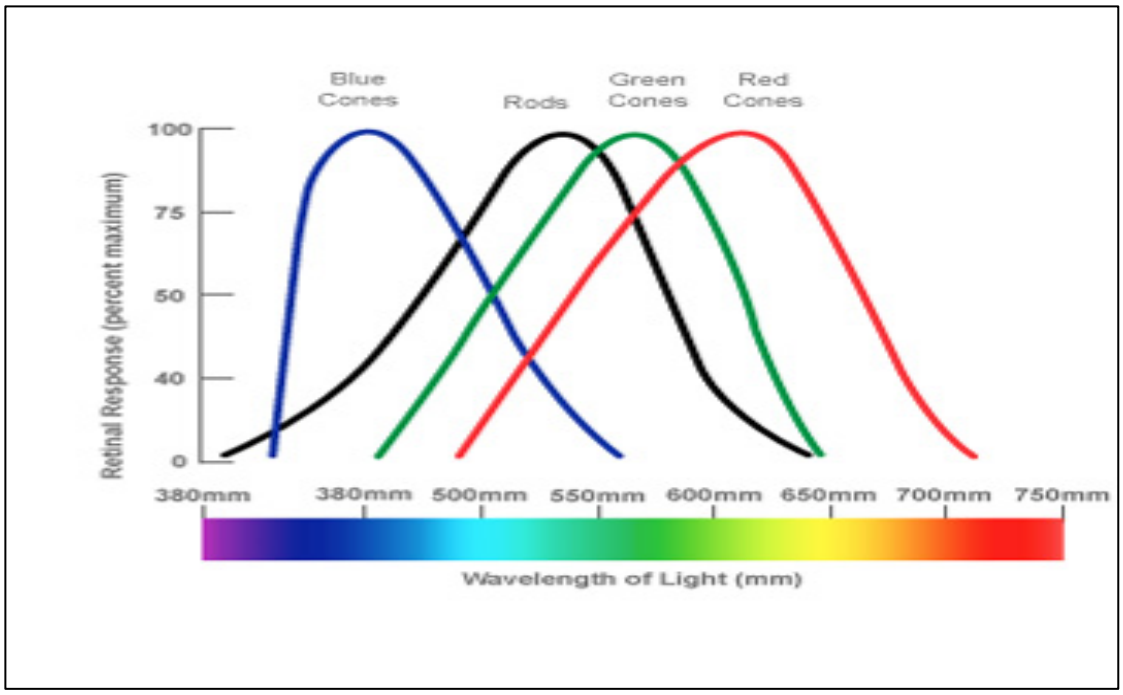

Figure 2.12: Spectral sensitivity of human rod and cone (Bulmer 2012)

2.4.4 Colour Space

A colour space is a method by which colour can be specified, created and visualized (Hunt, Pointer 2011). As humans we may define a colour by its attributes of brightness, hue and colourfulness (King 2005). A computer may describe a colour using the amounts of red, green and blue phosphor emissions required to match a colour (Ford, Roberts 1998).

A printing press may produce a specific colour in terms of the reflectance and absorbance of cyan, magenta, yellow and black inks on the printing paper (Ford, Roberts 1998).

A colour is thus usually specified using three co-ordinates, or parameters. These parameters describe the position of the colour within a colour space (Hunt, Pointer 2011).

2.5 Chromatic Transformation

The tri-chromatic theory of colour describes the way three separate lights (red, green and blue) can match any visible colour based on the eye's use of its three colour sensitive sensors. This is the basis on which photography and printing operate, using three different coloured dyes to reproduce colour in a scene. It is also the way that most computer colour spaces operate, using three parameters to define a colour (Ford, Roberts 1998).

2.5.1 Tristimulus Colorimetry

Tristimulus colorimetry is based on the assumption that any colour can be matched by a combination of three primary colours, red, green and blue. The CIE (Commission International de l'Eclairage) system is an internationally agreed set of primary colours and corresponding overlapping spectral responsivity functions (Hunt, Pointer 2011, CIE 1931) shown in figure 2.13. This means that a large spectral signature can be quantified by a smaller number of parameters.

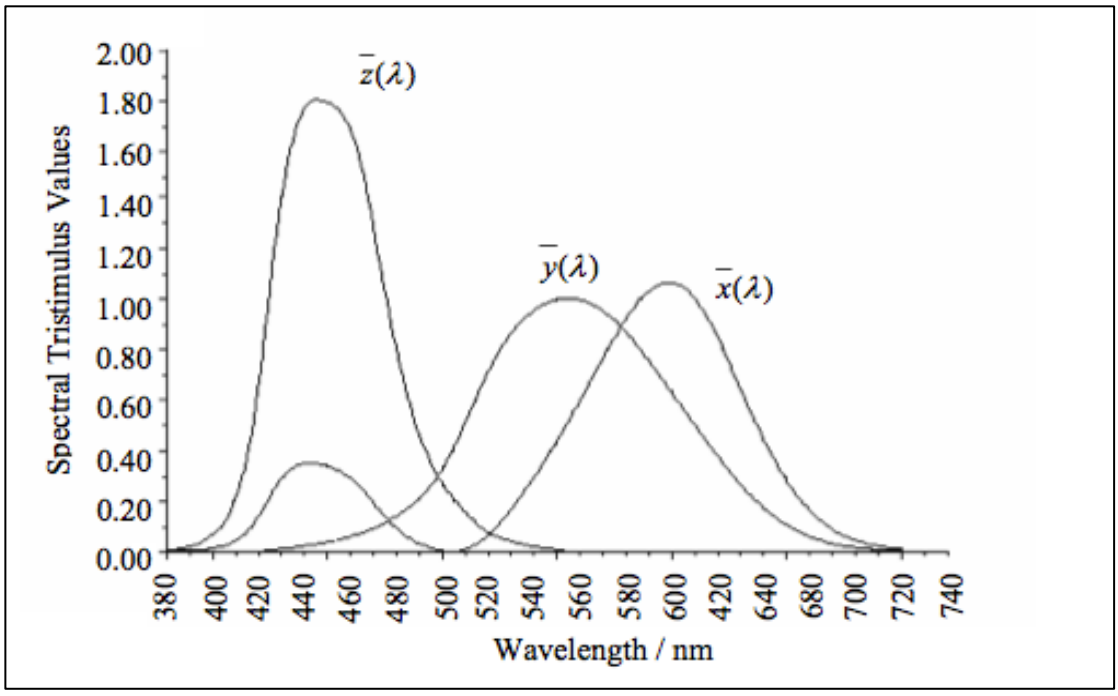

Figure 2.13: CIE Tristimulus colour-matching functions (Ross 2005)

The measured spectral power distribution of a source *P(λ)* can be addressed by these three functions to produce an integrated response value for the red, green and blue detectors over the wavelength range λ_1 to λ_2. The integrated spectral values are the three tristimulus values, *X*, *Y*, and *Z*. These values are coefficients of a vector in three-dimensional colour space given by the relationship of the measured spectral power distribution to the responsivities of the detectors R(λ) and the data increment d(λ). The output of each detector is given by:

$$i_n = \int_{\lambda_1}^{\lambda_2} P(\lambda)R(\lambda)d(\lambda) \tag{2.9}$$

Equation 2.9 is applied to the CIE tristimulus response curves of figure 2.13, the relationships become (Hunt, Pointer 2011)

$$X = \int_0^{\infty} P(\lambda)\bar{x}(\lambda)d(\lambda) \tag{2.10}$$

$$Y = \int_0^{\infty} P(\lambda)\bar{y}(\lambda)d(\lambda) \tag{2.11}$$

$$Z = \int_0^{\infty} P(\lambda)\bar{z}(\lambda)d(\lambda) \tag{2.12}$$

The CIE designed a horse-shoe shaped CIE Chromaticity diagram (figure 2.14) in order to represent the three dimensional representation of colour in a two dimensional form.

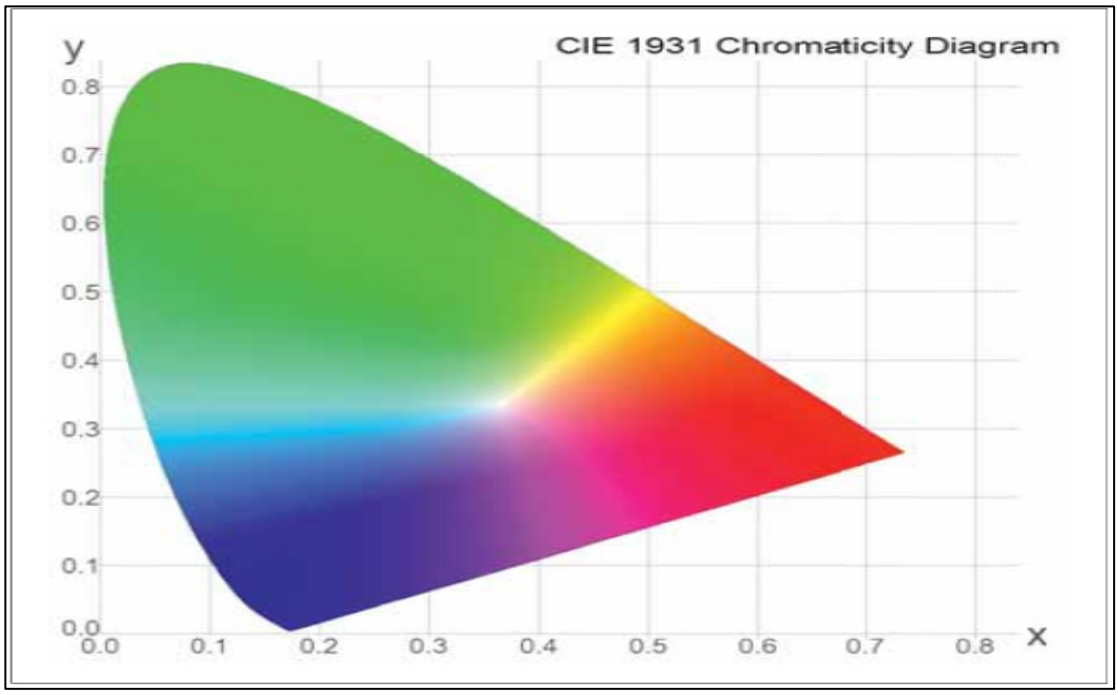

Figure 2.14: CIE Chromaticity Diagram (CIE 1931)

The two axes of the diagram are the chromaticity coordinates *x* and *y* for any given colour and are calculated from the Tristimulus values X, Y and Z thus:

$$x = \frac{X}{X+Y+Z} \tag{2.13}$$

$$y = \frac{Y}{X+Y+Z} \tag{2.14}$$

$$z = \frac{Z}{X+Y+Z} \tag{2.15}$$

Addressing colours in terms of the co-ordinates *x* and *y* defines exactly the hue and saturation of any given colour (Levkowitz, Herman 1993). The brightness *L*, of the spectra is the sum of all three detectors outputs.

$$L = X + Y + Z \tag{2.16}$$

At the boundaries of the CIE chromaticity diagram the hues are pure saturated colours and are non-uniformly spaced. Toward the centre of the diagram the hues become less saturated, to a point defined by: x=y=z=0.33.

This point is known as the point of achromaticity where pure white light exists. It is sometimes called the *'equal power'* point because achromatic colours are produced by spectral power distributions having equal power at all wavelengths.

For a colour mapped on the diagram (figure 2.15) at point C a straight line can be drawn through the achromatic point S, and C. The point W at where this line intersects with the spectral locus gives rise to a value that represents a single wavelength. This single wavelength is then referred to as the weighted average or dominant wavelength.

The Hue of point C is calculated from the simple equation (Levkowitz, Herman 1993):

$$H_{xy} = \left(\frac{x-x_s}{y-y_s}\right) \tag{2.17}$$

Where x_s and y_s are thr coordinates x and y of the achromatic point S colour mapped to point C. The saturation of light can be obtained from the ratio of points SC to SW (Levkowitz, Herman 1993).

$$Saturation = \frac{SC}{SW} \tag{2.18}$$

SC is the distance from the point S to point C and *SW* is the distance from the point S to the spectrum locus.

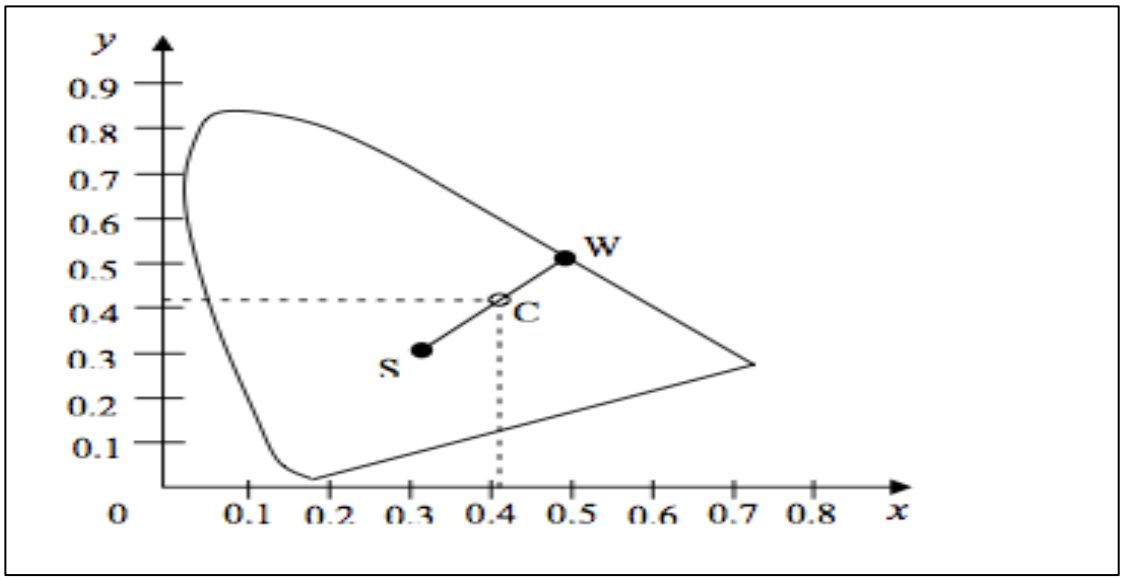

Figure 2.15: CIE Lxy System for representing a colour (Ross 2005)

2.5.2 Linear Colour Space (RGB)

The simplest means of representing a spectral signature is using an RGB 3-dimentional-colour cube (Ford, Roberts 1998) (figure 2.16). Each colour is broken down into its relative intensity in the three primaries red, green and blue. These values are plotted along the three axes of the cube to define a point in three-dimensional space. This point is representative of the original colour and will move in the RGB space in accordance with spectral changes (Hunt, Pointer 2011).

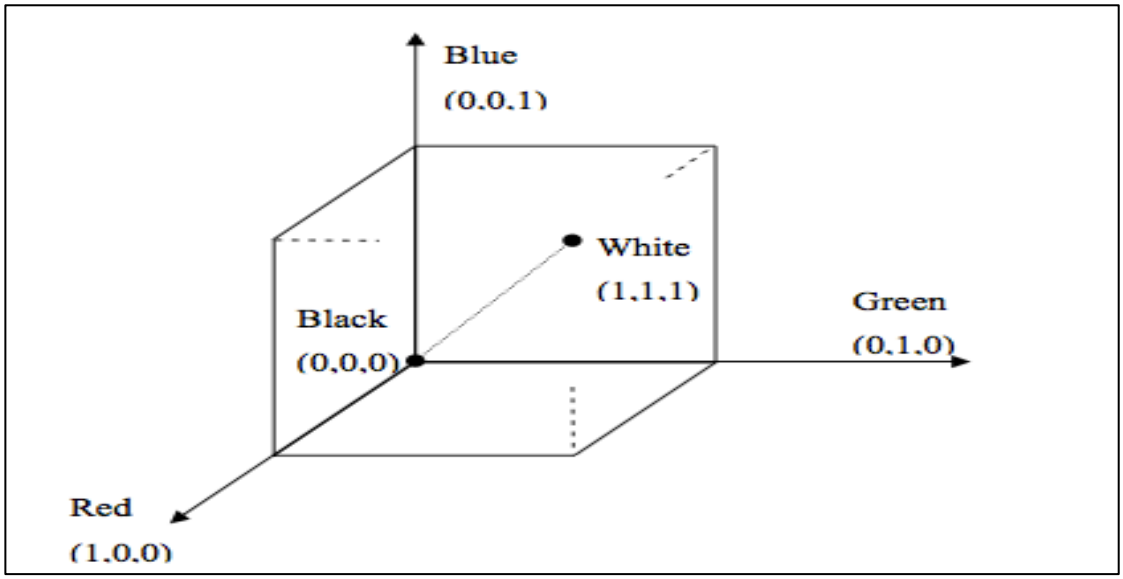

Figure 2.16: Colour space tristimulus cube RGB (Ross 2005)

Mathematically R, G and B colour parameters are defined by equation (2.10), (2.11) and (2.12) with X = R(λ), Y= G(λ) and Z= B(λ).

Where R(λ), G(λ) and B(λ) are the responsivties of the red, green and blue detectors respectively.

This simple representation has a distinct disadvantage in that the information pertaining to HSL by which a colour may be defined is not obvious (Ford, Roberts 1998) and distinguishing far fewer colours than can be perceived by the human eye (Chapman 2000).

2.5.3 Non-linear colour system (HLS)

The HLS colour space is the representation of a colour spectrum in terms of dominating wavelength (Hue), brightness (Lightness) and depth of colour (Saturation) (Billmeyer, Saltzman 1981). Figure 2.17 shows a HLS coordinate system.

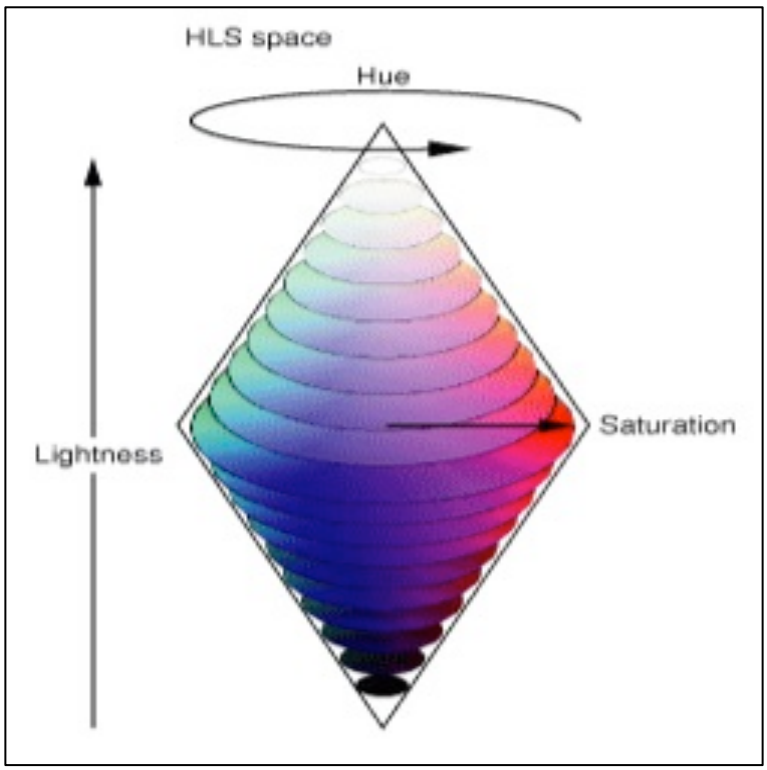

Figure 2.17:Double cylindrical coordinate HLS (Elzagzoug 2013)

The transformation from RGB colour space to an HLS space is non linear and can be described by the following algorithms (Jones G. R, Deakin A. G et al. 2008):

$$H = 240 - 120 \times \frac{g}{g+b} \qquad r = 0 \tag{2.19}$$

$$= 360 - 120 \times \frac{b}{b+r} \qquad g = 0$$

$$= 120 - 120 \times \frac{r}{r+g} \qquad b = 0$$

$$L = (R + G + B)/3 \tag{2.20}$$

$$S = [\max(R, G, B) - \min(R, G, B)]/[\max(R, G, B) + \min(R, G, B)] \tag{2.21}$$

Where

$$r = R - \min(R, G, B) \tag{2.22}$$

$$g = G - \min(R, G, B) \tag{2.23}$$

$$b = B - \min(R, G, B) \tag{2.24}$$

2.6 Chromatic Monitoring Principles & Modeling Maps

2.6.1 Basic Principles

Chromatic maps are used to display data extracted from a complex condition by transforming the extracted data from non-orthogonal processors such as RGB Gaussian processors (figure 2.18). This enables different information to be conveniently distinguished on 2–D polar diagrams, Cartesian XYZ diagram, etc (Jones G. R, Deakin A. G et al. 2008).

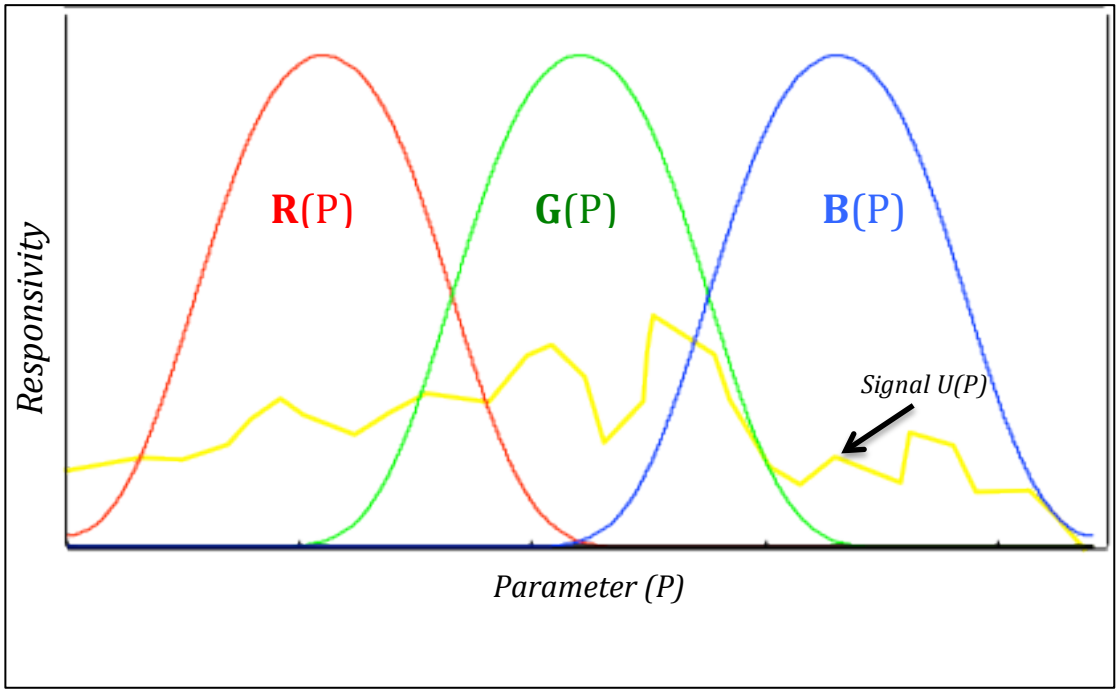

Figure 2.18: Gaussian Signals Processing Filters RGB

The characteristic shown in figure 2.18 is typical of R,G,B tristimulus chromatic system. This tristimulus system has important properties for extracting information from complex signals (Jones G. R, Deakin A. G et al. 2008). The outputs of R, G and B are defined mathematically by equations (2.10), (2.11) and (2.12) respectively (Jones G. R, Deakin A. G et al. 2008).

The outputs of R, G and B in response to an irregular spectrum “yellow” (figure 2.18) that contain significant levels of information. This maybe illustrated via the colored images shown in figure 2.19 of a scene obtained via different optical filters (Cyan, Green and Magenta). When the image is viewed separately, fragments of information are apparent. However, when the three images are superimposed, considerable information is apparent, which is greater than the discerned from the sequential viewing of the individual images. This illustrates the power of superposition in enhancing information without loss of breadth (Jones G. R, Deakin A. G et al. 2008).

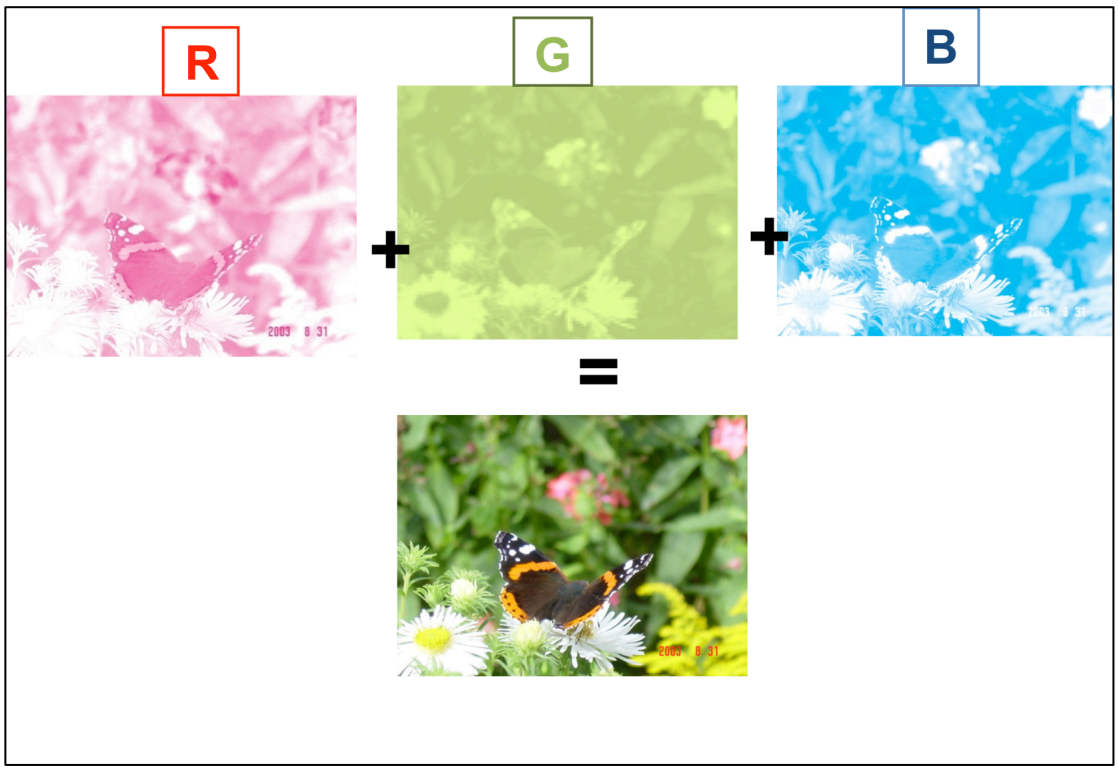

Figure 2.19: Illustration of information gain by overlapping three receptors R, G and B.

2.6.2 Effect Of Varying Processor Profiles

The information that appears following such a procedure of addressing with three overlapping processors RGB, depends upon the characteristics of the processor, e.g. their degree of non-orthognality, their profile form, width and relative amplitudes. These effects maybe perceived in visual images recorded via different optical filters with particular characteristics to modify the spectral response of the detector. Figure 2.20 illustrates an example of three chromatic images obtained with three different systems two from nature and one technically produced. The colours of an object observed by a human eye (figure 2.20(a)) are different from those observed by a honeybee (figure 2.20(b)) because of the latter's quest for pollen. An electronic system can be produced to give yet a different rendering depending upon the information sought (figure 2.20(c)).

The examples show how changing a processor response profile in one aspect affects the colour balance and so the information perceived (Jones G. R, Deakin A. G et al. 2008).

(a) **(b)** **(c)**

Figure 2.20: Effect of varying responses of chromatic parameters (Schmitt 2009).

2.6.3 Two–Dimensional Polar diagram

Hue, lightness and saturation are chromatic parameters obtained from the transformation of the signal captured with RGB filters. Hue (H), Lightness (L) and Saturation (S) may be represented on 2–D polar diagrams of hue-lightness (H–L) or hue-saturation (H–S) (Jones G. R, Deakin A. G et al. 2008). With Hue being the azimuthal coordinate and L or S as the radial coordinates.

The polar plot of figure 2.21 has H versus L with H ranging (0-120 = Red-Green, 120-240 = Green-Blue, 240-360 = Blue –Red) i.e. (0 = pure Red, 120 = pure Green, 240 = pure Blue). Lightness is the radial parameter from the origin (0,0) to the circumference (L=1.0). Alternatively H–S can be represented on a polar diagram.

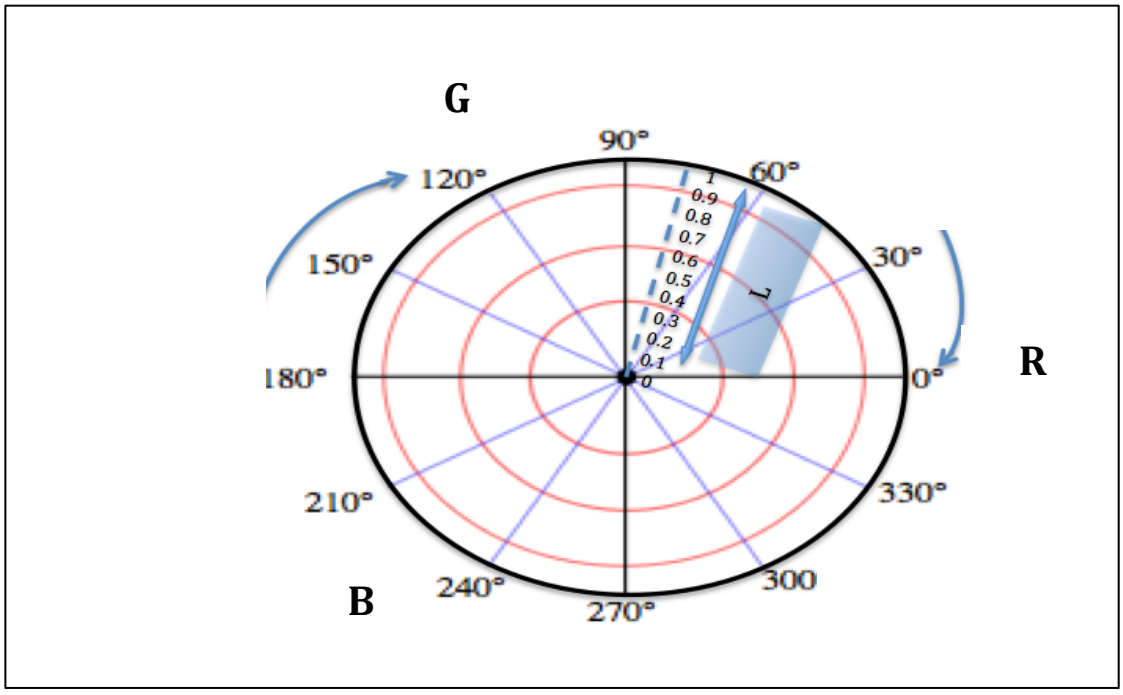

Figure 2.21: Polar diagram of H-L

2.6.4 Gaussian HLS Signal

The values of HLS may be regard as representing a complex signal as an equivalent Gaussian signal (figure 2.22). Where (H) is the dominant wavelength, (L) is the amplitude and (1-S) is the spread of the signal.

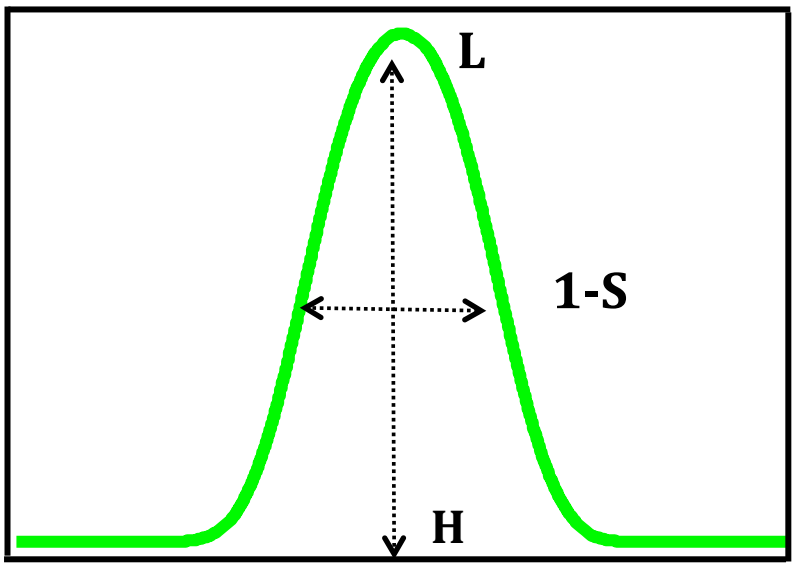

Figure 2.22: Gaussian HLS signal.

2.6.5 XYZ Cartesian Diagram

A Cartesian X, Y, Z diagrams can be used to illustrate details about the spectral distribution. Figure 2.23 shows such a typical XYZ diagram.

X, Y and Z respectively indicate the proportions of R, G and B components in the spectrum as defined by Equations (2.13), (2.14), (2.15) and (2.10), (2.11), (2.12), Section 2.5.1.

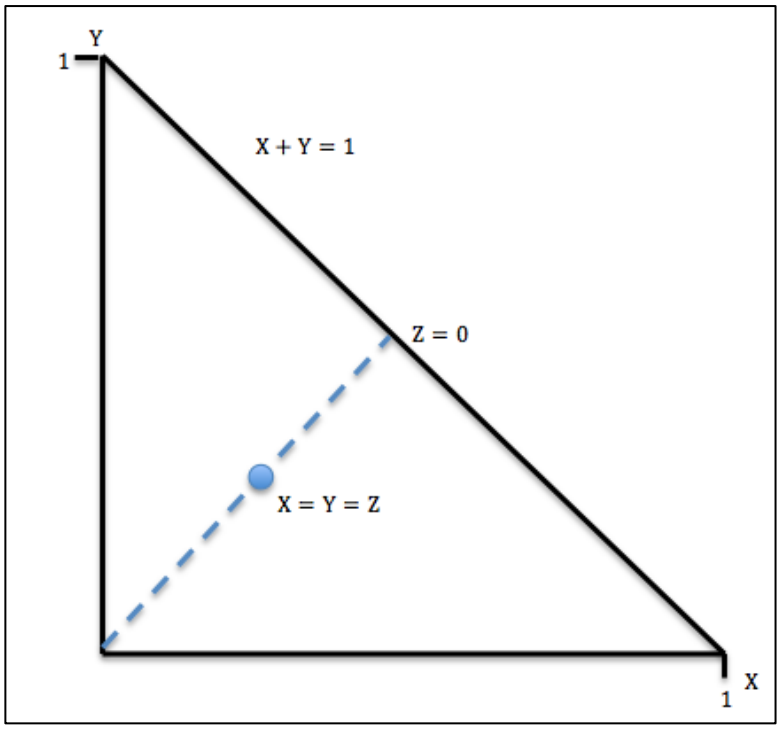

Figure 2.23: Cartesian XYZ diagram

The Cartesian diagram has the following properties:

1. XYZ are independent of effective light intensity (X + Y + Z) (Equations (2.20), Section 2.5.1)
2. X + Y + Z = 1.
3. Locus X+Y =1 corresponds to Z=0.
4. X=Y =0 corresponds to Z=1.
5. X = Y = Z = 0.33 represents the point at which R, G and B are equal.
6. X/Y = R/G is a distmulus dominant wavelength.

X + Y + Z = 1 means that if two terms are known the third term can be obtained. In this way, three dimensions can be represented on the 2-dimension of graph.

2.7 Summary

This chapter has summarized the properties of light, particularly those relevant to addressing liquids including transmission and absorption of light along with reflection, refraction, scattering, fluorescence and polarization.

The significance of polychromatic light and the concept of colour discrimination with the human vision system have been described. The manner in which quantification methods of colour science can be extrapolated for the more general case of chromaticity has been explained.

The fundamental concepts of chromatic techniques that enable information contained in polychromatic light to be extracted has been considered which are relevant to addressing complex liquids.

Chapter 3

Complex Liquids & Their Measurement Techniques

3.1 Introduction

Complex natural systems are unpredictable, non linear and tend to occur in a dynamic order. However, complex man made systems are characterized by their stability and order, but there are possibilities that they can fail and can cause chaos (Jones G. R, Deakin A. G et al. 2008).

Assessing the state of health of a complex system from a number of parameters and different conditions is difficult because complex systems do not operate individually, therefore intelligent monitoring systems to asses and assure the overall system behavior is required (Jones G. R, Deakin A. G et al. 2008).

Complex liquids are an example of a complex system, their complexity arises from dynamical combination of particles. The dynamics of their structure is dominated by the particles redistribution between different regions in their dynamic mixture.

This chapter describes briefly complex liquids and the dynamic combination of molecules from the physical/ chemical level and various examples of complex liquids is also given.

Honey as a particular form of a complex liquid is introduced together with its complex composition and the various ways that lead to honey adulteration (i.e. honey fraud). The link between the optical parameters being measured and the optical properties of honey is also evaluated.

The optical techniques for addressing honey complex liquid is reviewed in this chapter together with the recent development in chromatic techniques that address complex liquids in a convenient and cost effective manner.

3.2 Complex Liquids

In the state of matter (figure 3.1), the liquid state potential and kinetic energies are characterized by similar values, differently from the gas or solid phases (Gispert 2008). The intermolecular forces and molecular motions are strictly interconnected, producing the atypical features of liquid phases. Figure 3.2 shows the attractive force (hydrogen bond) between water molecules responsible for keeping matter in the liquid phase, hydrogen bonds are a much stronger type of intermolecular force (Hart, Craine et al. 1999).

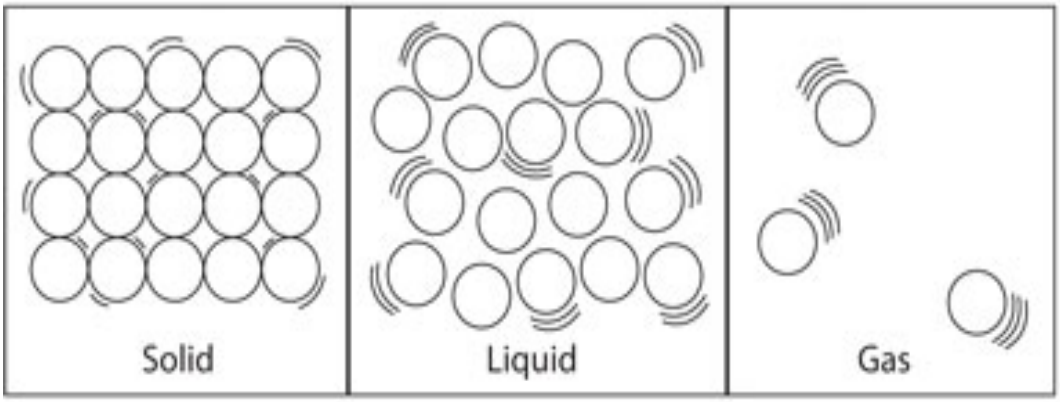

Figure 3.1: State of matter phases

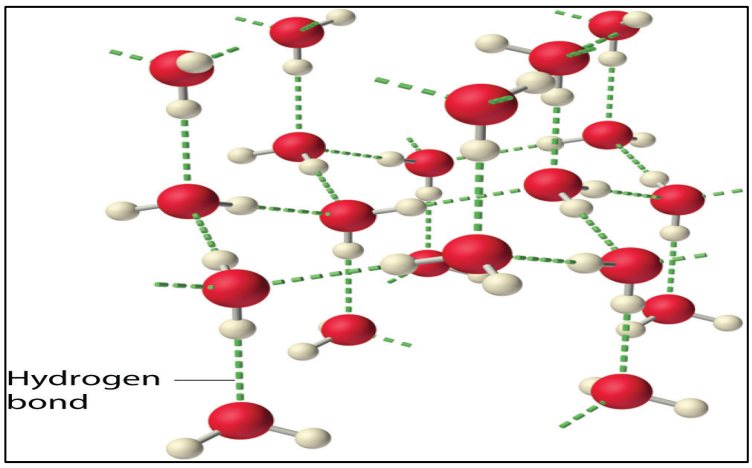

Figure 3.2: Hydrogen bond between adjacent water molecules (Hart, Craine et al. 1999)

The relative motions and correlations between molecules in liquids are a direct consequence of the intermolecular potential, which can be related to the fluctuation and dissipation processes that govern the physical behavior of the liquid as well as dictate the course of reactions (Torre 2007).

In complex liquids, there are number of contributions to the intermolecular potential that lead to stronger attractive forces and greater correlations than in free liquids. Molecules are free to diffuse relative to one another in the liquid state and it is possible to attain high densities of reactive species in solution phase. Both effects greatly increase collision frequencies above alternative media and accounts for the fact that most chemistry is explored using solution phase processing. The advantage of complex liquids is that the additional intermolecular forces such as hydrogen bonding and electrostatic terms can act to further lower barriers in reaction complexes and in the extreme case of biological systems, resulting in preferred orientation to the point of molecular self-assembly (Torre 2007).

The common defining feature of a complex liquid is the presense of *a mesoscopic length scale particles (*intermediate scale between molecular and macroscopic), their atoms and molecules are organized in a hierarchy of structures of mesoscopic scale (which in turn make up the bulk material), playing a key role in determining the properties of the system (Deshpande, Murali Krishnan et al. 2010).

The rheological behavior of complex liquids is almost nonlinear, because the large viscous torques exerted on the particles (Gelbart, Ben-Shaul 1996). Similarly, the electric, magnetic and optical responses are strong.

Understanding the liquid state has been a long-standing goal in physical chemistry as most chemical and biological processes occur in solution (Gispert 2008). Optical methods have been applied to the study of complex liquids to provide a window on the motion of molecules that distinguish the dynamics of the liquid state (Torre 2007).

3.2.1 Examples Of Complex Liquids

Water is a pure liquid but when adding tea to water it changes the molecular structure of the pure liquid and the relative bond between molecules, therefore affecting the optical transmission properties of light. A further complex mixture is formed by adding milk to the clear liquid (water and tea). Milk produces a turbid condition in a clear liquid and is often used for controlled exploratory tests involving turbidity (Prerana, Shenoy et al. 2008). Water, tea and milk mixtures represent the further complex condition of optically different clear liquids with a turbid medium.

Another form of complex bio liquid is urine. As a biological waste material, urine typically contains metabolic breakdown products from a wide range of foods, drinks, drugs, environmental contaminants, endogenous waste metabolites and bacterial by-products (Bouatra, Aziat et al. 2013). This chemical complexity had made urine a particularly difficult substrate to fully understand, therefore improved methods capable of quantifying complex changes in optical spectra is needed in the health industry for the characterization of human urine.

The study of complex liquids and the degree of dynamic correlations is an important introduction to understanding the more structured environment in biological systems. Complex biological liquids such as blood has been widely studied and portable instrumentations such as pulse oximetry have been introduced to measure the oxygen level in the blood which varied with the wavelengths of the absorbed and scattered light by the various forms of hemoglobin such as oxy-hemoglobin (HbO) and reduced hemoglobin (RHb) (Severinghaus, Kelleher 1992).

Dielectric liquids such as mineral oil that has the ability to cool transformers and provides a dielectric insulation between live parts of transformers is another example of a complex liquid. Their dielectric properties maybe subjected to corona, arcing, sparking etc. which will lead to the oil being contaminated by different types of gases, therefore changing the structural bonding of the

hydrocarbon molecules of the mineral oil (Naredo, Fuerte et al. 2001, Lorin 2005).

Mechanical stress and electrical failure could result in affecting the oil and insulation materials, which lead to the mineral oil being contaminated due to chemical interaction with the windings and insulation papers caused by high temperature operation. This affects the molecular structure of the pure oil (Naredo, Fuerte et al. 2001, Lorin 2005).

Industrial liquids such as petroleum fluids and vacuum pump oil exhibit this complex behavior which affects the light propagation through such liquids (Jones G. R, Deakin A. G et al. 2008). Understanding the behavior of such complex liquids is also very important in industrial and utility companies worldwide.

Many molecules also have the ability to rotate the plane of incident polarized light through some angle; such molecules are termed optically active (Hart, Craine et al. 1999). The phenomenon of optical activity arises from the physical structure of molecules, where two forms of its molecules exist the mirror image of the other; both forms have similar chemical properties but are not physically super-imposable on each other (Clayden, Greeves et al. 2012).

Complex liquids with sugar mixtures such as honey and syrup are optically active because of the complex asymmetric structure of the sugar molecules such as (sucrose, glucose fructose). Honey's property of rotating the plane of polarized light depends largely on the sugars composition, their types and relative proportions (White 1975).

Honey is a very complex liquid composed of major compounds including sugars such as glucose, fructose, water and minor components such as amino acids, enzymes, vitamins and minerals (Crane 1975, White 1975, Martin, Bogdanov 2002, Havenhand 2010). Its optical properties differ and vary in a regular manner with its composition contents which will affect its liquid dynamics. Monitoring such a complex liquid has been of great importance to the food industry (White 1975, Crane 1975, Martin, Bogdanov 2002, Pilizota V, Nedic Tiban N 2009).

3.2.2 Classification Aspects Of Complex Liquids

3.2.2.1 High Voltage Transformer Oil & Different Ageing Properties

High voltage transformers are important devices used for the supply of electricity (Lorin 2005). They enable electricity to be transmitted effectively from a substation to consumers. Modern growth in population makes increasing demands on power supplies and on the load on the transformers. Consequently improved maintenance and care of transformers is considered to be essential. Recent research (Lorin 2005, Naredo, Fuerte et al. 2001) has indicated that a key failure is due to the degradation of the electrical insulation of the transformer, including the mineral oil used to cool transformers (Elzagzoug 2013). Thus monitoring of oil degradation becomes an important issue, as it can be an early indication of transformer failures. This indication can help in solving the faults, with advantages of producing a longer reliable operation of the transformers and a robust supply of power.

3.2.2.1.1 Degradation Of mineral oil

Mechanical stress and electrical failure could result in affecting the oil and insulation materials, which lead to the mineral oil being contaminated due to chemical interaction with the windings and insulation papers caused by high temperature operation (Elzagzoug 2013). As a result the oil chemical chain (figure 3.3) will tend to break down, resulting in the oil being degraded over many years, and with the consequence of the oil losing its desirable properties. In addition, the oil may be subjected to corona, arcing, sparking etc. which will lead to the oil being contaminated by different types of gases (Elzagzoug 2013).

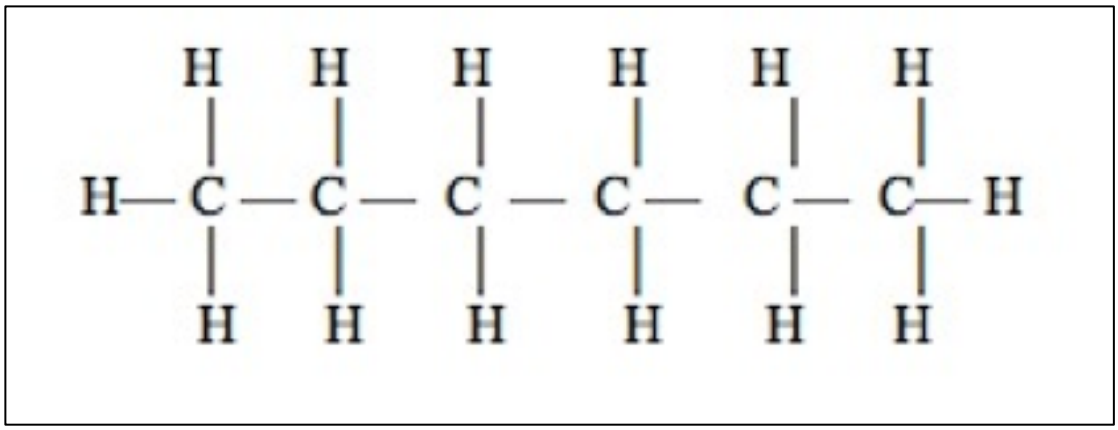

Figure 3.3: Mineral oil molecular structure (Elzagzoug 2013)

(a) Optical Degradation

There are several ways in which the degradation of transformer oils is monitored. They include a visual inspection of the colours of the oil and analysis of various gases dissolved in the oil. Visual inspection in values, comparing the perceived colour of the oil with a colour scale (figure 3.4) ASTM (D1500) (Golden, Craft et al. 1995). However human colour perception is not always a reliable guide to indicate the quality of the oil condition (Dervos, Paraskevas et al. 2005)

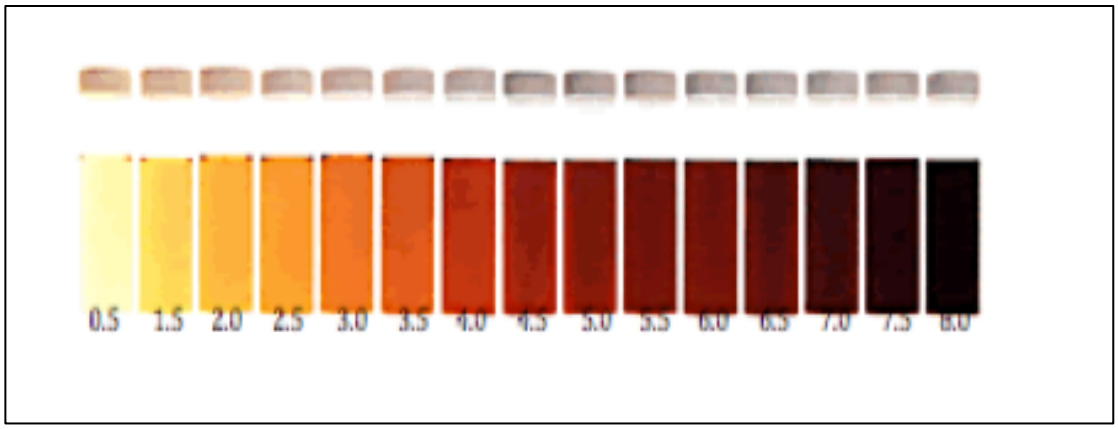

Figure 3.4: ASTM D1500 colour scale (Golden, Craft et al. 1995)

(b) Liquid Degradation

The approach of monitoring the gases dissolved in the oil as a degradation indication is based upon the fact that as various materials in the oil age, therefore producing changes in water and oxygen contents of the oil. These in turn lead to chemical reaction with metallic compounds in the transformer oil tank and acids, during which produces different gases such as (Methane, Ethane, Carbon-dioxide, etc.) are produced and dissolved in the oil (Naredo, Fuerte et al. 2001, Elzagzoug 2013).

3.2.2.2 Degradation Of Vacuum Pump Oil

The degradation of the liquid in vacuum pumps has been monitored via the spectral distribution of the transmitted light through the liquid using fiber optic sensors. Changes in the dominant wavelength of the spectra indicated the purity of the oil (Jones G. R, Deakin A. G et al. 2008).

3.2.2.3 Aircraft Fuels Discrimination

Aircraft use a number of fuel grades that are available in the aviation sector (AVGAS, AVCAT and AVTUR), these fuels contain similar hydrocarbon chains structures, which have different spectral characteristics. Also agitated mixtures of water and fuel that represent a two phase mixed fluid have differences in the optical signatures of light transmitted through mixtures having various proportions of water and fuel (Jones G. R, Deakin A. G et al. 2008).

3.2.2.4 Rotatory Active Liquids

Certain liquids have the property of rotating the phase of polarization of light propagating through the liquid. The rotation maybe clockwise (dextrorotatory) or anticlockwise (laevorotatory) (Hart, Craine et al. 1999).

Complex sugar molecules with more than four carbon atoms have ring structures, which have an asymmetric nature forming two isomers of D-glucose (α-D-glucose and β-D glucose) (figure 3.5) (Hart, Craine et al. 1999). These two ring structures are different and cannot be superimposed on one another, i.e. optically active in aqueous solutions. These structures may interconvert (mutarotation) via an intermediate open chain structure (Egan 2006).

The concentration of the rotary active material in a solution allows the concentration of the optically active material to be determined. Polarized light of different wavelengths will have their plane of polarization rotated by different amounts, the longer wavelengths being rotated more than the shorter ones (rotary dispersion) (Jones G. R, Deakin A. G et al. 2008).

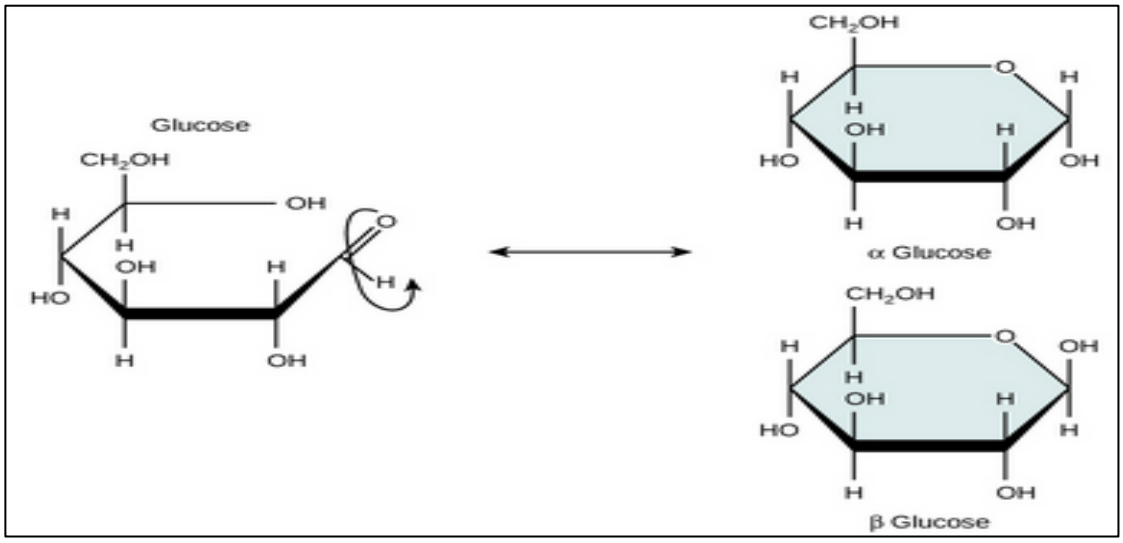

Figure 3.5: Ring form of glucose (Egan 2006)

3.2.2.5 Urine Contamination By Bacteria

Bactria in the urine such as Ecoli are the most common cause of Urinary tract infection (UTI) (Nordstrom, Liu et al. 2013). Currently used POCTs for diagnosing UTI include a chemical dipstick test of a urine sample for elevated nitrite levels and the presence of leucocytes. Visual inspection of the urine sample for possible cloudiness (turbidity) may also indicate, for example, high white cells count which could be associated with a bacterial infection (Deakin, Jones et al. 2014).

However, there are some problems with dipsticks in that they are not generally considered to be very accurate and reliable, with a wide range of performance reported (Othman, Yook et al. 2003)

Dipstick testing involves judgment in visually comparing the dipstick results (colour changes) to the manufacturer's template of predicted colour changes and estimating whether the sample is positive or negative for the indicators. It also requires an interpretation of the combination of indicator results(Deakin, Jones et al. 2014).

Visual turbidity estimates are qualitative, and although urine interpreted as clear (no turbidity) could be classed as non-infected, therefore, turbid urines could be positive or negative for a UTI (Health Protection Agency 2002)

3.2.2.6 Urine Contamination By Infection diseases

Genital chlamydial infection is also currently the most common sexually transmitted infection (STI) in the United Kingdom (Health Protection Agency 2002). Molecular diagnostic methods can complement existing tools to improve the diagnosis of Chlamydia. However, they require good laboratory infrastructure thereby restricting their use to reference laboratories and research studies.

Recently developed Loop-mediated isothermal amplification (LAMP) is a novel method that rapidly amplifies target DNA with high specificity under isothermal conditions. It has been applied as a diagnostic tool for several infectious diseases, including viral, bacterial, and parasitic diseases (Iseki, Takahashi et al. 2010)

In LAMP, a large amount of DNA is synthesized, yielding a large pyrophosphate ion by-product that forms as a precipitate of magnesium pyrophosphate; pyrophosphate ion combines with divalent metallic ion to form an insoluble salt (Tomita, Mori et al. 2008).

The process of LAMP reaction can be monitored by observing the white turbidity of magnesium pyrophosphate produced as a result of combination with magnesium ion in the reaction solution. However, the signal can be weak for visual detection. Clear signal detection can be achieved by monitoring the change in the metallic ion concentration during the reaction. There are several methods that determine the concentration of metallic ion in a solution, amongst these methods is the colorimetric methods using metal indicators where the concentration is measured by colorimetric change of the sample solution. Metal indicator such as (Calcein) yields strong fluorescence by forming complexes with divalent metallic ions such as calcium and magnesium, which can be optically detected (Tomita, Mori et al. 2008). This protocol as the results of the LAMP reaction enables discrimination of results without costly specialized equipment, which makes it feasible for point-of-care testing (Tomita, Mori et al. 2008, Abdul-Ghani, Al-Mekhlafi et al. 2012).

3.3 Honey

Honey is defined as “a sweet, sticky yellowish-brown fluid made by bees from nectar collected from flowers” (Stevenson 2010). The Honey (England) Regulations 2003 (Food England 2003) gives more precise definition: “honey” means the natural sweet substance produced by Apis mellifera bees from the nectar of plants or from secretions of living parts of plants or excretion of plant-sucking insects on the living parts of plants which the bees collect, transform by combining with specific substances of their own, deposit, dehydrate, store and leave in honeycombs to ripen and mature (Davis 2007).

3.3.1 Background Of Honey

3.3.1.1 Brief History

Havenhand (2010, p.40) stated, “The oldest evidence of a man collecting honey is to be found in prehistoric paintings found in caves near Valencia, Spain. Painted in red, it is though to be some fifteen thousand years old, originating in the Stone Age when in order to find shelter from predators, mankind might have lived in caves. The use and enjoyment of honey predates civilization, but once human society began to develop, the bee was adopted as a sign of mankind’s ingenuity. As long ago as 3000BCE, the bee was adopted as the hieroglyph of the rulers of Lower Egypt and carved on tombs of innumerable pharaohs as a never- ending symbol of power, industry and production”.

Honey comes wrapped in beeswax, which preserves it for seemingly endless years. The Roman, Egyptians, Babylonians and Arabs used honey for embalming their loved ones and leaders, the Egyptians in particular used honey as a currency while Romans paid their taxes in honey (Havenhand 2010). Before the discovery of sugar, honey was the only sweetener available because it provided a source of energy-rich food for people (White, Jonathan 1978).

Two thousand years ago, Greek athletes would indulge themselves with substantial amounts of honey throughout their training for the great Olympiad (Havenhand 2010). Honey was endowed with many mystical qualities and along with the bees that produced it, was present in the symbolism associated with most religions, ancient and modern. Even today it retains this air of wonder and mystery and many people swear by its ability to promote health and longevity (Davis 2007).

3.3.1.2 Relationship Between Flower Nectar, Honeybee and Honey

Honeybees are invaluable pollinators and such a huge importance to mankind as they have the ability to provide mobile pollination services to aid crop production. However most beekeepers keep bees in the fervent hope that they will produce large crops of honey. Understanding this substance (what it contains and what its properties) is important in order to obtain the best possible application of its potential.

Flower Nectar

Once the honeybee is ready to fly into the big wide world beyond its hive, it proceeds to collect two main commodities in order to produce honey. These are nectar and pollen. The Bee's basic energy food is nectar and it is therefore the raw material upon which the beekeepers base their activities. Plants produce nectar as a method of controlling the concentration of their plant sap (Davis 2007). Plant sap is the fluid that flows through the plant, carrying substances that the plant needs. Nectar is a means of removing excess water from the plant. It is water (30-90 %) containing a number of dissolved substances such as sugars, vitamins, minerals, organic acids, aromatic compounds, and minerals (Davis 2007). Nectar is found in flours but it may also be found elsewhere on the plant (Davis 2007).

There are factors that can influence the nectar secretion in flowers such as environment and plant condition. Temperature, humidity, soil moisture, nature of soil and topography can all influence the quality and the rate of nectar production in flowers which attracts pollinators (Davis 2007, White, Jonathan 1978). This explains the different variety and the quality range of honey produced by honeybees around the world. The honey produced by honeybees from such flowers nectar is called blossom honey (Bentabol Manzanares, García et al. 2011).

Nectar To Honey

(a) Physical Change

The worker honeybee collects nectar and carries it back to the hive in its honey stomach to be transferred to a storage area. The bees in the storage area reduce the water content of the nectar by taking a drop onto her proboscis and rolling it up and down so that the drop is exposed to the high temperature in the hive (35.5 degrees Celsius). As a result, the water content evaporates from the nectar. The humidity in the hive is also maintained and water drawn out from the hive by fanning bees. Once the water content is reduced to around 18%, the worker bees seal the cell with wax capping so that air and water are excluded (Davis 2007).

(b) Chemical Change

Nectars contain sugars, mainly sucrose, fructose and glucose. Honeybees convert most of the sucrose in nectar into two constituent parts and produce two enzymes, which act on sugars (Davis 2007):

Invertase: which acts as a dilute acid, in converting a molecule of sucrose into a molecule of glucose plus a molecule of fructose. The invertase comes from the bee hypopharyngeal glands. The bee adds the invertase to the nectar when it collects it and the processing continues so that most of the sucrose is converted into glucose and fructose by the time the honey is ripe.

Glucose oxidase: produced in the hypopharyngeal glands and is added to the nectar. This acts on some of the glucose, breaking it down into hydrogen peroxide and gluconic acid. The hydrogen peroxide is particularly important as it destroys bacteria.

Pollen Grains In Honey

Pollens are small structures produced by the anther (section of the flower) containing the mail gamete (used in plant fertilization). Pollens are important for pollination (movement of pollen to another plant which may be some distance away). Intelligent insects such as honeybees usually pollinate flowers to aid crop production. A worker honeybee is equipped with a whole set of tools to enable it to collect and transport pollen for cross-pollination and for returning to the hive to be mixed up with honey (Davis 2007).

3.3.1.3 Honey In Medicine

In the long human tradition, honey has been used not only as a nutrient but also as a medicine. However, in the last few years, there has been a renewed interest in research that investigates the potential health benefits of natural and unprocessed honey in the management of various diseases including diabetes mellitus(Erejuwa, Sulaiman et al. 2012). This has resulted in findings that attribute several medicinal effects to honey. The main nutrition and health relevant components are the carbohydrates, which make it an excellent energy source especially for children and sportsmen(Bogdanov, Jurendic et al. 2008).

Besides its main components (the carbohydrates of fructose and glucose), honey contains a whole array of vitamins, minerals, amino acids plus the all important nutrients know as bioflavonoids, which keeps the immune system functioning robustly when faced with bacteria, viruses and parasites (Havenhand 2010).

Also there are a great number of other constituents in small and trace amounts, producing numerous nutritional and biological effects: antimicrobial, antioxidant, antiviral, anti-parasitic, anti-inflammatory, anti-mutagenic, anticancer and immunosuppressive activities. Different nutritional studies have confirmed various effects after honey ingestion, e.g. enhanced gastroenterological and cardiovascular health. Besides, honey showed physiological effects on blood health indicators as well as effects on hepatitis A and radiation mucositis patients. Honey compositions, and also its different biological effects, depend to a great extent on the botanical origin of the honey (Bogdanov, Jurendic et al. 2008, Cortes, Vigil et al. 2011).

3.3.1.4 Honey In The Quran

Honey and bees has been mentioned in the Holy Quran, where a whole chapter was named in the name of [The Bee] in order to draw attention to this small insect and its benefits and that honey is the most important and useful product made by this insect that can heal people. Figure 3.6 shows the verses 68 and 69 from chapter 16 in The Qur'an.

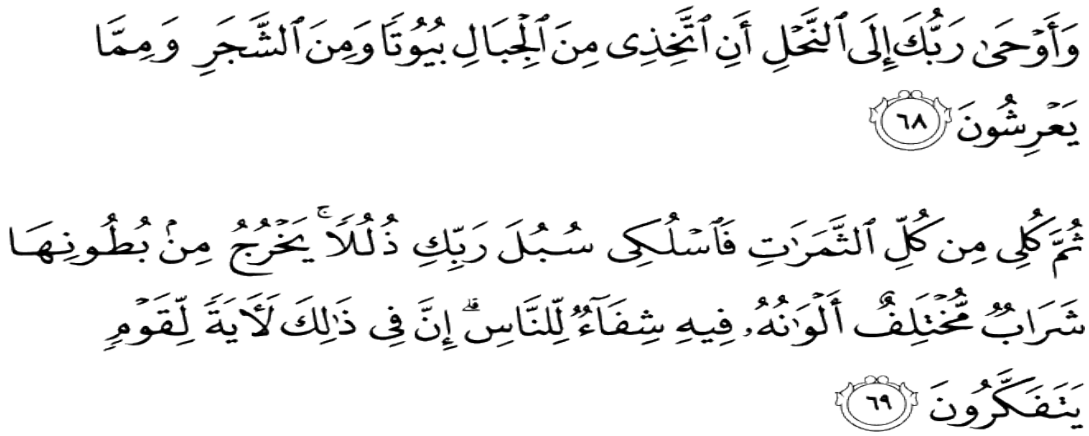

Figure 3.6: Verses 68 and 69 from Chapter 16 [The Bee], The Qur'an

The English translation of the verses in figure 3.6 is:

"And your Lord inspired to the bee, Take for yourself among the mountains, houses, and among the trees and in that which they construct" (The Qur'an 16:68).

"Then eat from all the fruits and show the ways of your Lord laid down for you. There emerges from their bellies a drink, varying in colours, in which there is a healing for mankind. Indeed in that this is a sign for a people who give thought" (The Qur'an 16:69).

From Tafsir Ibn Kaathir (a popular classic commentary of The Qur'an) the meaning of inspiration here is guidance (Al-Mubarakpuri 2003). The bee is guided to make its home in the mountains, in trees and in structures erected by man. The bee's home is a solid structure, with a hexagonal shapes and interlocking forms where there are no looseness in its combs (Davis 2007).

Bees are then ordered to go ahead to eat from all fruits wherever it wants in the vast spaces of the wilderness, valleys and high mountains in order to come back to the hive with the nectar (Al-Mubarakpuri 2003). The soil nutrition and weather conditions will all have an effect on the nectar composition, which varies as well depending on geographical location of the flowers and trees.

"There emerges from their bellies a drink, varying in colours" meaning honey that varies in colours depending on the different things that the bees eat (Al-Mubarakpuri 2003). The colour of honey is affected by the characteristics and the complex composition of the honey liquid.

"In which there is a healing for mankind" meaning that there is a cure in honey for diseases that people suffers from (Al-Mubarakpuri 2003).

3.3.2 Classification Aspects Of Honey

3.3.2.1 Composition Of Honey

Honeys vary considerably in their composition (Davis 2007, White 1975). Figure 3.7 gives an average breakdown of honey constituents. The composition of honey is influenced by a number of factors such as geographical origin, botanical sources of nectar, environmental and climatic conditions as well as processing techniques (White 1975, Crane 1975, Anklam 1998, Martin, Bogdanov 2002, Havenhand 2010).

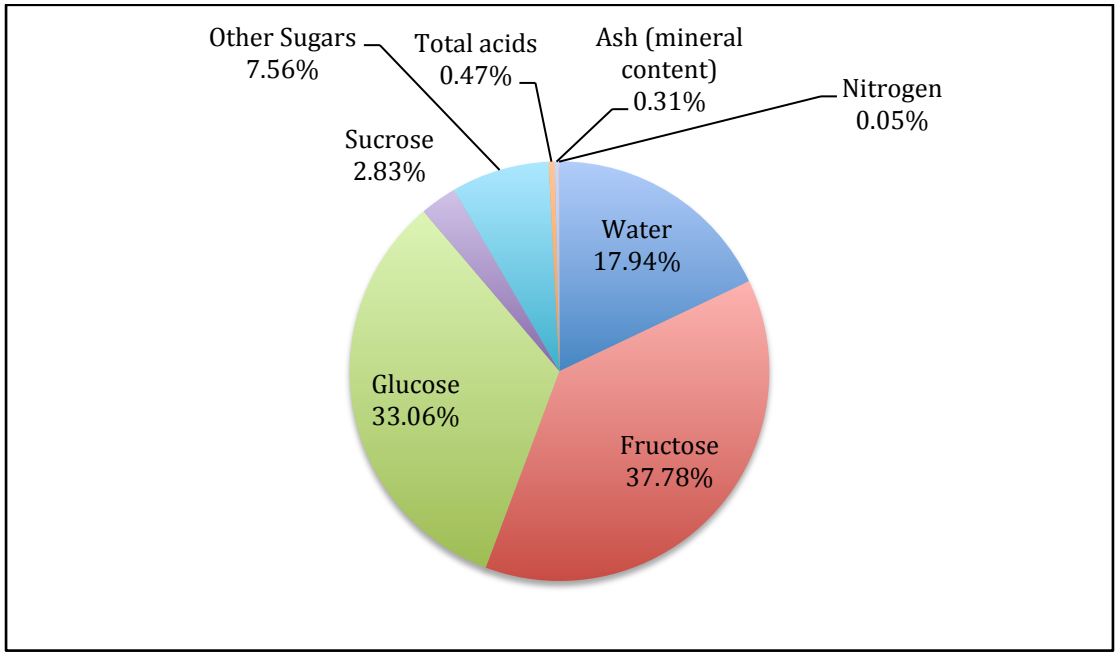

Figure 3.7: Average break down of honey constituents, amount as % of whole (Davis 2007)

3.3.2.2 Botanical Source Of Honey

Raw honey is a natural substance produced by bees. Figure 3.8 shows two different sources of honey, Blossom (floral) and Honeydew honey. Blossom are honeys produced from the nectar of flowers, while honeydew are produced by honeybees collecting nectar that is exuded from another insect such as an aphid or scale insect (Astwood, Lee et al. 1998, Bentabol Manzanares, García et al. 2011). Blossom honey may be divided into two other categories namely Mono-floral (made primarily from the nectar of one type of flower) and Multi-floral (made from many types of flowers) (Crane 1975, Anklam 1998, Martin, Bogdanov 2002, Havenhand 2010, National Honey Board 2013).

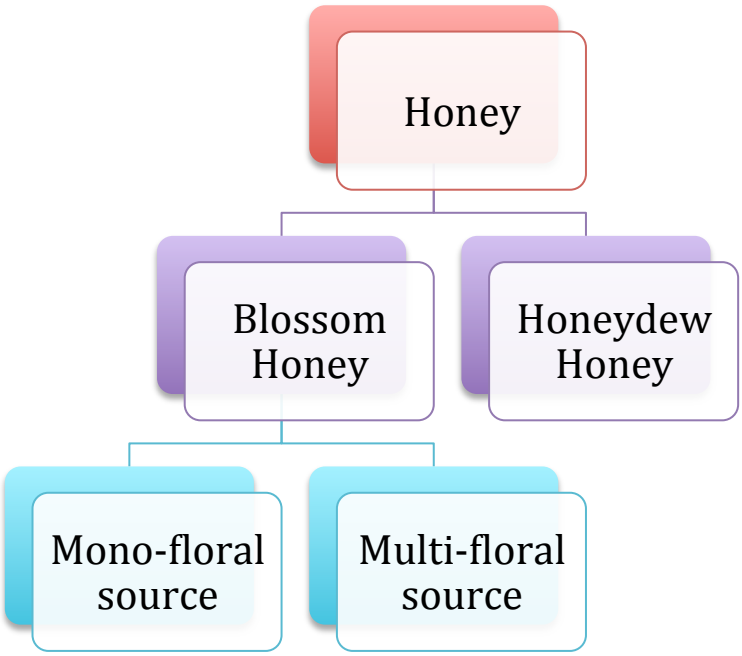

Figure 3.8: Honey types chart

Mono-floral honey typically has a high value in the marketplace due to its distinctive flavor. However, most commercially available honey is blended to include two or more honeys, differing in floral source, color, flavor, density, and geographic origin (National Honey Board 2013)

The classification of the botanical source basically depends on whether there is a dominating pollen grain from only one particular plant (Mono-floral) or no dominant pollen type in the sample (Multi-floral) (Davis 2007).

The pollens in honey samples usually enable an identification to be made of the botanical source, geographical region and whether the honey is raw. This is achieved by using methods such as Pollen Analysis and a number of chemical methods (Anklam 1998, Davis 2007, Martin, Bogdanov 2002). Raw honey has been shown to act as an antibiotic for hay fever and asthma because of the pollens within the honey (Havenhand 2010).

3.3.2.3 Regulatory standards of Honey

International honey standards are specified in the Codex Alimentarius (Codex Alimentarius Commission 1981) and in a European Honey Directive (Council Directive 2001/110/EC) Standards for Honey, both of which presently under revision.

The standards mentioned above include methods for the determination of the following quality factors: moisture, ash, acidity, hydroxymethyfurfural (HMF), apparent reducing sugars, apparent sucrose, diastase activity and water-insoluble matter. However during the last 30 years there are very few published works on reducing sugar and ash content of honey. Instead specific sugars such as (glucose/fructose/sucrose), moisture and electrical conductivity are mostly used.

Based on this data, international honey standards for the sum of fructose/glucose/sucrose content, moisture content and electrical conductivity are proposed. Besides, the use of other quality factors, like invertase acidity, hmf, proline and specific rotation are additionally used in many countries (Bogdanov, Lüllmann et al. 1999).

The proposed honey standards in the EU is similar to the Codex standard, but it contains fewer specific details dealing with contamination, hygiene and sugar adulteration, all of these being important quality factors nowadays. However, despite varying consumer preferences and price for different honey varieties (color and flavor), there are no criteria specified to distinguish between them as different grades (Bogdanov, Lüllmann et al. 1999).

The US provides specific standards (United States Department of Agriculture 1985) for the grading and classification of honey according to characteristics similar to CODEX and the EU. However they provides a mechanism to grade honey according to quality, clarity, and flavor. Nevertheless, classification according to these standards is voluntary for the importer or reseller of honey in the US as long as the product's import conforms to the regulations governing inspection and certification (USAID 2012). Similar grading mechanism is applied for the honey in Yemen.

Consumption of honey and honey products has grown considerably during the last few decades. However, at the present time, the traceability of this food is limited to the quality of each processor's documentation. In case of doubt or fraud, there is no standardized analysis available that can discriminate or determine the botanical (floral or vegetable) and geographical (regional or territorial) origin of the honey. Counterfeiting and product adulteration are now commonly practiced in the global food marketplace (Pilizota V, Nedic Tiban N 2009).

3.3.2.4 Adulteration of Honey

Honey is a natural food with a specific flavor, odor and nutritive value. Its composition and quality vary depending on the production method, climatic conditions of the region, conditions of handling and storage and the nectar, which is the source of the honey (Guler, Bek et al. 2008, Anklam 1998). No food component or food additive can be added into honey (Codex Alimentarius Commission 1981).

Adulteration of honey by means of feeding bees with different sugar syrups during honey production or adding different sugar syrups of certain ratios after production and incorrect statements about the honey's geographic and botanical origin causes serious problems for pure honey producers and consumers (Tosun 2013).

Various methods have been used to make fraudulent honey and many methods continue to evolve. For example, the original honey is blended with other less expensive components including inverted sugar (Martin, Bogdanov 2002). Alternatively, bees are intentionally fed sweeteners to increase their production in order to seek a quick profit (Martin, Bogdanov 2002, Pilizota V, Nedic Tiban N 2009).

These honeys are deceptively marketed on the basis that they are pure and natural. Adulteration of honey affects pure honey producers from the point of view of the economy and market while it also has negative effects on consumers' nutrition and health (National Honey Board 2013, Pilizota V, Nedic Tiban N 2009).

Invert sugar syrup

Invert sugar syrup is a mixture of glucose and fructose, it is obtained by splitting sucrose into these two components by hydrolysis reaction. The hydrolysis reaction can be induced by heating an aqueous solution of sucrose or a catalyst such as "invertase" can be added to accelerate the conversion.

The plane of polarized light is rotated to the right (+ve optical rotation) as it paase through a sample of pure sucrose solution (specific rotation ≈ +66°). As the solution is converted to a mixture glucose (specific rotation ≈ +52°) and fructose (specific rotation ≈ -92°), the resultant optical rotation converts to (-39°), i.e. direction of the total optical rotation is inverted to the left (-ve optical rotation).

Cane sugar and beet sugar are both relatively pure sucrose. While corn sugar is composed of approximately 24 % water and the rest sugars of sucrose, glucose and fructose. Corn syrup is a predominant sweetener used in processing foods and beverages. Honey typically has a fructose/glucose ration similar to corn syrup as well as containing some sucrose and other sugars. Because of the similar sugar profiles and low prices, corn syrup has been illegally used to fraud honey. As result, checks for adulteration of honey no longer test the levels of sucrose, but instead for levels of fructose/glucose.

3.3.2.5 Processing of Honey

Most honey found in the retail honey industry has been subjected to some form of processing during production. Today, most if not all-commercial honey is produced by centrifugation (Martin, Bogdanov 2002). Filtering of honey is also an important issue. In the regulations of many European beekeeping associations, use of honey filters is prescribed. Beekeepers should harvest honey by using filters with a mesh size not smaller than 0.2 mm in order to prevent pollen removal (National Honey Board 2013). On the other hand, some packers, according to the international honey legislation, should label such honey as “filtered”. However, the use of excessive heat for pasteurization and liquefaction might have adverse effects on honey quality, e.g. loss of volatile compounds and reduction of enzyme activity (Martin, Bogdanov 2002).

3.3.2.6 Honey Adulteration In Yemen

Honey has been a valuable commodity for centuries, but few places have a stronger tradition of honey making than Yemen, where beehives dot the country's landscape. The diversity of the fertile environment of Yemen as well as the variety of climate and pastures gives Yemeni honey the unique and highly prized flavours. The name of the honey has been associated with the different botanical types since immemorial time and with its nutrition and therapeutic benefits. People resort to this kind of honey as a medicine because it is free from any artificial additives.

However this international fame acquired by the Yemeni honey for its high quality and demand locally and globally, created a parallel market for fraudulent imitations, which deceives purchasers of the genuine product (Al-Muraqab 2012). These fraudulent practices have led to an increasing occurrence of adulterated honey. If ways of monitoring the honey are not urgently implemented, the reputation of the famous Yemeni industry will be destroyed (Hassan 2012, Al-Muraqab 2012).

Unfortunately, traditional methods currently used in Yemen to examine the honey to ensure quality through taste or smell is no longer feasible with the development of the new means and ways to produce fraudulent honey (Martin, Bogdanov 2002, Al-Muraqab 2012). Although other methods are available to test the quality of the honey (e.g. using different chemical procedures (Bogdanov 2002, Martin, Bogdanov 2002)), these can be expensive and time consuming because of the complexity of the composition of such liquid.

Recent work recently published by (Roshan, Gad et al. 2013) using optical UV spectroscopy techniques to detect genuine Sidr (Zizipu-spinachristi) honey samples from adulterated honey mixtures in Yemen. However, such method is expensive for a quick decision to be made on the condition of the honey sample and further studies still under investigation including incorporating more samples.

3.4 Optical Properties Of complex Fluids affecting Properties Of Light (Transmission, Reflection, Fluorescence, Polarization)

From the physical viewpoint, honey is an aqueous dispersion of material covering a wide range of particle size from inorganic ions and saccharides and other organic materials in true solution, colloidally dispersed macromolecules of protein and polysaccharide to spores of yeasts and moulds and the largest particles pollen grains (White 1975).

The largest portion of honey composition represents carbohydrates and water, where fructose and glucose are the most abundant sugars found. The minor components are more diverse such as flavonoids, (which consider the main group of antioxidant in honey), carotenoids, vitamins, minerals and traces of pollens. The properties of honey depend on the floral or honeydew sources collected by the bees as well as the humidity and climate conditions (Davis 2007, Havenhand 2010, White 1975).

3.4.1 Moisture Content

Moisture affects the physical properties of honey (viscosity, refractive index, density), they differ somewhat from those of an invert-sugar solution of the same water content. These properties vary in a regular manner with the moisture content of honey, but some uncertainty as to actual values is caused by a lack of accuracy in methods for determining water content and by the possible effects of differences in ratios of the various sugars and in amounts of the more important minor components. Even so, each of these properties has been used as a means of measuring the moisture content of honey a value of great importance to the honey producer, packer, and merchant, since it bears a direct relation to the likelihood of undesired processing and fermentation (White 1975). Freshly collected honey is a viscous liquid and has a greater density than water; these molecules have been used as indicator to determine the quality of commercial honey samples (Sanz, Sanz et al. 2005).

3.4.2 Sugar Content

Sugars are by far the most important constituents in honey. The gross physical attributes of honey are largely determined by the kinds and concentrations of the carbohydrates. That these properties are expressed in ranges rather than by constants reflects the variability in honey composition.

The sugars are responsible for much of the physical nature of honey, its viscosity, granulation properties, energy values, etc. (Davis 2007). The two sugars fructose (laevulose) and glucose (dextrose) account 75 % of honey carbohydrates (White 1975, Fujita 2013, Davis 2007).

3.4.3 Acid Content

The levels of acidity of honey contribute to its stability towards microorganisms and can be examined in tow ways, the kind of acids present and their relative or total amounts can be considered, or the affect of acid and other minerals which affect acidity, such as minerals can be expressed in terms of the concentration in the honey of hydrogen ions, which all acids have in common (White 1975). .

A measure of the total concentration of hydrogen ions provides information on the strength of acidity and allows comparisons between materials. They are normally expressed in logarithmic PH scale and honey fall in the range 3.2 to about 4.5 averaging 3.9. This value is affected somewhat by the amounts of the various acids present, and other ash constituents. Honey rich in ash generally show high PH values (White 1975).

3.4.4 Mineral Content

The scientific literature on honey ash falls into three categories (amounts of total ash, amounts of principle constituents, the identities of minor metallic constituents). Mineral elements in honey are mainly Potassium, Sodium, Calcium, Magnesium, Phosphorous and Sulphur (White 1975).

3.4.5 Enzymes

Honey also contains proteins that include a number of enzymes and amino acids Enzymes in the honey such as (invertase and diastase) are sensitive to heat and storage temperatures, which allows the detection of overheating in honey.

3.4.6 Hydroxymethylfurfural (HMF) Content

HMF is an organic compound containing aldehyde and alcohol function group. It's a naturally occurring compound found in sugar containing food such as honey. HMF is an intermediate product of the acid-catalyzed dehydration reaction that occurs in hexoses such as fructose. Its also produced as intermediate product of the Maillard and creamelisation reaction (Lynn, Englis et al. 1936).

HMF is it self subject to degradation. Consequently the amount of HMF detected on analysis is the result of equilibrium between its formation and degradation. Length of storage time and heat can shift this equilibrium, increasing the quantity of HMF present thus its subject to debate. The quantity of HMF presents in honey currently used as indicator of shelf life and the amount of heat applied to honey.

Molecules of HMF have been reported by (Sanz, Del Castillo et al. 2003) to be present in honey at different levels, fresh honey samples obtained from reliable beekeepers were found to have lower HMF where as commercial honeys samples obtained had higher levels of HMF. The same research also reported that low level of HMF found in fresh samples indicate that the samples un-heated or submitted to low heat treatment.

The most common analytical method of HMF is based on optical UV/Visible fluorescence spectrophotometry, which doesn't need a chemical procedure and sample extraction (Karoui, Dufour et al. 2007).

3.5 Conventional Optical Measuring Techniques

Complex liquids have certain physical properties that govern how they behave. Honey for example has different optical characteristics that can enable to be classified according to its botanical source, geographical origins and quality attributes. This section will outline the optical measurement techniques used for complex liquids and in particular honey in the food and research industry.

3.5.1 Refractive index

Refractometers are instruments used to measure substances dissolved in water and certain oils. They use the property of refractive index to determine the amount of dissolved solids in liquids by passing light through a sample and showing the refracted angle on a scale.

The refractive index of a solution is determined using transmitted light refractometry (Stockley, Oxlade et al. 2007). A light beam propagates through the solution and is refracted at the interface of a prism. The angle of refraction is measured by a detector and calculated from the angle of refraction using Snell's law of refraction (Ryer 1997).

The scale most commonly used is referred to as the Brix scale, which represents the total concentration of soluble solids in the sample. The Brix scale is based on sucrose (sugar) and water solution (Ball 2006, Knecht 1990). For liquids, which contain substances other than, sugar, (minerals, salts, proteins, etc) such as oils and other industrial fluids, a conversion chart from the Brix percentage to the sample total concentration may be necessary (Ball 2006). The moisture content of honey must not exceed 21-23% and the refractive index of honey varies in the range of 1.3 – 1.7 nD (70-88 in Brix scale) according to official methods for water determination.

Fig 3.9 shows a schematic diagram of a typical refractometer. The light emitted by the LED is collimated before it propagated through the fluid to be measured. At the surface of a measuring prism, the light beam is refracted and split in two. On the CCD (Charged Coupled Device) sensor behind the prism, two separate signals are detected. The distance between them is correlated with the refraction index through Snell's law together with the measured media temperature (Flexim GmbH).

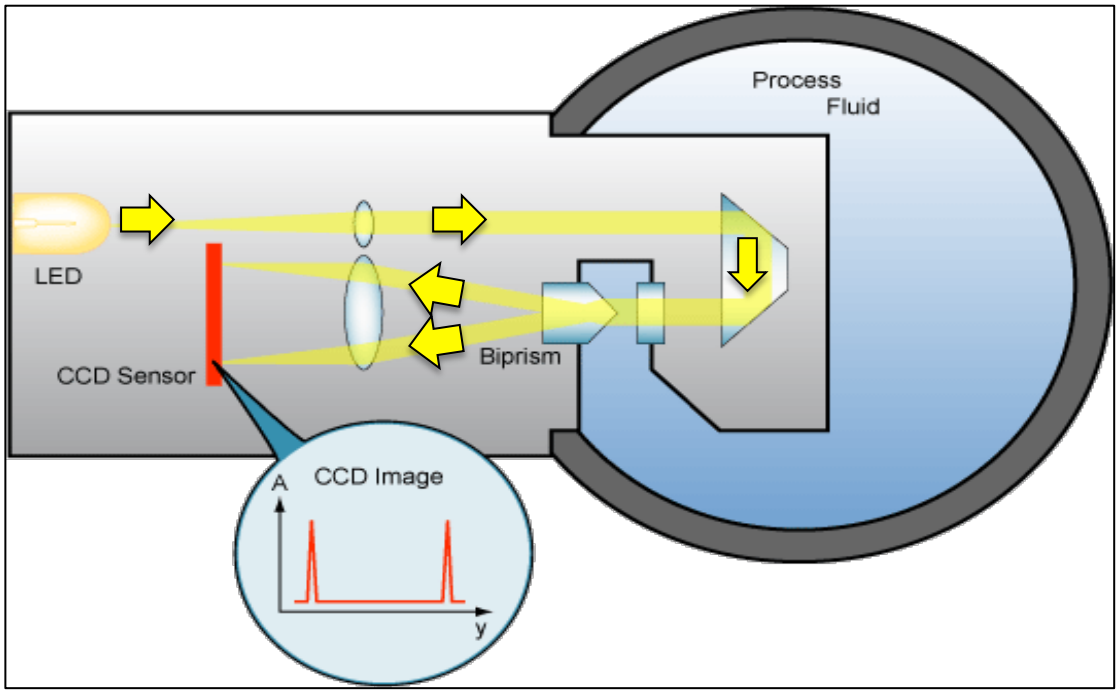

Figure 3.9: Schematic diagram of a honey refractometer (Flexim GmbH)

The refractometer is a readily available instrument and comparatively inexpensive. Since the refractive index varies with temperature, the instrument is often calibrated for use at a specific temperature (Ball 2006, Knecht 1990).

Beekeepers and honey packers use refractometers to measure the moisture content of honey (Davis 2007). Figure 3.10 shows a typical image of a honey refractometer used in the honey industry (ATAGO CO). Many authors (Bentabol Manzanares, García et al. 2011, Serrano, Villarejo et al. 2004, Popek 2002, Guo, Zhu et al. 2010) have suggested the use of refractive index as measurement criterion of the water content of honey. However, the Refractive index approach may result in a loss of water and makes a comparison with liquid honey measurement at room temperature difficult for creamy (crystallized honey samples because they must be heat-treated before analysis (Isengard, Schulthei et al. 2001). Another difficulty is that the comparison of solid content using refractive index measurements varies from one type of honey to another. In addition chemical reactions can take place at elevated temperatures (Mailard reaction), which leads to the formation of water in sample under drying conditions, on the other hand, very tightly bound water may escape detection (Isengard, Schulthei et al. 2001)

Figure 3.10: Honey refractometer (ATAGO CO)

3.5.2 Spectrophotometry

Spectroscopy is a term used to refer to the measurement of radiation intensity as a function of wavelength and is often used to describe experimental spectroscopic methods. Spectral measurement devices are referred to as (spectrometers, spectrophotometers, spectrographs or spectral analyzers).

Spectrophotometry is the quantitative measurement of the transmission or reflection properties by a substance as a function of wavelength (Wyszecki, Stiles 1982). It is more specific than the general term electromagnetic spectroscopy in that spectrophotometry deals with visible light, near ultraviolet and near infrared (Sommer 2012).

A spectrophotometer is a photometer that can measure light intensity as a function of the light source wavelength. Important features of spectrophotometers are spectral bandwidth and linear range of absorption or reflectance measurement (Wyszecki, Stiles 1982).

Figure 3.11 shows a schematic diagram of a single UV/Visible beam wavelength spectrophotometer. The monochromatic light is obtained by allowing the beam of light to pass through a monochrometer (prism of diffraction grating). The monochromatic light is directed (by suitable optics) through a cuvette containing the sample, some of the light will be absorbed by the sample and the remaining light is detected by a suitable detector. For absorption measurements, Beer-Lambert law is then applied to determine the concentration of the sample at a specific wavelength (Sommer 2012). Figure 3.12 shows a typical spectrophotometer that operates in the visible range 340nm-1000nm and used for honey testing.

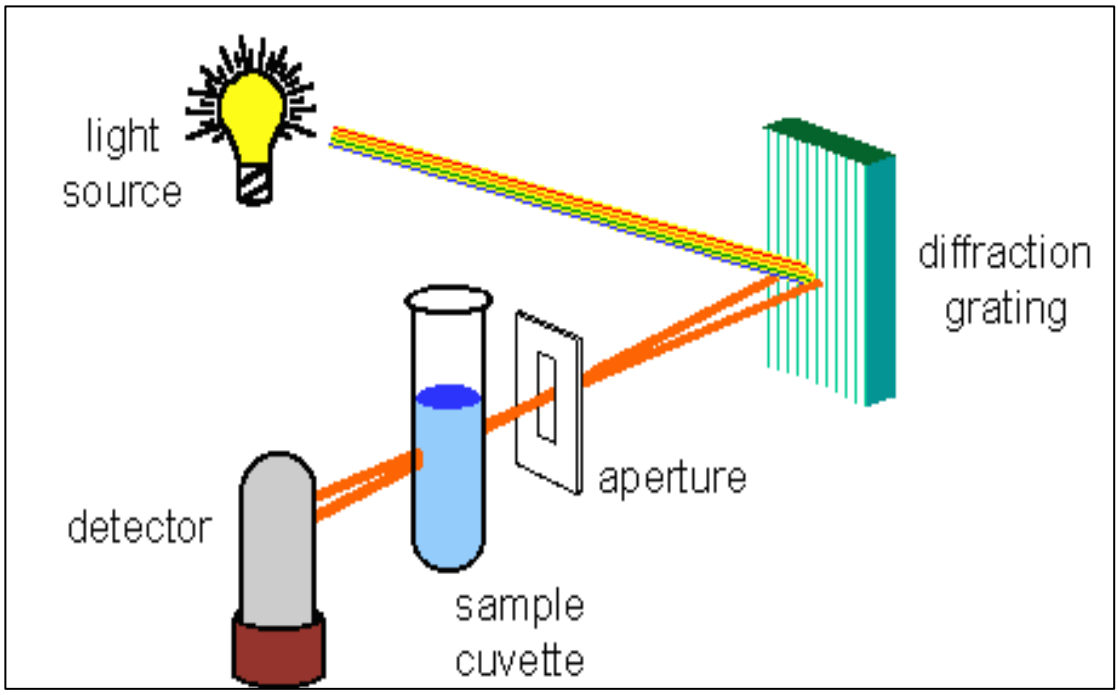

Figure 3.11: Schematic diagram of a wavelength selectable single beam UV_VIS Spectrophotometer (Tissue 2003)

Figure 3.12: Visible Spectrophotometer 340nm-1000nm from (Trontech)

Several honeys from Yemen and Saudia Arabia have been tested for quality and safety for human consumption thorough determining the concentrations of minerals and trace elements by physical properties such as optical absorption measures at 530nm using spectrophotometer measurements (Alqarni, Owayss et al. , AL-Zoreky, Alza'aemy et al. 2001).

Recent work has been developed by (Roshan, Gad et al. 2013) using UV spectroscopy to study the absorption of UV bands (200-400nm), which are ususally associated with the presence of different phenolics and flavonoids which are used as markers for determination of adulterated samples of Yemeni Sidr honey resulting from mixtures with honeys of lower quality price as well as the authentication of genuine Sidr honey.

Spectrophotometers designed for the infrared region are quite different because of the technical requirements of measurement in that region. One major factor is the type of photo sensors that are available for different spectral regions, but infrared measurement is also challenging because virtually everything emits IR light as thermal radiation.

The near infrared (NIR) spectroscopy has been used to classify the floral origin of European honey samples (Davies, Radovic et al. 2002) and for the detection of honey adulteration by addition of fructose and glucose (Downey, Fouratier et al. 2003).

(Bertelli, Plessi et al. 2007) reported that the mid-infrared region potentially has advantages over the NIR for the analysis of food. This is because NIR is limited in its usefulness for spectral interpretation, due to the many overlapping bands, whereas the MIR region is rich of information related to the molecular structures of compounds present in the samples. Therefore Fourier transform mid-infrared spectroscopy was used as an optical sensing technique to obtain classification of Italian honey.

3.5.3 Spectro-photocolorimeter

Spectrophotometers can also be designed to measure the reflectivity both at selected fixed wavelengths or perform scans over the complete wavelength range using different controls and calibrations. Reflectance measurements are of great value in providing a reference standard for the comparison of the colour of different samples (Wyszecki, Stiles 1982).

Reflected colour of a given sample can be measured by taking different readings in the visible light range (400-700 nm). These readings are typically used to draw the sample's spectral reflectance curve (reflection of light as a function of wavelength).

Figure 3.13 shows a schematic diagram of the principle of a spectrocolorimeter that combines a monochromator with a normalized light source. For each wavelength, the light reflected by the sample is compared to the light reflected by a reference white surface under the same conditions of lighting and observation. One can then determine the (diffuse) reflectance spectrum R(λ) of the sample (figure 3.14).

There are two types of spectrocolorimeters that are used depending upon the type of photo detector employed (Breteau 2007).

- A single detector that captures the light dispersed by the monochromator: in this case the diffraction grating of the monochromator is rotated using a precision stepper motor.
- A photodiode array is set at the exit of the monochromator in order to acquire the spectrum in one single step (Optical Multichannel Analyzer).

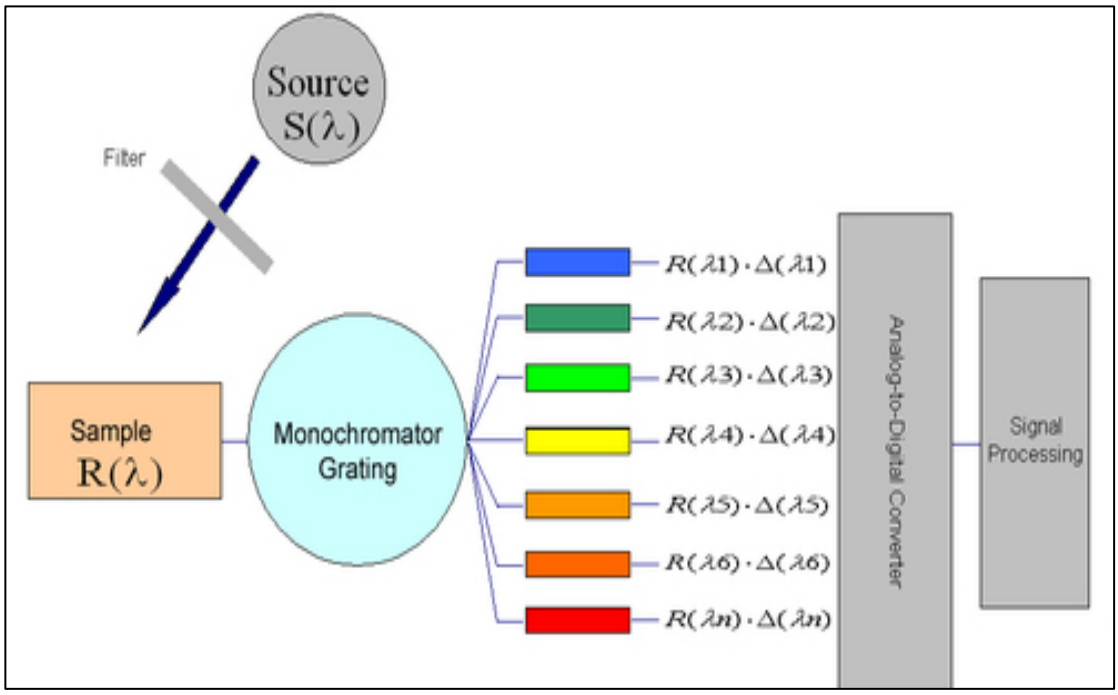

Figure 3.13: Schematic diagram of the principles of a spectrocolorimeters (Breteau 2007)

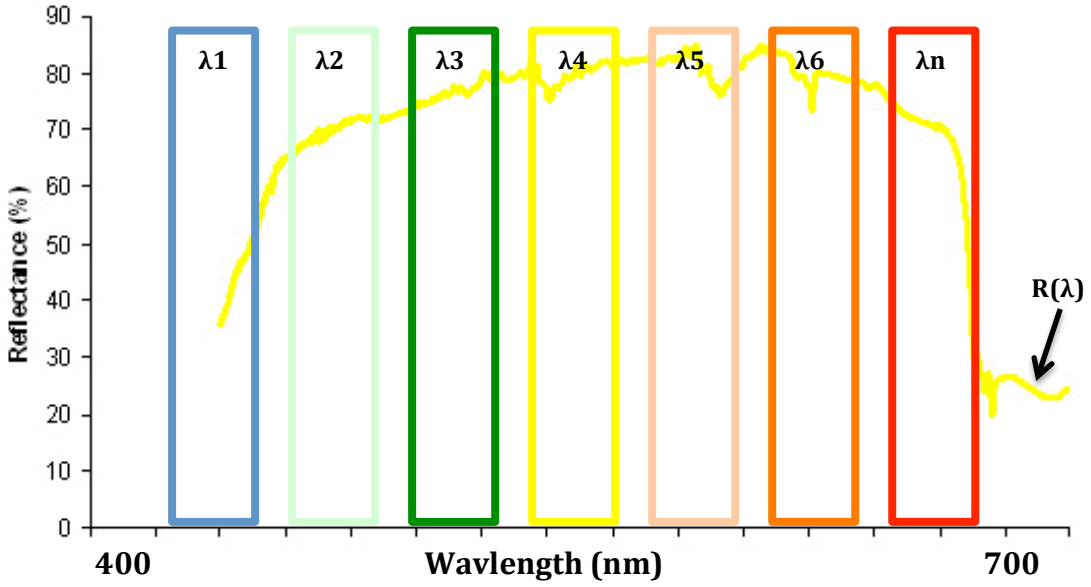

Figure 3.14: An overview of atypical monochromator response spectra (λ1-λn >> response filters, Rλ=reflectance spectra of sample)

3.5.4 Spectrocolorimeters

Measurements of reflectance found at various wavelengths under specified light conditions may then be used to compute absolute colour concept values. Among the different spectrophotometric systems, the tristimulus CIE (International Commission on Illumination) chromaticity coordinates has been the most used since it has been intended to be comparable to the scale of human visual perception (Schanda, Eppeldauer et al. 2007). Instrumental techniques that use spectrocolorimeters or colorimeters which require less time and provide easily comparable results, have been used more often for research and routine daily analysis (Storozhuk 2010).

Figure 3.15 shows a schematic diagram of a colorimeters based on the optical filters (Red, Green and Blue). It is made of three different photo detectors, operating simultaneously and having spectral sensitivities corresponding to the colorimetric tristimulus functions (Figure 2.13, Chapter 2). The trichromatic components of a sample are measured after calibration with a reference source whose spectrum is close to the spectrum of a normalized illuminate.

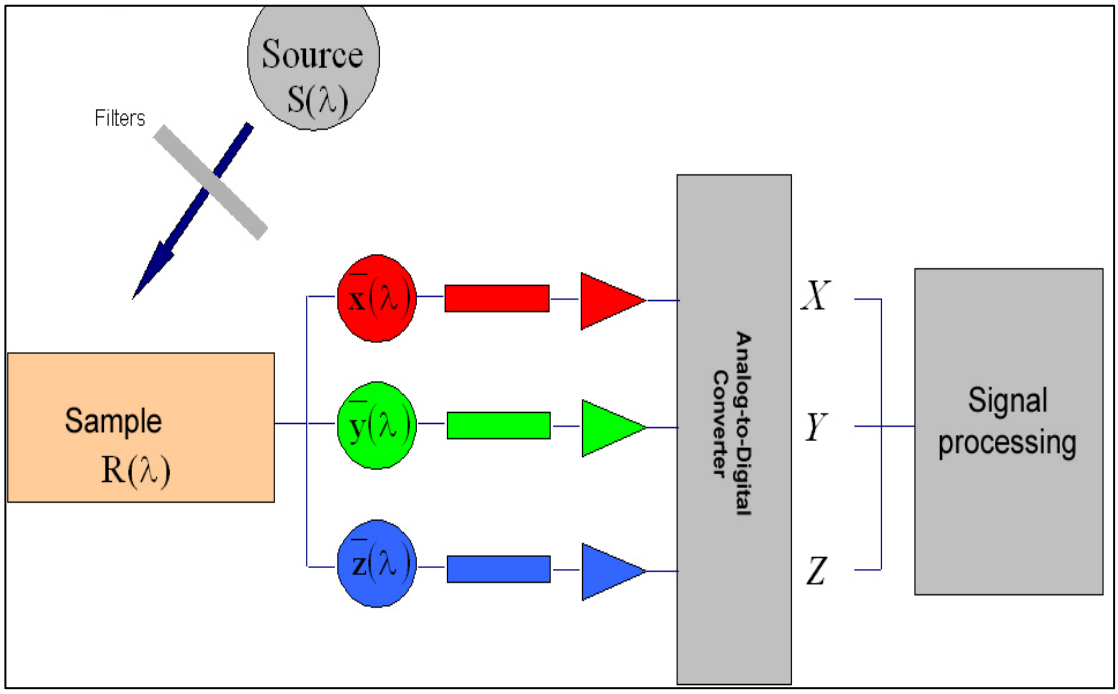

Figure 3.15: Schematic diagram of the principle of colorimeter based tristimulus filters (Breteau 2007)

The color of complex liquids such as honey can be used to make judgments on its quality or to distinguish variations due to different botanical sources or production peculiarities in honey. Visual investigation of honey colour may help to evaluate its botanical source, the degree of thermal treatments, and the presence of defects like fermented products (Tuberoso, Jerković et al. 2014). Physical examination of honey colour has been used in establishing the current U.S. Department of Agriculture grade colours of honey. This was achieved by recording spectrophotometric data for several characteristic honeys in all colour ranges and calculating CIE colorimetric data (White 1975).

Colour has been useful in the classification of mono-floral honeys produced from the nectar/honeydew that mainly originates from specific plant species and that have distinctive sensory characteristics. The high antioxidant and the content of phenolic compounds has been associated with the darker colour commonly observed in honeydew honeys (Bentabol Manzanares, García et al. 2011).

Furthermore, (Gonzales, Burin et al. 1999) have stated that the colour shade of honey is related to the composition of the honey and the storage temperature. It was also indicated that the cause of darkening in the honey maybe attributed to fructose crystallization and amino aminoacidaldol reactions in the honey. Factors like the ratios of glucose to fructose, nitrogen content, moisture and amino acids content are possible affects determining the rate of honey colour darkening. Measurements were done using spectrocolorimeter and the colour functions were calculated through the tristimulus values XYZ. The results displayed on a CIE chromatic diagram allowed an objective approach to color grading of honey samples.

Colour parameters measured using CIE L a* b* together with other physiochemical parameters have been used by (Popek 2002, Bertoncelj, Doberšek et al. 2007) to determine the quality of various honeys, while CIE XYZ tristimulas values were assessed by (Tuberoso, Jerković et al. 2014) to measure the transmittance of the whole visible spectrum (380-780nm) to assess the colour of honey in order to discriminate mono-floral honey types from different geographical locations in Europe.

3.5.5 Fluorescence Spectroscopy

Fluorescence spectroscopy is a type of spectroscopy that analyses fluorescence from a sample. It involves using a beam of light, usually ultraviolet light that excites the electrons in molecules of certain compounds and causes them to emit light (typically visible light) (Lakowicz 2006).

Devices that measure fluorescence are called fluorometers or fluorescence spectrometers. Figure 3.16 shows a simple schematic diagram of a fluorescence spectrometer. The component parts necessary include incident photon source, monochromators (used for selecting particular incident wavelengths), focusing optics, photon collecting detector (single or multiple channel), cut-off filters and a control software unit. This intrinsic sensitivity of fluorescence is also its biggest problem and care must be taken to record a true fluorescence signal of interest. Figure 3.17 shows typical fluorescence spectrophotometer device from JASCO that is normally used in biomedical and food research.

The application of fluorescence in analysis of food has increased during the last decade, probably due to the propagated use of chemometrics. In addition, fluorescence spectroscopy offers several inherent advantages for the characterization of molecular interactions and reactions. Firstly, it more sensitive than spectrophotometric techniques and secondly its extremely sensitive to their environments. However such devices are expensive.

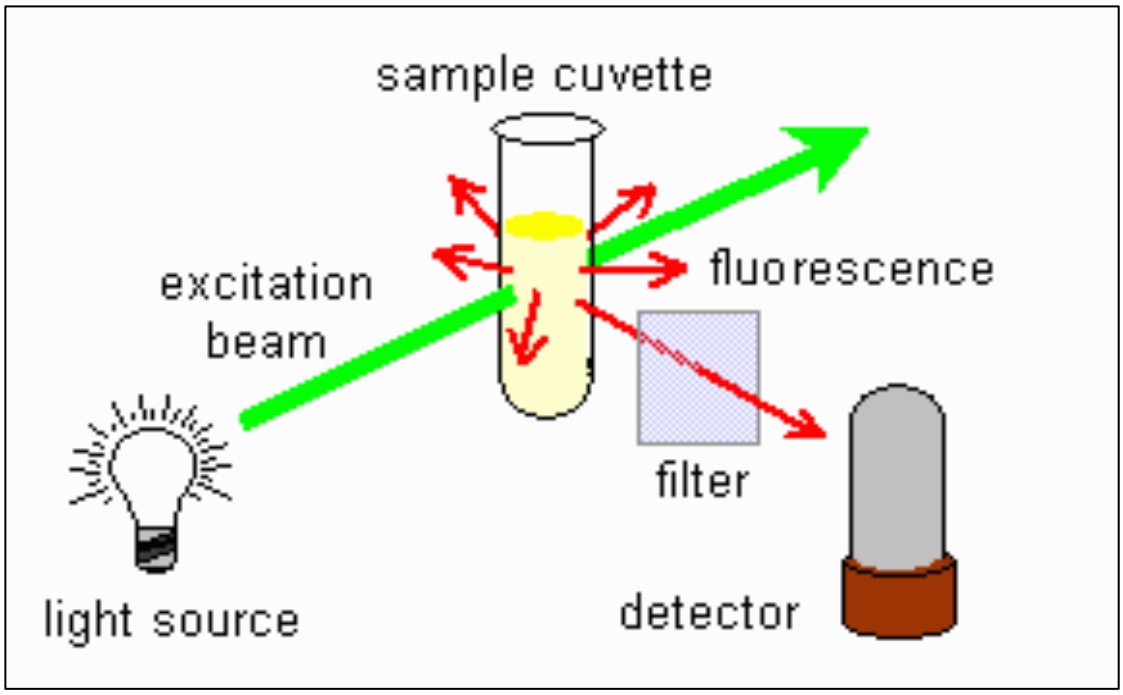

Figure 3.16: Schematic diagram of simple fluorescence spectroscopy with one band bass filter (Tissue 2003)

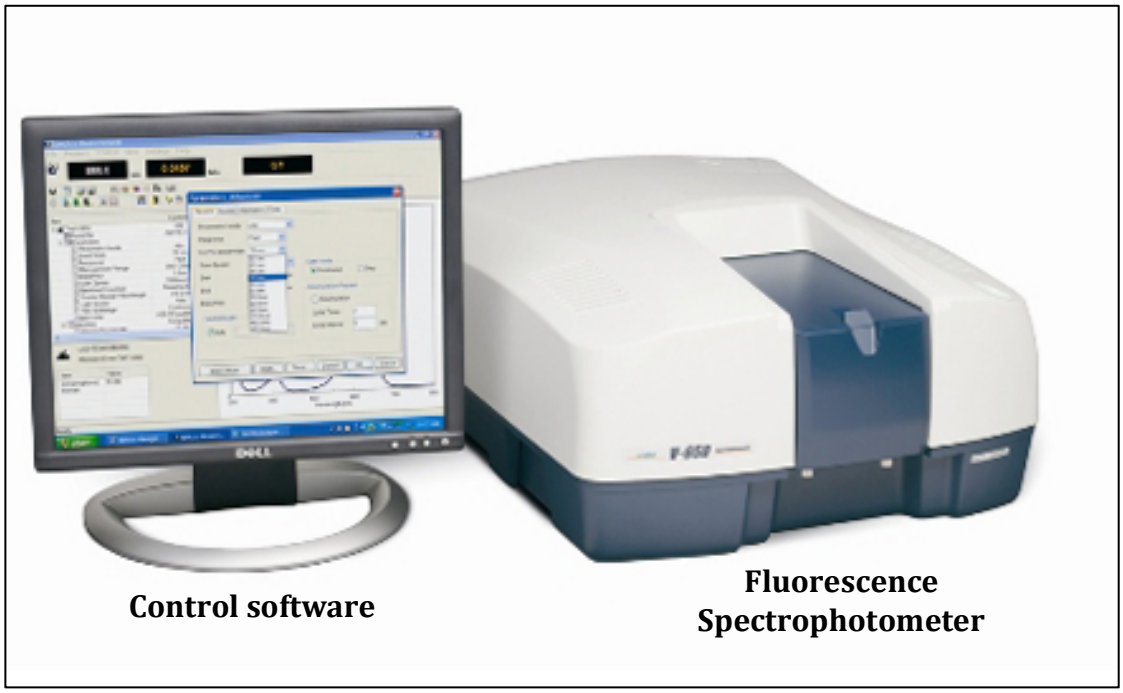

Figure 3.17: UV/VIS/NIR spectrophotometer from (JASCO)

It has also been shown that fluorescence spectroscopy can discriminate milk samples subjected to heat treatment from those subjected to homogenisation and to characterise mild heat treatment applied to milk (Karoui, Dufour et al. 2007).

Front-face fluorescence spectroscopy has demonstrated its feasibility to classify Swiss honeys from seven different floral sources with the fluorescence emission spectra being analyzed at (280-480nm), (305-500nm) and (380-600nm) using excitation wavlengths 250, 290 and 373nm respectively to investigate the fluorescence of aromatic amino acids (maximum emission 340nm), as well as fluorescent of furosine, HMF and phenolic compounds present in the honey samples (maximum emission 440nm and 425nm) as a result of the Maillard reaction used as indicator to determine the quality of commercial honey samples (Karoui, Dufour et al. 2007). The high presence of HMF usually formed during acid hydrolysis of sucrose, high levels of his compound suggest the possibility that the honey been adulterated with invert syrup.

The presence of fluorophors in the form of aromatic amino acids, vitamins, cofactors and phenolic compounds in honey makes fluorescence spectroscopy a valuable technique to determine the botanical origins of such products (Karoui, Dufour et al. 2007). However, the relatively limited number of samples were involved and further study should be done to discriminate between floral origins using front face fluorescence spectroscopy.

Fluorescence spectroscopic properties of honey and cane sugar syrup were also investigated by (GHOSH, VERMA et al. 2005) to explore the detection of adulterated honey with cane sugar syrup. Measurement showed that the major contributor to fluorescence of cane sugar syrup is the reduced form of nicotimide adenine dinucleotide (NADH) which had an emission peak at 430nm and 440nm for adulterated honey samples when excited at 340nm, while the fluorescence of pure honey samples is dominated by the existence of flavins (emission peak 520nm), therefore fluorescence spectropic measurements was used to monitor adulteration of honey with cane sugar syrup.

There has been some work on optical glucose sensing in biological fluids using fluorescence spectroscopy (Loschenov, Parfenov et al. 2001). The most glucose fluorescence detecting method is based on oxidation of glucose-by-glucose oxidase to generate peroxide and gluconoleactone. However a chemical dye is used in theses reactions for the detection of the peroxide in biological samples such as honey (Loschenov, Parfenov et al. 2001).

3.5.6 Raman Spectroscopy

Raman spectroscopy is a spectroscopic technique used to observe vibrational, rotational, and other low-frequency modes in a system (Graves, Gardiner et al. 1989). It relies on inelastic scattering, or Raman scattering, of monochromatic light, usually from a laser in the visible, near infrared, or near ultraviolet range. The laser light interacts with molecular vibrations, phonons or other excitations in the system, resulting in the energy of the laser photons being shifted up or down. The shift in energy gives information about the vibrational modes in the system (Graves, Gardiner et al. 1989, Smith, Dent 2005).

Raman scattering is fundamentally a weak process in that only one in every 10^6–10^8 photons that scatter, therefore very high power modern lasers and microscopes are delivered to very small samples to make the process sensitive (Smith, Dent 2005).

Figure 3.18 shows the basic processes that occur for one vibration. At room temperature, most molecules, but not all, are present in the lowest energy vibrational level. Since the virtual states are not real states of the molecule but are created when the laser interacts with the electrons and causes polarization, the energy of these states is determined by the frequency of the light source used. The Rayleigh process will be the most intense process since most photons scatter this way. It does not involve any energy change and consequently the light returns to the same energy state. The Raman scattering process from the ground vibrational state (m) leads to absorption of energy by the molecule and

its promotion to a higher energy excited vibrational state (n). This is called Stokes scattering. However, due to thermal energy, some molecules may be present in an excited state (n). Scattering from these states to the ground state (m) is called anti-Stokes scattering and involves transfer of energy to the scattered photon (Smith, Dent 2005).

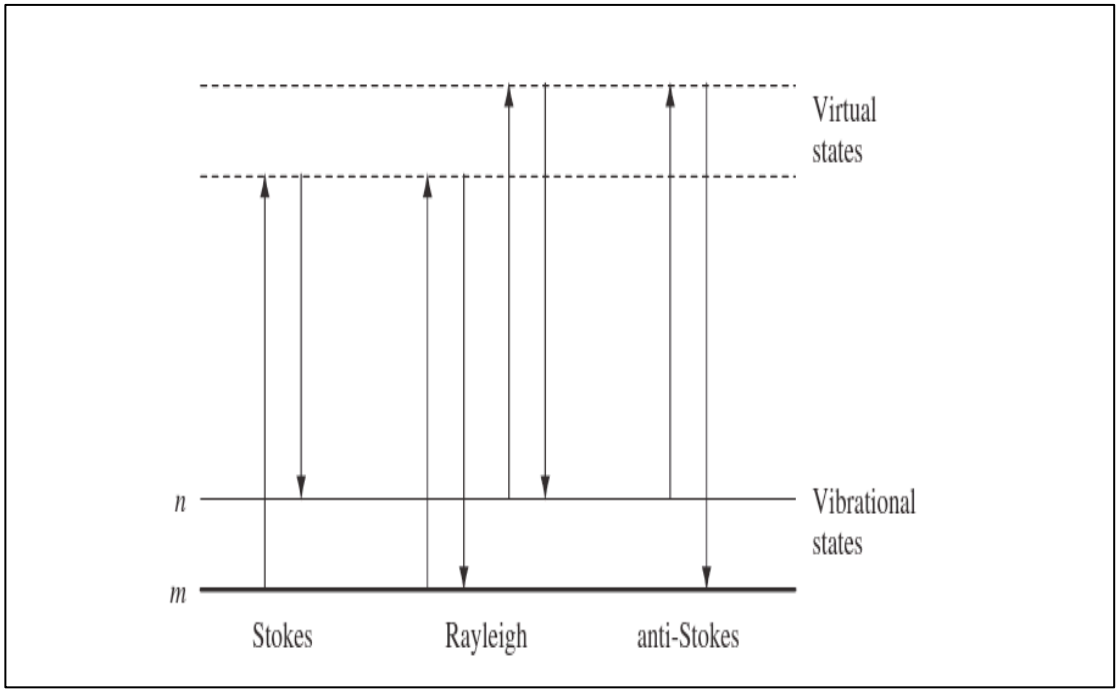

Figure 3.18: Diagram of Rayleigh and Raman scattering processes (Smith, Dent 2005)

The way in which radiation is employed in infrared and Raman spectroscopies is different. In infrared spectroscopy, infrared energy covering a range of frequencies is directed onto the sample. Absorption occurs where the frequency of the incident radiation matches that of a vibration so that the molecule is promoted to a vibrational excited state. The loss of this frequency of radiation from the beam after it passes through the sample is then detected. In contrast, Raman spectroscopy uses a single frequency of radiation to irradiate the sample and it is the radiation scattered from the molecule, one vibrational unit of energy different from the incident beam, which is detected. Thus, unlike infrared absorption, Raman scattering does not require matching of the incident radiation to the energy difference between the ground and excited states (Smith, Dent 2005, Graves, Gardiner et al. 1989).

To help provide a better visualization of the operation of Raman spectroscopy, a generic diagram is given in figure 3.19. A sample is illuminated with a laser beam (infrared region), which is then scattered by the sample. The scattered light passes through a filter to remove any stray light that may have also been scattered by the sample. The filtered light is then dispersed by the diffraction grating and collected on the detector (Graves, Gardiner et al. 1989).

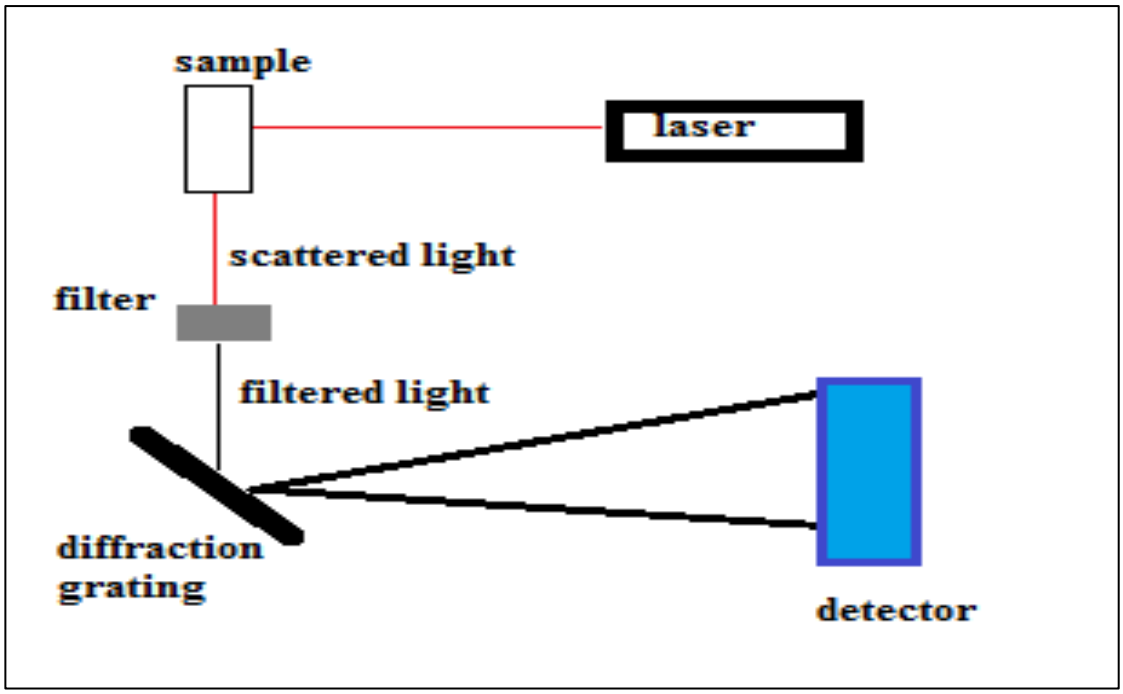

Figure 3.19: Simplified diagram of how a Raman spectrometer works (www.chemwiki.ucdavis.edu)

The main difficulty with Raman spectroscopy is separating the weak inelastically scattered light from the intense Rayleigh scattered laser light. Historically, Raman spectrometers used holographic gratings and multiple dispersion stages to achieve a high degree of laser rejection. In the past, photomultipliers were the detectors of choice for dispersive Raman setups, which resulted in long acquisition times. However, modern instrumentation almost universally employs band pass filters for laser rejection and CCD detectors (Graves, Gardiner et al. 1989).

Raman spectroscopy is increasingly used as an analytical technique for the evaluation of food safety and quality. The determination of glucose content in the

beverage industry (Delfino, Camerlingo et al. 2011) and the discrimination of sugar additives in honey as adulteration (Özbalci, Boyaci et al. 2013) have been preformed using Raman instrumentation.

The continued improvements in modern optics including small diode lasers, improved simple detectors and fiber optic coupling have all led to the ability to use Raman scattering for liquid analysis. Although the technique is limited by the fact that it is a weak effect, to some extent this can be overcome where the power density is high by the use of a microscope or particular forms of fiber optics. However these can be very expensive optical equipment's. Another disadvantage this creates is that the range of choice requires an understanding of the subject and cannot be made simply on the basis of the purchase of one simple instrument (Graves, Gardiner et al. 1989, Smith, Dent 2005).

3.5.7 Optical Rotation

Quantification of glucose is also based on the phenomenon of optical rotatory dispersion whereby a chiral molecule (molecules that has non-superposable mirror image) in an aqueous solution will rotate the plane of linearly polarized light passing through the solution (Hart, Craine et al. 1999, Egan 2006).

A number of techniques for obtaining optical rotation measurements generally fall into two categories: those which utilize crossed polarizers to measure rotation via amplitude changes and those which measure the relative phase shift of modulated polarized light passing through the sample (McNichols, Coté 2000).

Polarimetry is an instrumental analytical method using rotation of polarized light by some substances as a measure of their concentration in a solution (Hart, Craine et al. 1999). The instrument used is called a polarimeter. When it is adapted for measuring quality of sugar the instrument is named saccharimeter (Topac Inc).

In both instruments it is the rotation of polarized light by a substance in a solution that is measured. Usually, it is only one instrument that has two interchangeable scales, one labeled in angular degrees, the other in units Z (named International Sugar Scale (I.S.S.)) (Ball 2006, Knecht 1990).

Figure 3.20 shows a schematic diagram of a polarimeter consisting of a monochromatic light source, a polarizer, a sample cell and a second polarizer called the analyzer. Un-polarized light from the light source is first polarized. This polarized light passes through a sample cell. If an optical active substance is in a sample tube, the plane of the polarized light waves is rotated. The rotation is noticed by looking through the analyzer as a change in intensity of illumination. To reach the same illumination as was without an optical active sample the analyzer must be turned through an angle. Readings are taken in degrees angle (+/- 360°) or sugar degrees Z (International sugar scale +/- 250° Z) (Ball 2006).

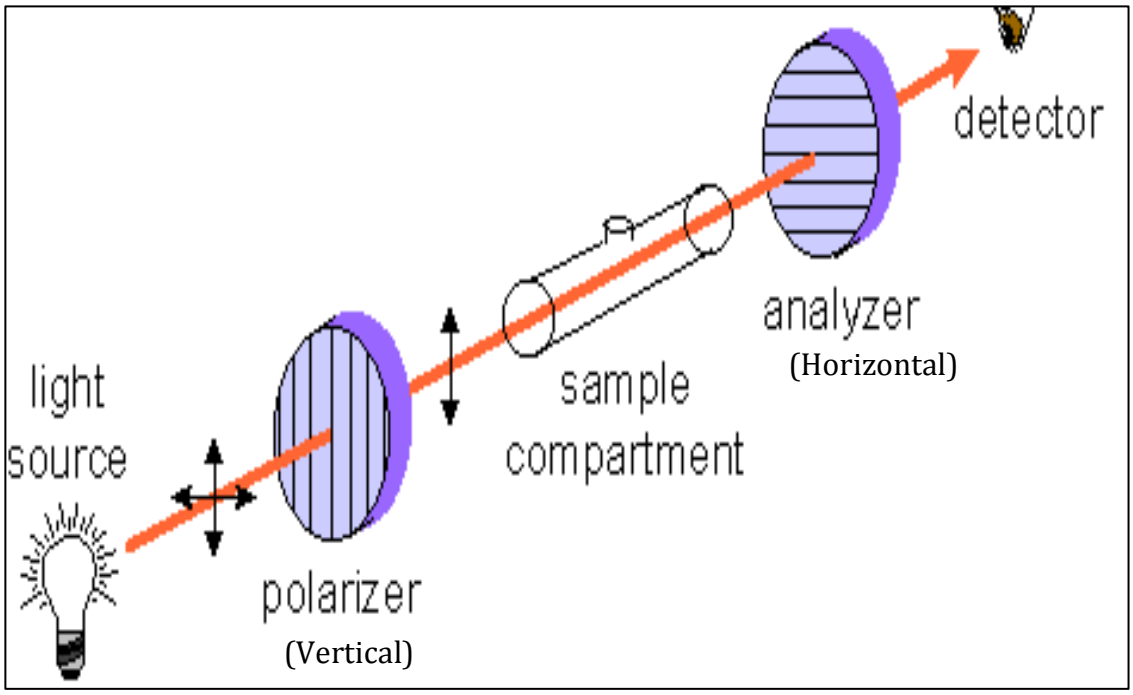

Figure 3.20: Schematic diagram of a polarimetre (Tissue 2003)

Among many other materials of natural origin, honey has the property of rotating the polarization plane of polarized light. This is one further property that depends largely on the sugars of honey-their types and relative proportions. Since each sugar has a specific and consistent effect, and the total optical rotation is dependent on concentration. Early analysts used optical rotation under various specified conditions as a means of sugar analysis and it was extended for sugar analysis of honey (White 1975).

Determination of optical rotation amongst other optical properties were used by (Nanda, Sarkar et al. 2003, Pridal, Vorlova 2002) to characterize various honey samples from different sources. Floral honey showed the property of rotating the polarization plane of polarized light and optical rotation was levorotatory (anticlockwise, i.e. –ve angular rotation). In contrast, adulterated honey samples and some honeydew where dextrorotatory (clockwise, i.e. +ve angular rotation). This is a consequence of normal preponderance of fructose in floral honey, which shows negative specific rotation over glucose.

The overall value for the optical rotation is a result of the values of the different honey sugars and because of the complex structure, only broad indication can be done. The measurement of specific rotation is currently used in India, Greece, Italy and UK to distinguish between blossom, honeydew and adulterated honey samples.

3.6 A Summary Table Of The Conventional Instrumentation Performance & Optical Properties Measured

Table 3.1 summarizes the optical techniques, the optical properties, the identification parameters measured and the performance of such techniques for analyzing honey samples.

Optical Technique	Optical Property	Identification Parameters	Measured Parameters	Indicator	Performance
Refractometere	Refractive Index	Water content	% Soluble solids/ % Moisture	Quality	Indirect measurement using empirical formula or conversion table/ variation of water content due to temperature and humidity
Spectrophotometry	Transmission/ Reflection	Mineral content/ liquid content/ Turbidity/ sediments	Absorption spectral signatures (UV/VIS/IR regions)	Quality/ botanical classification	Expensive equipment's/ precise optics needed
Photo-colorimeter	Reflection	Colour	CIE Colour measurement (VIS region) / Pfund scale (0-140mm)	Quality/ botanical classification	Not reliable as honey colour varies over time due to storage temperature and long shelf-life
Fluorescence spectroscopy	Fluorescence	Flurophor/ furosine/ HMF/ Flavonoids/ Aromatic Amino acids/ etc.	Spectral emission signatures (UV-VIS region)	Quality/ authenticity/ adulteration	Expensive equipment's/ precise optics needed and optical filters
Polarimetry	Optical rotation of polarization	Average concentration of sugar solution (fructose/ Glucose)	Intensity measured at a specific angle of rotation (+/- 360°) or in International sugar scale (+/- 250° Z)	Quality/ Adulteration	Specific angle of rotation must be selected at specific wavelength for optimum measurement/ precise optic needed.
Raman spectroscopy	Scattering	Sugar content	Vibrational rotation and low frequency modes	Quality/ adulteration	Weak effect/ require understanding of the subject /expensive equipment's
Pfund grader	Optical density	Colour	Pfund scale (0-140mm)	Classification	Visual perception, not accurate and not reliable

Table 3.1: A summary table of the conventional measurements techniques performance and optical properties measured

3.6 Chromatic Techniques Applied To Complex Liquids

Optical monitoring of high voltage transformer oil using the chromaticity of polychromatic light transmitted through the oil is a convenient and a cost effective method for monitoring oil degradation (Elzagzoug 2013, Elzagzoug, Jones et al. 2014). The technique uses readily available and portable instrumentation and was based upon a mobile phone camera, LED source and a VDU computer screen. Details of changes in the optical transmission spectra of oils have been obtained together with the possibility of detecting different levels of micro particles in the oil, which provided additional information about changes in the transformer oil.

Chromatic monitoring and analysis of urine is providing a novel approach for improving point of care diagnosis of Urinary tract infection (UTI) (Deakin, Jones et al. 2014). It is capable of quantifying complex changes in optical spectra of urine samples and the results can be presented in a convenient manner for decision-making with high levels of traceability. The approach used a webcam-computer and a computer VDU screen as tunable illumination source. The system has been shown to be capable of operating in a robust manner under ambient lightning conditions and with potential for use as a point of care test in primary care.

Chromatic-based fiber optics sensors have been used to monitor different complex industrial liquids that include vacuum pump oil and various aviation fuels (Jones G. R, Deakin A. G et al. 2008). It was capable to quantify complex spectral changes of propagated/ reflected light from a controlled source.

It has also been shown that chromatic analysis could be applied for distinguishing between various broadband absorption spectra of liquors and also their classification (Jones, Deakin et al. 2009). Three chromatic coordinates quantified the absorption spectra and a scheme was produced for differentiating

and classifying various spectra at different levels of detail for checking the authenticity of whisky liquors.

Chromatic techniques based on polychromatic light source have also been used to address complex liquids of optically active compounds such as (sucrose) in aqueous solutions (Egan 2006, Jones G. R, Deakin A. G et al. 2008). The different rotation of the various wavelengths using a polychromatic light lead to the color of light viewed through the analyzing filter varying with the angle of the polarizer. The optical activity was determined in practice without the need to rotate the analyzing filter but via the colour of the emerging light, which was quantified using the chromatic approach.

3.7 Summary

Complex liquids have been concidered and described. Various examples of complex liquids have been given including water-tea-milk mixtures, urine, blood, high voltage transformer oils, petroleum fluids, vacuum pump oil, optically active liquids, syrup and honey.

Honey, regarded as a complex liquid has been introduced, its various aspects considered and the mannar in which honey is classfied was also described.

Optical properties of complex liquids affecting transmission, reflection, polarisatin and flourescence have been described. Optical techniques addressing such liquids are also considered.

Recent ways of chromatic techniques are described which provide a convienient, cost effective and robust monitoring approach.

Chapter 4

Experimental setup

4.1 Introduction

This chapter describes the equipment that has been used for this research project and the procedure adopted. An overview of the complete system is presented first, followed by more detailed information on the major components used. The experimental procedures observed are described for the different types of experiments that have been preformed. The method used for computational data processing is also described.

4.2 The Chromatic Monitoring System

This section describes the chromatic optical instrumentation developed for addressing complex liquids over the course of this research. The optical systems developed included the following:

- An optical system for monitoring the optical transmission through and the light scattering by the sample. It was used for addressing a cuvette containing a complex liquid (e.g. honey) sample. It was based upon a VDU screen as a controllable uniform light source and a webcam for capturing images of the cuvette and the computer screen.
- An optical system used for monitoring the optical polarization of light passed through a complex liquid (e.g. honey) sample contained in a cuvette and based upon a VDU screen, 2 polarizing filters and a webcam for capturing images.
- An optical system for monitoring the optical fluorescence of the sample. This was used for addressing a cuvette containing a complex liquid (e.g. honey) sample and was based upon a VDU screen, a collimated LED light system design and a webcam for capturing images.

4.3 Apparatus Used For Addressing Complex Liquids

4.3.1 Sample Cuvettes

A cuvette is one of the primary elements that are used for all the experiments performed. The cuvette was used to contain the honey (or the calibration mixture) sample, transparency being an essential feature of the cuvette to allow light to be transmitted through a sample.

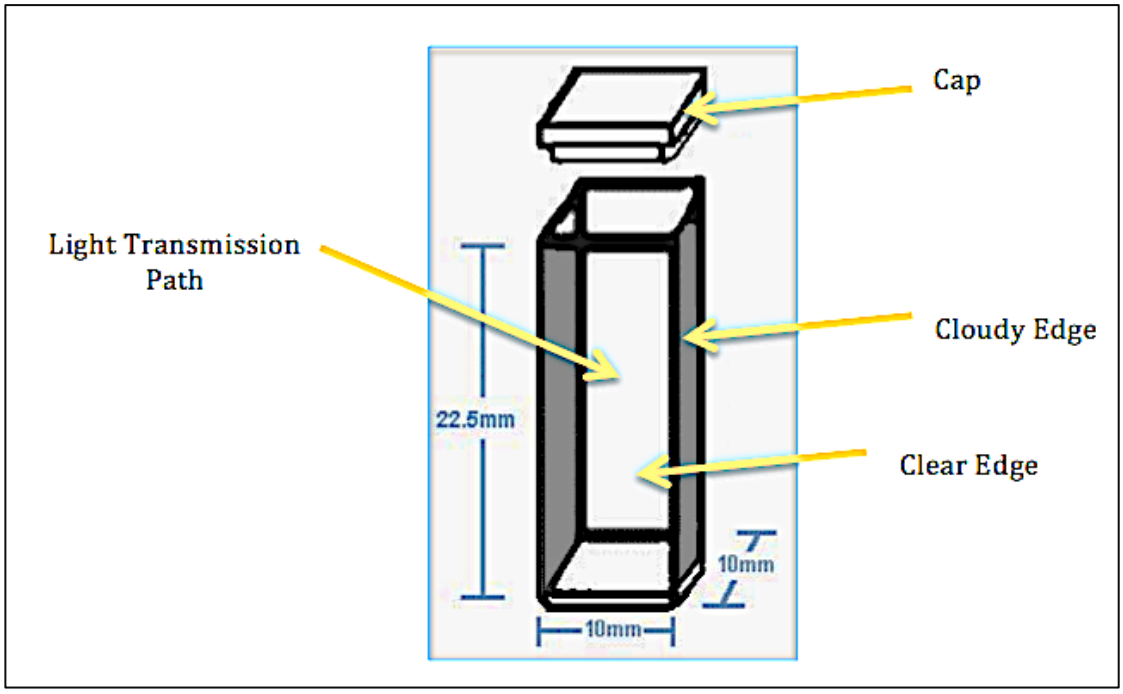

Figure 4.1: Schematic of the cuvette structure

Figure 4.1 shows a schematic diagram of the plastic transparent cuvette made from methacrylate material with useable range (280-800nm). It consisted of a small tube of square cross section closed at one end and open at the other. These cuvettes were made to hold samples for spectroscopic experiments (Perfector Scientific 2014). Two opposite surfaces of the cuvette were clear for light to be transmitted and scattered through each and the other two side faces were cloudy. A cap was used to keep samples separate from the surrounding environment such as air etc.

4.3.2 Light Sources

There was a requirement for a polychromatic light source, which needed to be stable and have a long lifetime. Two different types of light sources were used, a VDU laptop screen and a collimated LED light. For each type of light source a stable power supply was used.

4.3.2.1 VDU Screen

VDU stands for (Visual Display Unit). A VDU displays images generated by a computer or other electronic device. The term VDU is often used synonymously with monitor, but it can also refer to another type of display, such as a digital projector. Visual display units may be peripheral devices or may be integrated with the other components. For example, laptop computers (figure 4.2) use an all-in-one design, in which the screen and computer are built into a single unit.

Figure 4.2: VDU Laptop screen

A uniform illumination was obtained using the screen of a VDU as a light source described by (Jones, Deakin et al. 2009). Polychromatic light transmitted through a sample can provide useful information about the sample condition via preferential absorption or scattering within various wavelength bands. This also provided the possibility of tuning the spectrum of the illumination from the VDU via software installed on the connected laptop. This system maintained a uniform back illumination of the sample.

The VDU screen used was a Liquid Crystal Display (LCD), its an electronically modulated optical device made up of a number of segments filled with liquid crystals that are sandwiched between polarizers in front of a light source (backlight) to generate visual colour sensation. The screen resolution is 1200 × 800 and the wavelengths emitted are RGB colour bands. Tuning the VDU involved adjusting the gains of the (R), green (G) and blue (B) screen channals to change their relative intensities in accordance with the optical spectra of typical liquid sample (e.g. honey). In this manner the sensitivity of the monitoring system could be varied to optimize the performance. A combination of R,G,B gains is used to generate white light perception on the eye a standard to illuminate the samples. Trail and error led to the choice of gains of 0.7 for R, G and B in the experimental tests.

4.3.2.2 LED Light

A light-emitting diode (LED) is a semiconductor light source that can provide an intense source of polychromatic light. The LED light that was used in this research was violet InGaN (Indium gallium nitride) type from Roithner LaserTechnik GmbH (Appendix I). Figure 4.3 shows the measured emission spectrum of the violet light LED at short wavelengths which peak at 405nm and has a narrow bandwidth. This wavelength range was chosen carefully to excite the sample in order for it to emit characteristic light (fluorescence) at longer wavelengths so that the excitation spectrum would not interfere with the emission spectra of the samples fluorescence.

HMF and phenolic compounds in the honey can fluoresce at (≈ 440nm) causing fluorescent shift of 35nm when excited at around 380nm. High levels of this compound indicate adulteration of honey by invert syrup. Flavins in the honey are also an indicator of honey authenticity and they also fluoresce at ≈ 520nm causing a fluorescent shift of 115nm when excited at the short wavelength 370-420nm.

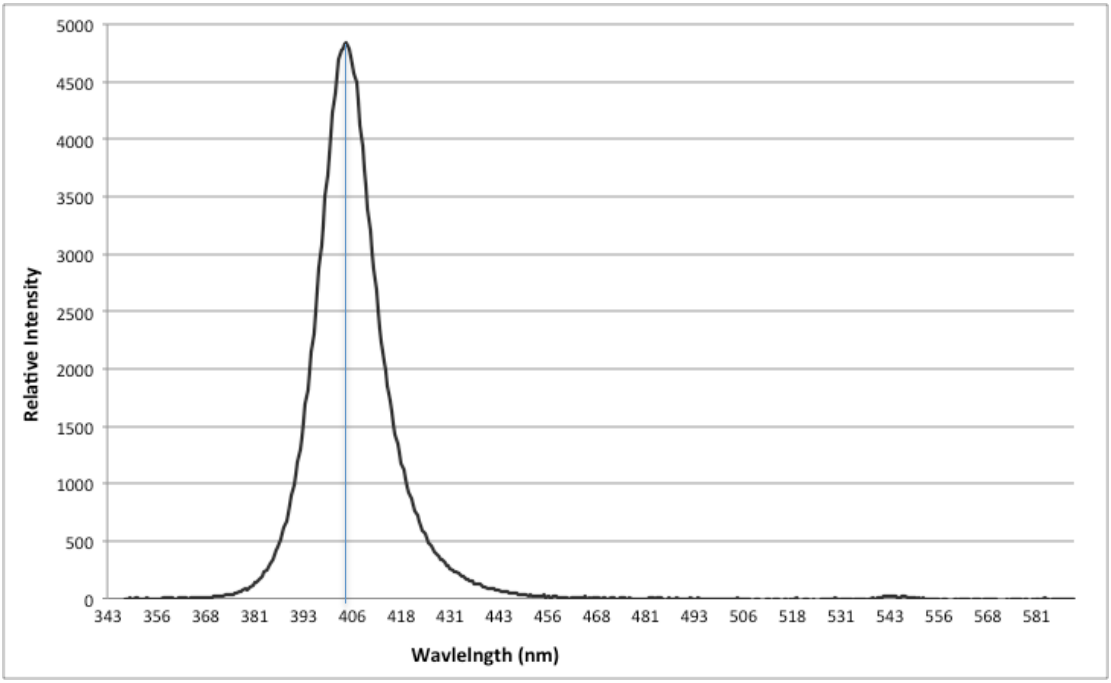

Figure 4.3: Measured spectrum of Violet light LED (Peak ~405nm)

A simple circuit was designed and built to provide a stabilized constant current for the LED light. The circuit regulates to 5V when connected to a 12V power supply adapter. The circuit has been designed so the current can be varied from 9.6mA to 41mA to suite the power requirements of the LED source used. The circuit diagram is attached in the (Appendix I).

4.3.3 Detector

4.3.3.1 Colour CCD Camera

The detector that was used in this research was a small CMOS (Complementary metal-oxide-semiconductor) image sensor webcam based module (Genius VideoCAM Trek) with high frame rate video 320 × 240 or 640 × 480 video at 30 frames per second connected to a computer via a USB cable. Figure 4.4 shows a measured spectral sensitivity of a CMOS colour sensor given by (Frey, Parrein et al. 2011) I.

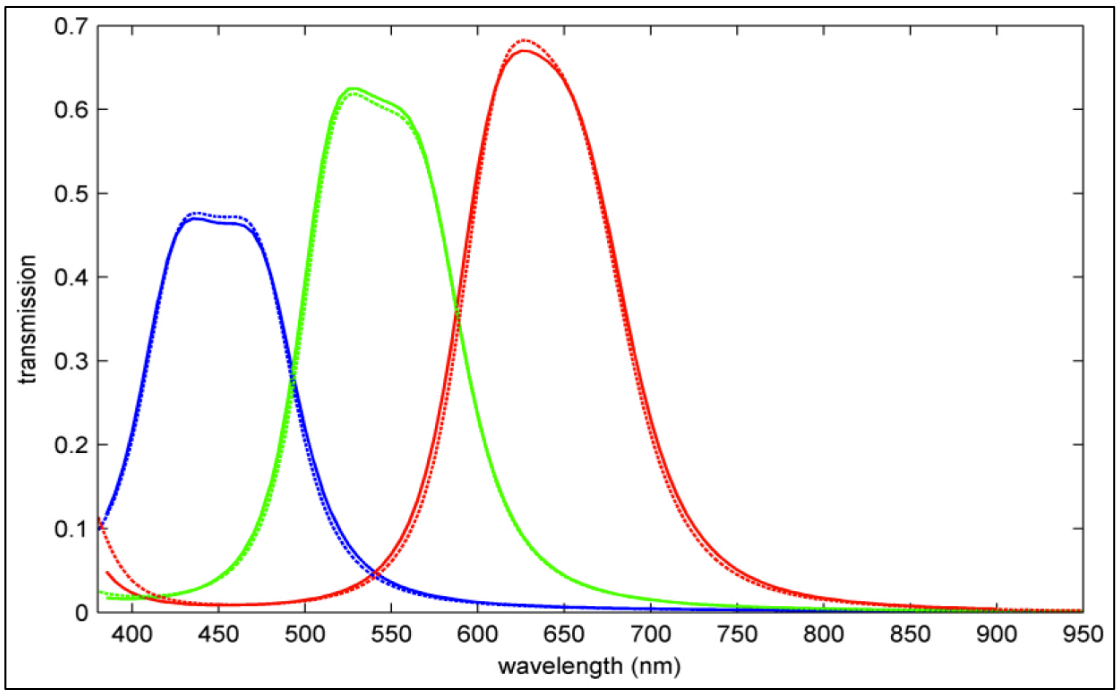

Figure 4.4: Relative spectral sensitivity of a CMOS colour sensor (Frey, Parrein et al. 2011)

Images were captured via the computer and stored for later processing. These images where processed using Capsoft Software (Appendix I) to obtain RGB information for analysis. Processing of these images involved the averaging of the pixels over a 7×7 pixel area centered on the image as illustrated in figure 4.5. The average of the pixels in this 7×7 area was outputted to a text file as R, G, and B (Red, Green and Blue) values in the range of 0-255 and H, L and S (Hue, Lightness and Saturation). This file was easily imported into a spreadsheet that used a set of functions to calculate various chromatic parameters (Chapter 5). Graphing and further processing could then be preformed sub-sequentially.

The webcam was adjusted so that the full illumination area provided on the VDU screen (174 X 128mm) filled the camera image area. The webcam's resolution (320 x 240) was not critical in affecting the results obtained. The R, G, B values of the screen areas on either side of the cuvette were tuned via trial and error for providing a means for any image illumination correction and to stabilise the webcam response as described by (Jones, Deakin et al. 2009).

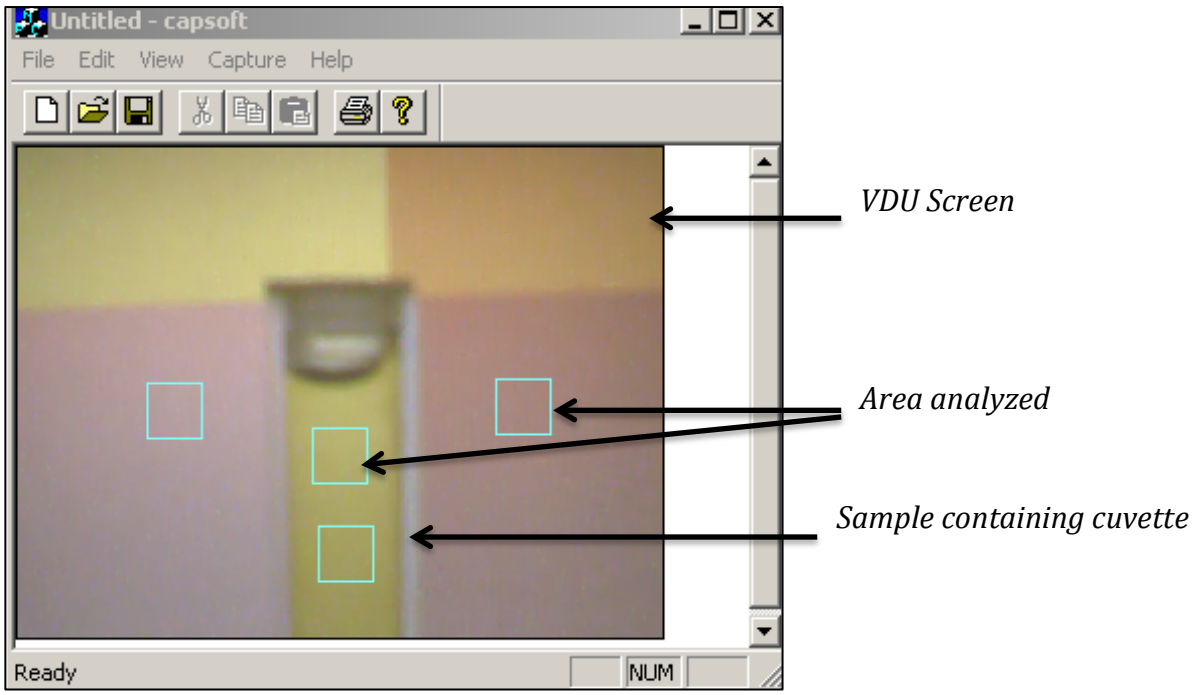

Figure 4.5: Image analysis window

A camera based detector has an advantage over other types of detectors in that, due to its integrated lens, it has a large viewing angle, so would in theory be able to resolve many light sources at once if used with suitable computer hardware and software that would be able to process the information. Also using a webcam camera can be cost effective and have the advantage of being portable for use on site.

4.3.4 Optical filters

Standard and cost effective optical wavelength polarizers (Plastic Linear Polarizing Film, made by TECHSPEC) were used in this research to examine the polarization change as light passes through both the sample and polarizers to be incident on the detector.

4.3.4.1 Polarizing Filters

The first polarizing filter was arranged to allow only vertically polarizing light to be transmitted through the sample. The second polarizer (or analyzer) was movable via rotation relative to the first polarizer against a fixed angular scale.

4.3.5 Limitations Of Components

The low cost and high volume manufacture VDU and Webcam components are not intended for analytical or optical measurements, so their performance may change with time, age manufacture or batch, but the calibration and ambient light rejection procedures developed in this project allow for those changes to be compensated for, but there are some limitations. The limitation in the web camera is the different setting by different manufacturers, these settings such as (exposure, brightness, white balance, etc.) must stay the same for all the tests, therefore, camera stetting's has to be noted and used the same for all cameras.

4.4 Systems & Procedures

4.4.1 General Procedures

There were several general procedures adopted as a matter of routine during all experiments.

- All samples were handled carefully
- All containers of honey samples were kept sealed and out of extreme temperatures and light
- Sample cuvettes and filling apparatus were kept clean before and after use
- Samples of honey (and calibration mixtures) were added to the cuvettes carefully
- Sample cuvettes were stored in a cool dry place out of extreme temperatures' and light between experiments
- The apparatus was treated with care, parts were not moved unnecessarily between experiments and not at all if the experiments were being repeated

4.4.2 Portable Chromatic Optical Transmission System

The portable chromatic optical transmission system has been designed for the purpose of laboratory and field tests. Figure 4.6 shows a schematic diagram of such an optical system setup. A light source provided back illumination for a cuvette that contained the sample. The cuvette was positioned 1cm away in front of the light source. The detector captured the transmitted light from the sample and was positioned 10cm away from the sample in cuvette.

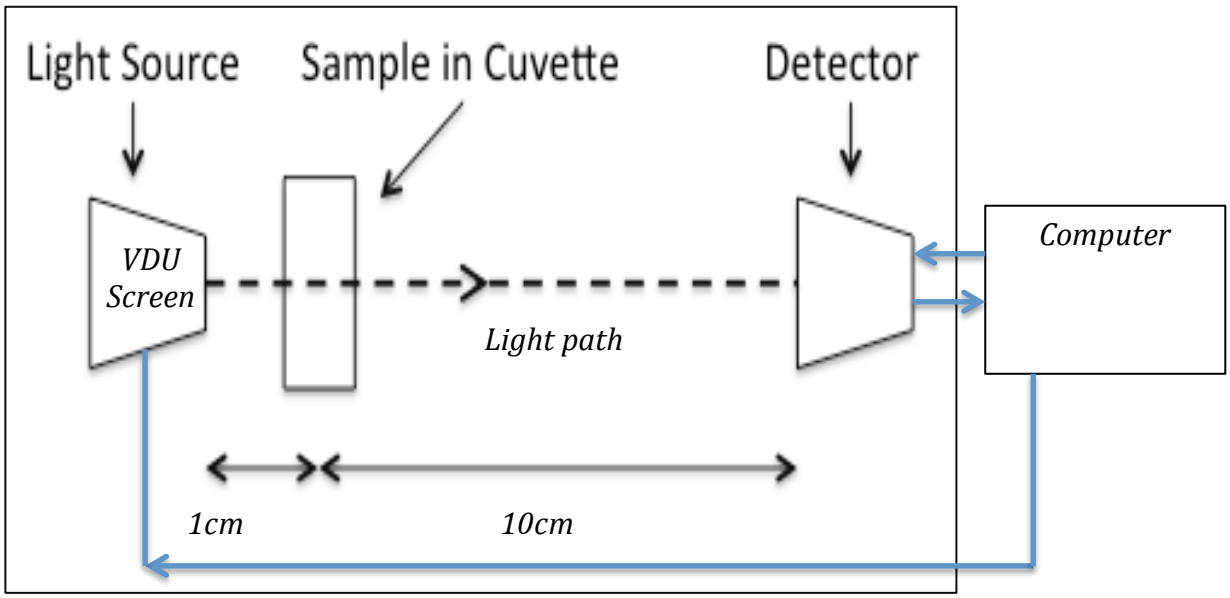

Figure 4.6: Schematic diagram of the chromatic optical transmission system

Figure 4.7 shows an image of the system setup. The VDU screen formed a tool for providing a uniform of light source passed through the sample in the cuvette and was then captured for analysis using a CMOS webcam as the detector. The processed data was formatted in a text file as R, G and B (Red, Green and Blue) (Appendix I). Examples of images of various honey sample taken obtained with the CMOS webcam and VDU background screen are shown on figure 4.8.

The optical system setup (figure 4.7) was also adapted to capture the reflected ambient light from the calibration mixture samples. This was achieved by changing the illumination behind the sample cuvette to be black (i.e.no light) or by placing a black and a white card in turn between the sample and the VDU screen in order to stop light propagating through the sample.

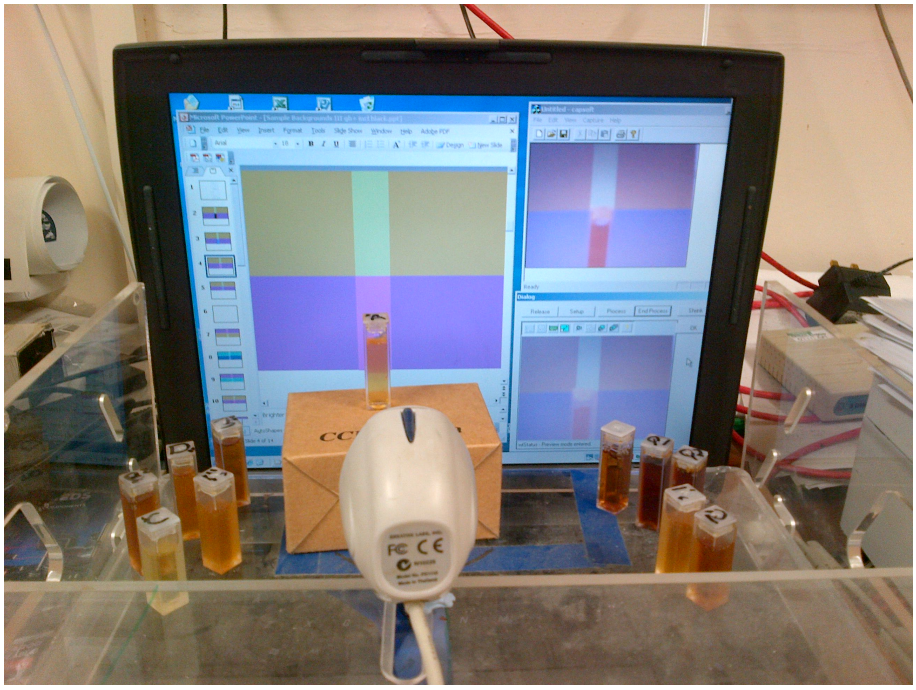

Figure 4.7: Image of the chromatic transmission systems setup

Example of Images of various honey samples taken from a webcam with a VDU screen as the light sources are shown on figure 4.8.

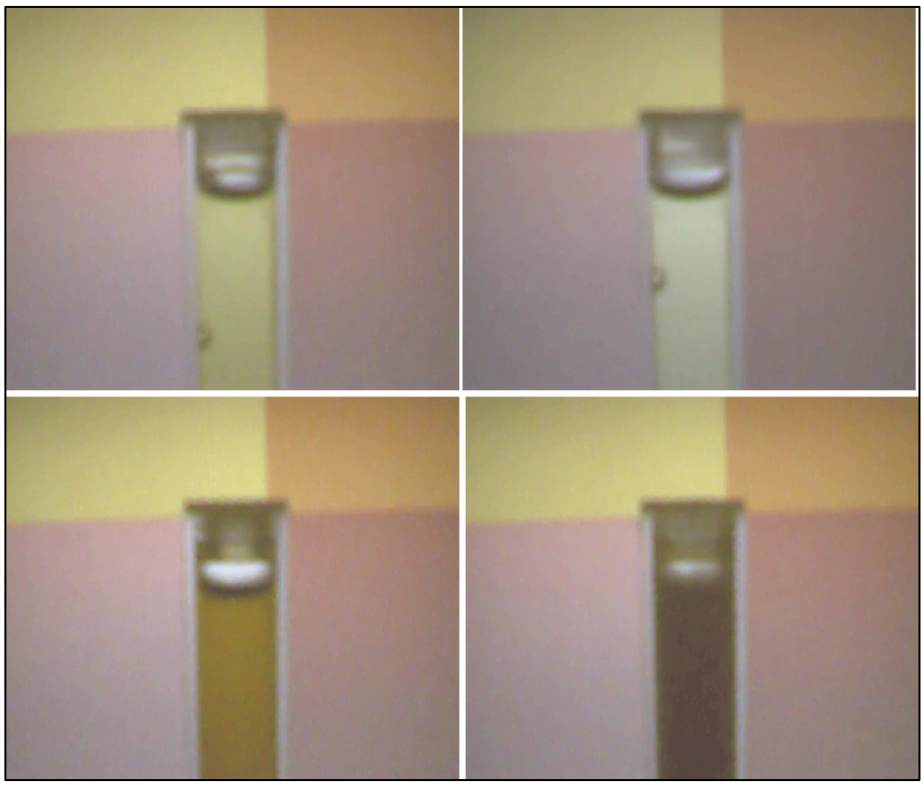

Figure 4.8: Examples of honey images taken the chromatic transmission systems setup

4.4.3 Portable Chromatic Optical fluorescence System

The portable chromatic optical fluorescence system is a system designed for the purpose of laboratory and field tests. Figure 4.9 shows the schematic diagram of such an optical system setup. Two light sources were positioned 6cm away from the sample in the cuvette and 6cm apart from each other and positioned at 45-degree angles with respect to the line of sight. This is to provide a forward illumination towards the center of the cuvette containing a honey (or a calibration mixture) sample. A black card is also positioned directly behind the cuvette to prevent any light provided by the VDU screen propagating through the sample and also for enhancing the images of scattered fluorescent light from the sample for enhanced detection. The detector capturing the fluorescent light from the sample is positioned 10cm away from the sample in cuvette.

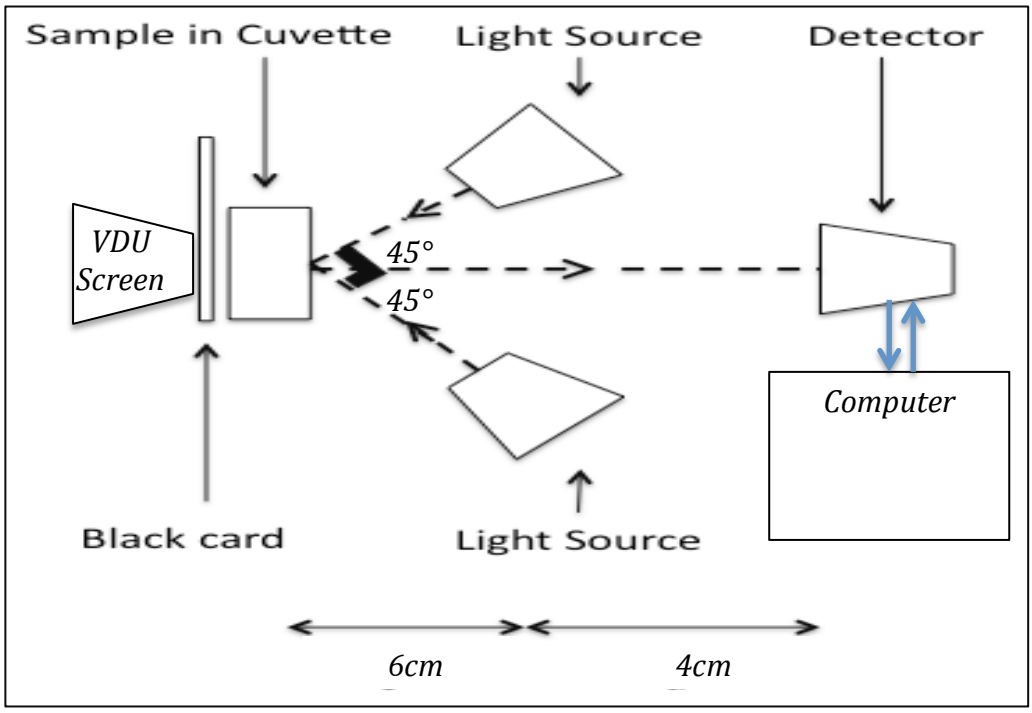

Figure 4.9: Schematic diagram of the chromatic optical flourecsence system

Figure 4.10 shows an image of the system setup. The two violet LED's provided uniform light sources and were driven by a stable current source circuit designed for maintaining stable light source through out the experiments. The two violet LED's provided forward illumination that passed through the front surface of the sample cuvette. The scattered fluorescent light from the front surface of the sample in the cuvette was then captured for analysis using the CMOS webcam as the detector. The processed data was formatted in a text file as R, G and B (Red, Green and Blue).

Figure 4.10: Image of the chromatic fluorescence systems setup

Examples of Images of various honey samples taken from the CMOS webcam with violet LED's as the light sources are shown on figure 4.11.

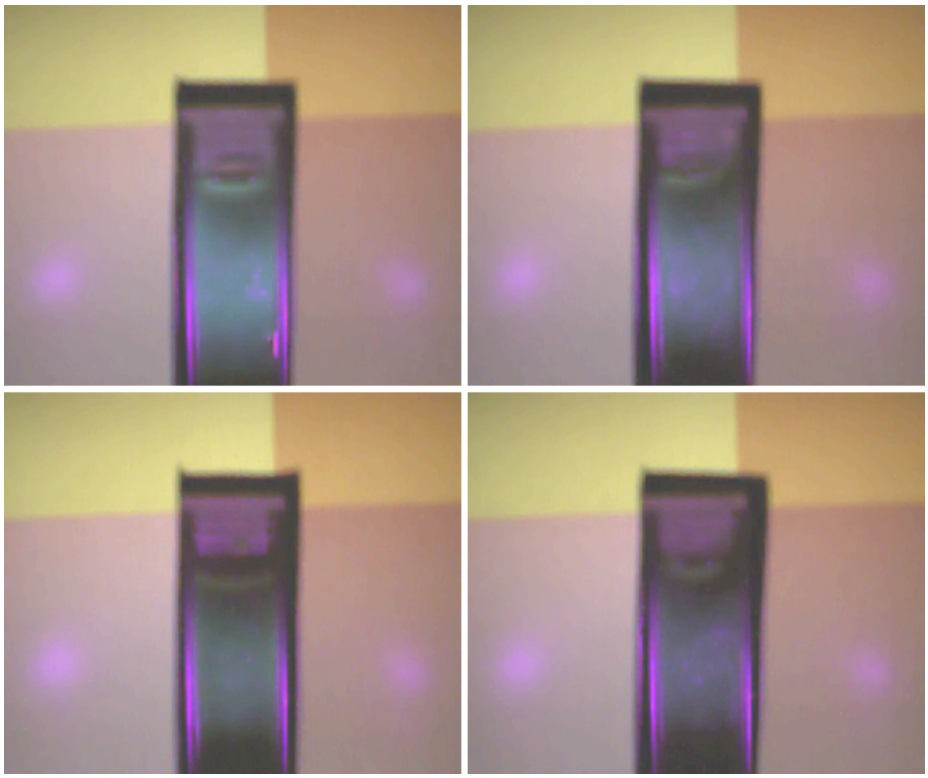

Figure 4.11: Examples of honey images using the chromatic fluorescence systems setup

4.4.4 Portable Chromatic Optical Polarization System

The portable chromatic optical polarization system was designed for the purpose of laboratory and field tests. Figure 4.12 shows a schematic diagram of such optical system with light source providing the back illumination, a fixed polarizing filter 1 positioned between the light source and the sample containing cuvette in front of the light source. A second rotational polarizing filter (analyzer) is positioned in front of the detector that is capturing the propagated light through the sample positioned.

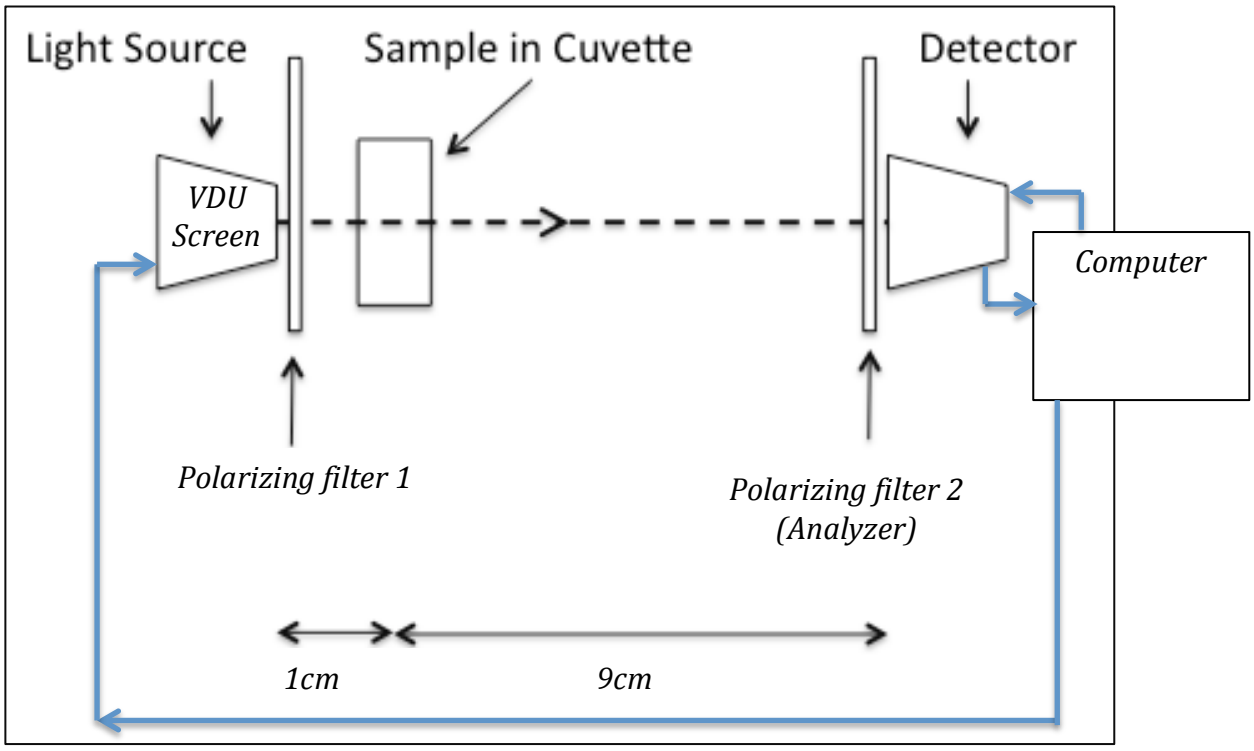

Figure 4.12: Schematic diagram of the chromatic optical polarisation system

The VDU screen formed a tool for providing uniform illumination. The light from the screen passed through the first fixed polarizing filter, the sample in the cuvette and the second rotational polarizing filter (analyzer) respectively. The transmitted polarized light is then captured for analysis using the CMOS webcam as the detector. The first fixed polarizing filter was oriented vertically and was been kept fixed at this position through out all the experiments. The second rotational polarizing filter (analyzer) was placed at various angles (0°, 30°, 45°, 70°) in turn. The processed data was formatted in a text file as R, G and B (Red, Green and Blue).

Examples of images of honey sample taken at (0°, 30°, 45°, 70°) rotational angles taken with CMOS webcam and VDU screen light source are shown on figure 4.13.

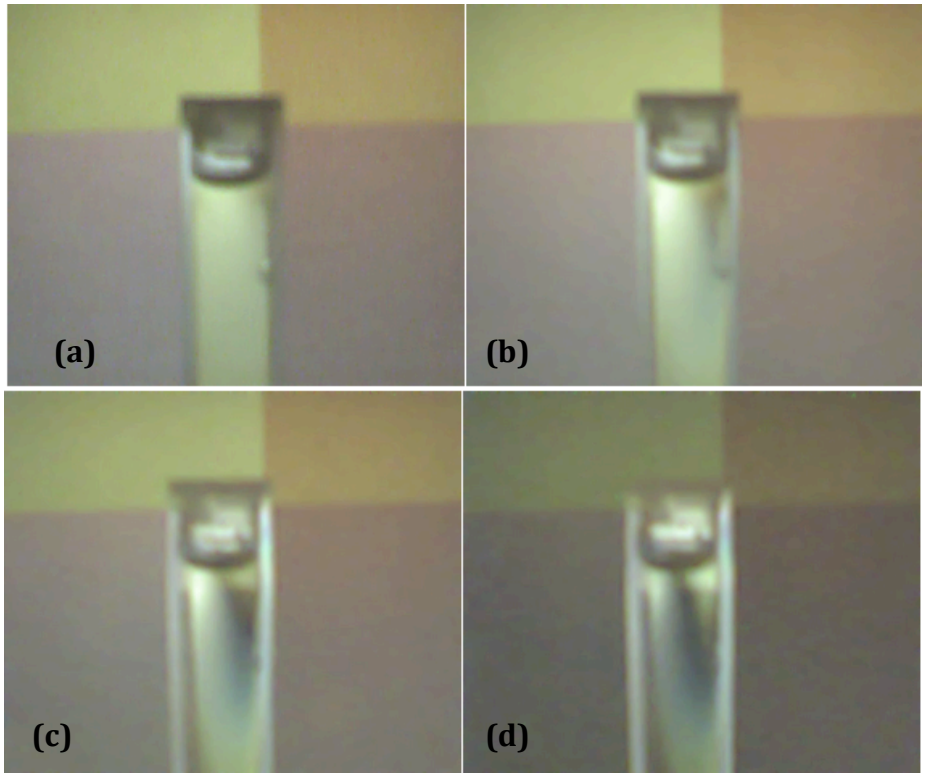

Figure 4.13: Examples of honey images taken using the chromatic polarisation systems setup at diffrent rotational angles((a) 0° angle, (b) 30° angle, (c) 45° angle, (d) 70° angle).

4.5 Summary

This chapter has described the three optical chromatic systems (transmission, polarization and fluorescence) for addressing complex composition liquids such as honey.

The handling and processing procedures of the test samples has been described, followed by a description of the optical systems used for extracting data for chromatic processing.

The cuvette for holding the samples to be addressed has been described, followed by a description of the methods used to capture images of honey and calibration mixture samples for additional chromatic analysis.

The honey sample contained in a cuvette was first addressed optically using a portable chromatic optical system with illumination provided by a VDU computer screen to monitor the optical transmission of light. A second system is described for illuminating the honey samples in a cuvette using a violet LED to produce the optical fluorescent light. The third system is described with illumination provided by a VDU computer screen and two polarization filters to address the optical rotation of light for optically active complex liquid samples.

Chapter 5

Chromatic Analysis Procedures

5.1 Introduction

The experimental and test data results for the honey and calibration samples presented in later chapters may be analyzed chromatically for accommodating the large amount of data without unacceptable loss of sensitivity and for extracting meaningful information from them.

The procedures and methodology for analyzing the test data are described in this chapter that are original and are new contribution to knowledge and to the chromatic analysis techniques. The manner in which referencing used for measuring test to test aberrations is described followed with procedures for normalizing the signal parameters. This leads to chromatic parameters suitable for use in chromatic calibration charts and maps. The production of primary chromatic maps is first described followed by the production of secondary chromatic maps.

5.2 Test Procedures

The processing procedures in each case involved capturing signals (S1, S2, Lref and Rref) from references placed in the test window (figure 5.1) followed by the test sample in the window.

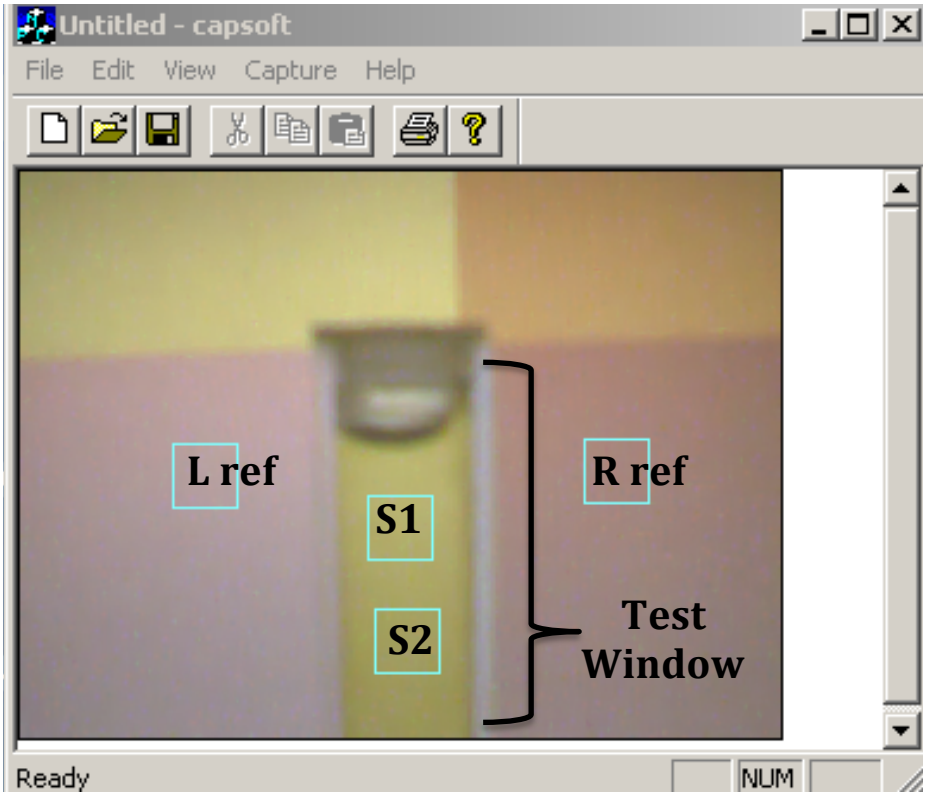

Figure 5.1: An example of a sample image with two reference areas Lref and Rref along with two sample addressing area S1 and S2

The reference elements represented the high and low ranges, which were different from each of the four optical tests (Transmission, reflection, Fluorescence and Polarization). RGB values of the high and low references were then used to normalize the sample RGB values. Figure 5.2 shows a general procedure chart from sample testing with different forms of light (Transmission, reflection, Fluorescence and Polarization).

This involved selecting

(1): Appropriate Illumination (transmission, reflection, polarization, and fluorescence) (Table5.1).

(3): Chromatic high and low references for each illumination (Table 5.1)

(4): Capturing R, G, B outputs

(a) R, G, B outputs for (i) Test sample, (ii) High reference, (iii) Low reference

(b) R, G, B outputs for the same reference area (Lref & Rref) for: (i) Test sample, (ii) High reference, (iii) Low reference

(5): Correcting the window R,G,B in each case with the corresponding reference area R, G, B.

(6): Normalizing on a scale (0-1) the corrected sample R, G, B's using the corrected window references.

(7): Using the normalized R, G, B for chromatic characterization (choosing the appropriate R, G and B parameters for each illumination (Table 5.1)

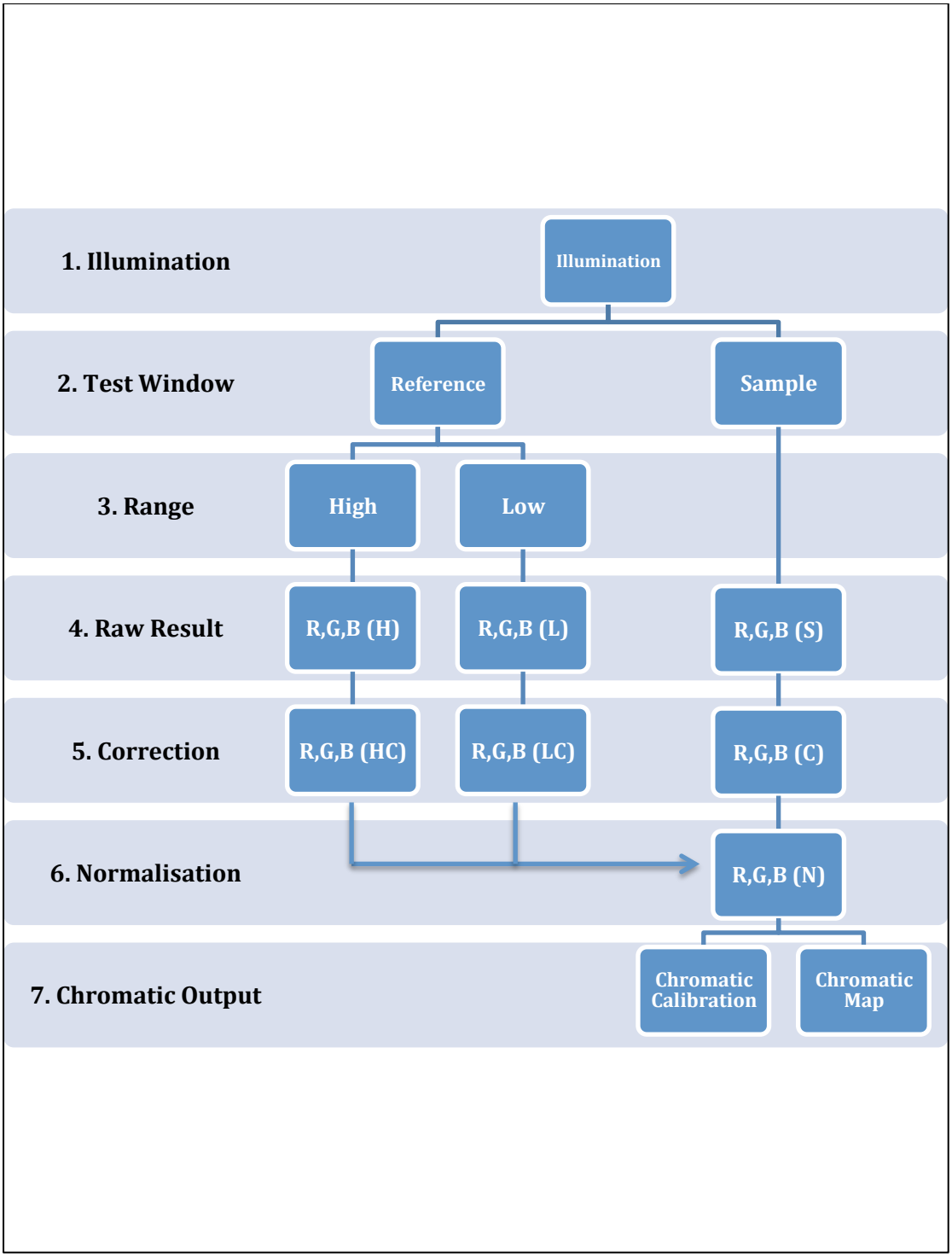

Figure 5.1:General flow chart for chromatic processing of different processing signals including (Transmission, Reflection, Fluorescence and Polarization), (1, 3 and 7 are different for the different illumination see (Table 5.1)).

Table 5.1 lists the particular forms of illumination, range reference and chromatic parameters used for each of the four types of optical signals for the procedure shown on figure 5.2

Light from	**Transmission**	**Reflection**	**Fluorescence**	**Polarization**
(1) Illumination	*VDU Screen*	*Ambient*	*Violet LED*	*VDU Screen + polarizing filters*
(3) Range reference **<u>High</u>**	*Water*	*Water + White card*	*Maximum sample + Black card*	*Maximum sample*
<u>Low</u>	*Minimum sample*	*Water + Black card*	*Water + Black card*	*Minimum sample*
(7) Primary Chromatic Parameters	*B : R*	*B : R*	*G : B*	*R : B*

Table 5.1: Particular forms of illuminations, window reference range and chromatic parameters used with each type of optical signal (Transmission, Scattering, Fluorescence, Polarization) in flow chart (figure 5.2).

With the optical transmission, the illumination was from a VDU screen, the reference ranges in the window used water (high) and a minimum sample, the preferred chromatic parameters being R and B.

For light reflection, ambient light was used with window reference ranges of water with white card (high) and black card (low) references, the preferred chromatic parameters being R and B.

For the fluorescence tests illumination was produced by a violet LED, the high and low reference ranges were respectively a maximum sample and water both with black card and the preferred chromatic parameters were G and B.

The polarization tests used the VDU screen illumination with a polarizing filter (the camera viewing this with a rotated polarizing filter) with high and low reference ranges of maximum and minimum samples and the preferred chromatic parameters were R and B.

The R, G and B output values of the experimental tests are checked with regard to their relative magnitudes. If any of the outputs approach saturation (i.e. R, G, B → 0, R, G, B → 1) then that output is eliminated from further analysis since it has effectively lost sensitivity.

The correction factor ($\mathbf{L_{cf}}$) for the sample and the reference in the test window for any aberrations that may occur from test to test is given by:

$$L_{cf} = \frac{L(benchmark)}{Lref} \tag{5.1}$$

Where L(benchmark) is the R, G, B benchmark values chosen for the colour background of the reference check area and Lref is the captured R, G, B values of the left reference check area.

In all cases the corrected values ($\mathbf{X_c}$) of the sample and references in the test window were given by:

$$X_c = X_s \times L_{cf} \tag{5.2}$$

Where $\mathbf{X_s}$ is the raw R, G, B of the test window sample and $\mathbf{L_{cf}}$ is the correction factor.

The normalized values in each case were:

$$X_N = \frac{X_c\,(s) - X_c\,(min)}{X_c\,(max) - X_c\,(min)} \tag{5.3}$$

Where $\mathbf{X_c(s)}$, $\mathbf{X_c(min)}$, $\mathbf{X_c(max)}$ are the corrected values of the sample, minimum reference and maximum reference respectively.

A more detailed discussion of the correction and normalization procedure for (Transmission, Reflection (i.e. Turbidity), Polarization and fluorescence) tests together with list of equation used for analyzing raw RGB data are given in Section 7.4, Chapter 7.

5.3 Production Of Chromatic Maps

Two sets of chromatic maps are produced

1. Maps for checking data validity (Primary Calibration Graphs)
2. Maps for use by the "user" (User Graphs)

5.3.1 Primary Calibration Graphs

Primary Check Graphs have two subsets:

(a) Raw data checks – for checking validity of measured parameters

(b) Reference area checks – for checking variability of image reference areas "choosing the most responsive parameters from trial tests minimizes the numbers of graphs."

5.3.1.1 Sample Calibration

The data calibration graphs are of the form shown on figure 5.3 which shows the variation of the corrected values $\mathbf{X_c}$ = R, G, B for each of the four different optical domain signals i.e. liquid transmission, reflection, polarization and fluorescence over the measurement range.

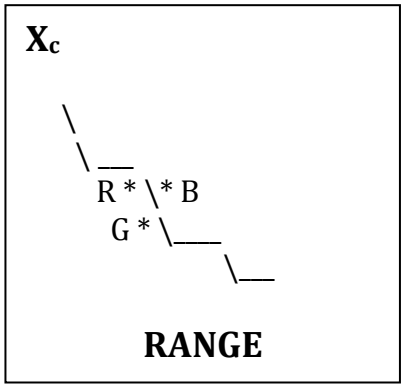

Figure 5.3: Sample calibration graph applicable to (Liquid Transmission {X(liq)=R(liq), B(liq)}, Reflection {X(tur)=R(tur), B(tur)], Polarization {X(pol)=R(pol), B(pol)}, Fluorescence {X(flo)=G(flo), B(flo)])

5.3.1.2 Reference Area Checks

The RGB data of the reference areas on each image are checked for the level of repeatability and for any variations from test to test. $\mathbf{X_{ref}}$ = R, G, B is the channel outputs from image reference area for each of the four different optical domain signals i.e. liquid transmission, scattering, polarization and fluorescence over number of tests (figure 5.4).

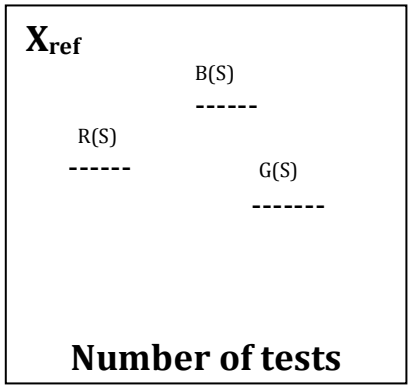

Figure 5.4: Reference area check graph for the three optical domain tests (Liquid Transmission, Reflection, Polarization, Fluorescence). X_{ref} is the range on graph

The horizontal dotted lines shows the set calibration level. This is to show the difference in the reference area values compared with the sample in the cuvette that can be corrected for any aberrations.

5.3.2 User Graphs

The types of user graphs that have been developed are:

(a) Calibration Graphs – chromatic parameter versus calibrated concentrations (liquid, turbidity, polarization, fluorescence)

(b) Primary Chromatic Maps – for distinguishing selected clusters of interest for the measured samples

5.3.2.1 Chromatic Calibration Graphs

Four calibration graphs are produced corresponding to each of the type of the optical signals monitored i.e. transmission, turbidity, fluorescence and polarization. Each type of optical signal chromatic parameter $\mathbf{X_N}$ normalized according to (Equation 5.3) are plotted as a function of the range (figure 5.5). (Where $\mathbf{X_N}$ = R(N), G(N), B(N), B/R (N), G/B (N), etc.)

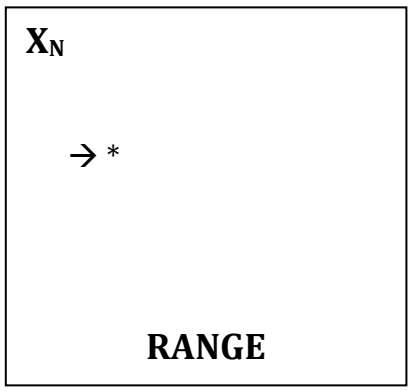

Figure 5.5: Chromatic calibration graph X_N vs. Range applicable to (Liquid Transmission {X_N=R(liq)N, B(liq)N}, Turbidity {X_N =R(tur)N. B(tur)N}, Polarization {X_N=R(pol)N, B(pol)N}, Fluorescence {X_N =G(flo)N, B(flo)N}).

5.3.2.2 Primary Chromatic Cluster Maps

Likewise four cluster maps are produced corresponding to the optical signals monitored. In this case selected Chromatic parameters normalized with (Equations 5.3) are plotted against each other. An example of such a map is shown on figure 5.6 Where (liq), (turb), (pol), and (flo) are type of test, for example (optical liquid, turbidity, polarization, fluorescence).

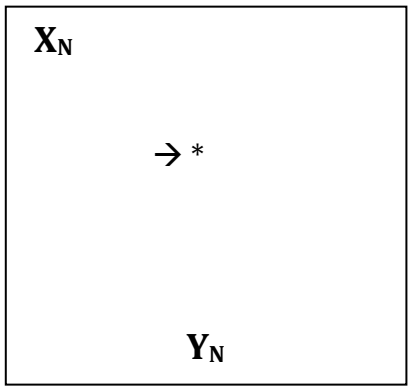

Figure 5.6: Primary Chromatic cluster map of X_N : Y_N applicable to(Liquid Transmission {X_N =R(liq)N, Y_N=B(liq)N}, Turbidity {X_N=R(tur)N, Y_N=B(tur)N}, Polarization {X_N=R(pol)N, Y_N=B(pol)N, Fluorescence {X_N =G(flo)N, Y_N=B(flo)N}).

5.4 XYZ Secondary Chromatic Mapping Procedures

Cartesian X, Y, Z diagrams (Section 2.6.5, Chapter 2) can be used to illustrate details about the sample distribution. Figure 5.7 shows such a typical X,Y,Z diagram with relevant relationships between X, Y, Z indicated.

The normalized parameters Rliq(N), Bliq(N), Rturb(N), Bturb(N), Gflo(N) ,Bflo(N), Rpol(N), Bpol(N) and the B/R liq(N), G/B flo(N) and B/R pol(N) can be used to form XYZ maps.

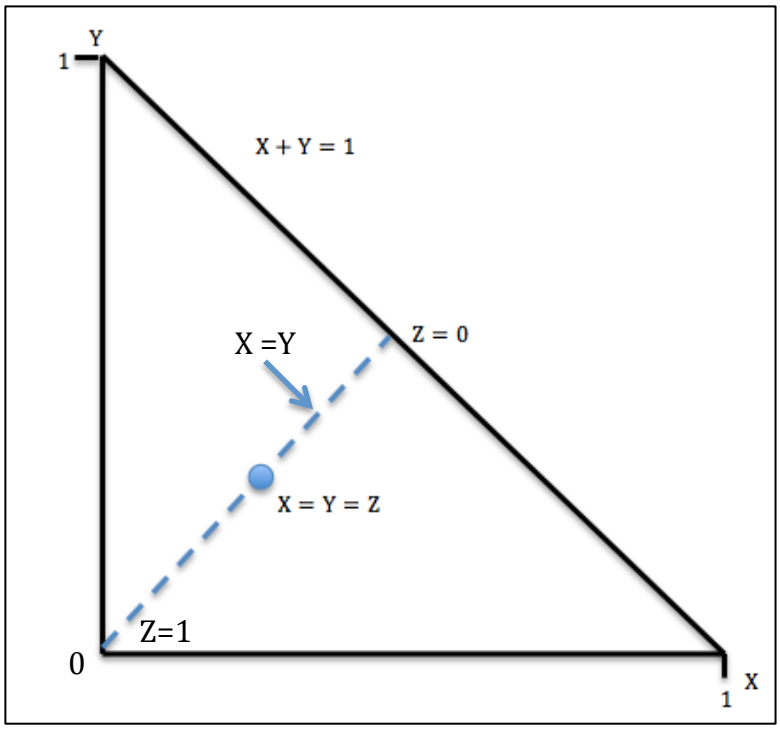

Figure 5.7: Cartesian X, Y, Z diagram

Secondary chromatic XYZ maps have been used to combine the various sets of results (transmission, fluorescence and polarization). This enables results to be presented on a single diagram for extracting relevant information from the chromatic signatures. It distinguishes the relative significance of transmission, polarization and fluorescence components.

The chromatic parameters used for the XYZ maps were the ratios of the normalized dominant wavelengths B/R or G/B (i.e. the gradient of the locus connecting the sample point to the origin on the R:B and G:B maps) for the different optical signals (transmission, polarization and fluorescence). These parameters are defined mathematically by the following equations:

$$Fluorescence\ parameter\ (Z) = \frac{G}{B}\ flo(N) \tag{5.4}$$

$$Transmission\ parameter\ (X) = \frac{B}{R}\ liq(N) \tag{5.5}$$

$$Polarisation\ parameter\ (Y) = 1 - \frac{B}{R}\ pol(N) \tag{5.6}$$

With

$$3L = (Z + X + Y) \tag{5.7}$$

5.5 Assessment Flow Chart

An assessment flow chart showing the philosophy for relating optical properties of light and visually observed properties of complex liquid to decision making on the condition of the sample is one single graph analysis is shown in chapter 9 and discussed for application use in honey quality decision making.

5.6 Calibration Mixtures

To indicate the form and features of chromatic cluster maps and to address the issue of the effect of complex liquid mixtures on chromatic signatures, preliminary tests were performed on controlled mixtures of some common clear and turbid liquids plus some laboratory prepared honey and syrup mixtures.
This section describes tests with liquid components mixtures of water-tea-milk and mixtures of water- syrup-honey.

5.6.1 Water, Tea, Milk Calibration Mixtures

The water and tea mixtures were used to represent optical variations produced by changes in relative concentrations of two clear liquids with different polychromatic optical transmission properties. Tests with water and milk are representative of optical variations produced by changes in relative concentrations of components, one of which (milk) produces turbid condition in a clear liquid. Milk is often used for controlled exploratory tests involving turbidity (Prerana, Shenoy et al. 2008) and it was chosen for the present controlled tests to form mixtures with water and tea. Tests with tea, water and milk represent the further complex condition of optically different clear liquids (water and tea) with a turbid medium (milk).

5.6.2 Water-Syrup-Honey Mixtures

The water, syrup and honey mixtures tests include additional optical phenomena to transmission and absorption to be considered. These are polarization and fluorescence. Tests with water-syrup and water-honey are representative of optical variations produced by changes in relative concentrations of components, one of which (glucose/fructose) produces a sugar solution mixture condition in a pure liquid. Tests with honey-syrup represent the further complex condition of optically different viscous liquids (honey and syrup) with an invert sugar medium (syrup).

5.7 Summary

This chapter has presented the procedures for chromatically analyzing test data that leads to chromatic parameters suitable for use as chromatic calibration charts, primary plus secondary cluster maps for the various types of optical signals (liquid transmission, Turbidity, Polarization and fluorescence).

It has also described the procedure used in referencing to correct test-to-test aberrations and for normalizing test samples within a reference range.

Chromatic cluster maps are also described which accommodate large amount of data obtained from various optical tests for relevant extraction of information.

The use of an assessment flowchart relating to the optical characteristics and properties of liquid for decision-making capability on the condition of the sample has been described.

The use of turbid and clear complex liquids mixtures used for calibration has been described and have related to back to optical properties in liquids.

Chapter 6

Experimental Results

6.1 Introduction

This chapter will present the raw experimental results that were gathered initially from the optical experimental systems (Chapter 4). The purpose of this chapter is to review some experimental data to give the reader an introduction to examples of visual images taken by such a monitoring system and the raw RGB data results. Test calibrations and system stability results also presented for mixtures of pure, clear and turbid liquids (water, tea and milk) using transmission and reflection/scattering of light. Other test calibrations have been presents for mixtures of pure and viscous liquids (water, syrup and honey) using transmission, fluorescence and optical polarization of light. Finally the raw RGB data results of honey samples (which represent a mixture of clear, turbid and viscous liquids) are presented including the use of transmission, fluorescence and polarization, each being shown as visual images and the basic output parameters RGB.

6.2 Calibration Mixtures (Water-Tea -Milk)

Prior to the test sequence, water image sample is to be taken with:
(a) Screen illumination (+ reference screen either side) this is the screen light and ambient light.
(b) Black Screen illumination (+ reference screen either side) this is to measure the reflection/scattering of the ambient light.

For each test, a sample image is taken with:
(a) Screen illumination (+ reference screen either side) this is the screen and ambient light.
(b) Black Screen illumination (+ reference screen either side) this is to measure the turbidity from the ambient reflected/ scattered light.

In all cases the VDU screen was switched on to provide reference signals either side of the cuvette test region. Thus the screen illumination will contribute indirectly to the ambient Illumination.

6.2.1 Visual Examples Of Transmitted Light Images

Figure 6.1 shows example of four images of samples when light has been transmitted through pure clear liquid (water) and mixtures of clear liquid (tea) at weak and high concentration strength as shown on figures 6.1 (a), (b) and (c) respectively. The VDU sections around the cuvette holding the sample are used for referencing. The section with the VDU behind the cuvette holding the sample gives the light transmitted through the sample.

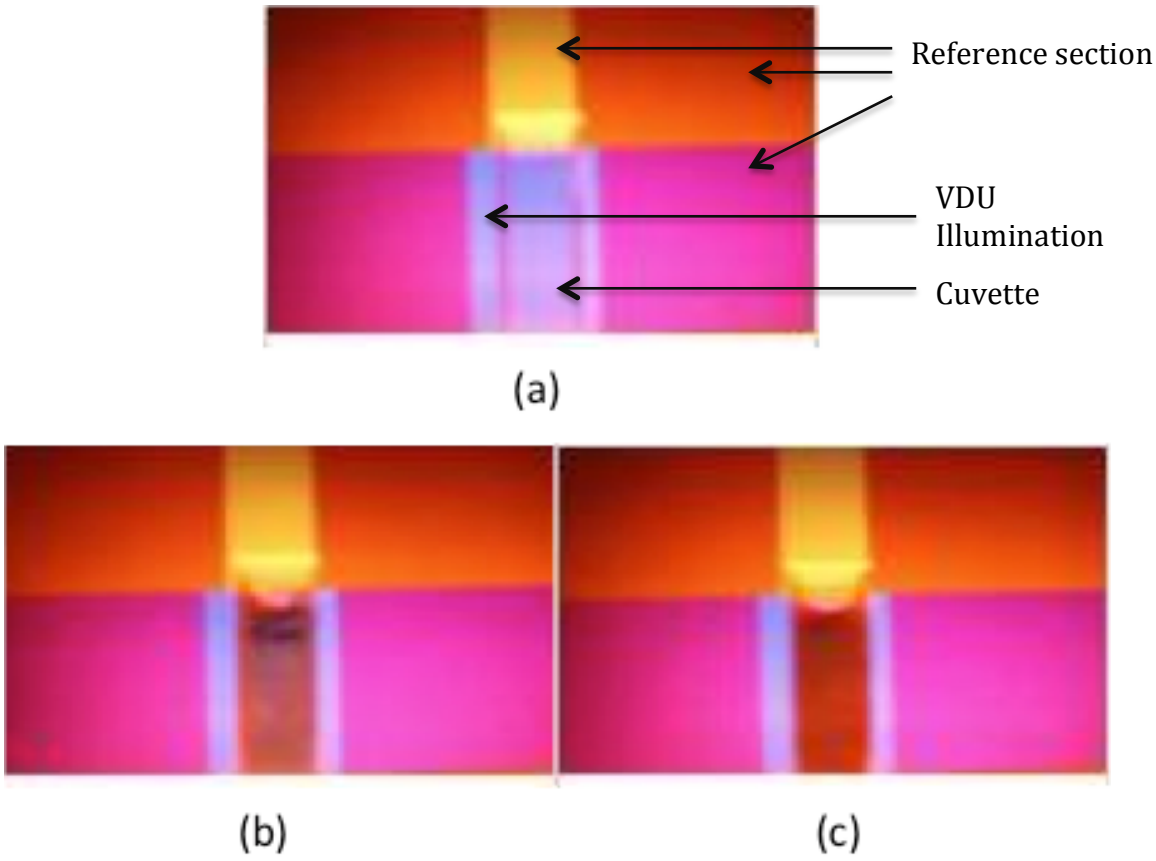

Figure 6.1: Visual images of (water-tea mixtures) with transmitted blue illumination behind cuvette

(a) Pure clear liquid [water]

(b) Clear liquid [tea weak concentration]

(c) Clear liquid [tea high concentration]

Figure 6.2 shows examples of three images of samples when light has been transmitted through a pure clear liquid (water), a mixture of medium turbid liquid (water and 5 drops of milk) and a mixture of highly turbid liquid (water and 10 drops of milk) (figures 6.2(a), 6.2(b) and 6.2(c) respectively).

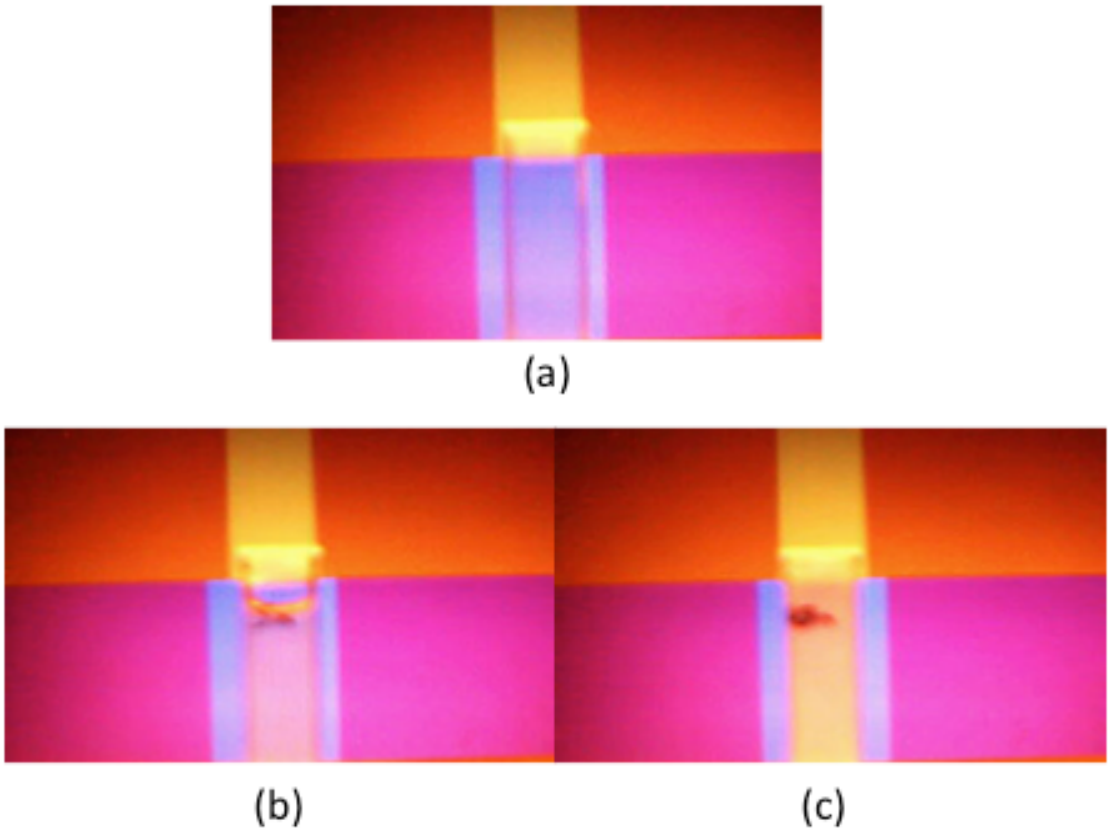

Figure 6.2: Visual images of (water-milk mixtures) with transmitted blue illumination behind cuvette

(a) Pure clear liquid [water]

(b) Turbid liquid [water + milk 5drops]

(c) Turbid liquid [water + milk 10 drops]

Figure 6.3 shows examples of four images of samples when light was transmitted through a mixture of medium clear and turbid liquids at different concentrations (tea and 5 drops of milk), (tea and 10 drops of milk), (tea and 15 drops of milk) and (tea and 30 drops of milk) as shown on figures 6.3(a), 6.3(b), 6.3(c) and 6.3(d) respectively.

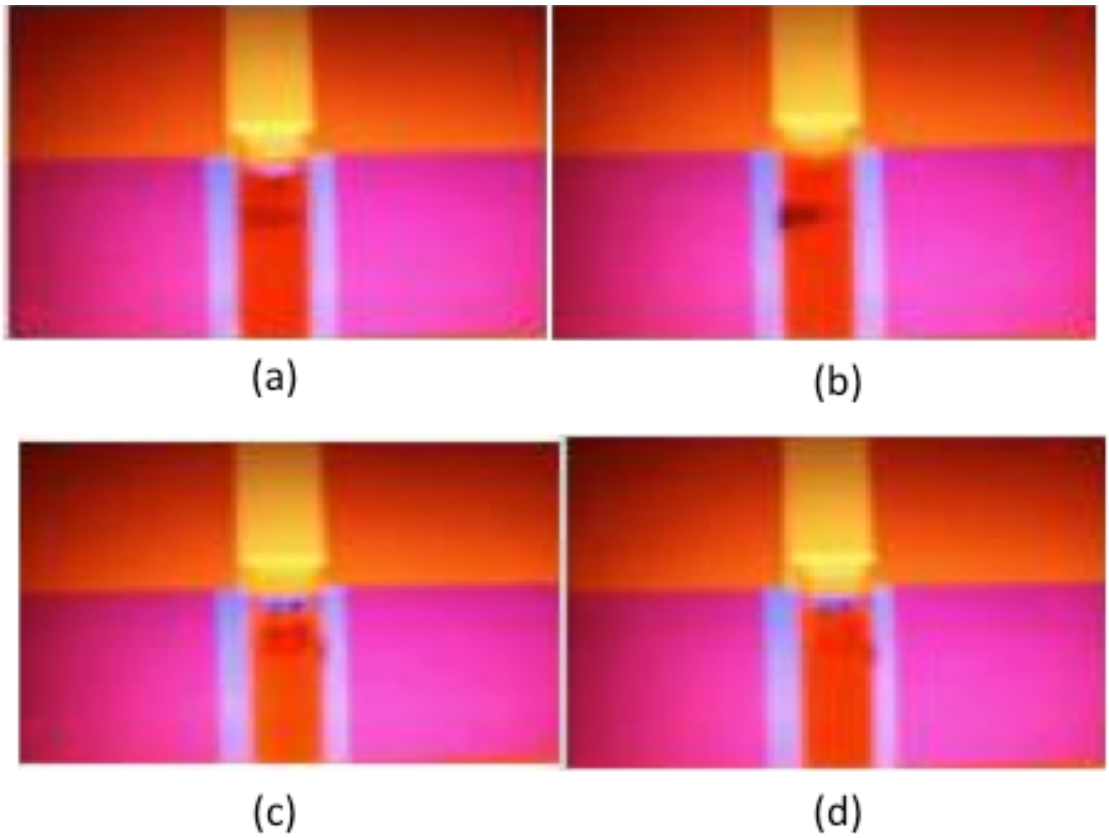

Figure 6.3: Visual images of (tea-milk mixtures) with transmitted blue illumination behind cuvette

(a) Mixture of Clear and Turbid liquid [tea+ milk 5 drops]

(b) Mixture of Clear and Turbid liquid [tea+ milk 10 drops]

(c) Mixture of Clear and Turbid liquid [tea+ milk 15 drops]

(d) Mixture of Clear & Turbid liquid [tea+ milk 30 drops]

6.2.2 RGB Outputs of sample Images Of Transmitted Light

R, G, and B data were extracted from a specified area on the various images as shown on the example image on figure 6.4 and were analyzed using the (Capsoft) software (Appendix I). The R, G and B raw data outputs for water, tea and milk tests are shown on figures 6.5, 6.6 and 6.7 obtained with blue screen illuminations respectively. The results illustrate the complex variation in the R, G and B values produced by the different samples.

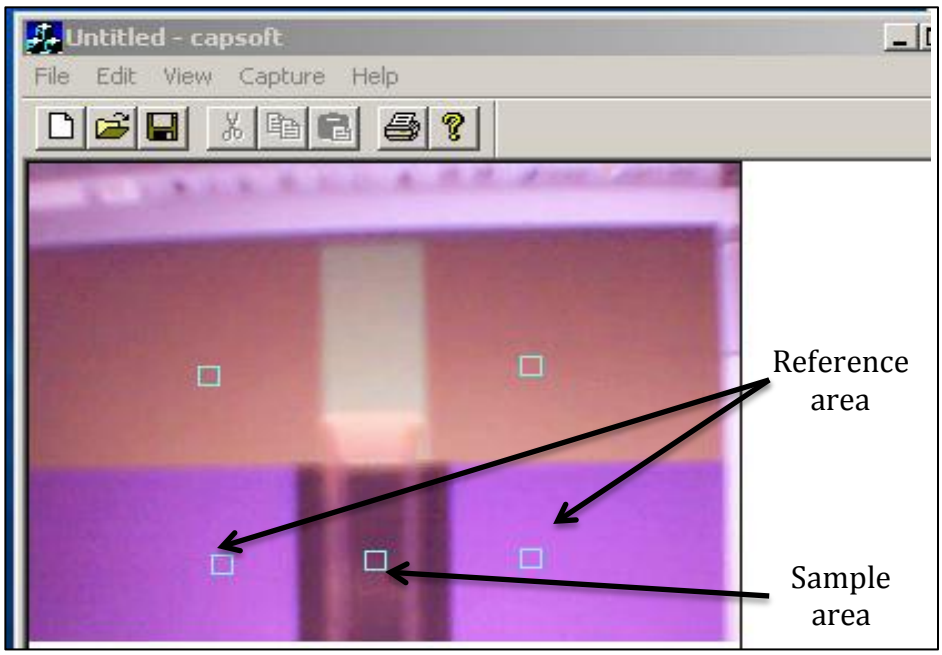

Figure 6.4: Example of a water sample image with Black screen illumination showing five specified areas were RGB data are extracted from

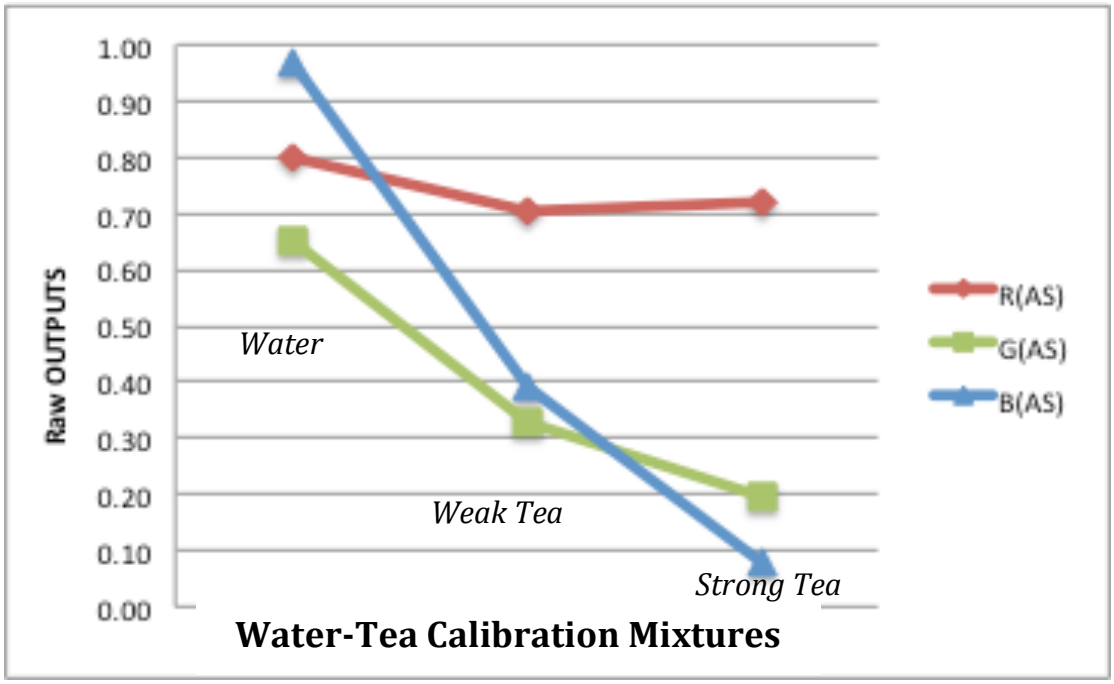

Figure 6.5: Raw RGB outputs vs water- tea mixtures with blue screen illumination

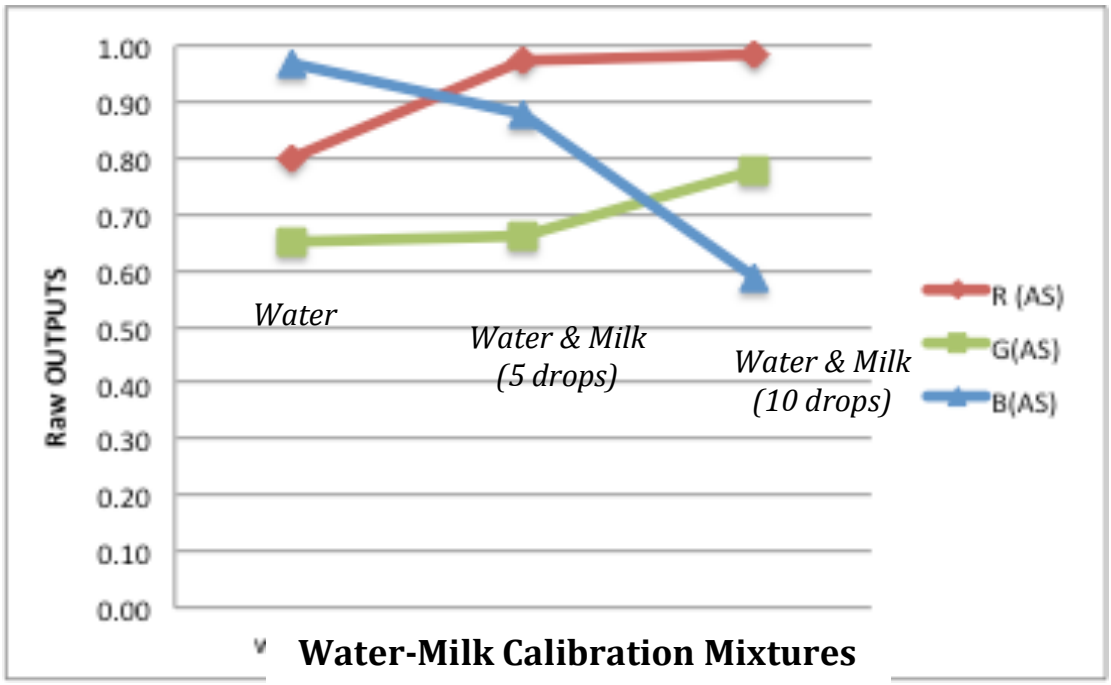

Figure 6.6: Raw RGB outputs vs water- milk mixtures with blue screen illumination

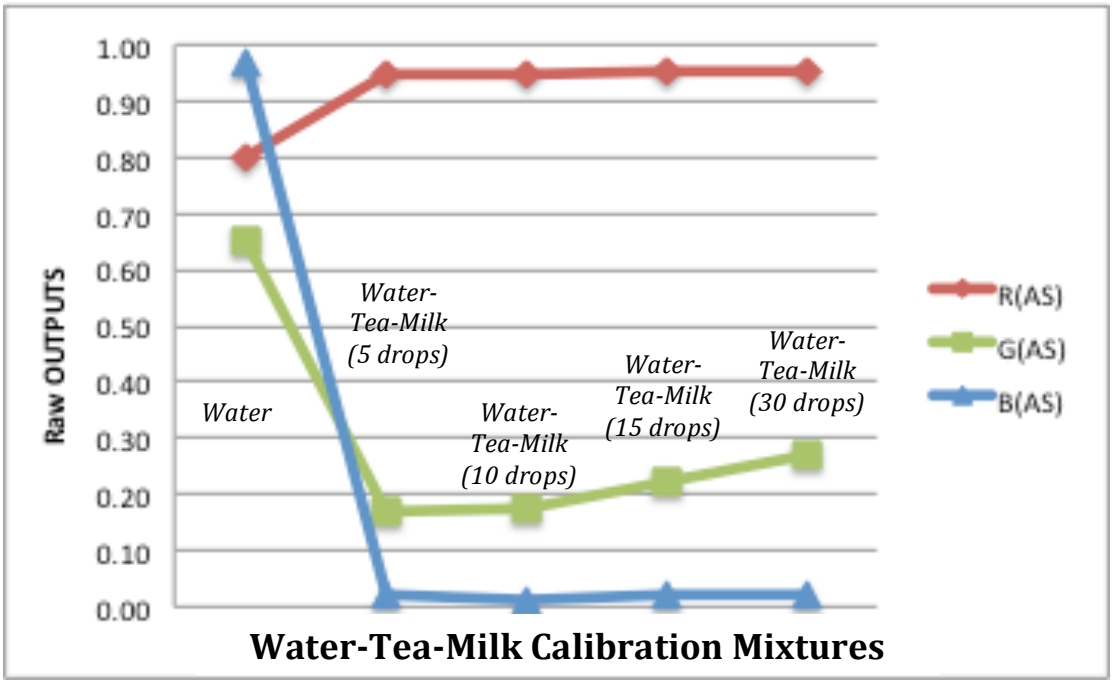

Figure 6.7: Raw RGB outputs vs water-tea-milk mixtures with blue screen illumination

6.2.3 Visual Examples Of Images Of Reflected Light

Figure 6.8 shows examples of three images of samples with a black screen behind the cuvette i.e. (black screen for minimum light transmission) in order to visualize ambient light reflected from a pure clear liquid (water) and mixtures of clear liquid (tea) at weak and high concentration strength (figures 6.8 (a), (b) and (c) respectively). The VDU sections around the cuvette holding the sample are used for referencing.

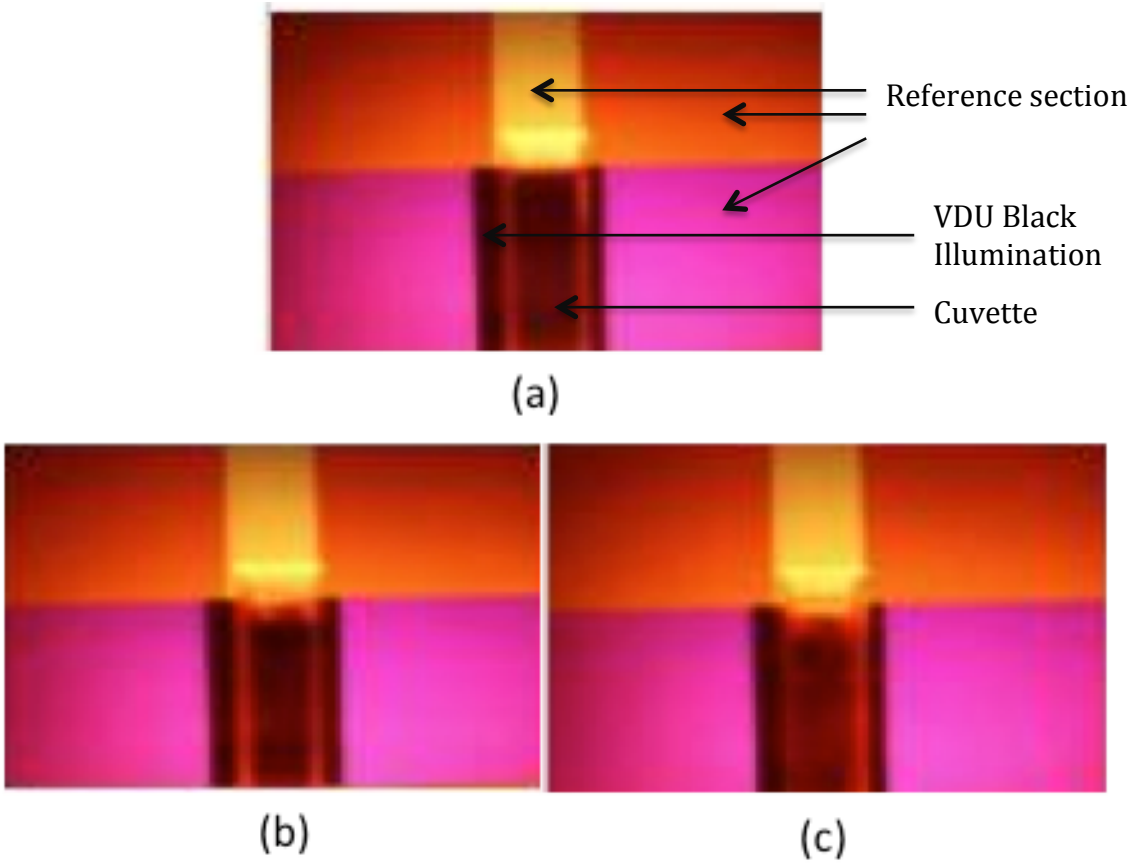

Figure 6.8: Visual images of water-tea mixtures with a black illumination behind cuvette:

(a) Pure clear liquid [water]

(b) Clear liquid [tea weak concentration]

(c) Clear liquid [tea high concentration]

Figure 6.9 shows examples of three images of samples when ambient light was scattered from a pure clear liquid (water), a mixture of medium turbid liquid (water and 5 drops of milk) and a mixture of high turbid liquid (water and 10 drops of milk) (figures 6.9 (a), (b) and (c) respectively).

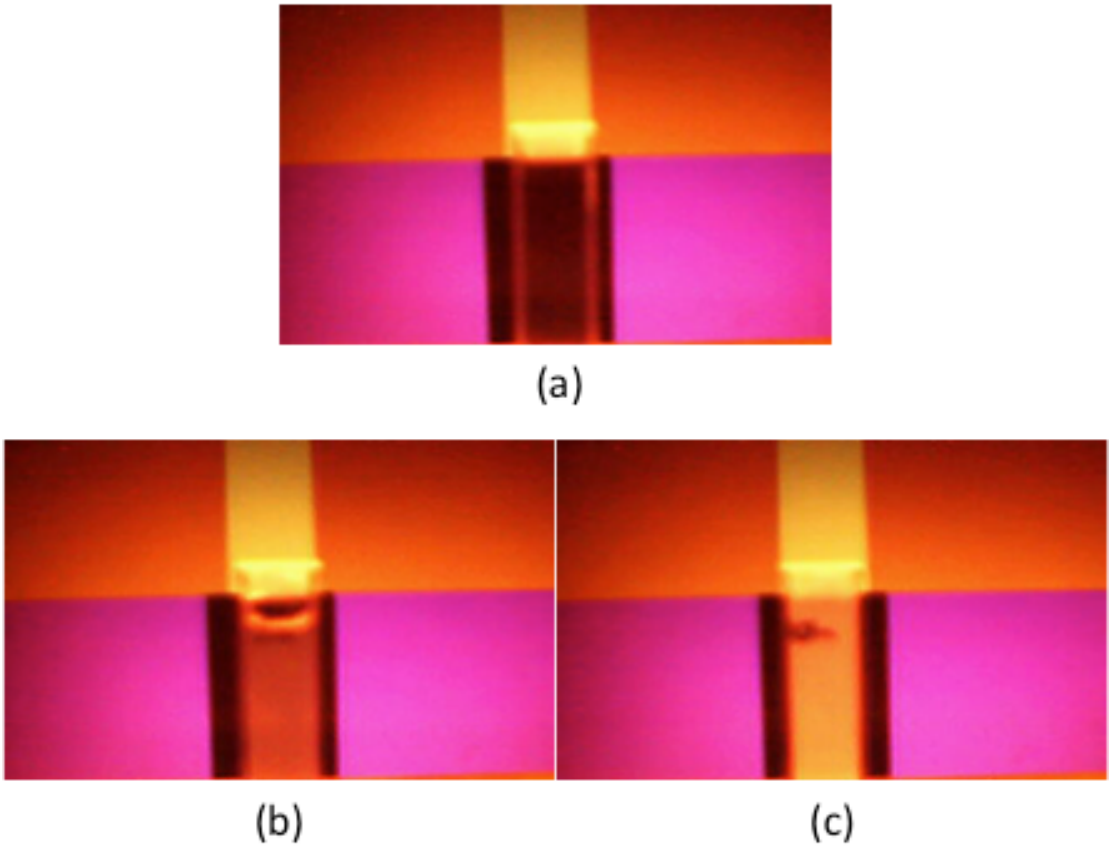

Figure 6.9: Visual images water-milk mixtures with a black screen illumination behind cuvette:

(a) Pure clear liquid [water]

(b) Turbid liquid [water + milk 5drops]

(c) Turbid liquid [water + milk 30 drops]

Figure 6.10 shows examples of four images of samples when ambient light was reflected from a mixture of medium clear and turbid liquids at different concentrations (tea and 5 drops of milk) , (tea and 10 drops of milk), (tea and 15 drops of milk) and (tea and 30 drops of milk) as shown on figures 6.10 (a), (b), (c) and (d) respectively.

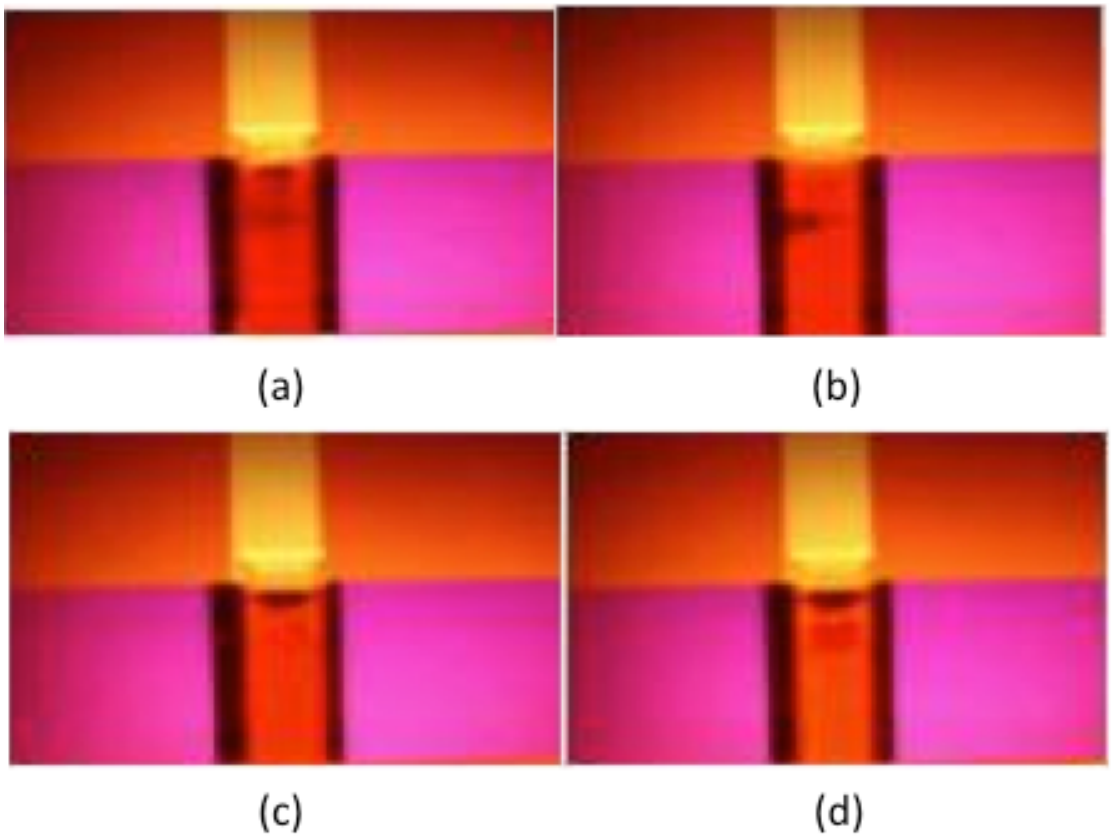

Figure 6.10: Visual images water-tea-milk mixtures with a black screen illumination:

(a) Mixture of Clear and Turbid liquid [tea+ milk 5 drops]

(b) Mixture of Clear and Turbid liquid [tea+ milk 10 drops]

(c) Mixture of Clear and Turbid liquid [tea+ milk 15 drops]

(d) Mixture of Clear & Turbid liquid [tea+ milk 30 drops]

6.2.4 RGB Outputs Of Example Images Of Reflected Light

The R, G and B raw data outputs for the water, tea and milk tests derived from the images of figures 6.8, 6.9 and 6.10 are shown on figures 6.11, 6.12 and 6.13 with black screen and reflected/scattered ambient light respectively. The results illustrate the complex variation in the R, G and B values produced by the different samples.

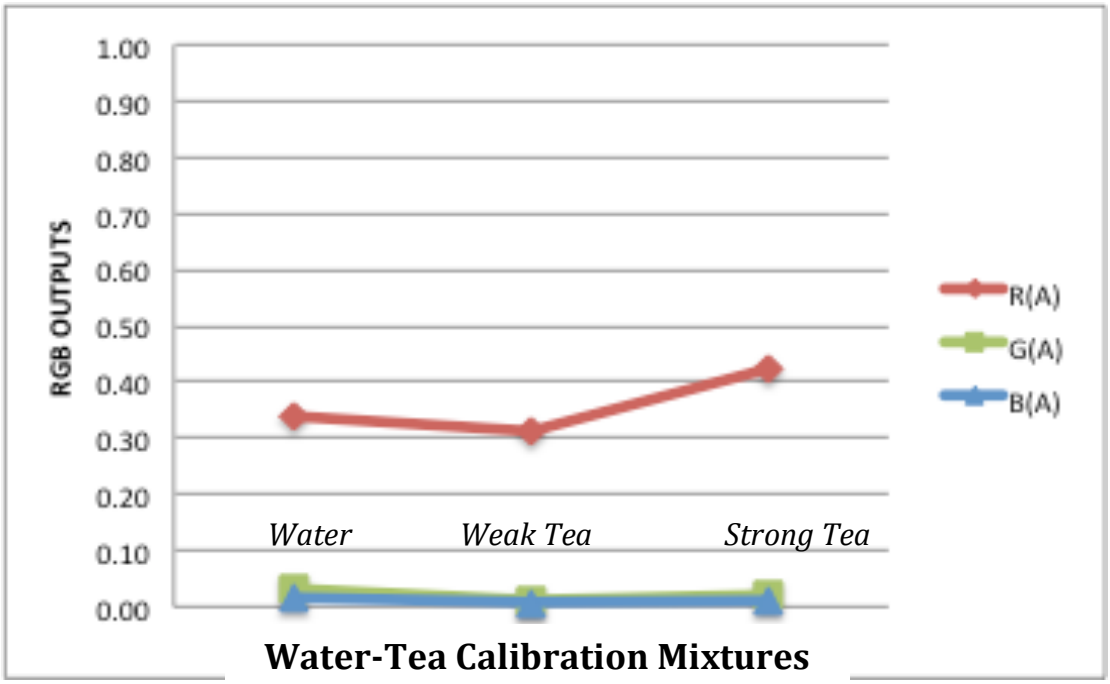

Figure 6.11: Raw RGB outputs vs. water -tea mixtures reflected/scattered ambient light

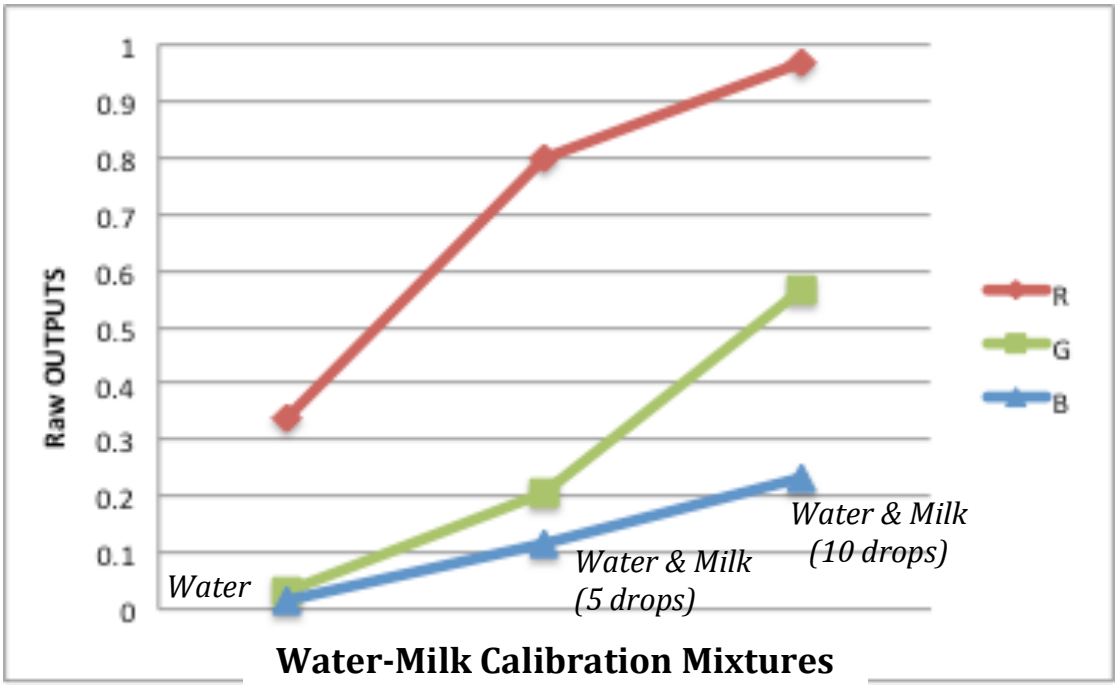

Figure 6.12: Raw RGB outputs vs. water -milk mixtures reflected/ scattered ambient light

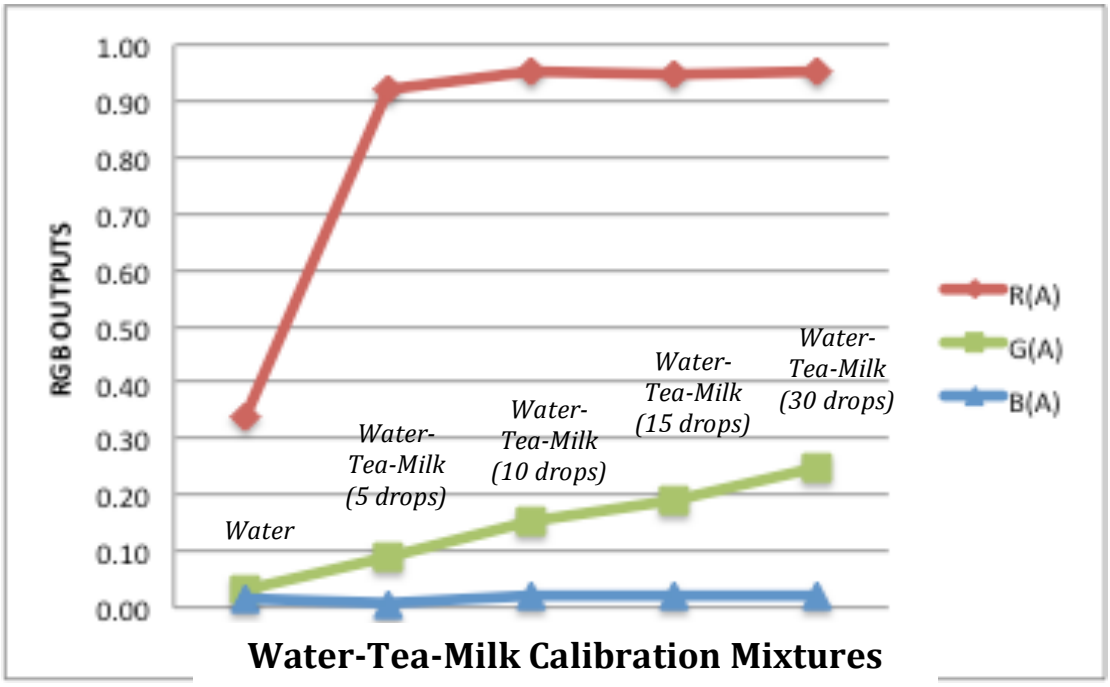

Figure 6.13: Raw RGB outputs vs. water-tea-milk mixtures, scattered ambient light

Figures 6.14 show the raw R, G, B data for the L (left) reference area with (water and tea), (water and milk) and (water, tea and milk) tests respectively. In all cases the VDU screen was switched on to provide reference signals either side of the cuvette test region. Thus the screen illumination and ambient illumination are both present.

The results show that in all cases an approximate level of repeatability for the RGB values of L (left) reference for all the tests. The results shows that the parameter values are all greater than 0.2, in all cases the G values are the lowest of the R, G, and B parameters and R is the highest of the order of 0.95.

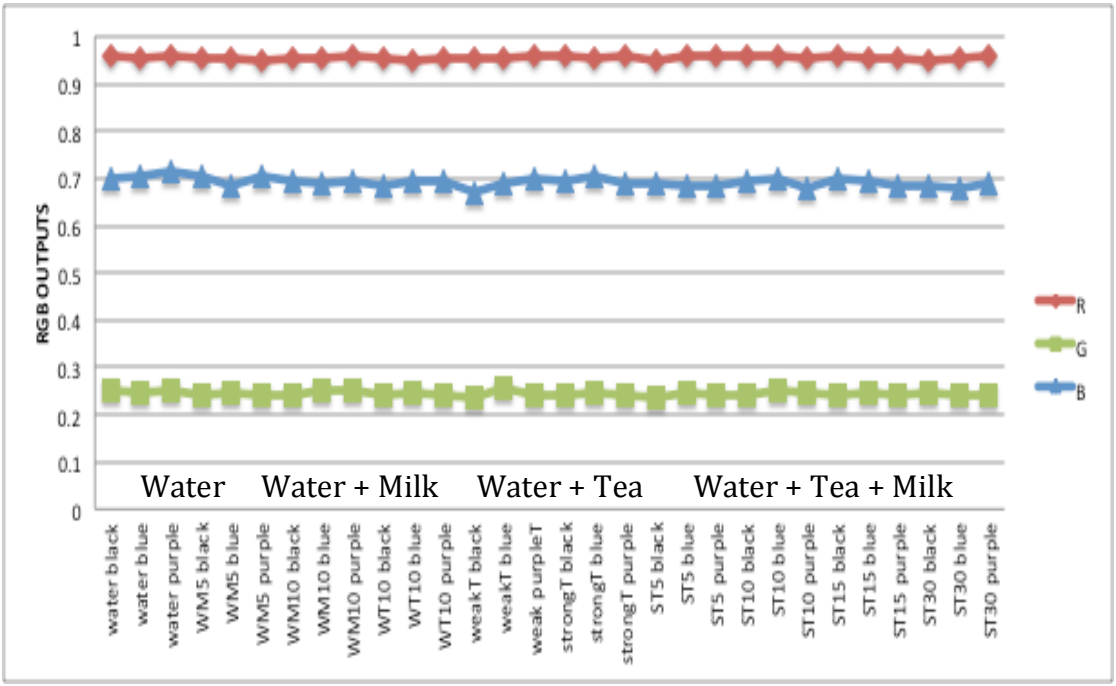

Figure 6.14: RGB outputs of the L (left) reference area with (water and tea), (water and milk) and (water, tea and milk) mixtures with VDU illumination and ambient light

6.3 Initial Honey Results Of The Optical Experiments

Prior to the test sequence, water image sample is to be taken with:
(a) Screen illumination (+ reference screen either side) this is the screen light and ambient light.
(b) Black Card placed between the water sample cuvette and the screen (+ reference screen either side) this is to measure the reflection of the ambient light.
(c) White Card placed between the water sample cuvette and the screen (+ reference screen either side) this is to measure the reflection of the Ambient light strength.

For each test, a sample image is taken with:
(a) Screen illumination (+ reference screen either side) this is the screen and ambient light.
(b) Black Card placed between the test sample cuvette and the screen (+ reference screen either side) this is to measure the turbidity from the ambient scattered light.

In all cases the VDU screen was switched on to provide reference signals either side of the cuvette test region.

6.3.1 Visual Examples Of Transmitted & Reflected Light Images

Figure 6.15 shows examples of images for water and four honey samples obtained with the CMOS webcam and VDU background illumination system (Chapter 4). These images show how the light transmission through the sample varies from little effect (sample SDR3 in figure 6.15(b)) to a high attenuation with little transmission (sample QDR1 in figure 6.15(e)).

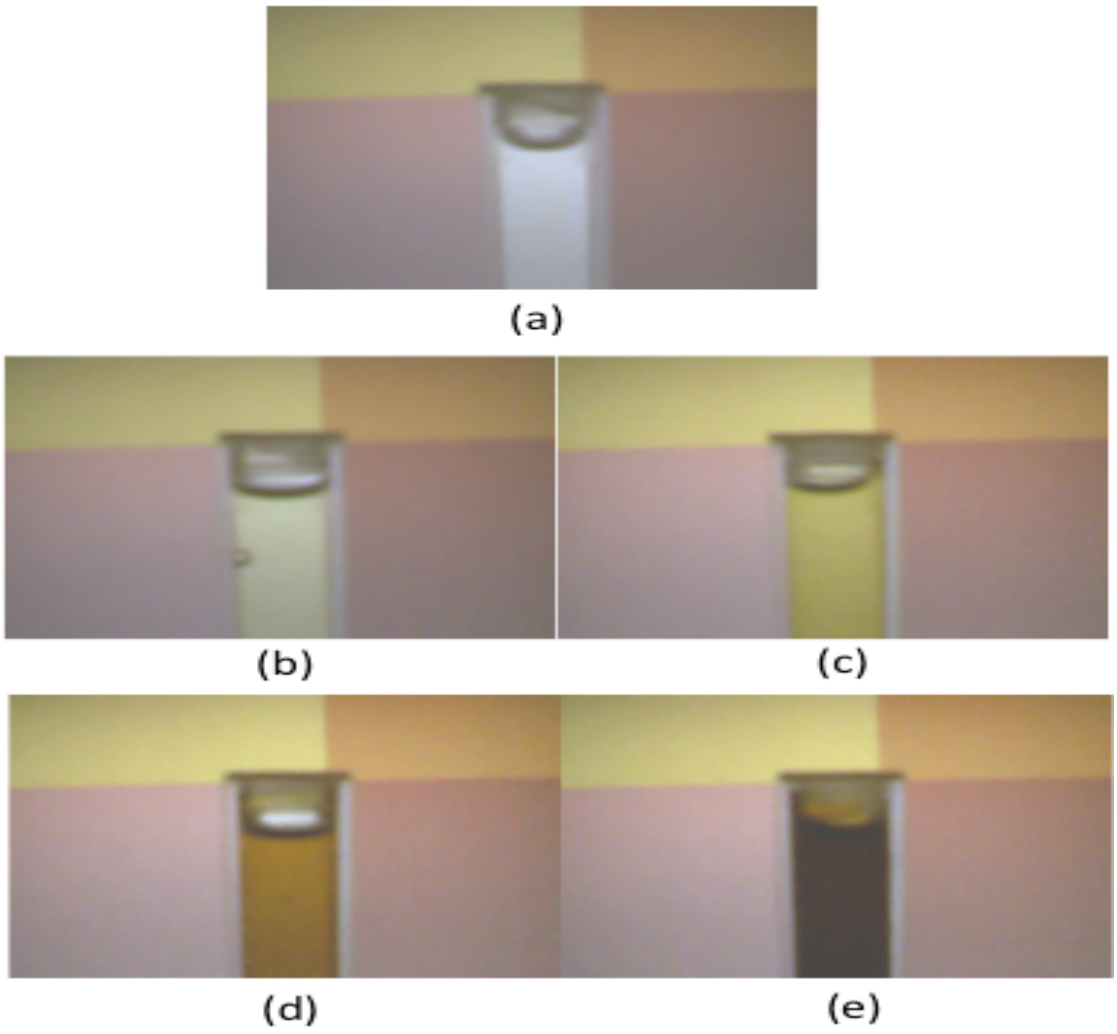

Figure 6.15: Examples of images of light transmitted through water and four different honey samples with white screen illumination: (a) water (b) SDR3 (c) SDR1 (d) SMR1 (e) QDR1

Figures 6.16 and 6.17 show examples of images of the same sample as figure 6.15 but with a different VDU illumination. Figure 6.15 shows an image captured with a white screen illumination, figure 6.16 shows an image captured with a blue screen illumination and figure 6.17 shows an image captured with a purple screen illumination. Differences in the appearance of the honeys samples with the three illuminations are visually apparent on the images of figures 6.15, 6.16 and 6.17.

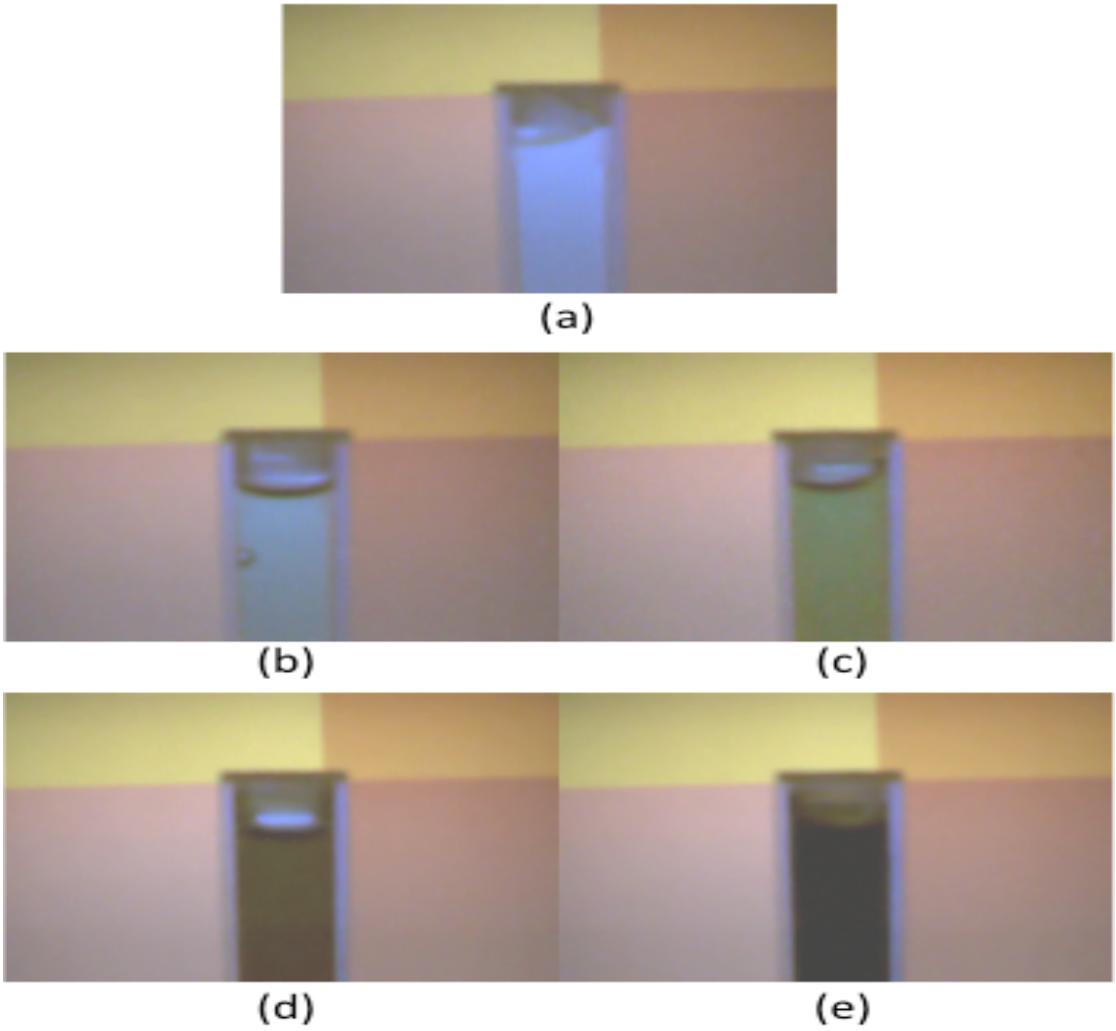

Figure 6.16: Examples of images of light transmitted through water and four different honey samples with blue screen illumination

(a) water

(b) SDR3

(c) SDR1

(a) SMR1

(d) QDR1

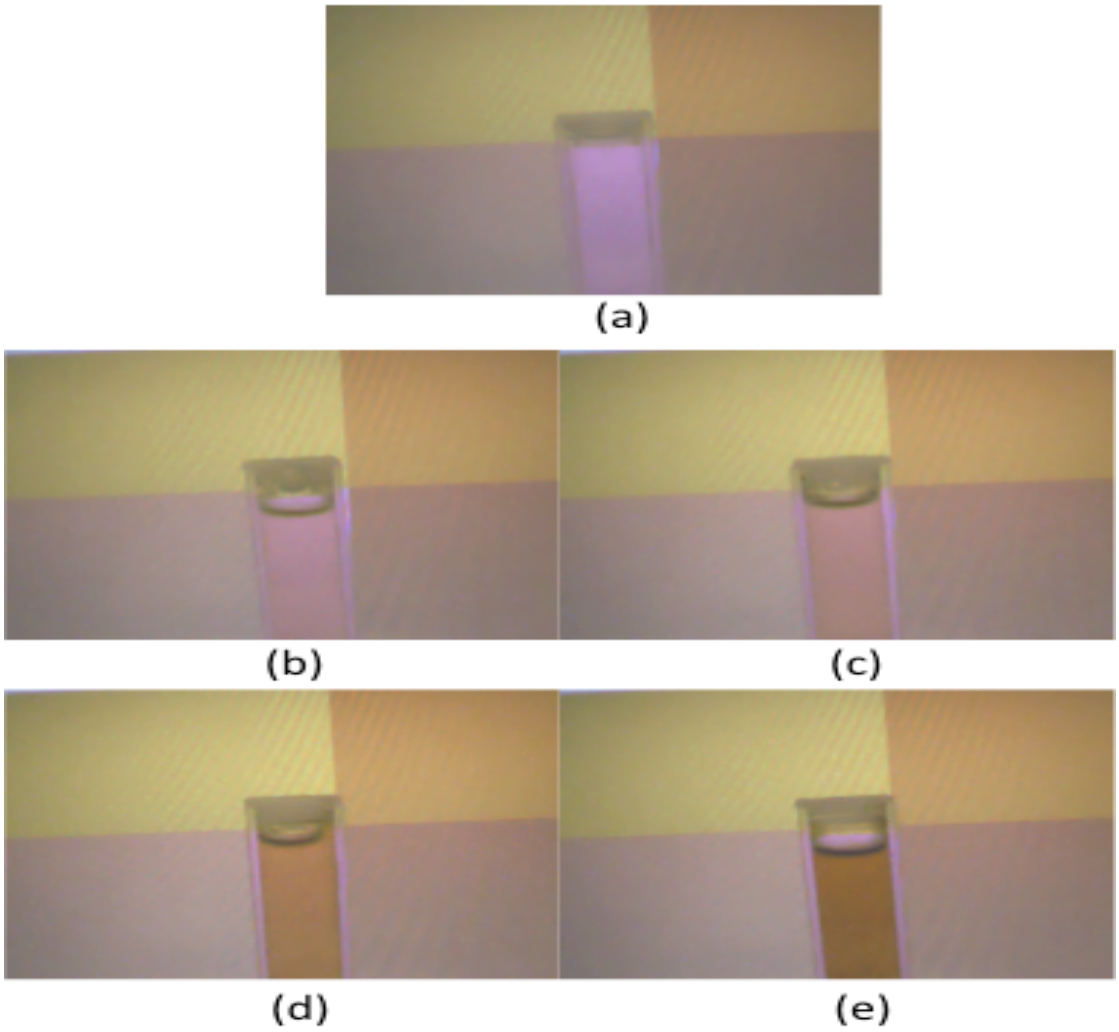

Figure 6.17: Examples of images of light transmitted through water and four different honey samples with purple screen illumination

(a) Water

(b) SDR3

(c) SDR1

(d) SMR1

(e) QDR1

R, G, and B data were extracted from a specified area on the various images as shown on the example image on figure 6.18 and were analyzed using the (Capsoft) software (Appendix I). The R, G and B raw data outputs of the test calibrations (Water, Honey and Syrup) are shown on figure 6.19 and the R, G and B raw data outputs for 32 different honey samples are shown on figures 6.20 and 6.21 with white and blue screen illuminations respectively.

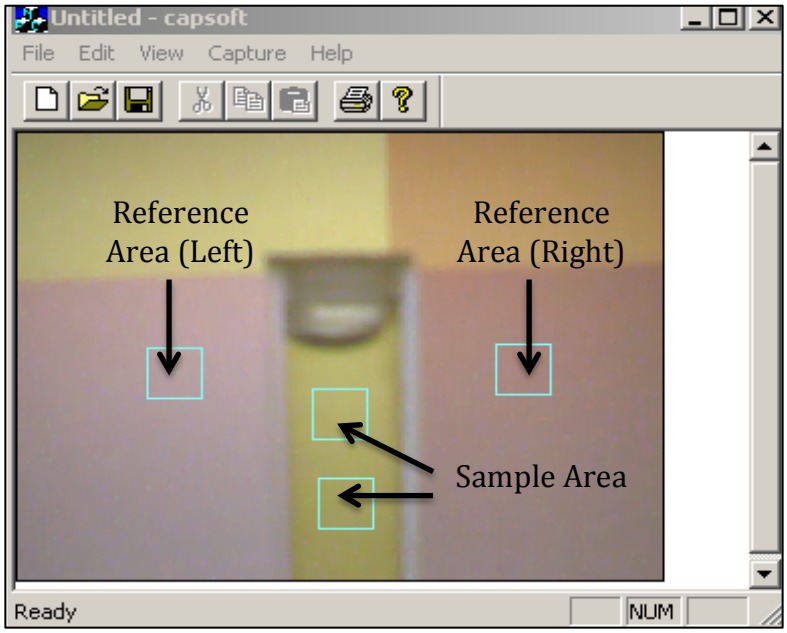

Figure 6.18: Example of honey sample image with white screen illumination showing four specified areas were RGB data are extracted from

6.3.2 RGB Outputs Of The Optical Transmission & Scattering System

6.3.2.1 Water-Syrup-Honey Mixtures

Water, syrup and honey mixtures enable additional optical phenomena to transmission and absorption properties when diluted in water. Figure 6.19 shows the RGB raw data outputs of water, syrup and honey mixtures. Figure 6.19(a) shows water-syrup at different concentrations, figure 6.19(b) shows water-honey at different concentrations and figure 6.19(c) shows tests with honey- syrup at different concentrations that represent a further complex condition of optically different viscous liquids (honey & syrup) with a sugar mixture medium (syrup).

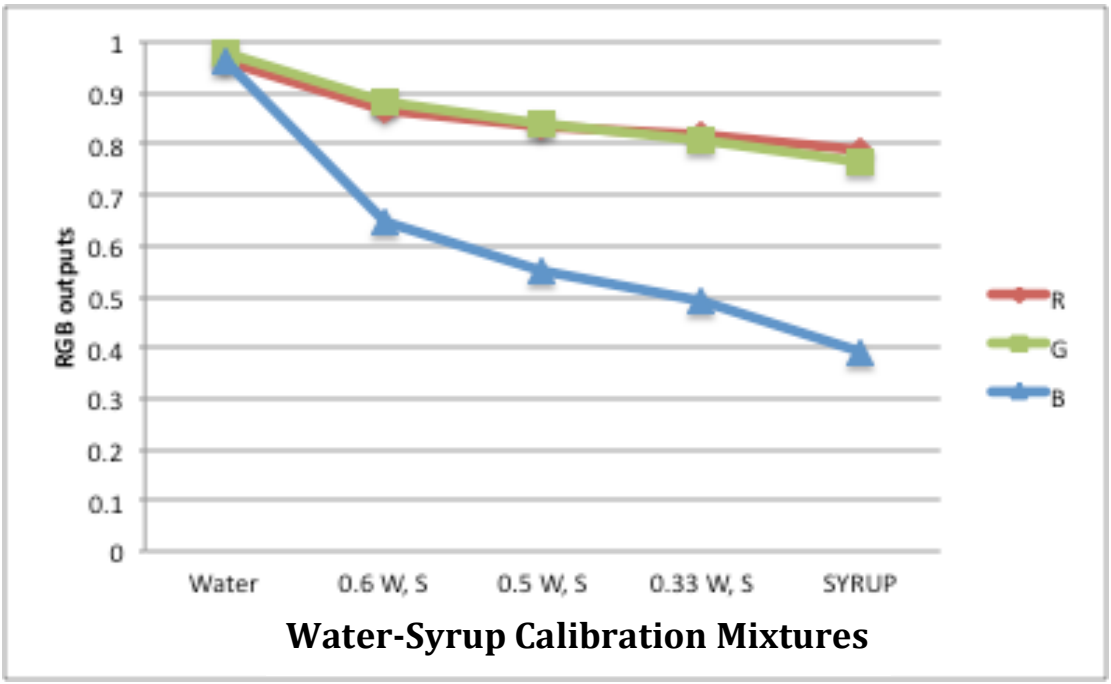

Figure 6.19 (a): Raw RGB outputs vs water and syrup mixtures with white screen illumination

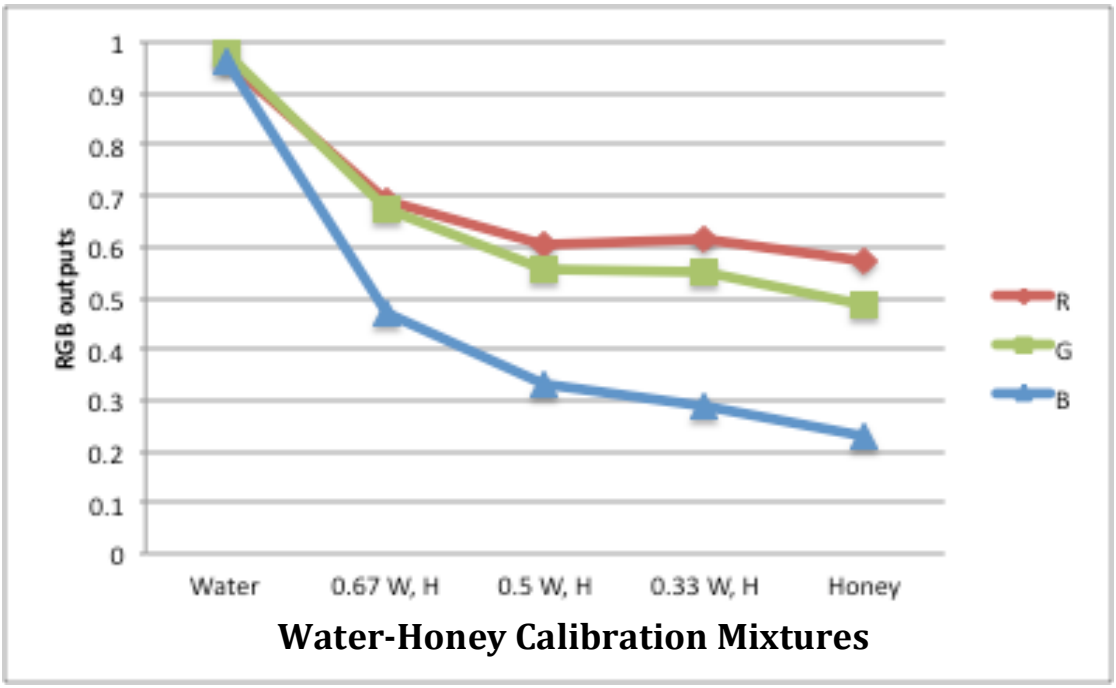

Figure 6.19(b): Raw RGB outputs vs water and honey mixtures with white screen illumination

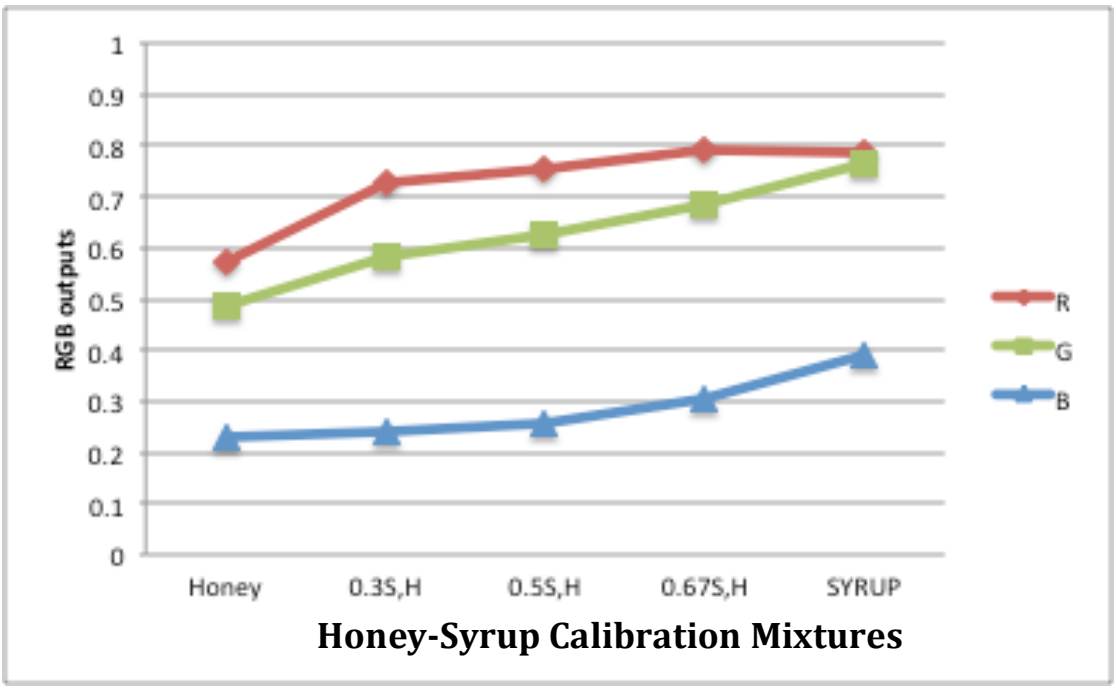

Figure 6.19(c): Raw RGB outputs vs honey and syrup mixtures with white screen illumination

Figure 6.19: Raw RGB outputs of (water-syrup-honey mixtures) with white screen illumination

(a) RGB outputs vs water and syrup mixtures

(b)RGB outputs vs water and honey mixtures

(c)RGB outputs vs honey and syrup mixtures

6.3.2.2 Honey Samples

Figures 6.20 show the raw RGB data outputs for 32 different honey samples with white screen illuminations. The results illustrate the complex variation in the R, G and B values produced by the different honey samples.

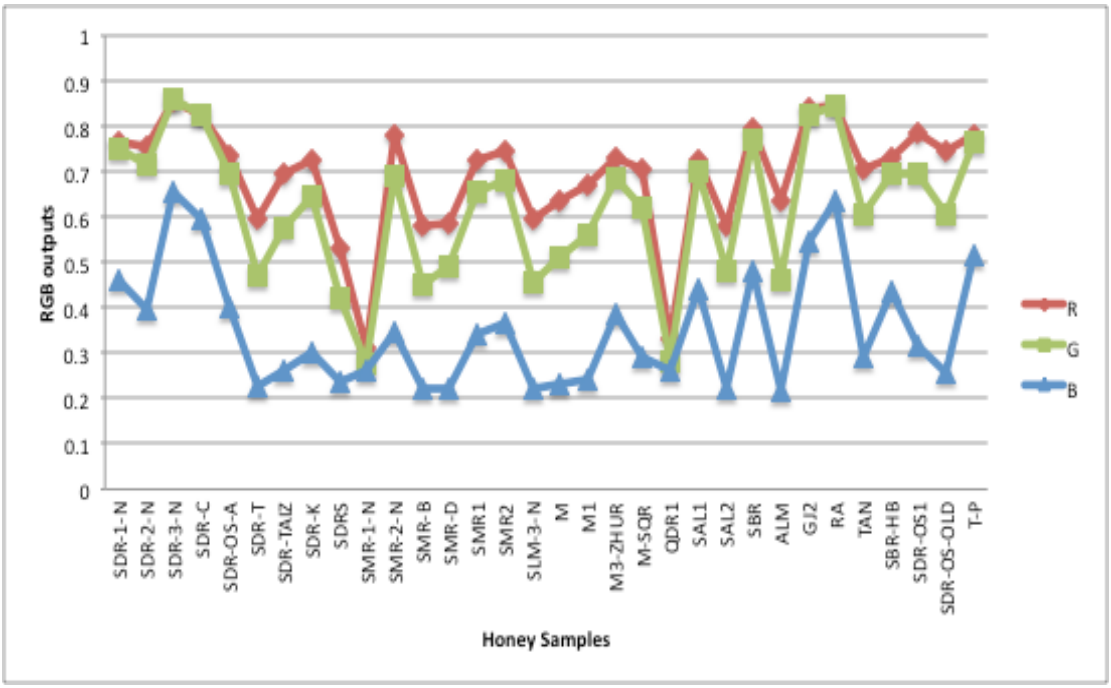

Figure 6.20: Raw RGB outputs vs. Honey samples with white screen illumination

Figures 6.21 show the raw RGB data outputs for the different honey samples with blue screen illuminations.

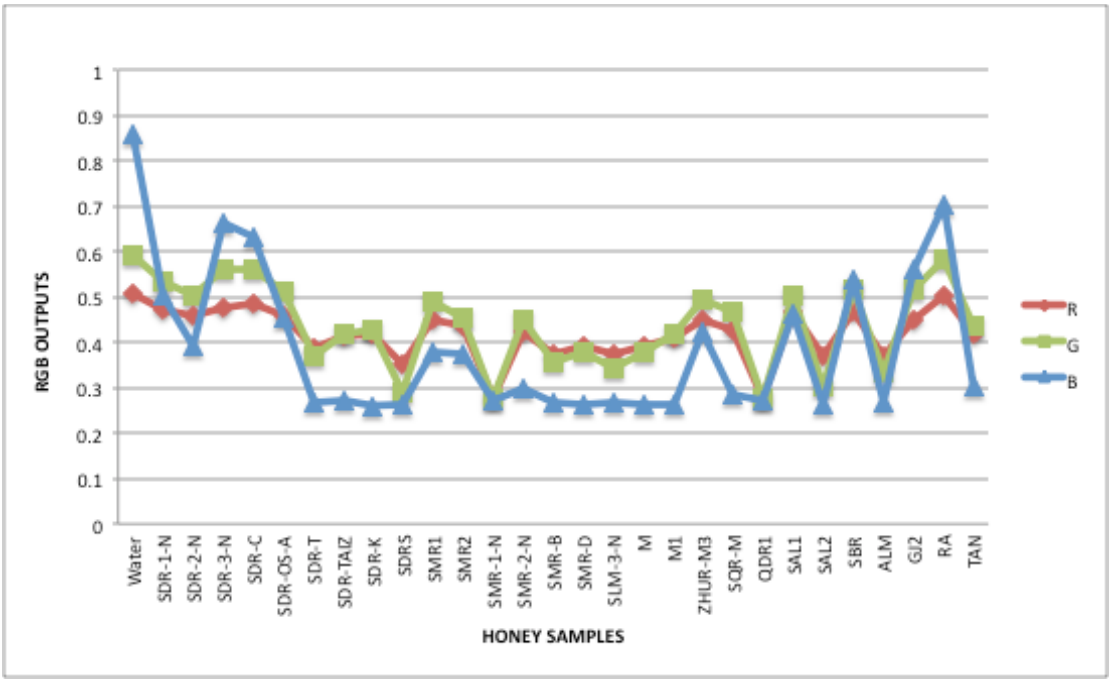

Figure 6.21:Raw RGB outputs vs. Honey samples with blue screen illumination

Figure 6.22 shows examples of images of water and honey samples obtained with the VDU background screen illumination and ambient light with white card (figure 6.22(a)) and black card (figure 6.22(b)& (c) inserted behind the cuvette with ambient room light.

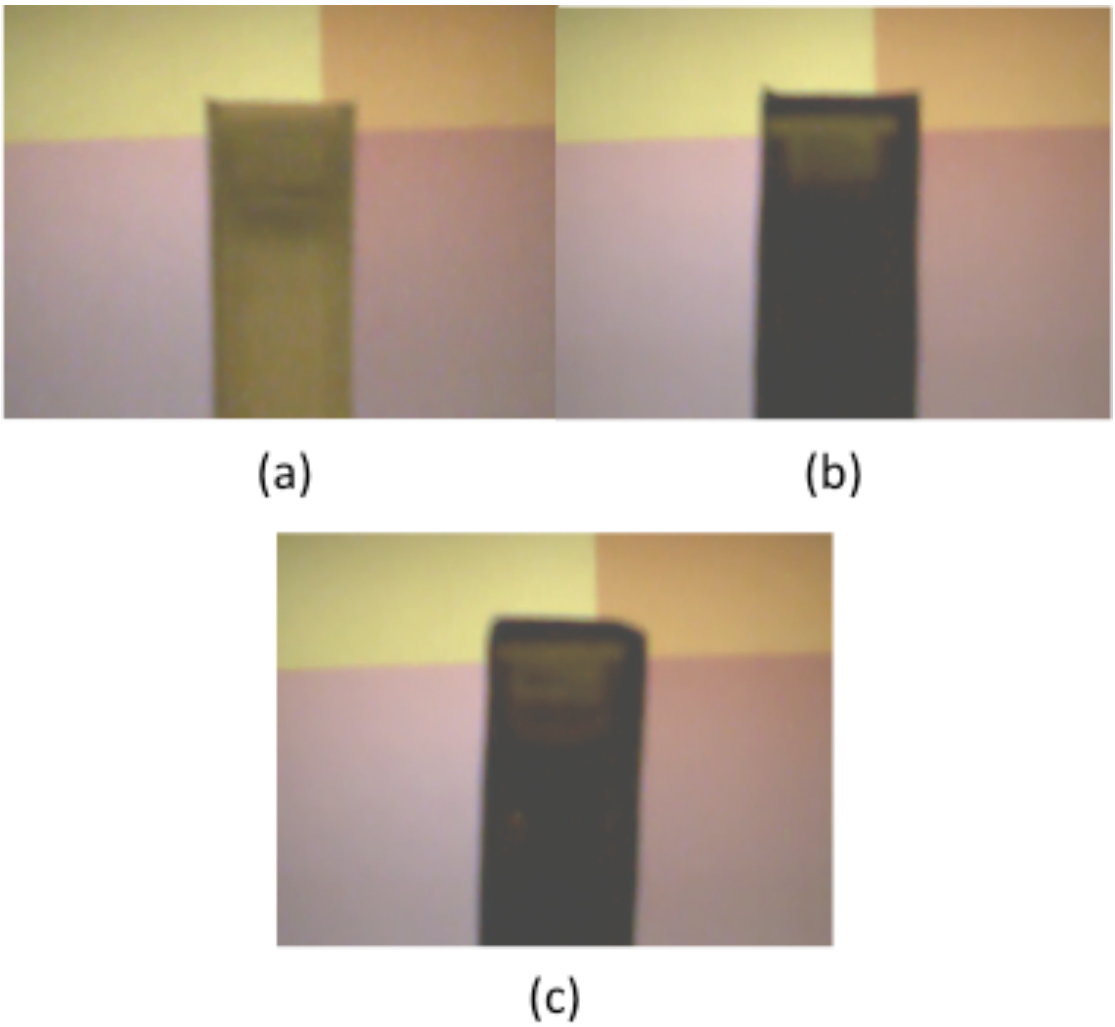

Figure 6.22:Examples of water and honey images with white and black card behind the cuvette:

(a) Water with White card

(b) Water with Black card

(c) Honey with Black card

The R, G and B raw data outputs are shown on figure 6.23 which correspond to the ambient light reflected from the water and the various honey samples.

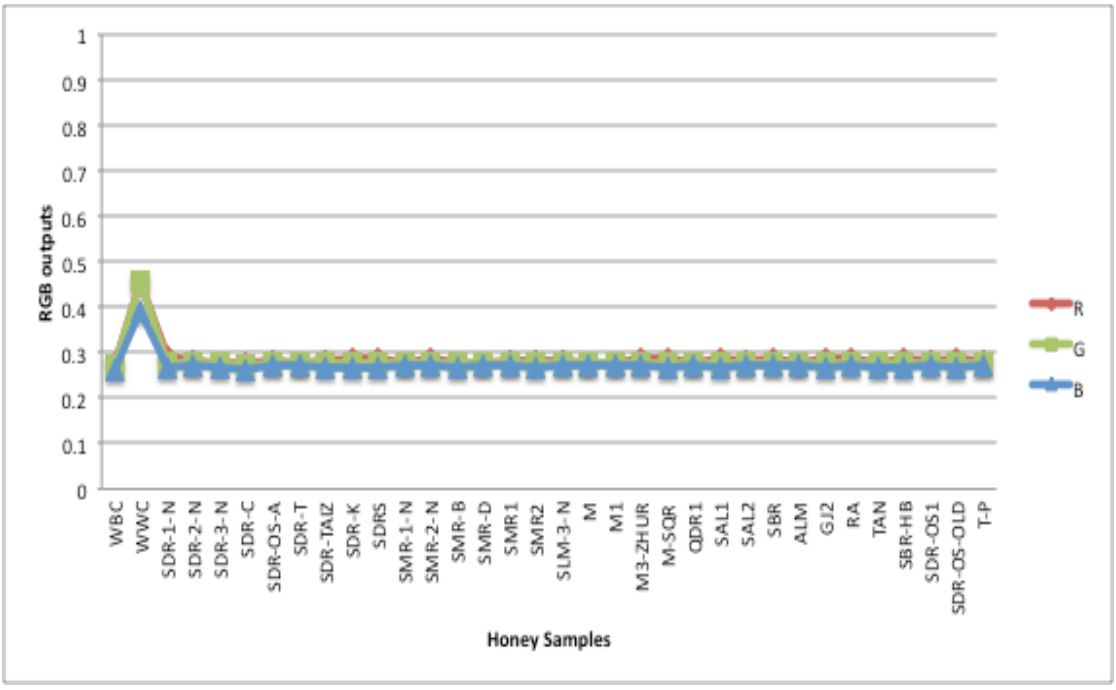

Figure 6.23: Raw RGB outputs vs. various Honey samples of reflected/ scattered ambient light using white and black card behind the cuvette.

Figure 6.24 shows the raw R, G, B data for the L (left) reference area tests with different honey samples. In all cases the VDU screen was switched on to provide reference signals either side of the cuvette test region. Thus the screen illumination and ambient illumination are both present. The results show some variations apparent of the RGB values of L (left) reference for all the tests.

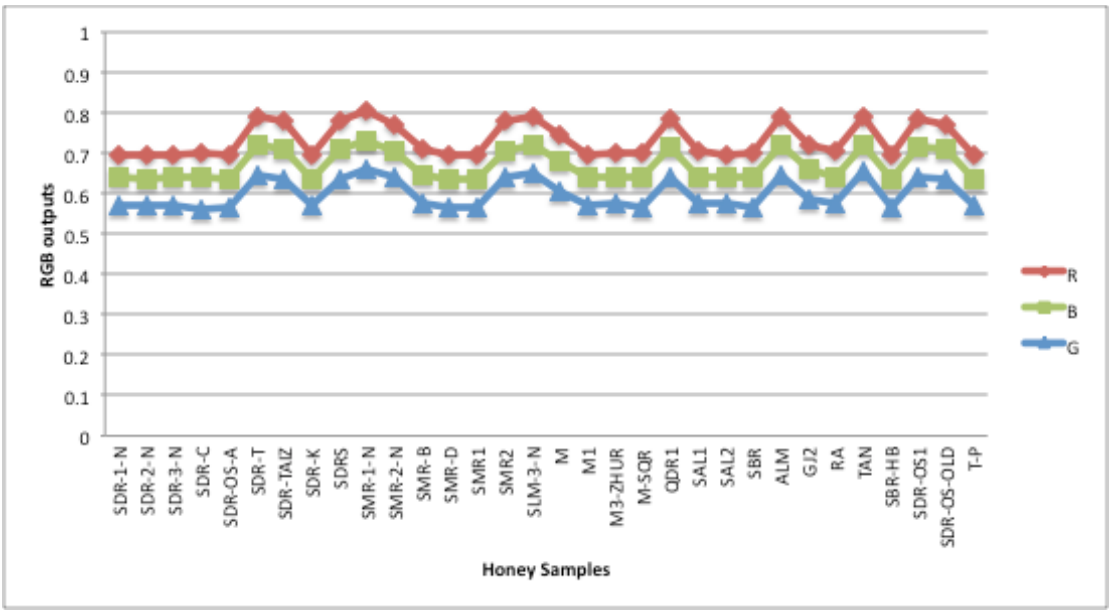

Figure 6.24: RGB output of the L (left) reference area with 32 different honey tests with white illumination behind the cuvette.

6.3.3 Visual Examples Of Fluorescent Images

Figure 6.25 shows examples of images of various honey samples obtained with the CMOS webcam and violet LED illumination (Chapter 4). The images show the fluorescence area when violet light excites the different honey samples.

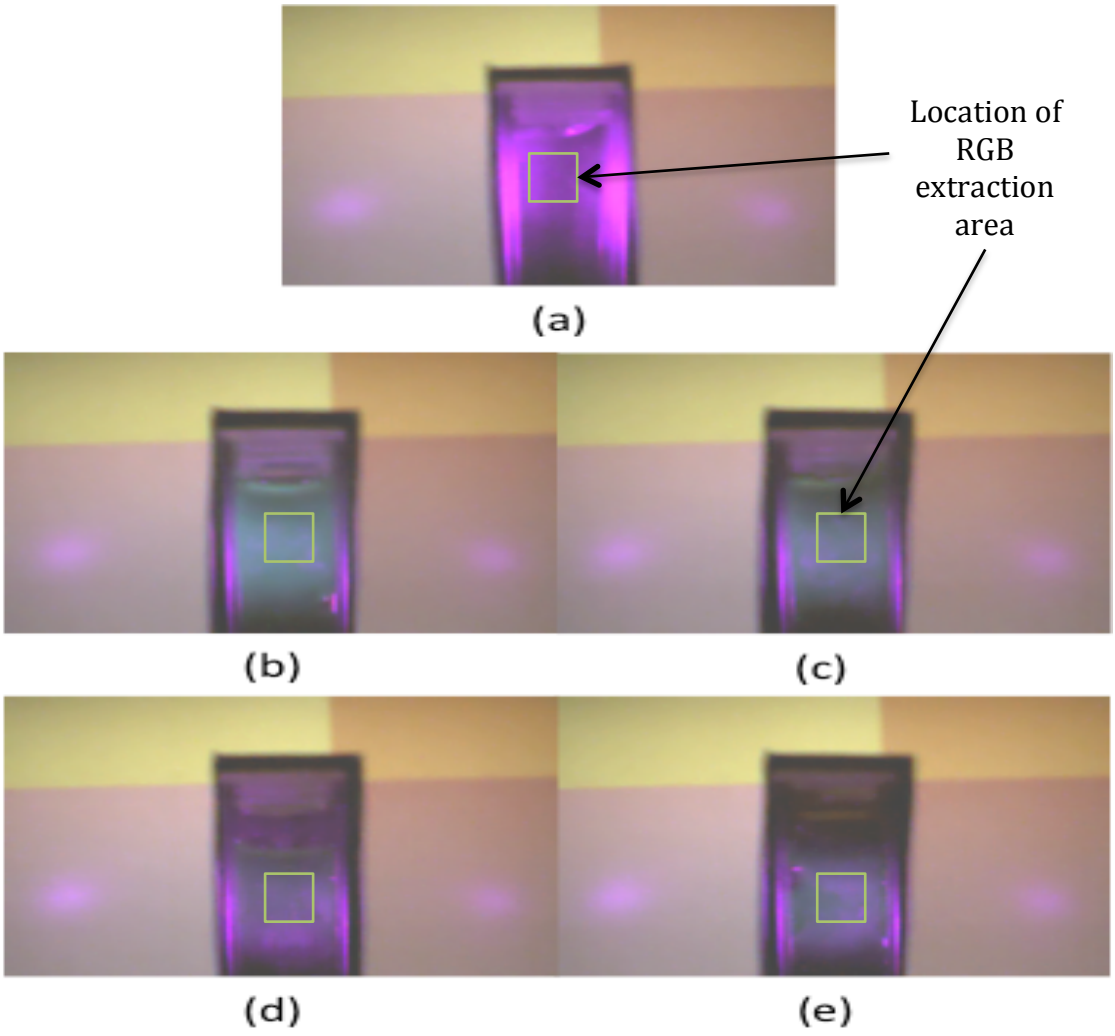

Figure 6.25: Examples of images of fluorecsent light of water and four different honey samples: (a) Water (b) SDR3 (c) SDR1 (d) SMR1 (e) QDR1

6.3.4 RGB Outputs Of The Optical Fluorescence System

6.3.4.1 Water-Syrup-Honey Mixtures

Figure 6.26 shows the RGB raw data outputs of water, syrup and honey mixtures. Figure 6.26(a) shows water-syrup at different concentrations, figure 6.26(b) shows water-honey at different concentrations and figure 6.26(c) shows tests with honey-syrup at different concentrations.

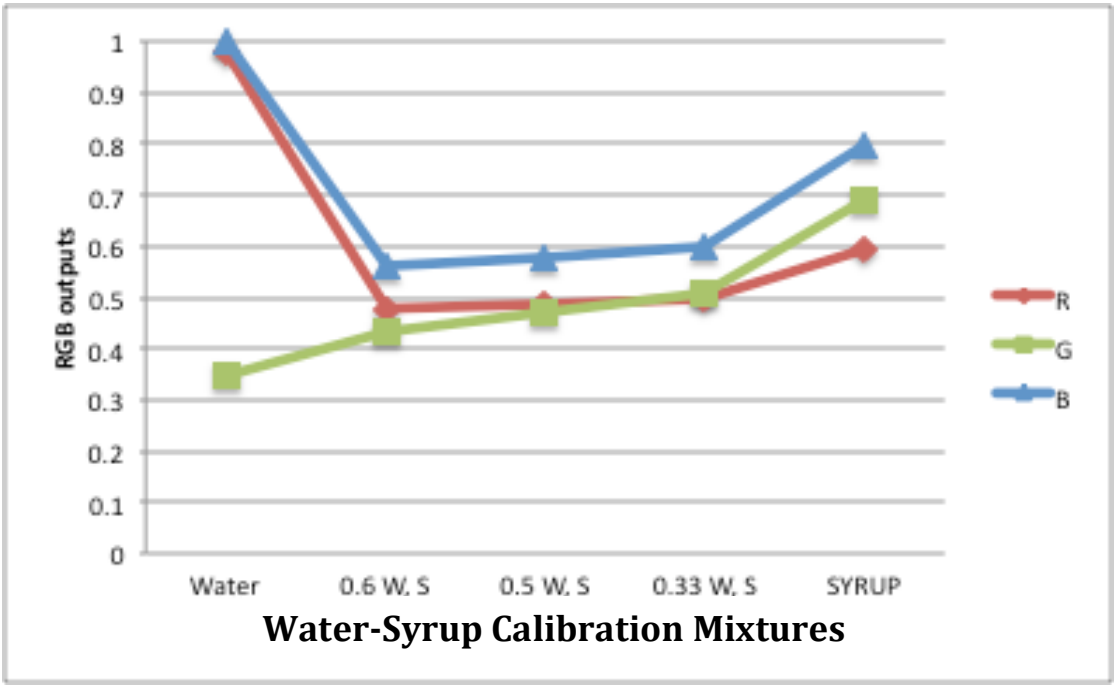

Figure 6.26(a): Raw RGB outputs Vs Water and Syrup mixtures with violet LED illumination.

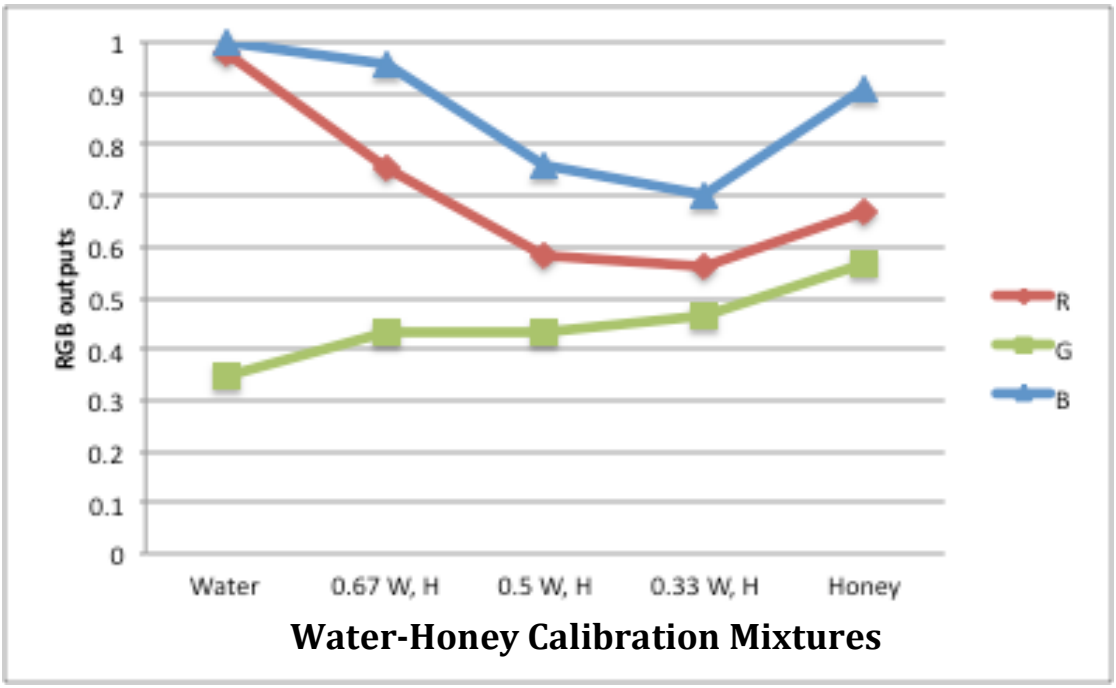

Figure 6.26(b): Raw RGB outputs Vs Water and Honey mixtures with violet LED illumination

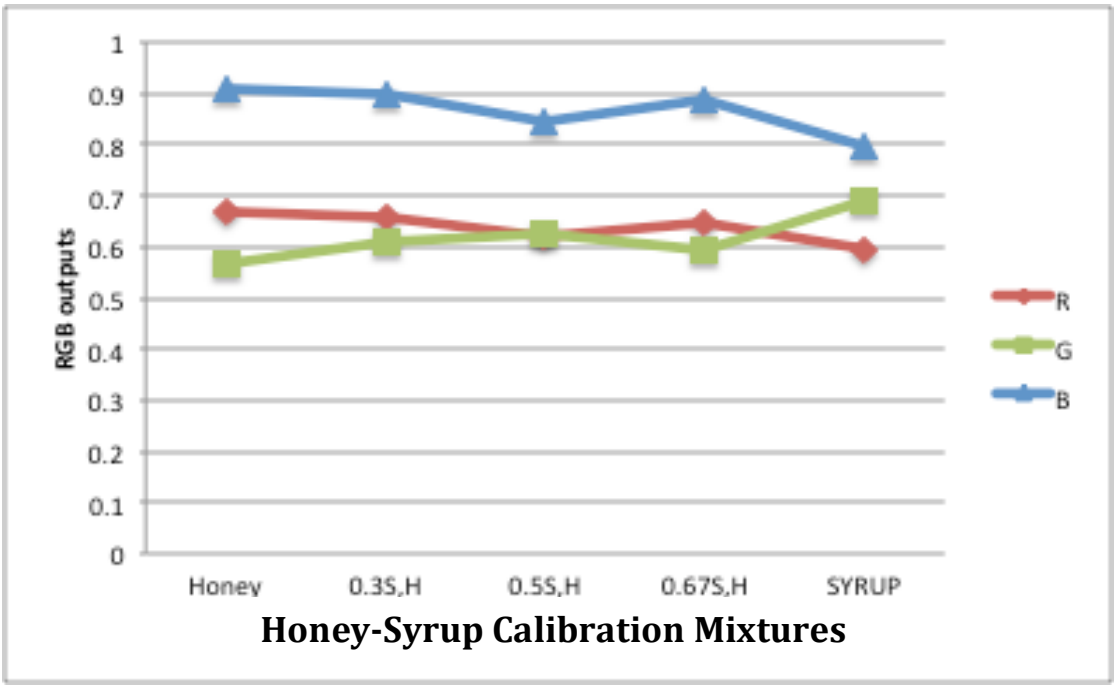

Figure 6.26(c): Raw RGB outputs Vs Honey and Syrup mixtures with violet LED illumination

Figure 6.26: Raw RGB outputs of (water-syrup-honey mixtures) with violet LED illumination illuminating the samples.

(a) RGB outputs vs water and syrup mixtures

(b)RGB outputs vs water and honey mixtures

(c)RGB outputs vs honey and syrup mixtures

6.3.4.2 Honey Samples

Figure 6.27 shows the R, G and B raw data outputs from each image for 32 different honey samples shown on figure 6.25. The results illustrate the complex variation in the R, G and B values produced by the different honey samples

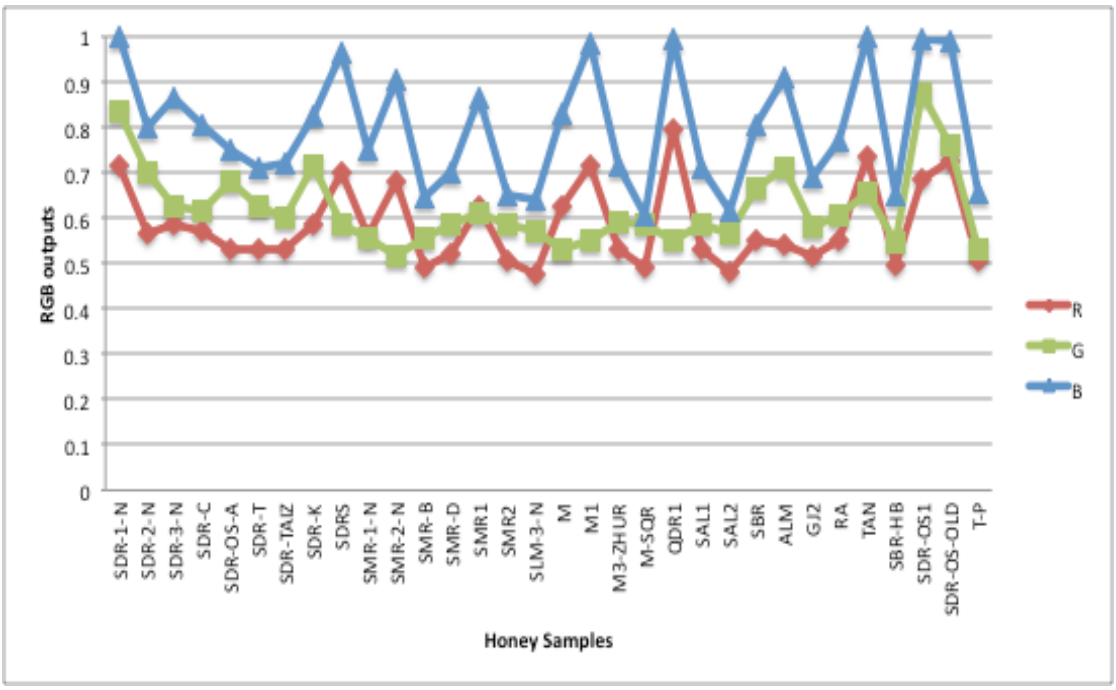

Figure 6.27: Raw RGB outputs vs. Honey samples with violet LED illumination illuminating the samples.

Figure 6.28 shows the raw R, G, B data for the L (left) reference area tests with different honey samples. In all cases the VDU screen was switched on to provide reference signals either side of the cuvette test region. Thus the screen illumination, ambient illumination and violet LED illumination are present.

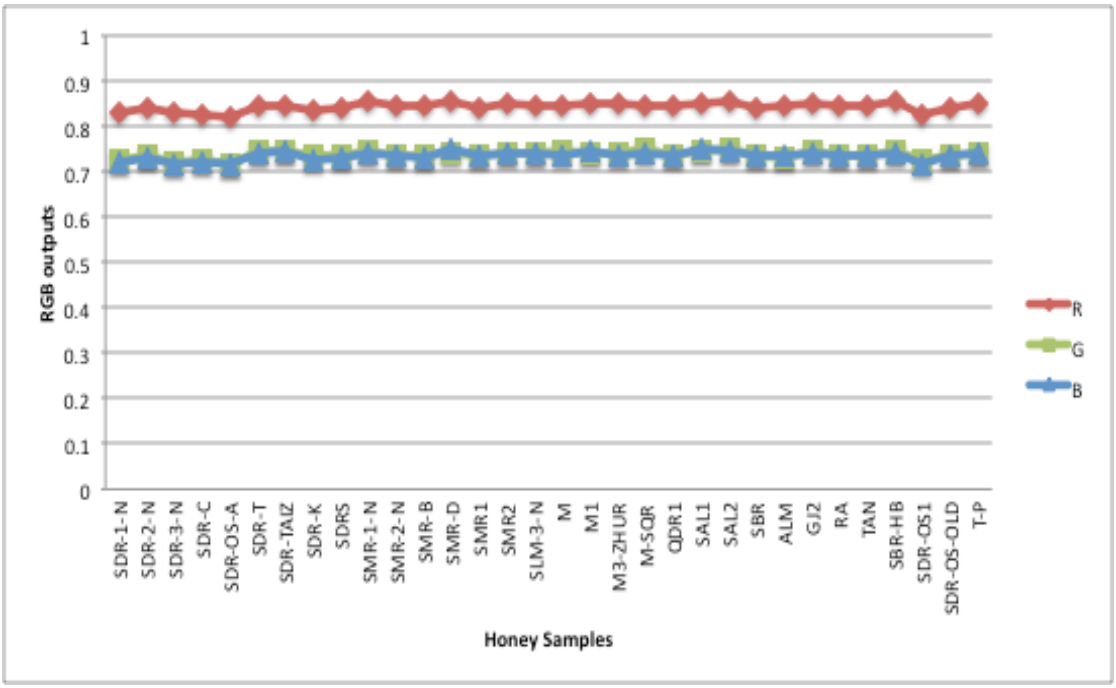

Figure 6.28: RGB output of the L (left) reference area with 32 different honey sample tests with violet LED illumination

6.3.5 Visual Examples Of Polarization Of Light Images

Figure 6.29 shows examples of images for various honey samples obtained with VDU background illumination screen and two polarizing filters rotated at a specific angle (Chapter 4) relative to each other of 45 degrees. Figure 6.30 shows examples of honey images of the same honey sample as figure 6.27(b) at different angles relative to each other at 0, 30, 45 and 70 degrees respectively.

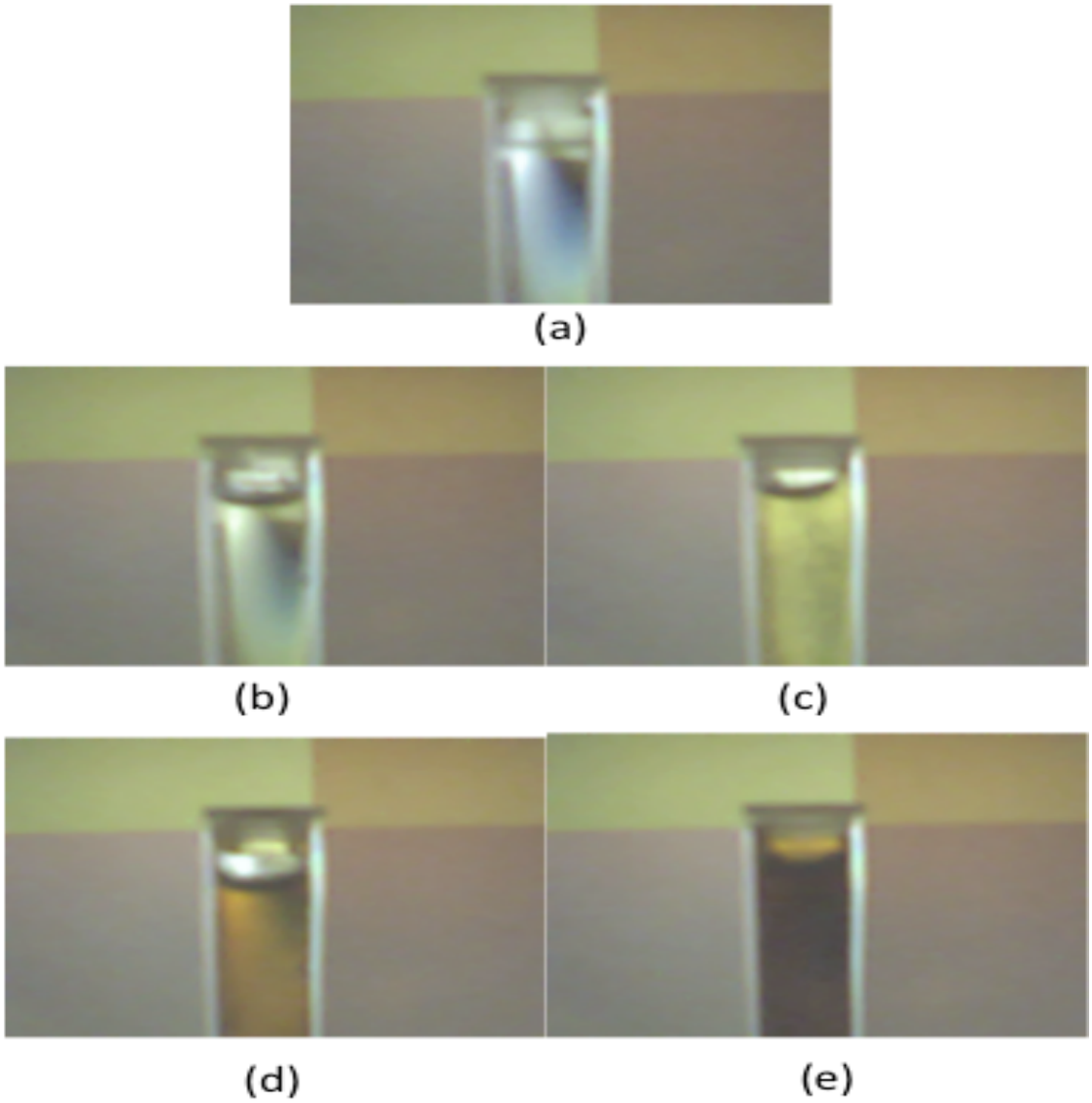

Figure 6.29: Example images of polarized transmitted light through water and four different honey sample using white screen illumination and polarizing filters at 45 degrees relative to each other: (a) Water (b) SDR3 (c) SDR1 (d) SMR1 (e) QDR1

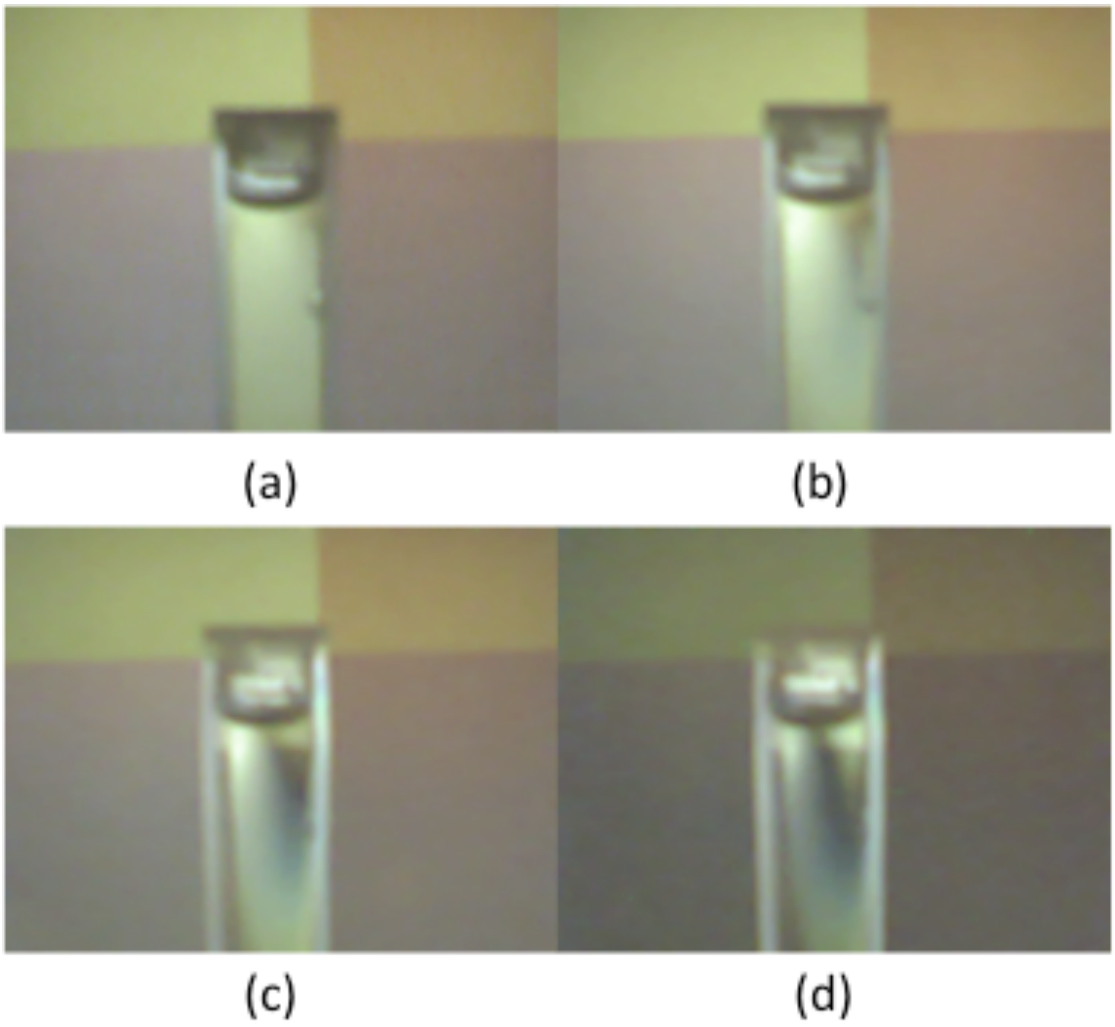

Figure 6.30:Example of images of polarized light transmitted through the honey sample (SDR3) using white screen illumination and polarizing filters at: (a) 0 degree (b) 30 degree (c) 45 degree (d) 70 degree relative to each other

6.3.6 RGB Outputs Of The Optical Polarization System

6.3.6.1 Water-Syrup-Honey Mixtures

Figure 6.31 shows the RGB raw data outputs of water, syrup and honey mixtures corresponding to 45-degree analyzer angle. Figure 6.31(a) shows water-syrup at different concentrations, figure 6.31(b) shows water-honey at different concentrations and figure 6.31(c) shows tests with honey-syrup at different concentrations.

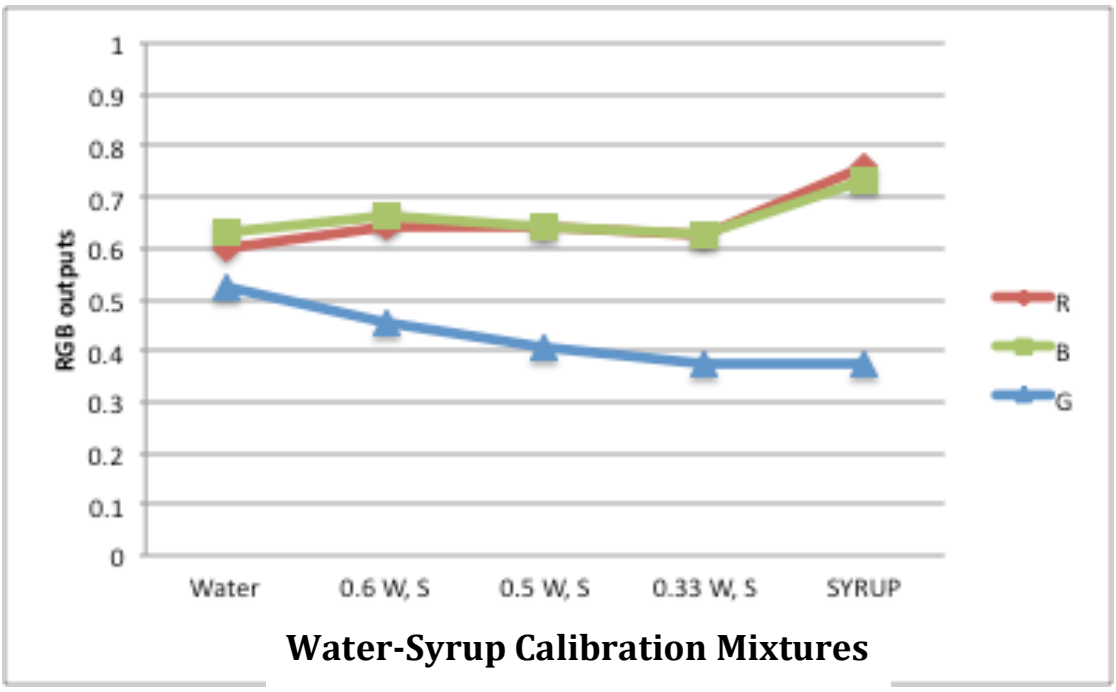

Figure 6.31 (a): Raw RGB outputs Vs Water and Syrup mixtures using white screen illumination and polarizing analyzer angle at 45-degrees

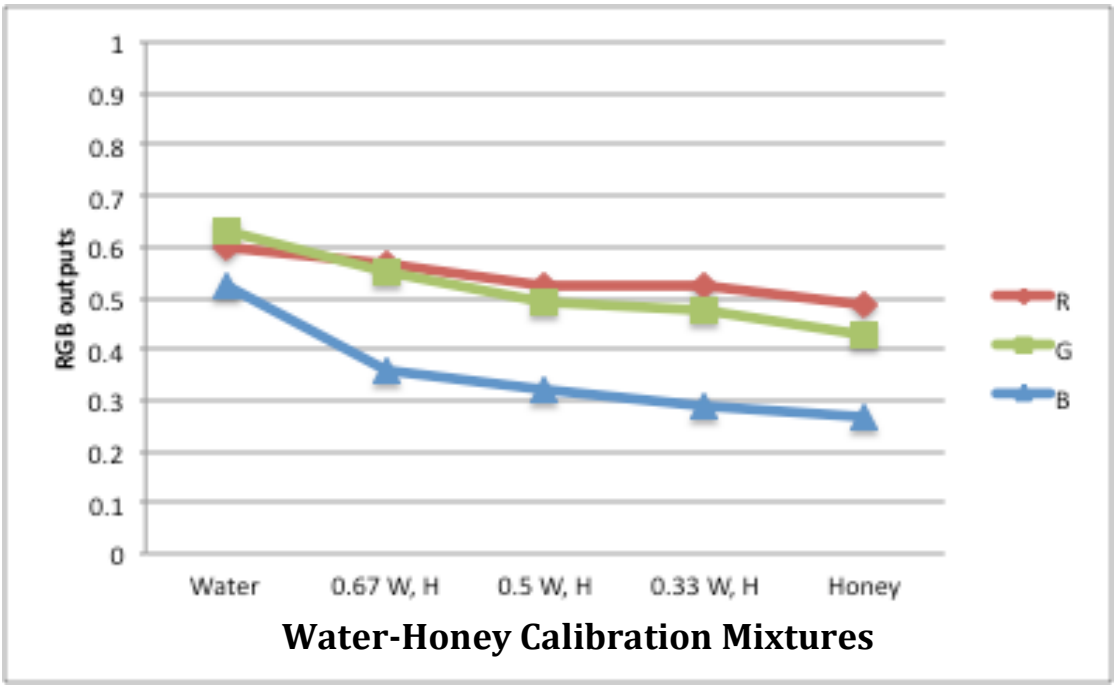

Figure 6.31(b): Raw RGB outputs Vs Water and Honey mixtures using white screen illumination and polarizing analyzer angle at 45-degrees

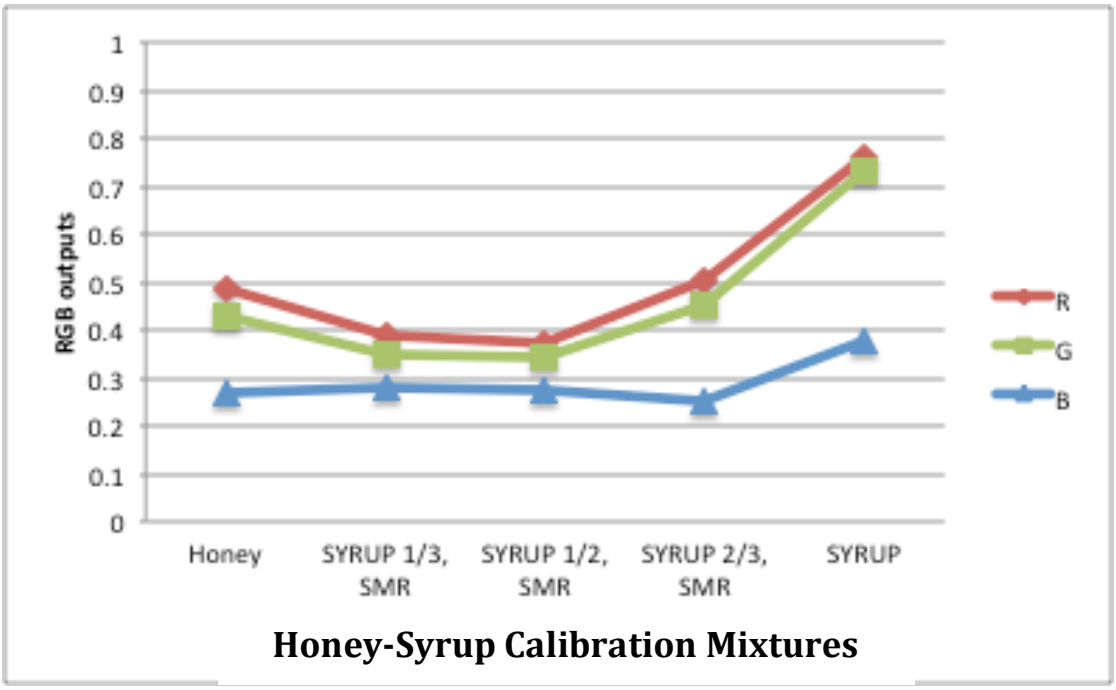

Figure 6.31(c): Raw RGB outputs Vs Honey and Syrup mixtures using white screen illumination and polarizing analyzer angle at 45-degrees

Figure 6.31: Raw RGB outputs of (water-syrup-honey mixtures) using white screen illumination and polarizing analyzer angle at 45-degrees.

(a) RGB outputs vs water and syrup mixtures

(b)RGB outputs vs water and honey mixtures

(c)RGB outputs vs honey and syrup mixtures

6.3.6.2 Honey Samples

Raw R, G and B data outputs derived from each of the images for 32 different honey samples are shown on figures 6.32 corresponding to 45-degree analyzer angle. The results illustrate the complex variation in the R, G and B values produced by the different honey samples. Other tests have been done using different angle of polarization (0, 30 and 70) respectively and the results are attached in the Appendix II section.

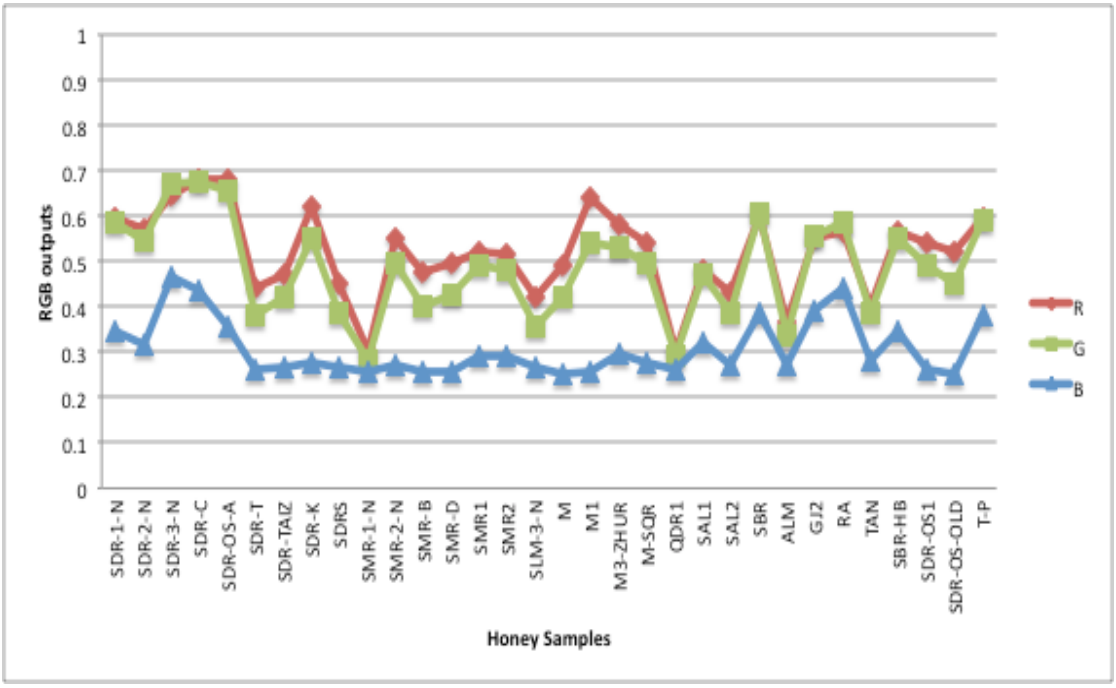

Figure 6.32: Raw RGB outputs vs. Honey samples using white VDU illumination and polarizing filter angle at 45 degrees

Figure 6.33 shows the raw R, G, B data for the L (left) reference area tests with 32 different honey samples corresponding to 45-degree analyzer angle. The VDU screen was switched on to provide reference signals either side of the cuvette test region. Thus the screen illumination and ambient illumination are both present.

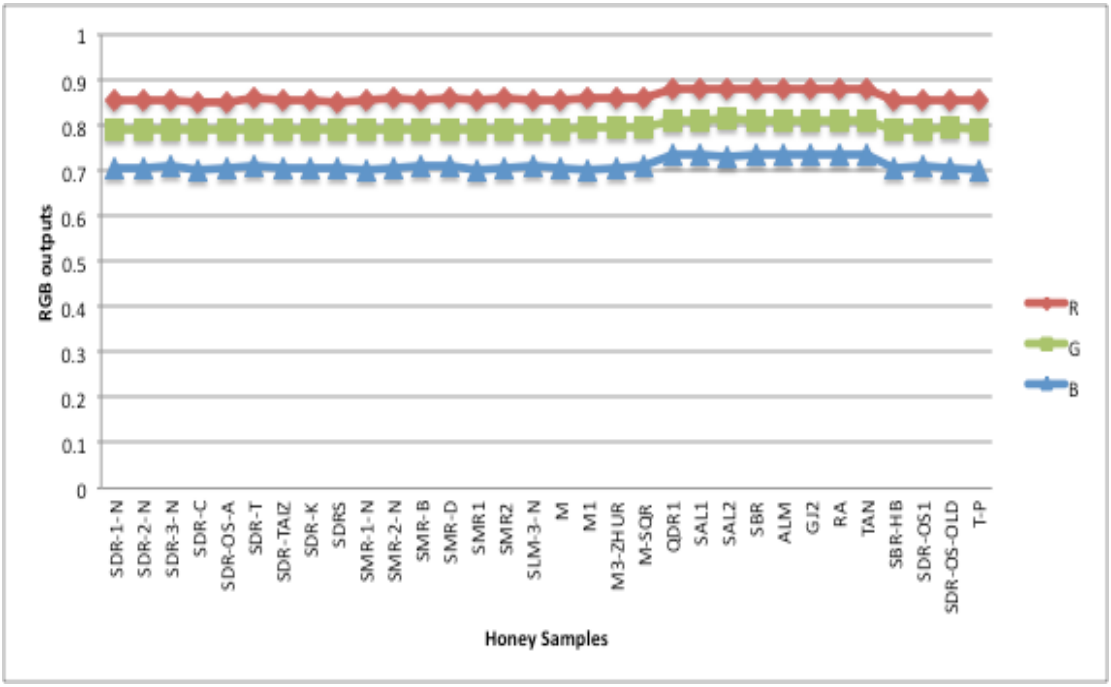

Figure 6.33: RGB outputs of the L (left) reference area with 32 different honey sample tests using white VDU illumination and polarizing filter angle at 45-degrees

6.4 Summary

This chapter has presented the results of experiments investigating the chromatic properties of various kind of liquids- clear (water, tea), turbid (water, tea +milk), viscous (water, syrup, honey), a further complex condition (honey, syrup) and 32 of different honey samples.

Images obtained with a webcam and VDU screen have been presented which emphasis the use of reference areas on the illuminating VDU screen.

The method in which the R, G and B values of both the sample and reference areas were extracted from the various images has been described. Graphical representations of these R, G, and B values have been presented.

The results provide the basis for applying various chromatic processing techniques for extracting the significance information of the various liquids investigated.

Chapter 7

Analysis of Result

7.1 Introduction

Chromatic techniques involve the representation of signals and information in terms of 3 outputs R, G, B from three non-orthogonal processors. This chapter describes methods for treating R, G, B outputs from a two dimensional array of detectors (e.g. polychromatic optical image) and means for overcoming aberrations, which may affect the values of R, G, B when monitoring under robust, operational conditions. Each of the three outputs is first preprocessed separately for referencing, correction and normalization before being combined for chromatic transformation.

Procedures are described for compensating for aberrations in the raw values of R, G, B from images used for chromatic monitoring. Some preliminary adjustments may be advantageously made to the values of R, G, B prior to such compensation procedures. Each of the raw chromatic outputs may then be separately compensated by the methods described below before combining the normalized values to optimize chromatic discrimination. This chapter includes the test analysis method of water, tea, milk mixtures, it also includes the test calibration methods and analysis of water, syrup, honey mixtures and various honey samples for chromatic features transmission, reflection, fluorescence and polarization signals.

7.2 Test Calibrations

7.2.1 Test To Test Correction Factor

An example of a two-dimensional image formed from a number of R, G, B pixels and used for referencing is shown on figures 7.1.

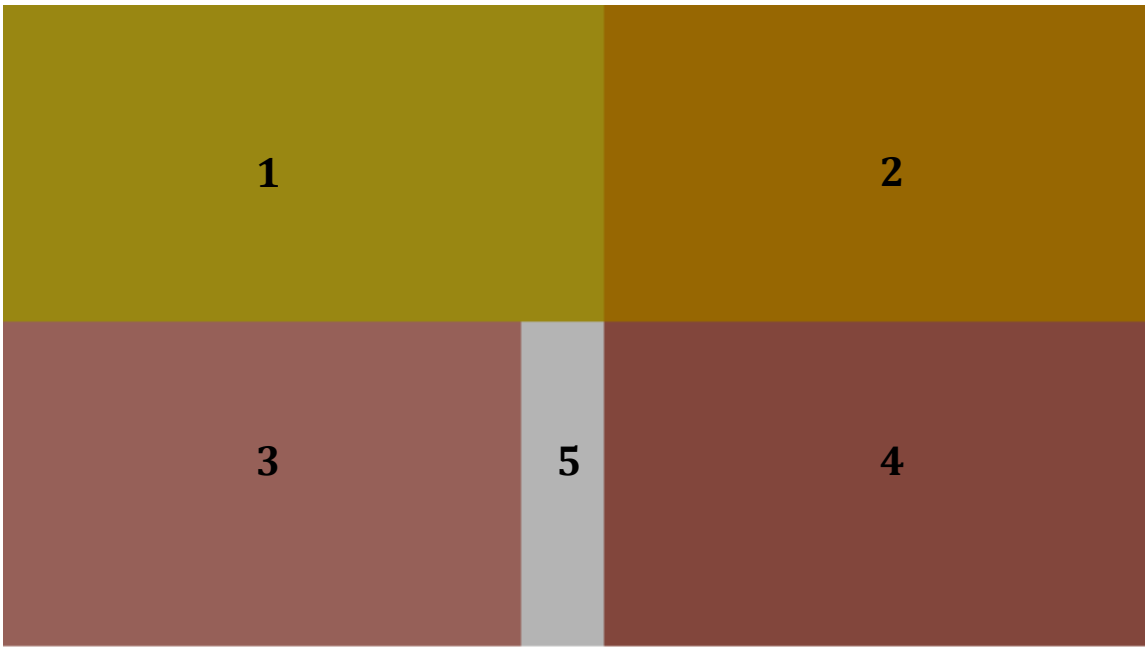

Figure 7.1: An example of two-dimensional image with attenuated white background and reference areas, the points on the image represents the following: (1) top left reference area, (2) top right reference area, (3) bottom left reference area, (4) bottom right reference area and (5) attenuated white illumination area

Figure 7.1 shows a basic image for monitoring light transmission from a VDU screen via a cuvette containing fluid. The VDU provides a single distributed source with a high degree of uniformity and whose spectral content and intensity is under control via the computer software. The screen is divided into five areas of different chromaticities. Each of the four reference areas (1,2,3 and 4) is located beside a narrower vertical strip (5). Area (5) provides the illumination for a liquid carrying cuvette placed in front this area. This area is bright to counter any reduced intensity produced by light absorption during transmission through the liquids (Water-Tea-Milk & Water-Syrup-Honey calibration mixtures and Honey samples) as shown on figure 7.2.

7.2.2 Compensation Procedures

Procedures for compensating for operating aberrations in the values of each of the outputs R, G, B from various image pixels may be employed based upon the use of the different reference areas on a captured image of the form shown on figures 7.2. The two reference areas (Lref) Left reference and (Rref) Right reference are shown along with two sample addressing areas (S1 and S2)

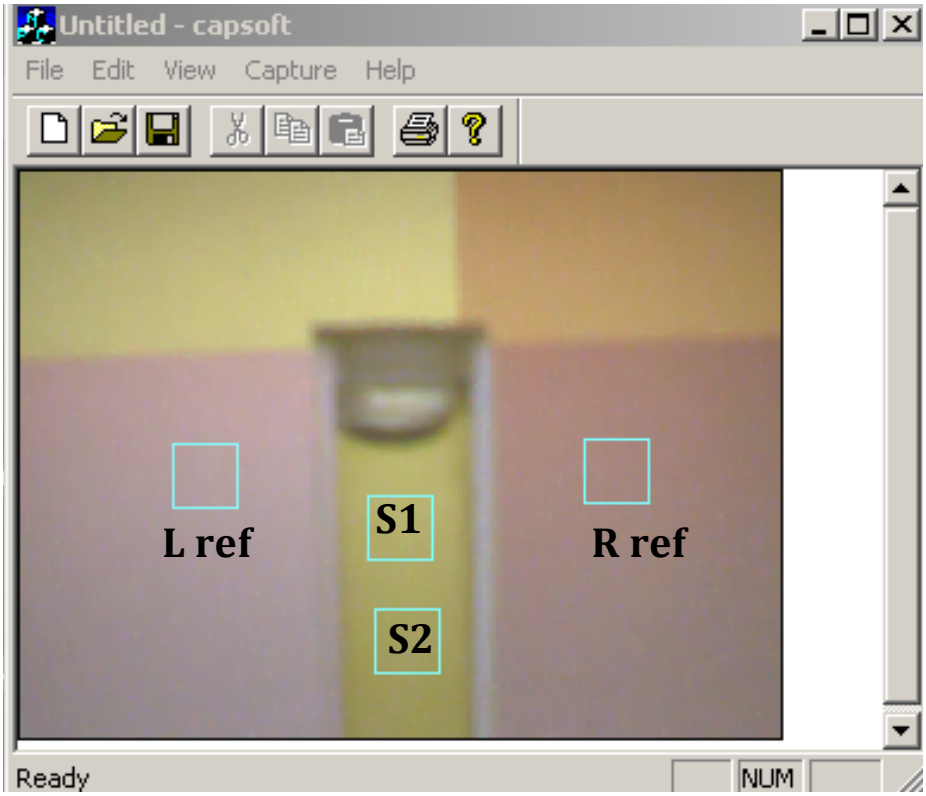

Figure 7.2: An example of a sample image with two reference areas Lref and Rref along with two sample addressing area S1 and S2

7.2.3 RGB Preprocessing

The raw R, G and B output values are first checked with regard to their relative magnitudes and three guiding criteria.

a) If any of the outputs approach saturation (i.e. R, G, B → 0, R, G, B → 1) then that output is eliminated from further analysis since it has effectively lost sensitivity.

b) Changing the amplification factor of one or two of the outputs R, G, B retrospectively via software is considered for improving discrimination of specific information. (E.g. R → (a1) R, G → G, B → (a3)B).

c) Changing the offset value of one or two of the outputs R, G, B retrospectively via software is considered for optimizing the discriminating effect of the outputs. (E.g. R → R + (a1), G → G + (a2), B → B)

Note: the values of (a1), (a2) and (a3) can be any nonmetric value.

These possibilities may be reviewed after a chromatic signature has been evaluated and a chromatic map formed. A further iteration using the compensating and chromatic procedures may be implemented to improve the chromatic discrimination of data on the chromatic map.

7.3 Water-Tea-Milk Calibration Mixtures

7.3.1 Raw RGB Results

The raw R, G, B data for the Lref area of the calibration mixtures tests (water-tea-milk) on (figure 6.14, Chapter 6) shows an approximate level of repeatability for all the tests, therefore no further correction to the raw data was made. In all cases the VDU screen was switched on to provide reference signals either side of the cuvette test region. Thus the screen illumination and ambient light are both present.

7.3.2 Normalization Procedure

The choice of chromatic parameters for monitoring complex liquid mixtures is assisted by simple mathematical modeling of polychromatic light interaction with such liquids. Both absorption of light transmitted through the liquid and the reflection of light from a separate source by the liquid are considered.

This section reports on the procedures developed for analyzing honey, urine or any complex liquids results from tests using computer screen illumination of various samples. In particular it addresses how information about the degree of turbidity and the surrounding liquid might be separated and further analyzed chromatically.

The new data collected may be summarized as follows:

- X (sample, white, blue or purple screen)
- X (sample, black screen)
- X (water, white, blue or purple screen)
- X (water, black screen)

Where X = R, G or B

The raw data are normalized and scaled within the range 0–1 using the following algorithms:

$$Xs(liq)N = \frac{XAS(sample,screen) - XA(sample,black\ screen)}{XAS(water,screen) - XA(water,black\ screen)} \quad (7.1)$$

$$Xs(turb)N = \frac{XA(sample,black\ screen) - XA(water,black\ screen)}{1 - XA(water,black\ screen)} \quad (7.2)$$

XA(sample, black screen), XA(water, screen) are measures respectively of a sample and water both with “ambient” light and no “direct” screen light.

XAS(sample, screen), XAS(water, screen) are measures respectively of the screen light transmitted through a sample, water.

7.3.3 Processed Results (Calibration Graphs)

The above algorithms have been used to produce values of Rs (liq), Gs (liq), Bs (liq) and Rs (turb), Gs (turb), Bs (turb) for the various liquid samples and conditions i.e. (water + tea), (water + milk) and (water + tea + milk).

7.3.3.1 Water – Tea Calibration Mixtures

Figure 7.3 shows results for the transmission and turbidity normalized chromatic parameters for water and tea mixtures.

Figure 7.3(a) shows a calibration graph of results for each of the transmitted light chromatic parameters Rs(liq)N, Gs(liq)N, Bs(liq)N derived from the measured parameters (figures 6.5 and 6.11, Chapter 6) and normalized with (Equation 7.1) for different concentration of tea in water. In all cases the three chromatic parameters (R,G,B) vary monochromatically approximately linearly with tea concentration.

Figure 7.4(b) shows a calibration graph of results for each of the reflected light chromatic parameters Rs(turb)N, Gs(turb)N, Bs(turb)N derived from the measured parameters (figure 6.11, Chapter 6) and normalized with (Equation 7.2) for different concentration of tea in water. In all cases the RGB chromatic parameters have no signal for the tea concentration except for the R parameter that increases to 0.17 at the high tea concentration.

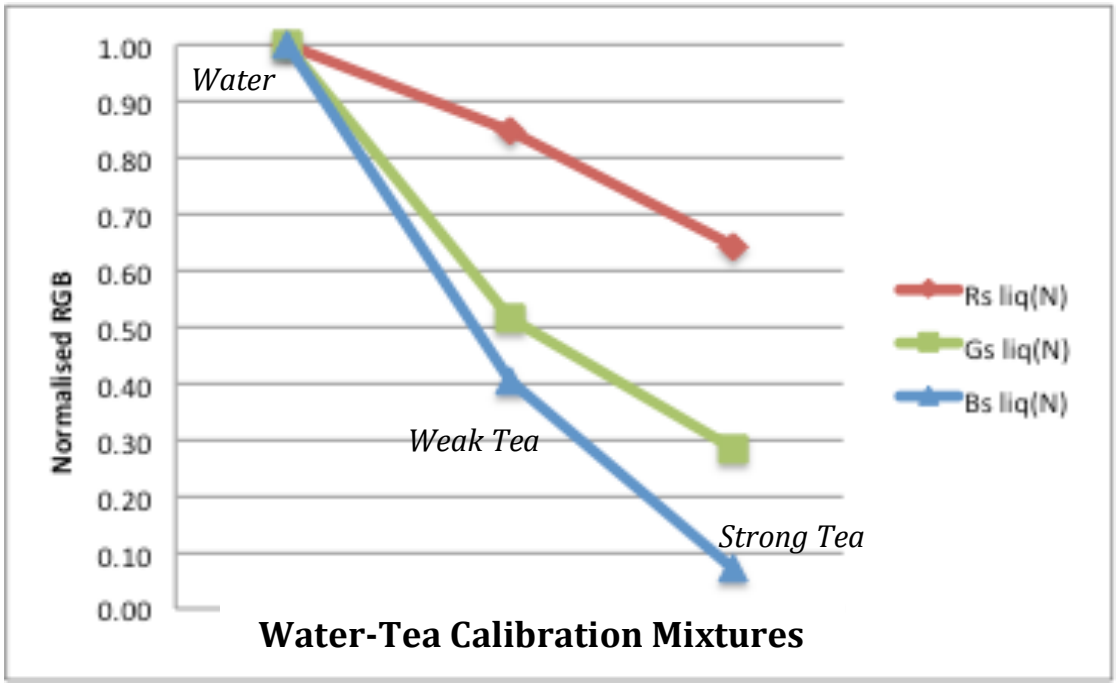

Figure 7.3 (a): Calibration graph of RGB liquid parameters light transmission against water & tea concentration samples

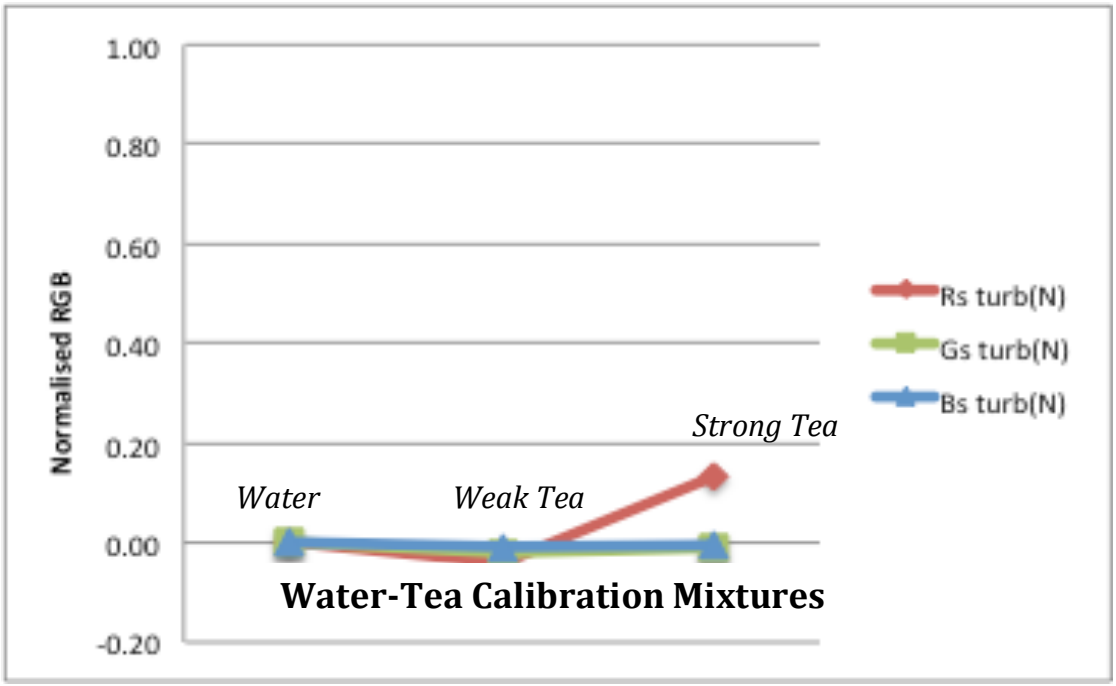

Figure 7.3(b): Calibration graph of RGB turbidity parameters of reflected light against water & tea concentration samples

Figure 7.3: Processed results for Water – Tea mixtures

(a) Calibration graph of RGB liquid parameters light transmission

(b) Calibration graph of RGB turbidity parameters light reflection

7.3.3.2 Water – Milk Calibration Mixtures

Figure 7.4 shows results for the transmission and turbidity normalized chromatic parameters for water and milk mixtures.

Figure 7.4(a) shows Rs(liq)N, G(liq)N, B(liq)N as a function of milk concentration in water derived from the measured parameters (Figures 6.6 and 6.12, Chapter 6) and normalized with (Equation 7.1) for mixtures of turbid milk in water.

Figure 7.4(b) shows Rs(turb)N, G(turb)N, B(turb)N as a function of milk concentration in water derived from the measured parameters (Figure 6.12, Chapter 6) and normalized with (Equation 7.2) for mixtures of turbid milk in water. In all cases the three chromatic parameters (R,G,B) vary monochromatically approximately linearly with milk concentration

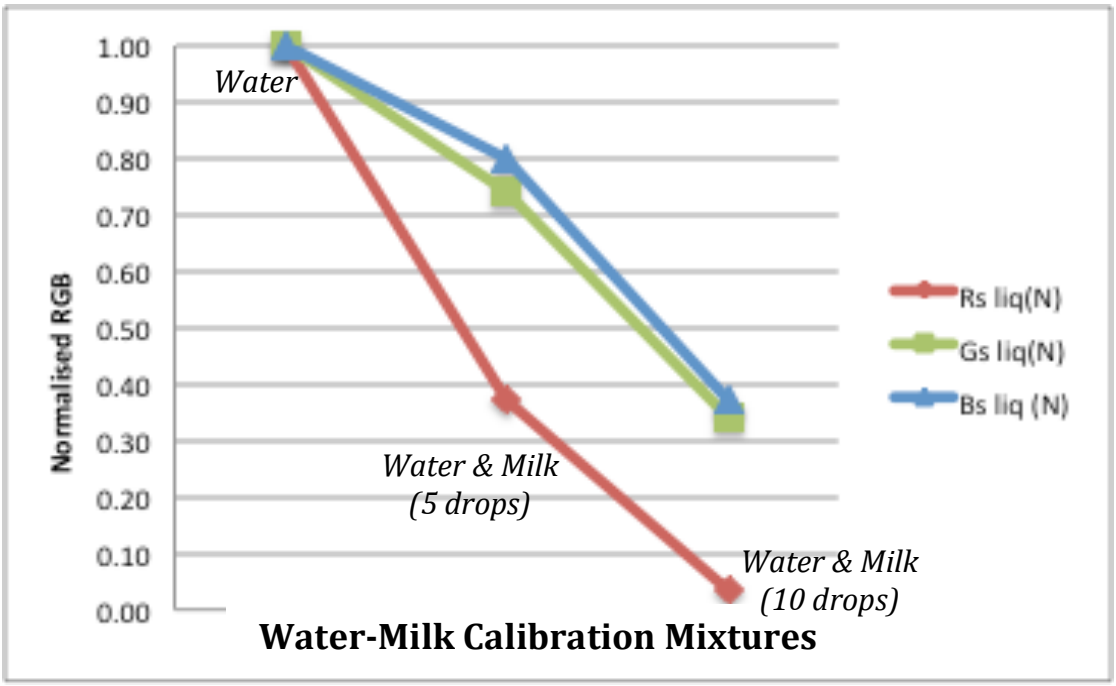

Figure 7.4: (a): Calibration graph of transmitted light liquid parameters against water & milk drops samples

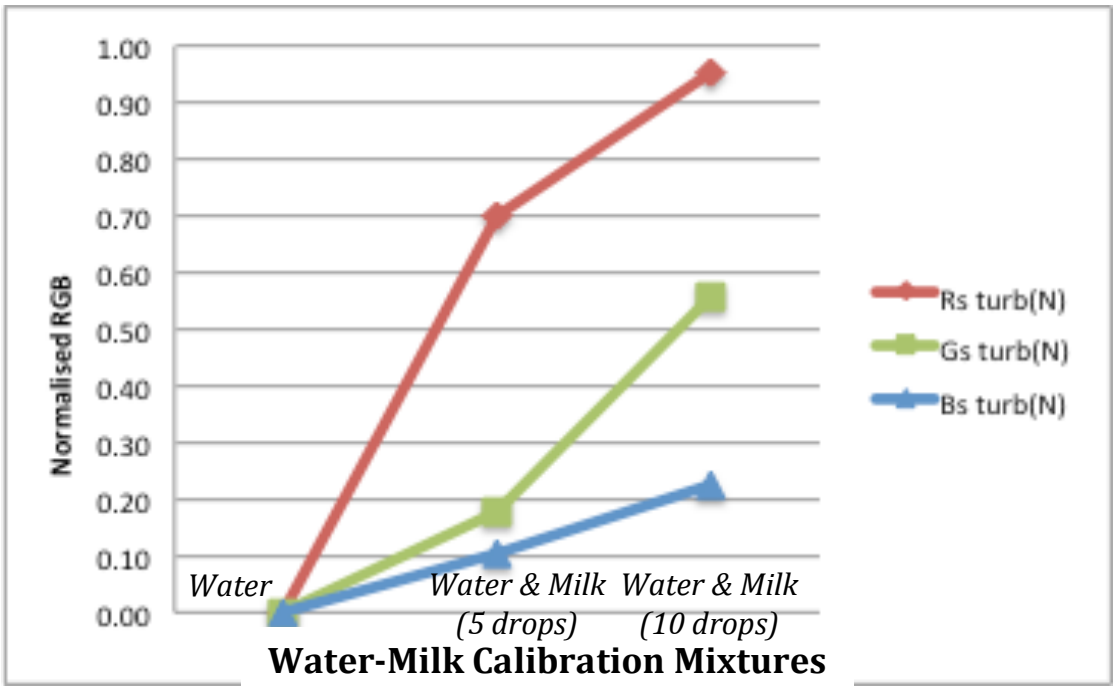

Figure 7.4(b): Calibration graph of reflected light turbidity parameters against water & milk drops samples

Figure 7.4: Processed results for water – milk mixtures.

(a) Calibration graph of transmitted light RGB liquid parameters

(b) Calibration graph of reflected light RGB turbidity parameters

7.3.3.2 Water – Tea – Milk Calibration Mixtures

Figure 7.5 shows results for the transmission and turbidity normalized chromatic parameters for water, tea and milk mixtures.

Figure 7.5(a) shows Rs(liq)N, G(liq)N, B(liq)N as a function of clear liquid (water and tea) when mixed with milk derived from the measured parameters (Figures 6.7 and 6.13, Chapter 6) and normalized with (Equation 7.1) for mixtures of water, tea and milk.

Figure 7.5(b) shows Rs(turb)N, G(turb)N, B(turb)N as a function of clear liquid (water and tea) when mixed with milk derived from the measured parameters (Figure 6.13, Chapter 6) and normalized with (Equation 7.2) for mixtures of turbid milk in water and tea.

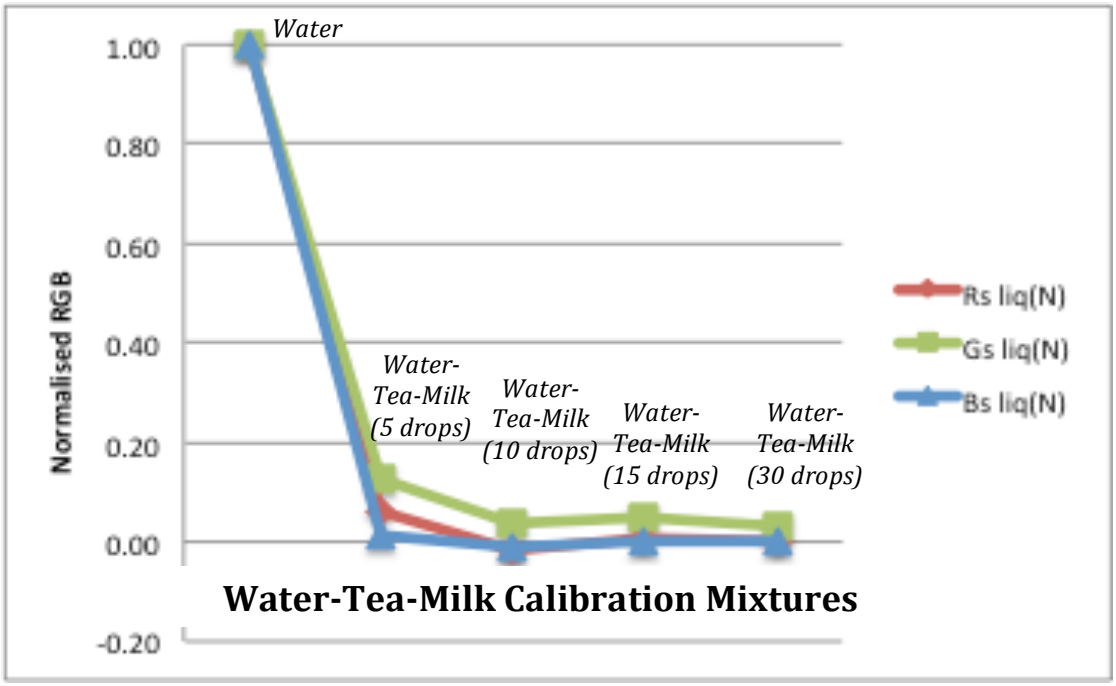

Figure 7.5 (a): Calibration graph of transmitted light parameters against water, tea & milk mixtures

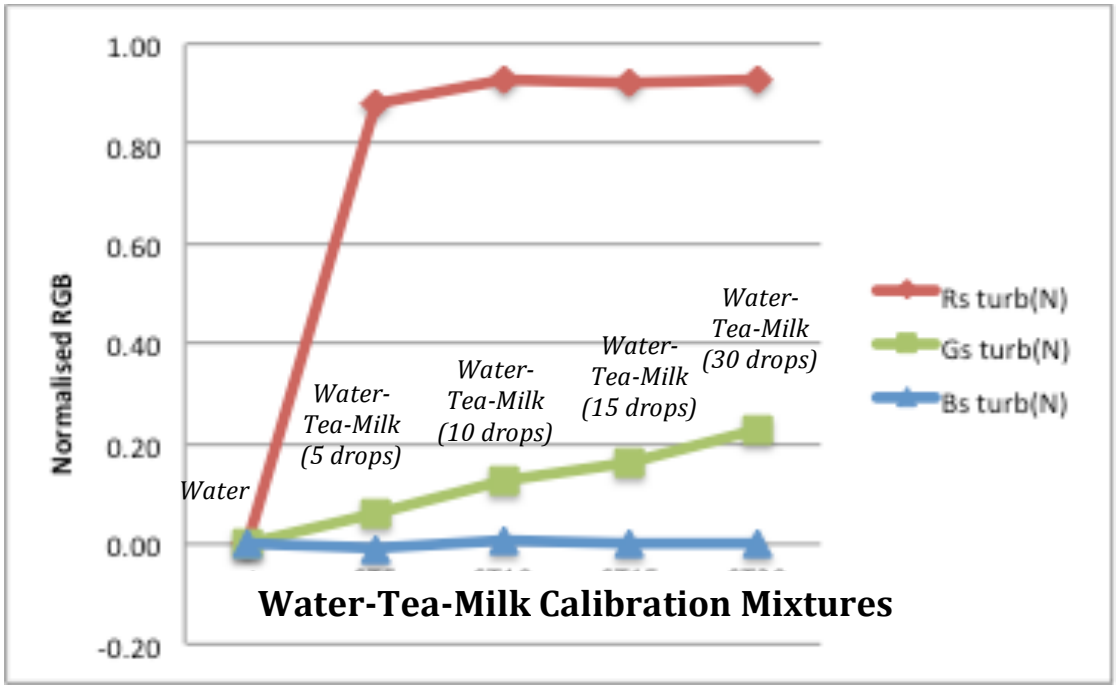

Figure 7.5(b): Calibration graph of reflected light turbidity parameters Vs water, tea & milk mixtures

Figure 7.5: Processed results for water – tea – milk mixtures.

(a) Calibration graph of transmitted light RGB liquid parameters

(b) Calibration graph of reflected light RGB turbidity parameters

7.3.4 Processed Results & Cluster Maps

The chromatic cluster maps were based upon the camera outputs R (long wavelengths) and B (short wavelengths) normalized (0-1) as shown on figure 7.6.

Figure 7.6(a) shows a (2-D) Rs liq(N) : Bs liq(N) chromatic map for optical transmission of the VDU illumination of water tea diluted with water, water with few drops (5,10) of milk, tea and milk mixtures(milk 5,10,15,30 drops) water and tea mixtures. The Rs liq(N) : Bs liq(N) results for the mixtures of water and tea (clear liquids) show that the Bs liq(N) reduces in strength with increasing tea concentration more rapidly than the Rs liq(N. The Rs liq(N) : Bs liq(N) results for mixtures of water and milk (turbid mixtures) show that the Rs liq(N) reduces in strength with increasing milk concentration more rapidly than the Bs liq(N).
The result for the more complex mixtures of water, tea and milk show that the Rs liq(N) : Bs liq(N) lies close to the origin. The locus line Rs liq(N)=Bs liq(N) denotes an equal strength.

Figure 7.6(b) shows a (2-D) Rs turb(N) : Bs turb (N) chromatic map for the turbidity with ambient light only for the liquid mixtures. The Rs turb(N) : Bs turb (N) results for the water and milk (turbid mixtures) show that the Rs turb(N) increases in strength with increasing milk concentration more rapidly than the Bs turb (N). The locus line Rs turb(N)=Bs turb(N) denotes an equal strength.

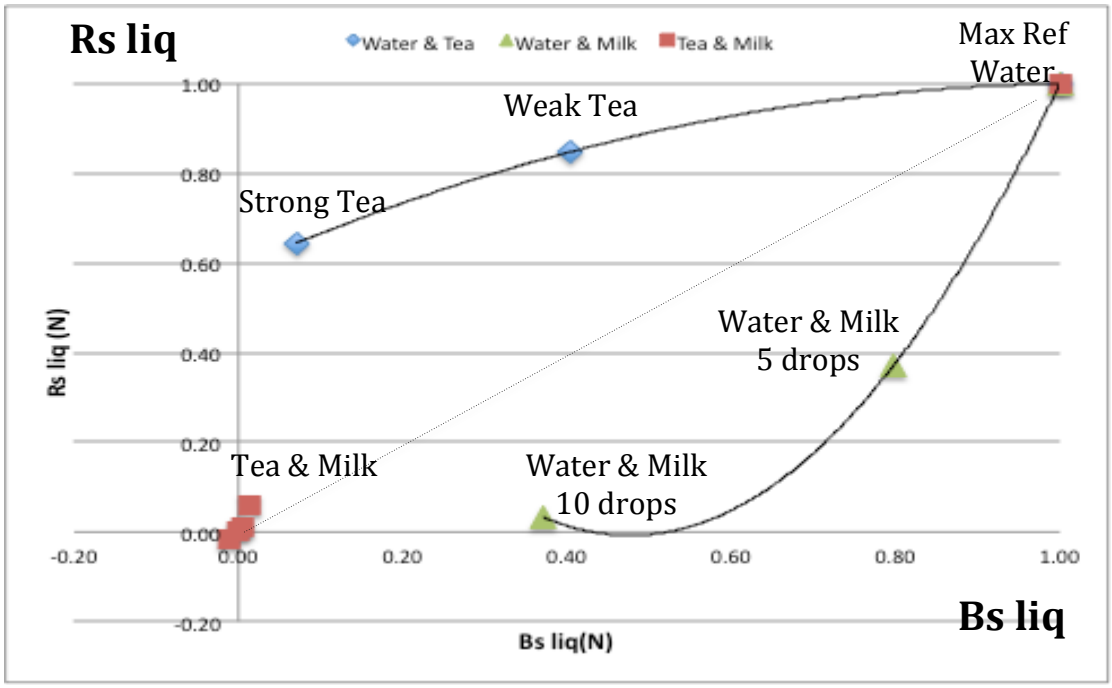

Figure 7.6 (a): Cluster map of transmitted light liquid parameter Rs liq(N):Bs liq(N) for water, tea and milk mixtures. (------ >> Rliq(N)=B(liq(N) locus)

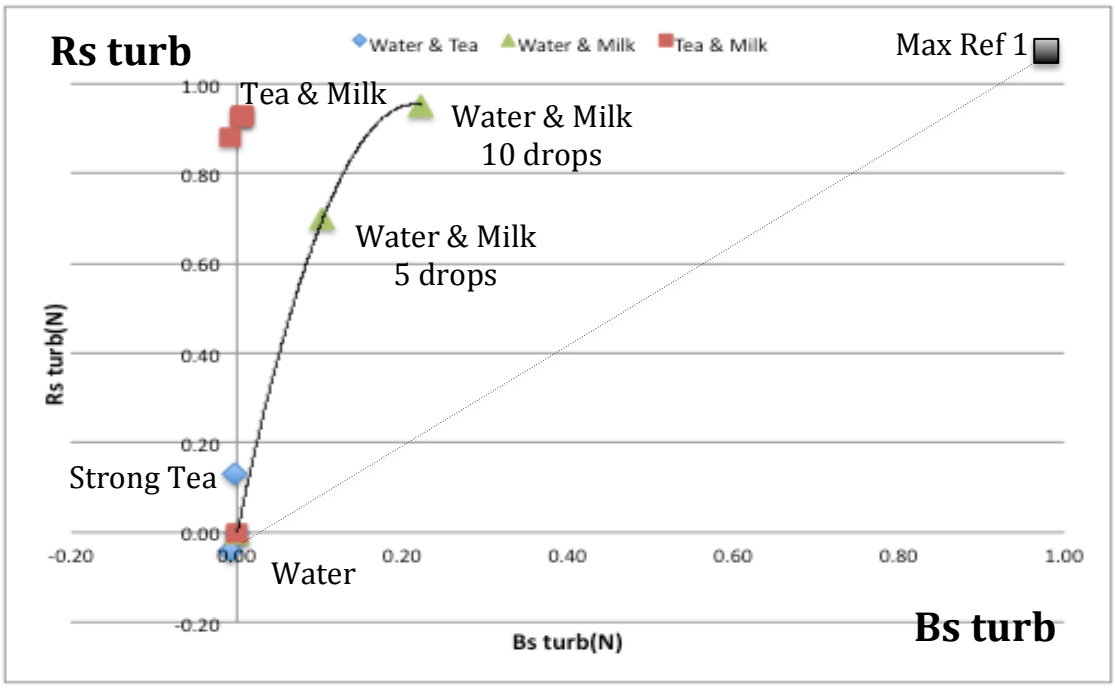

Figure 7.6(b): Cluster map of reflected light turbidity parameter Rs turb(N):Bs turb(N) for water, tea and milk mixtures. (------ >> Rs turb(N)=Bs turb(N) locus)

Figure 7.6: Chromatic cluster map for water, tea and honey mixtures

(a) Cluster map of transmitted light liquid parameter Rs liq(N):Bs liq(N)

(b) Cluster map of reflected light turbidity parameter Rs turb(N):Bs turb(N)

7.4 Water-Syrup-Honey Calibration Mixtures

7.4.1 Correction of Left Reference Area of the Images

Figure 7.7 shows the RGB data of the Left reference area of the image, Figure 7.7(a) shows the raw R, G, B data for the Lref area with difference honey samples. In all cases the VDU screen was switched on to provide reference signals either side of the cuvette test region. Thus the screen illumination and ambient light are both present.

The results show an approximate level of repeatability for the RGB values of L (left) reference for all the tests but with some variations apparent. These variations may be corrected with respect to a chosen benchmark value according to a correction factor $L_{ref\ correction\ factor} = \frac{L_{benchmark}}{L_{reference}}$. The benchmark values chosen were different to those chosen for the water, tea and milk test (Section 7.3) because a slightly different colour background was used in order to have a better camera focus, those values were chosen to be R = 0.588, G = 0.376 and B = 0.345 (these values were the RGB color values chosen to set the L reference area illumination). The values of the RGB correction factors for each honey test are shown on figure 7.7(b).

Figure 7.7 (c) shows the corrected values of RGB for the Lref area for various tests calculated in this manner.

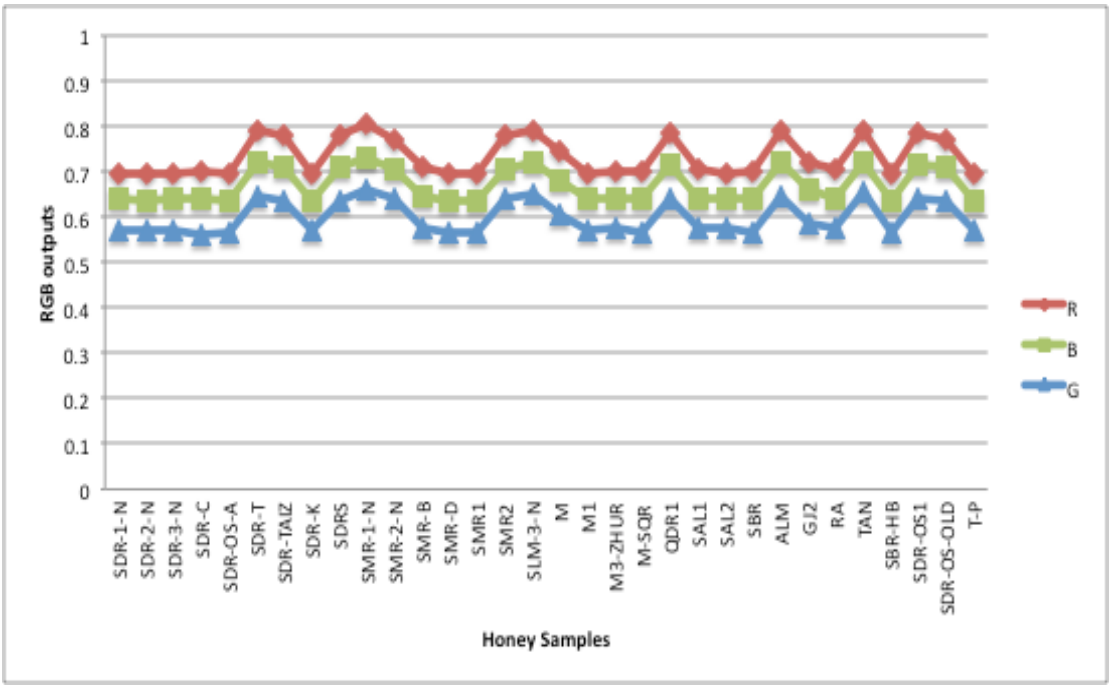

Figure 7.7 (a): RGB data output of Lref image area with 28 different honey tests

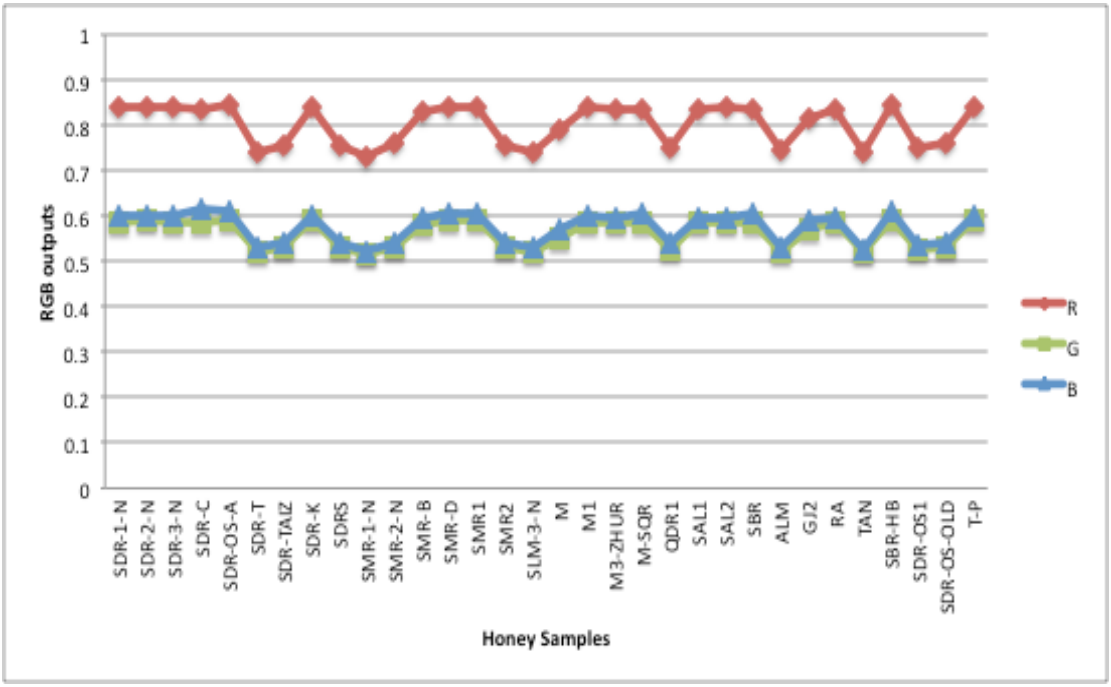

Figure 7.7(b): Correction factors for RGB data for each honey sample test, corrected with respect to the Lref area chosen benchmark

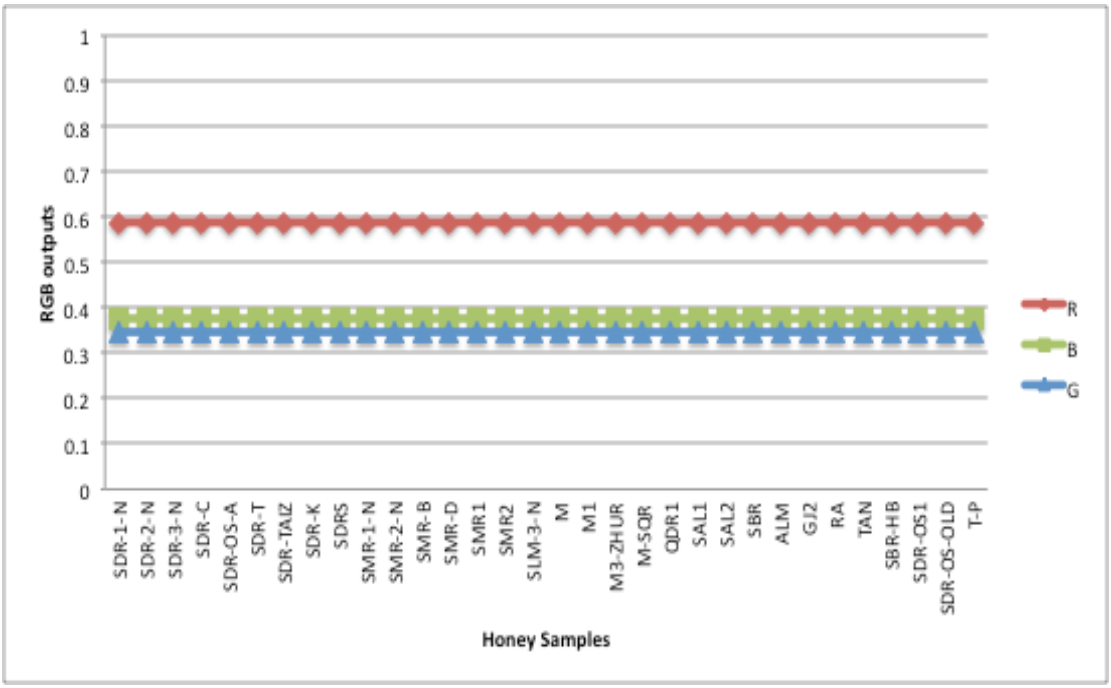

Figure 7.7(c): Corrected RGB data for the Lref areas for the various honey tests

Figure 7.7: RGB of the Left area of the image for various honey test samples.

(a) Raw output values

(b) Left reference area correction factor

(c) Corrected values of the Left reference area

7.4.2 Correction Of The Raw RGB Honey Data

Figure 7.8 shows the corrected RGB values for the various honey samples. Figure 7.8(a) shows the raw data R, G and B output (Figure 6.20, Chapter 6) whilst figure 7.8 (b) shows the R, G, and B data corrected using the measured levels from the Lref area correction factor (figure 7.7(b)).

These results show similar variations to those of the raw data on figure 7.8(a) but with shifts in the relative magnitudes of the R, G and B channels.

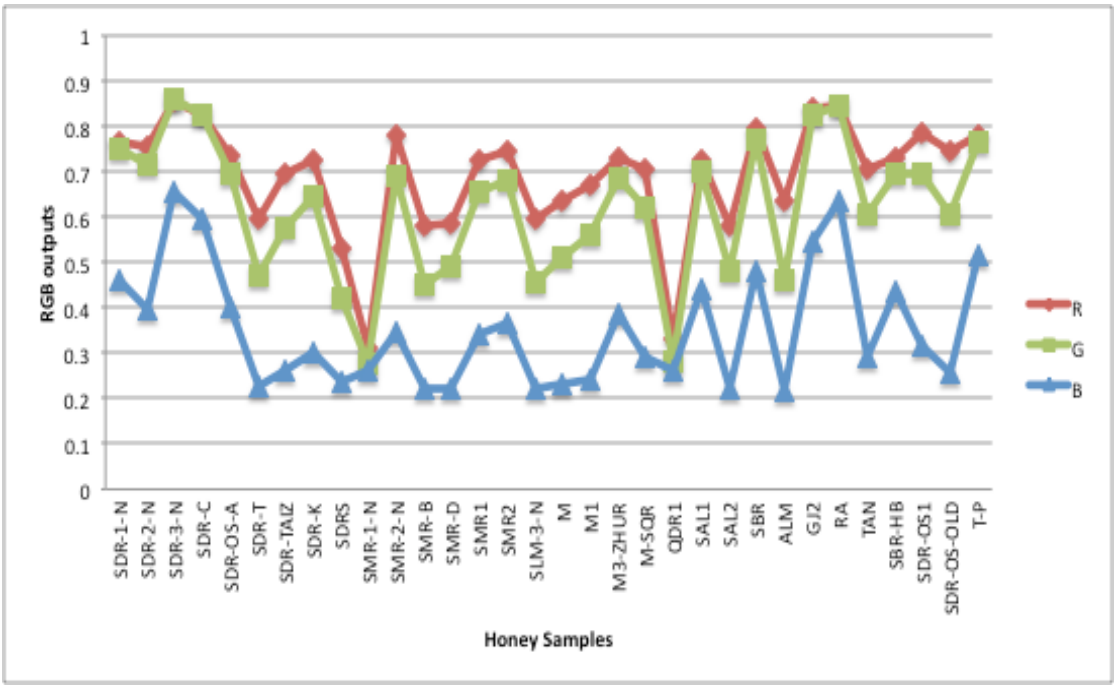

Figure 7.8(a): Raw RGB outputs

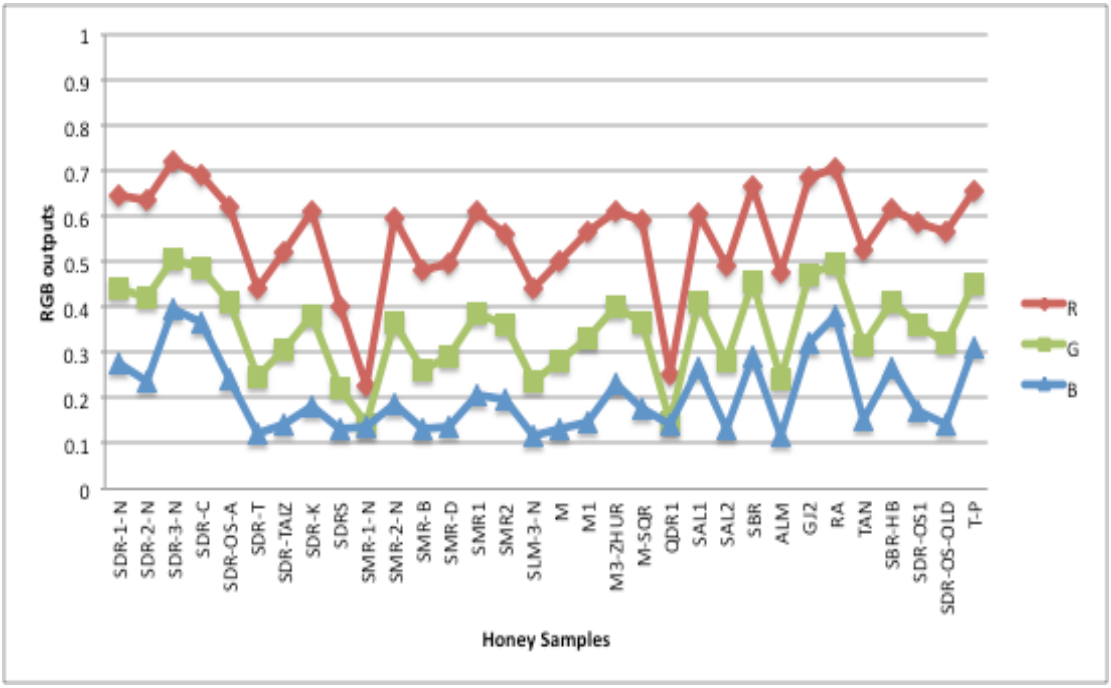

Figure 7.8 (b): Corrected RGB results

Figure 7.8: Correction of the raw RGB honey data vs. honey samples.

(a) Raw RGB outputs

(b) Corrected RGB results

7.4.3 Normalization Of The RGB Data For The Calibration Mixtures (Water-Syrup-Honey) & Honey Test Samples

A list of the range of data gathered for the honey test samples and calibration mixtures are given on table 7.1.

Sample	**Illumination**					
	Screen	*Black Card*	*White Card*	*Violet LED & Black Card*	*Polarizing Filters*	*Polarizing Filters & Black Card*
Honey Sample	X(S)Ws	X(S)Bc		X(S)UV	X(S)Pol	
Water	X(W)Ws	X(W)Bc	X(W)Wc	X(W)UVBc	X(W)Pol	X(W)PolBc

Table 7.1: Summary of test data collected for the experimental tests

DATA COLLECTED:

- X(S)Ws = X(sample, screen)
- X(S)Bc = X(sample, black card)
- X(W)Ws = X(water, screen)
- X(W)Bc = X(water, black card)
- X(W)Wc = X(water, white card)
- X(S)UV = X(sample(UV), (black card)
- X(W)UVBc = X(water(UV), black card)
- X(S)Pol = X(sample(θ), screen)
- X(W)Pol = X(water(θ), screen),
- X(W)PolBc = X(Water(θ), black card)

Where X = R, G or B

The raw data are corrected with respect to the reference area and then normalized and scaled within the range 0–1 using the following algorithms below.

Transmission of light equation (i.e. Liquid content):

The data that was collected have been normalized using equation 7.3 to give the level of the transmitted light (liquid content) though the test samples.

$$X(liq)N = \frac{X(sample,screen) - X(water,black\ card)}{X(water,screen) - X(ref,min)} \quad (7.3)$$

Where X = R, G, B

X(sample, screen), X(water, screen) are measures respectively of the screen light transmitted through a sample, water.

X(sample, black card), X(water, black card) are measures respectively of a sample, water with "ambient" light and no "direct" screen light.

X(water, white card) is a measure of the ambient light level reflected from a white card.

Fluorescence equation:

The data that was collected have been normalized using equations 7.4-7.6 to give the level of the fluorescence from the test samples.

$$R(flo)N = \frac{R(sample(UV),black\ card) - R(water,black\ card)}{R(ref(UV),max) - R(water,black\ card)} \quad (7.4)$$

$$G(flo)N = \frac{G(sample(UV),black\ card) - G(water(UV),black\ card)}{G(ref(UV),max) - G(water(UV),black\ card)} \quad (7.5)$$

$$B(flo)N = \frac{B(sample(UV),black\ card) - B(water,black\ card)}{B(ref(UV),max) - B(water,black\ card)} \quad (7.6)$$

R(sample(UV), black card), G(sample(UV), black card) and B(sample(UV), black card) are measures of a sample "fluorescent" light signatures at the Red, Green and blue wavelength respectively with "ambient light" and no "direct" screen light.
G(water(UV), black card) is a measures of water "fluorescent" light at the Green wavelengths with "ambient light" and no "direct" screen light.

R(water, black card), and B(water, black card) are measures of water with "ambient" light and no "direct" screen light.

R(ref, (UV),max), G(ref, (UV),max) and B(ref, (UV),max) are measures of the maximum "fluorescent" light of a reference sample at the Red, Green and Blue wavelength respectively with "ambient light" and no "direct" screen light.

Polarization equation:

The data that was collected have been normalized using equations 7.7 to give the level of optically rotated polarized light transmitted through the test samples.

$$X(pol)N = \frac{X(sample(\theta),screen) - X(water(\theta),black\ card)}{X(ref(\theta),max) - X(ref(\theta),min)} \qquad (7.7)$$

Where X = R, G, B

X(sample(θ), screen), X(water(θ), screen), are measures respectively of the screen light transmitted through a sample, water with two polarizing angles rotated with respect to each other.

X(water(θ), black card) are measures respectively of water with "ambient" light and no "direct" screen light and two polarizing angles rotated with respect to each other.

X(ref(θ), max) and X(ref(θ), min) are measures of the reference samples maximum and minimum rotated polarized light respectively.

7.4.4 Normalized Test Results

The above algorithms have been used to produce values of [R(liq)N, G(liq)N, B(liq)N], [R(flo)N, G(flo)N, B(flo)N] and [R(pol)N, G(pol)N, B(pol)N] for the (water- syrup-honey) calibration mixtures and various honey test samples. The results are given on figures 7.9 - 7.17.

7.4.4.1 Light Transmission Results

7.4.4.1.1 Water-Syrup-Honey Calibration Mixtures

Figure 7.9 shows the calibration curves for each of the three chromatic parameters, R(liq)N, G(liq)N, B(liq)N as a function of (water, syrup, honey) calibration mixture samples for the transmitted light , the values were obtained from (Equation 7.3)

Figure 7.9(a) shows calibration curves for each of the three chromatic parameters as a function of water and syrup mixture. Figure 7.9(b) shows calibration curves for each of the three chromatic parameters as a function of water and honey mixture and figure 7.9(c) shows calibration curves for each of the three chromatic parameters as a function of water and honey mixture

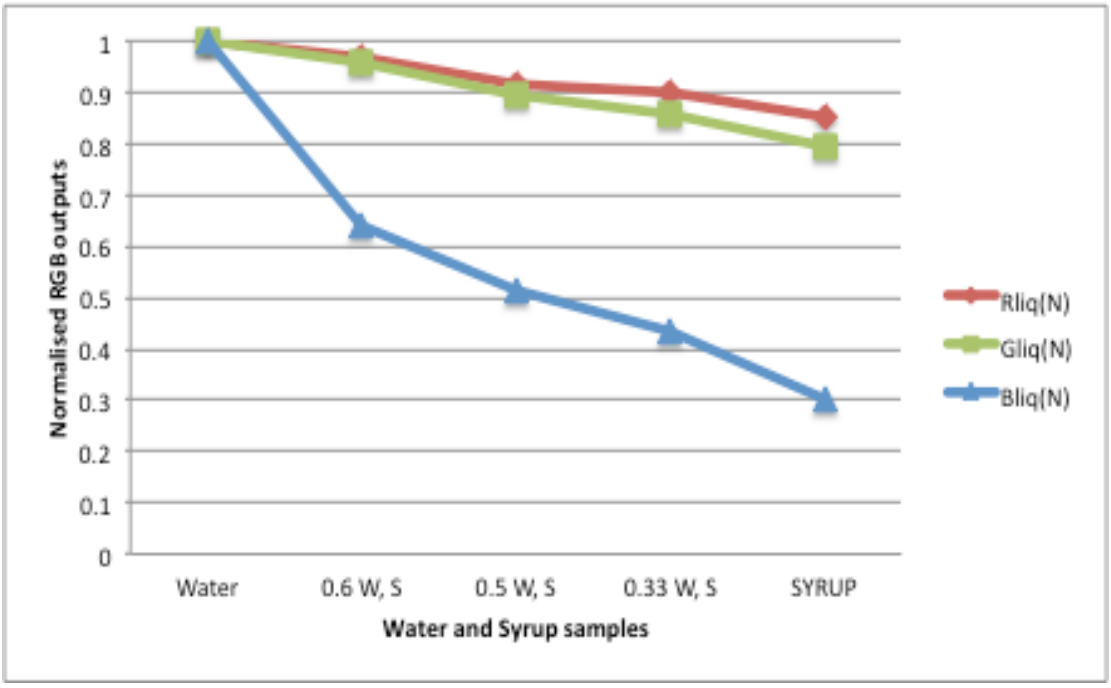

Figure 7.9(a): Calibration graph of RGB normalized parameters against Water & Syrup mixtures

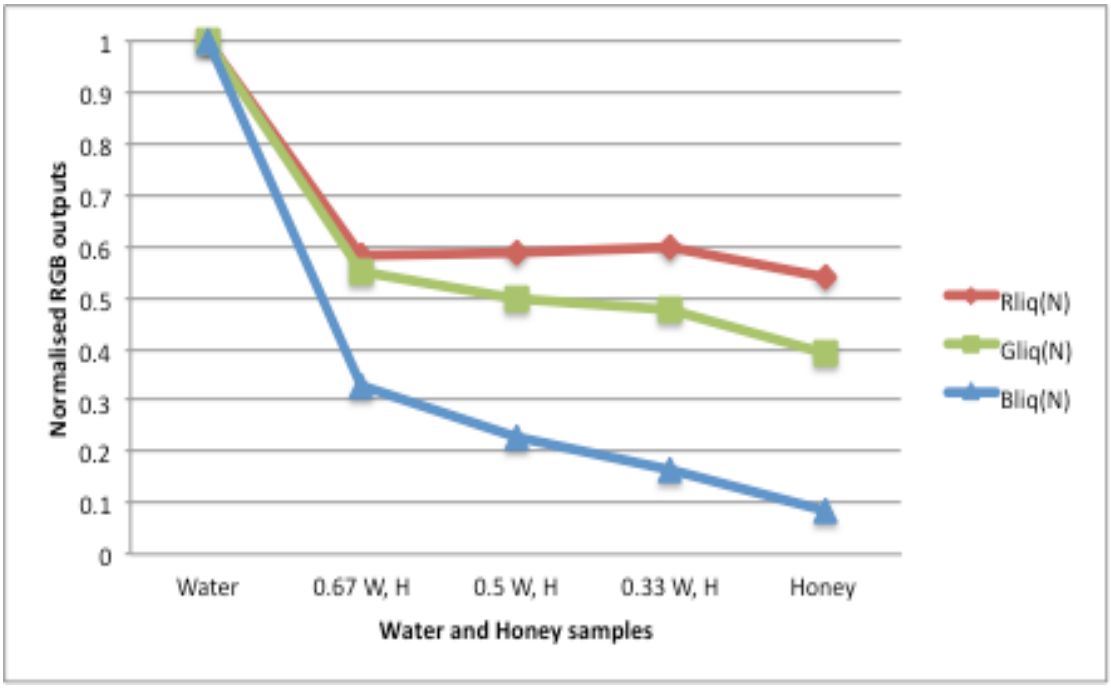

Figure 7.9(b): Calibration graph of RGB normalized parameters against Water & Syrup mixtures

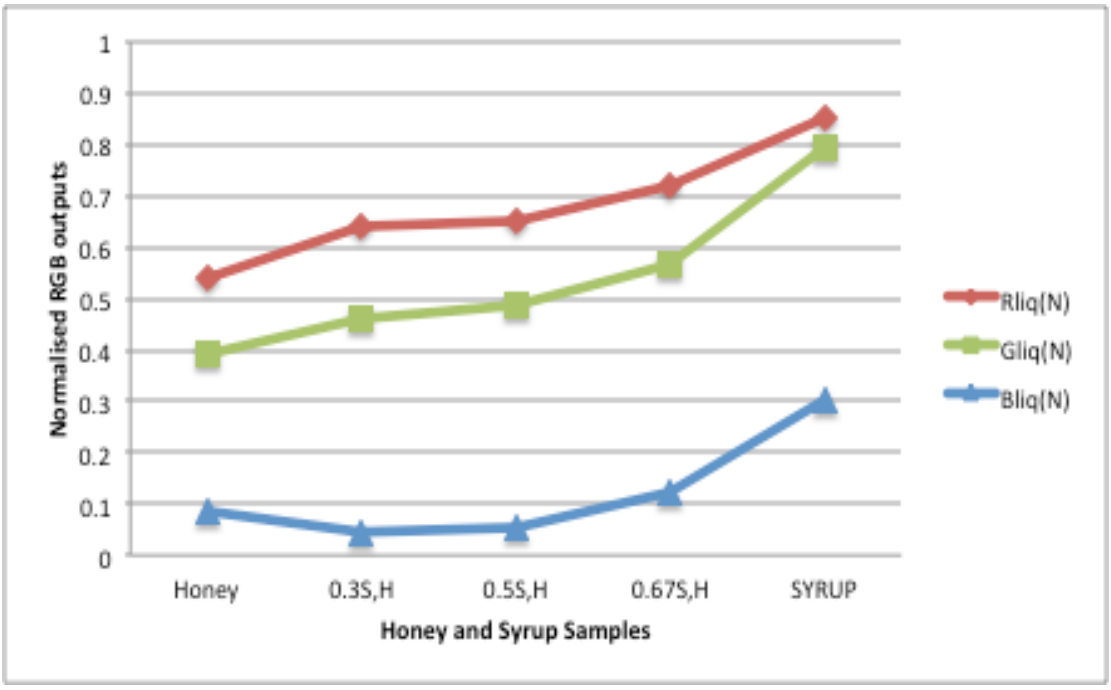

Figure 7.9(c): Calibration graph of RGB normalized parameters against Honey & Syrup mixtures

Figure 7.9: Calibration curves of the processed transmitted light result for (water, syrup, honey) mixtures s with white illumination screen

a) **Calibration graph of RGB normalized parameters against Water & Syrup mixtures**

b) **Calibration graph of RGB normalized parameters against Water & Honey mixtures**

c) **Calibration graph of RGB normalized parameters against Honey & Syrup mixtures**

Figure 7.10 shows a (2-D) Rliq(N) : Bliq(N) chromatic cluster map for the optical transmission of the VDU illumination of the syrup diluted with water, honey diluted with water and a further complex condition of honey and syrup (syrup 4g, 6g, 8g) mixture samples at different concentrations. The Rliq(N) : Bliq(N) results for the mixtures of water-syrup and water-honey (viscous sugar mixtures) show that the Bliq(N) reduces in strength with increasing syrup and honey concentrations respectively more rapidly than the Rliq(N). The result for the more complex condition of honey and syrup mixture (added sugar mixture) show that the Rliq(N) : Bliq(N) increases in strength with increasing syrup concentrations. The locus line Rliq(N)=Bliq(N) denotes an equal strength.

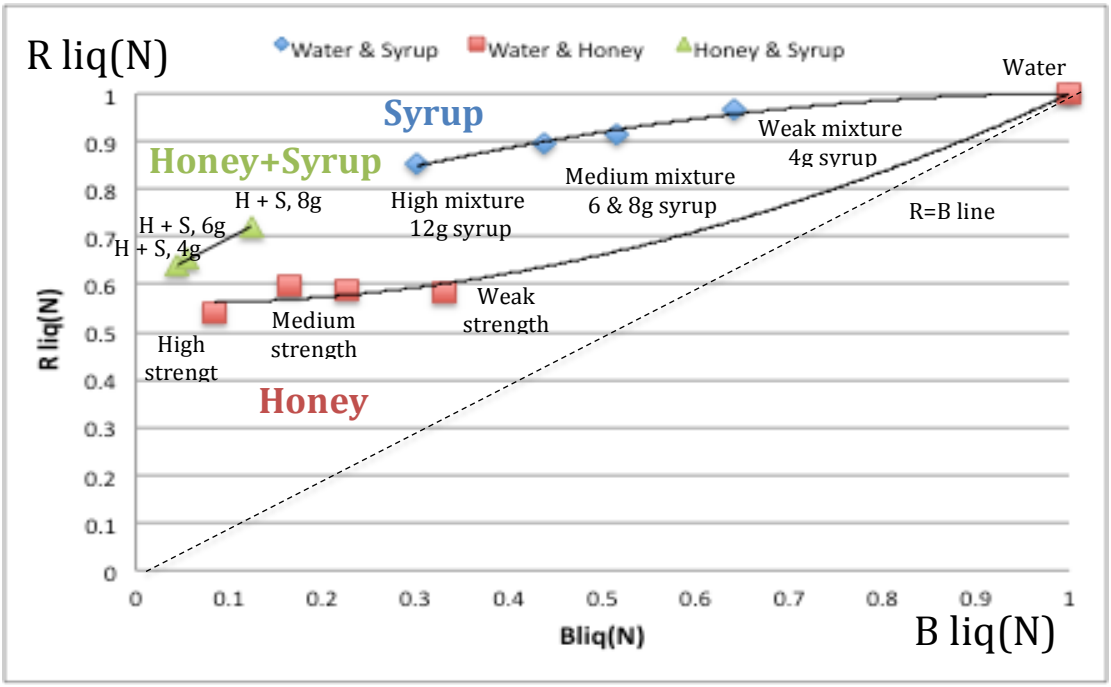

Figure 7.10: Chromatic cluster map of transmitted light parameter Rliq(N):B(liqN) for (water, syrup, honey) calibration mixture samples.

7.4.4.1.2 Honey Samples

Figure 7.11 shows the normalized results for the white light transmission through various honey samples the values were obtained from (Equation 7.3)

Figure 7.11(a) shows calibration curves for each of the three chromatic parameters, R(liq)N, G(liq)N, B(liq)N as a function of various honey samples with attenuated white illumination screen.

Figure 7.11(b) shows a chromatic cluster map Rliq(N) against Bliq(N) for various honey samples. This shows that for Rliq(N) ≤ 0.2 there is little variation in Bliq(N).

The normalized calibration curves and cluster map results for the blue light illumination through water and various honey samples are shown on the Appendix II section.

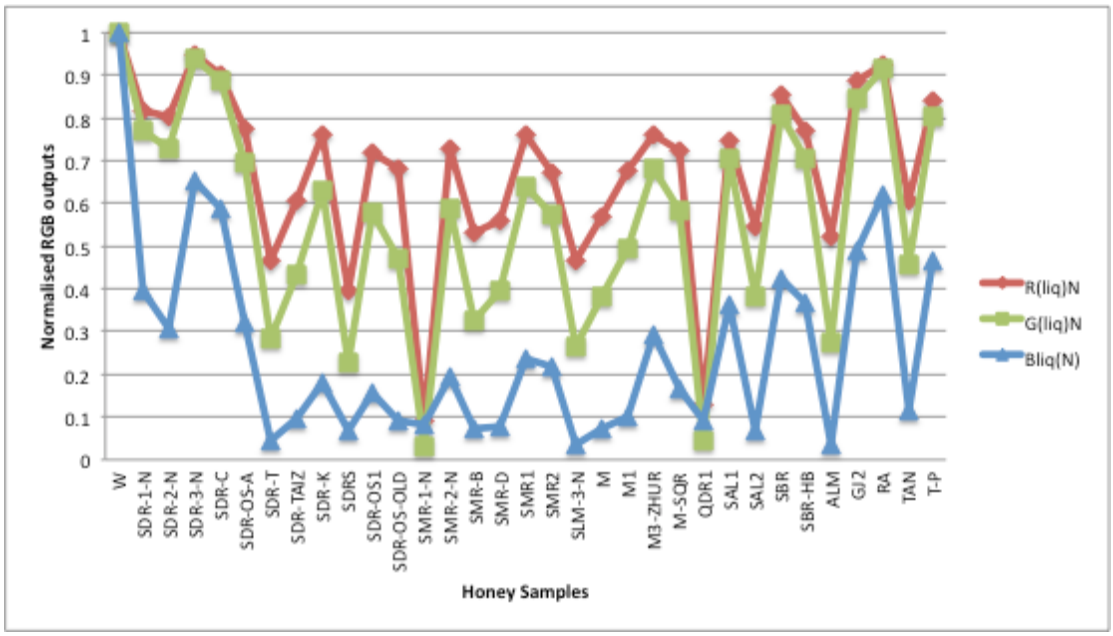

Figure 7.11 (a): Calibration graph of RGB transmitted light parameters against water and various honey samples

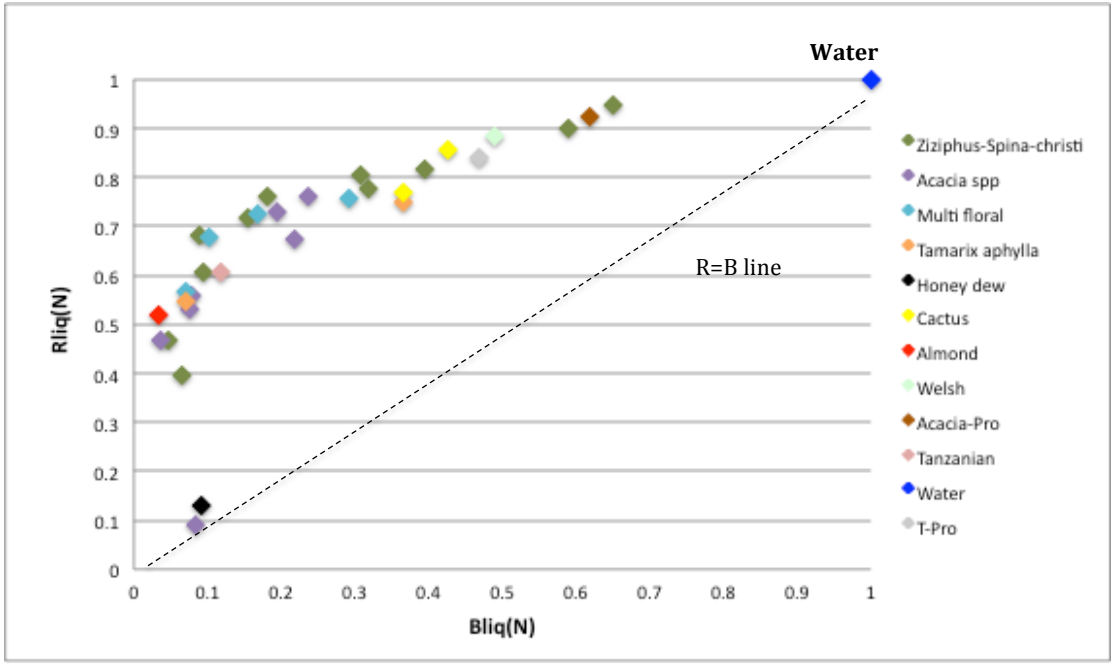

Figure 7.11(b): Chromatic cluster map of transmitted light parameter Rliq(N):B(liqN) for water and various honey samples

Figure 7.11: Processed Transmitted light result for various honey samples and water with attenuated white illumination screen

(a) Calibration graph of RGB transmitted light parameter against water and various honey samples

(b) Chromatic cluster map of transmitted light parameter Rliq(N):B(liqN)

7.4.4.3 Normalized Fluorescence Results

7.4.4.3.1 Water-Syrup-Honey Calibration Mixtures

Figure 7.12 shows the calibration curves for each of the three chromatic parameters, R(flo)N, G(flo)N, B(flo)N as a function of (water, syrup, honey) mixture samples for the scattered fluorescent light, the values were obtained from (Equations 7.4, 7.5 and 7.6 respectively).

Figure 7.12(a) shows calibration curves for each of the three chromatic parameters as a function of water and syrup mixture. Figure 7.12(b) shows calibration curves for each of the three chromatic parameters as a function of water and honey mixture and figure 7.12(c) shows calibration curves for each of the three chromatic parameters as a function of syrup and honey mixture

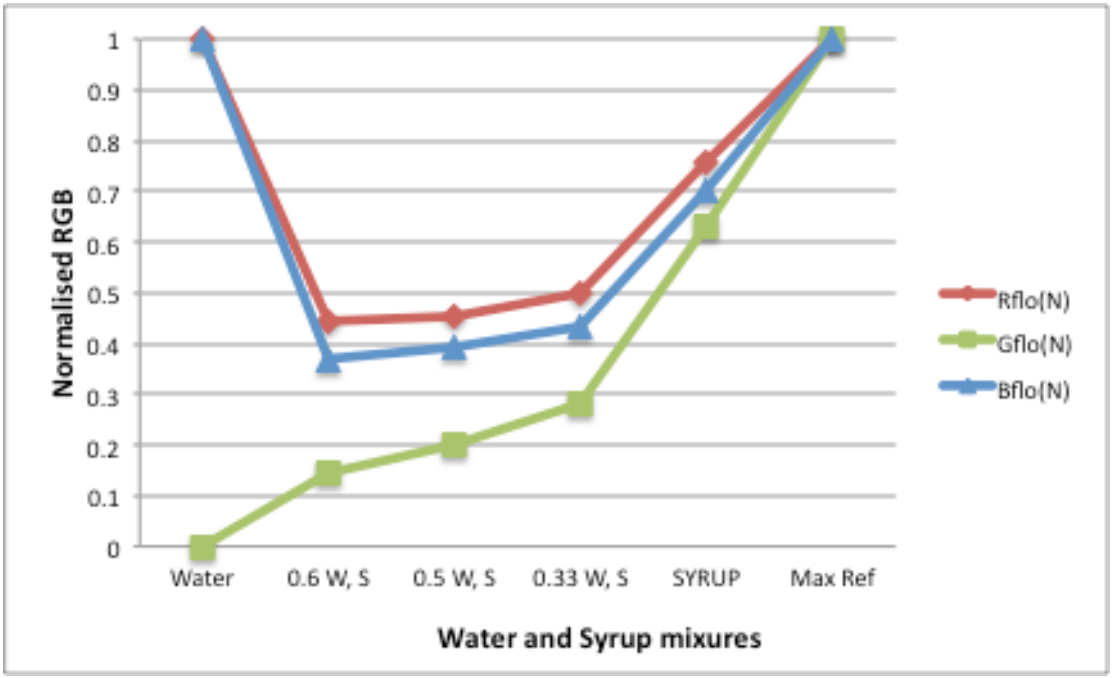

Figure 7.12 (a): Calibration graph of RGB normalized parameters against Water & Syrup mixtures

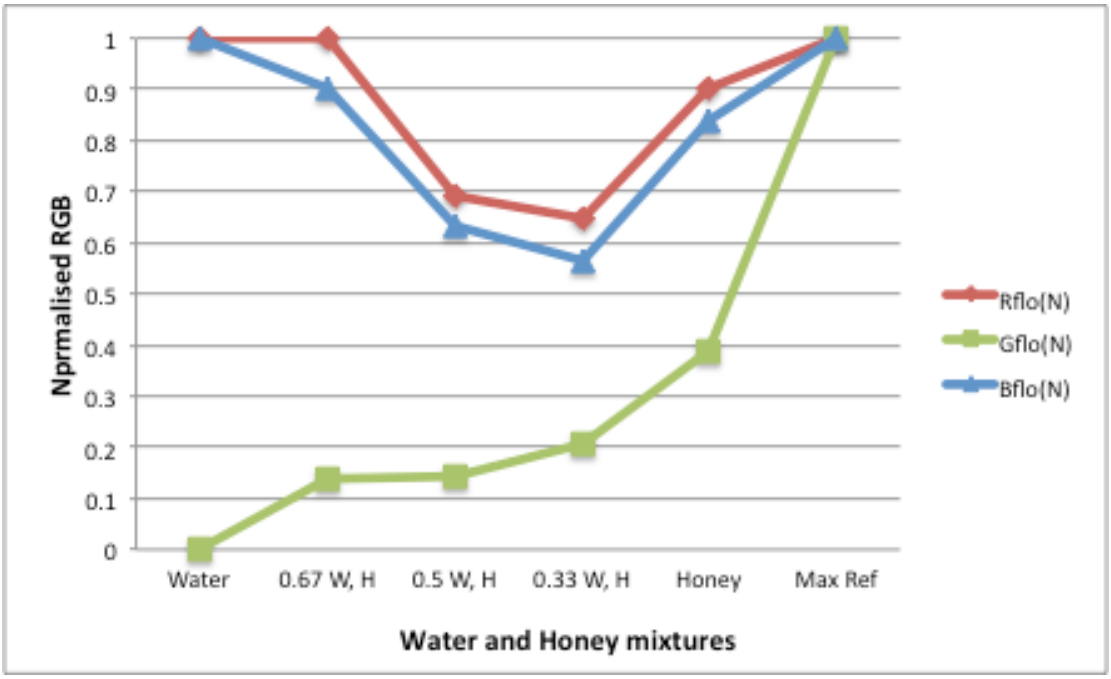

Figure 7.12(b): Calibration graph of RGB normalized parameters against Water & Honey mixtures

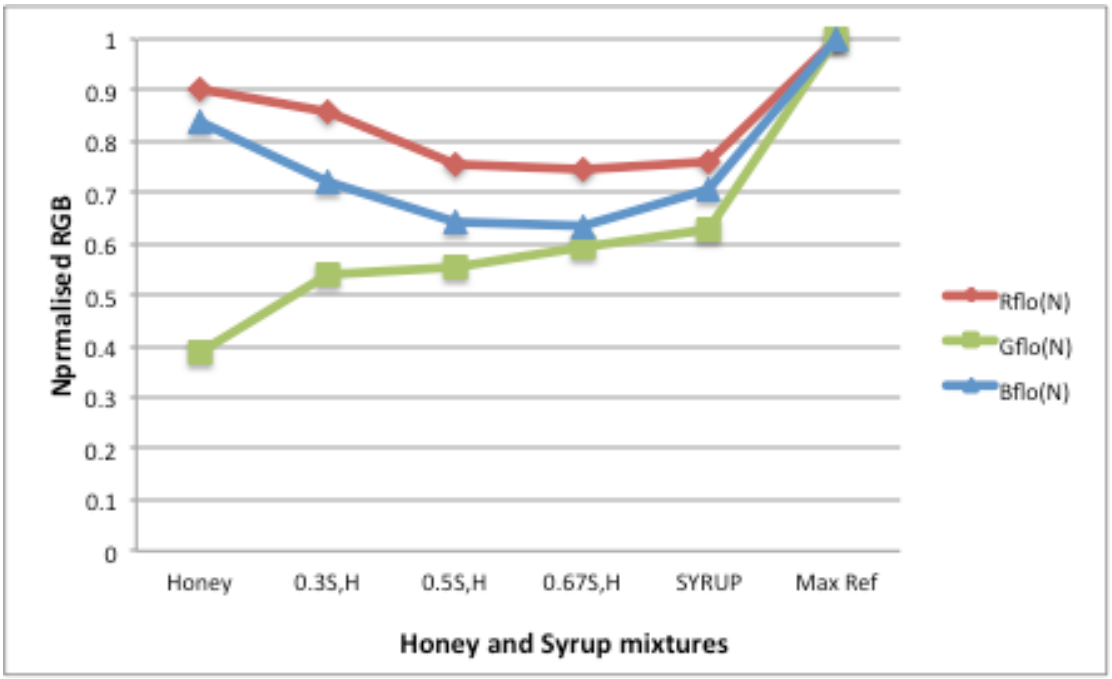

Figure 7.12(c): Calibration graph of RGB normalized parameters against Honey & Syrup mixtures

Figure 7.12: Calibration curves of the processed scattered fluorescent light result for (water, syrup, honey) mixtures s with violet LED illumination

a) Calibration graph of RGB normalized parameters against Water & Syrup mixtures

b) Calibration graph of RGB normalized parameters against Water & Honey mixtures

c) Calibration graph of RGB normalized parameters against Honey & Syrup mixtures

Figure 7.13 shows a (2-D) Gflo(N) : Bflo(N) chromatic cluster map for the optical light fluorescence when violet LED illumination excites the samples mixtures of syrup diluted with water, honey diluted with water and a further complex condition of honey and syrup (syrup 4g, 6g, 8g) mixture samples at different concentrations. The water-syrup Gflo(N) : Bflo(N) results are more closer to the locus line Gflo(N)=Bflo(N) than the water-honey Gflo(N) : Bflo(N) results . The result for the more complex condition of honey and syrup mixture (added sugar mixture) show that the as the syrup concentration increases, the points goes towards the locus line Gflo(N)=Bflo(N). The locus line Rliq(N)=Bliq(N) denotes an equal strength.

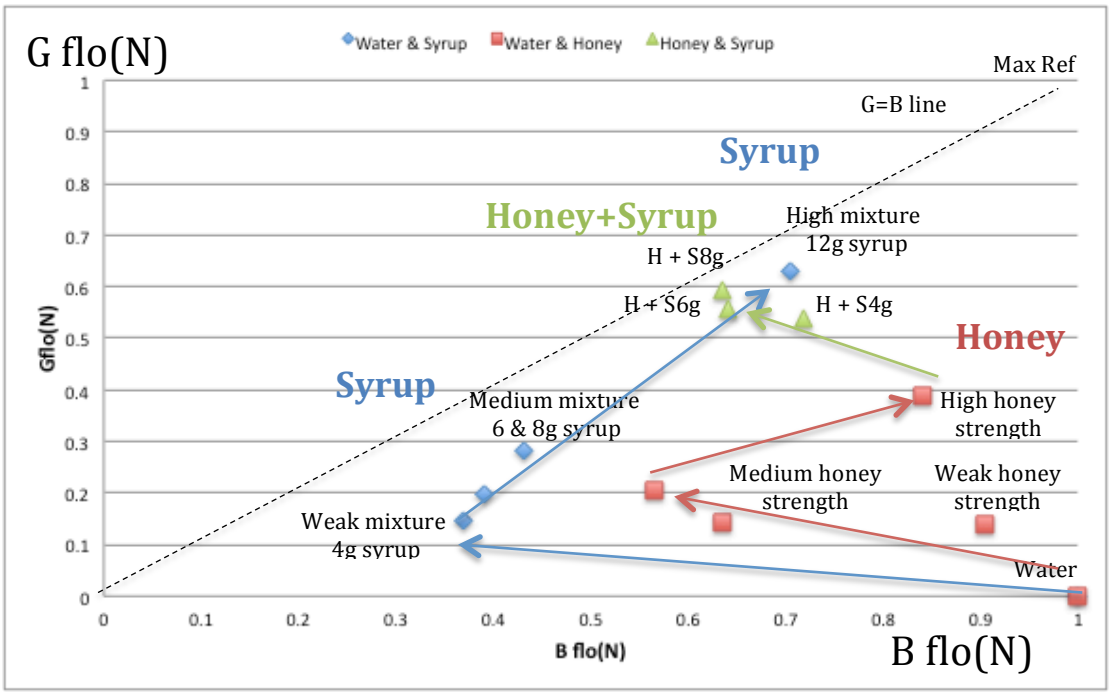

Figure 7.13: Chromatic cluster map of fluorescent light parameter Gflo(N):Bflo(N) for (water, syrup, honey) calibration mixture samples.

7.4.4.3.2 Honey Samples

Figure 7.14 shows the Normalized results R(flo)N, G(flo)N, B(flo)N scattered fluorescent light from various honey samples, the values were obtained from (Equation 7.4, 7.5 and 7.6 respectively).

Figure 7.14(a) shows calibration curves for each of the three chromatic parameters, R(flo)N, G(flo)N, B(flo)N as a function of various honey samples.

Figures 7.14(b) show chromatic cluster maps of Gflo(N): Bflo(N) for various honey samples.

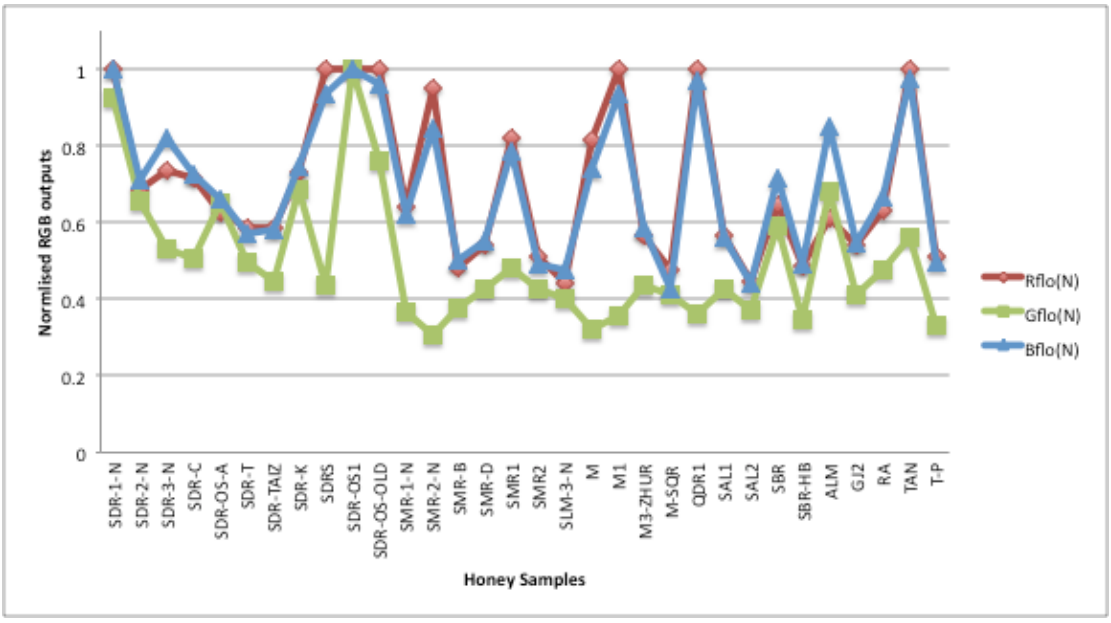

Figure 7.14 (a): Calibration graph of RGB scattered fluorescent light parameters against water and various honey samples

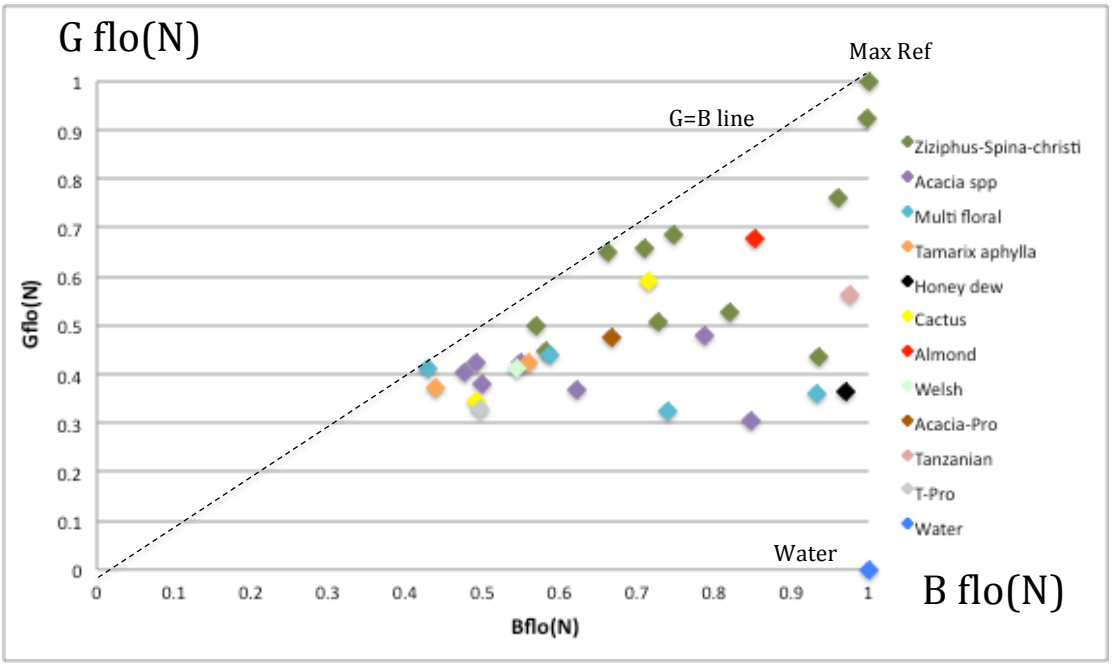

Figure 7.14(b): Cluster map of scattered fluorescent light parameter Gflo(N):Bflo(N)

Figure 7.14: Processed fluorescent chromatic parameters for various honey samples

(a) Calibration graph of RGB scattered fluorescent light parameters against various honey samples

(b) Cluster map of scattered fluorescent light parameter Gflo(N):Bflo(N)

7.4.4.4 Normalized Polarized Light Results

7.4.4.4.1 Water-Syrup-Honey Calibration Mixtures

Figure 7.15 shows the calibration curves for each of the three chromatic parameters, R(pol)N, G(pol)N, B(pol)N as a function of (water, syrup, honey) mixture samples for the polarized light, the values were obtained from (Equation 7.7) with polarizing filters indirection at 45 degrees to each other.

Figure 7.15(a) shows calibration curves for each of the three chromatic parameters as a function of water and syrup mixture. Figure 7.15(b) shows calibration curves for each of the three chromatic parameters as a function of water and honey mixture and figure 7.15(c) shows calibration curves for each of the three chromatic parameters as a function of syrup and honey mixture

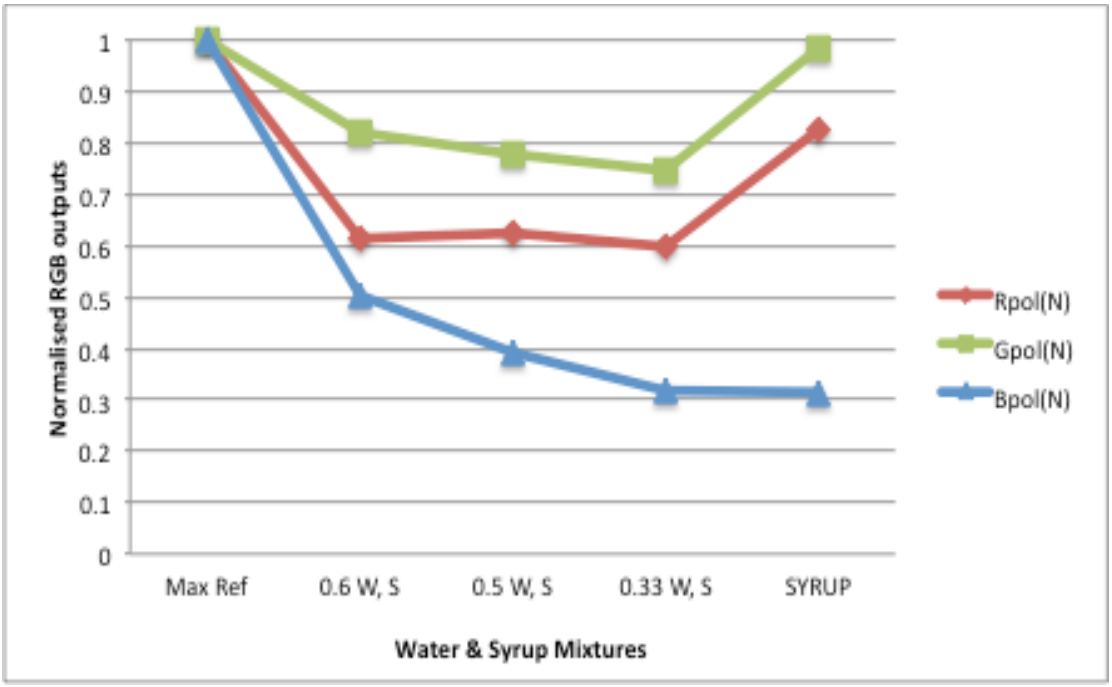

Figure 7.15 (a): Calibration graph of RGB normalized parameters against Water & Syrup mixtures

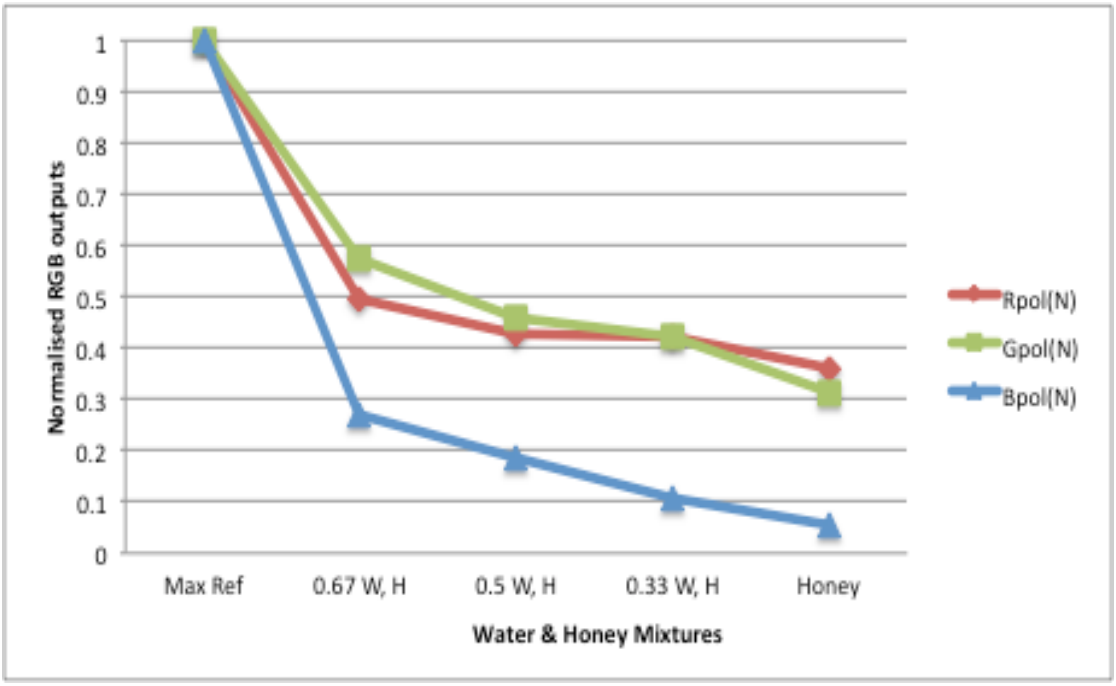

Figure 7.15(b): Calibration graph of RGB normalized parameters against Water & Honey mixtures

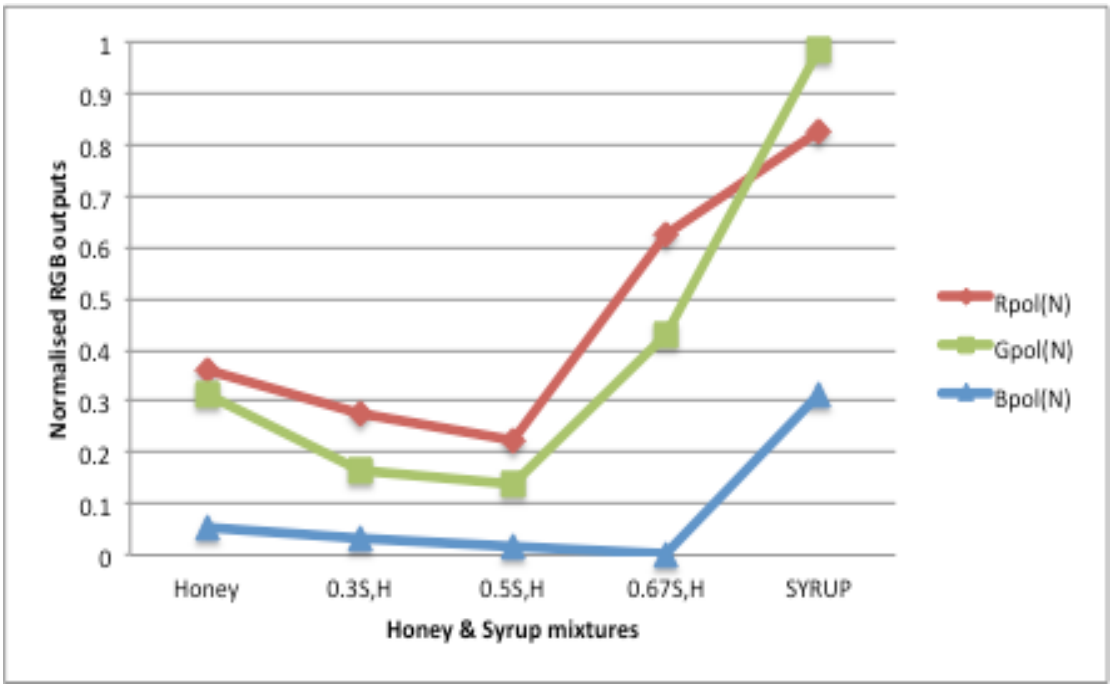

Figure 7.15(c): Calibration graph of RGB normalized parameters against Honey & Syrup mixtures

Figure 7.15: Calibration curves of the processed polarized light result for (water, syrup, honey) mixtures with angle of rotation at 45 degree and white VDU illumination

a) Calibration graph of RGB normalized parameters against Water & Syrup mixtures

b) Calibration graph of RGB normalized parameters against Water & Honey mixtures

c) Calibration graph of RGB normalized parameters against Honey & Syrup mixtures

Figure 7.16 shows a (2-D) Rpol(N) : Bpol(N) chromatic cluster map for the polarized light when a white VDU illumination is transmitted with polarizing filters indirection at 45 degrees to each other through the samples mixtures of syrup diluted with water, honey diluted with water and a further complex condition of honey and syrup (syrup 4g, 6g, 8g) mixture samples at different concentrations.

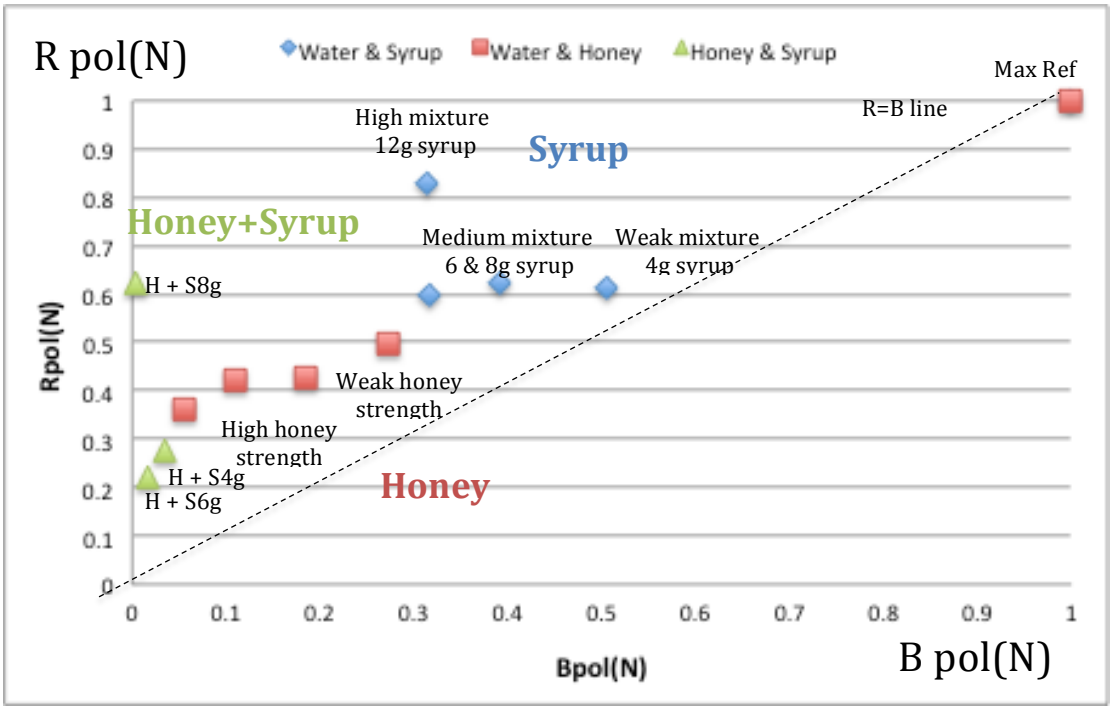

Figure 7.16: Cluster map of polarized light parameters Rpol(N):Bpol(N) at 45-degree polarizer angle

7.4.4.4.2 Honey Samples

Figures 7.17 shows R(pol)N, G(pol)N and B(pol)N results for the polarized light parameters through various honey samples, the values were obtained from (Equation 7.7).

Figure 7.17(a) shows calibration curves for each of the three chromatic parameters R(pol)N, G(pol)N and B(pol)N as a function of water and various honey samples with the polarizing filters indirection at 45 degrees to each other.

Figure 7.17(b) shows a chromatic cluster map Rpol(N) against Bpol(N) of various honey samples and water corresponding to this 45 degree relative indirection of the polarizing filters.

The normalized calibration curves and cluster map results for the polarized light parameters through various honey samples corresponding to 0, 30 and 70 degrees relative indirection of the polarizing filters are shown on the Appendix II section.

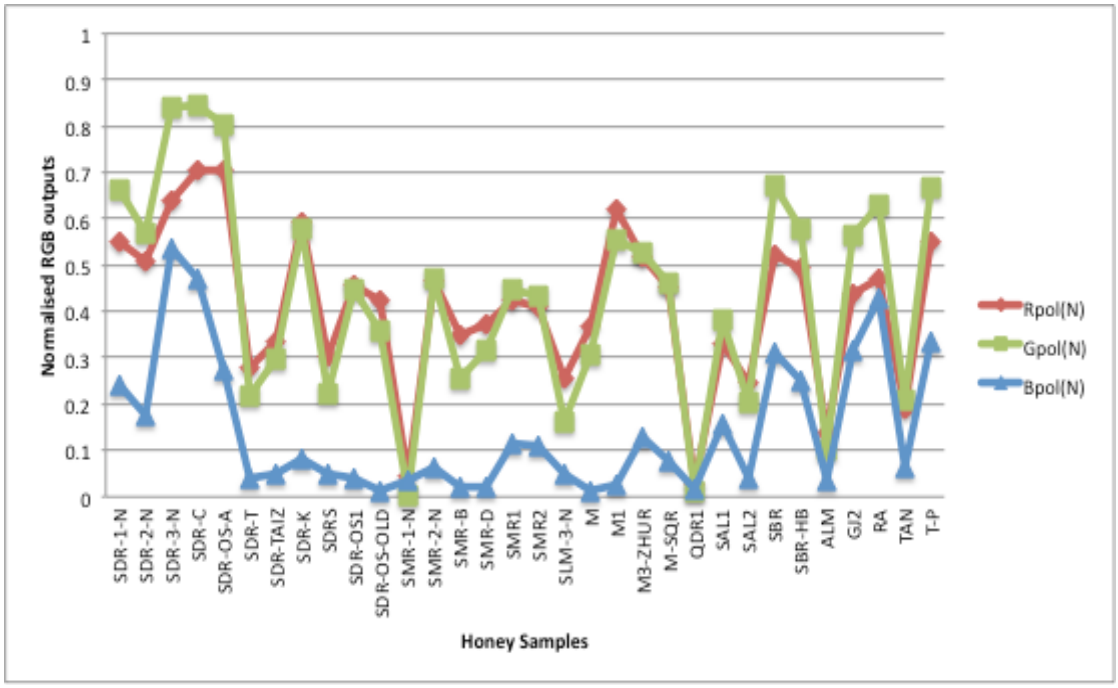

Figure 7.17:(a): Calibration graph of RGB polarized light parameters against various honey samples at 45-degree polarizer angle

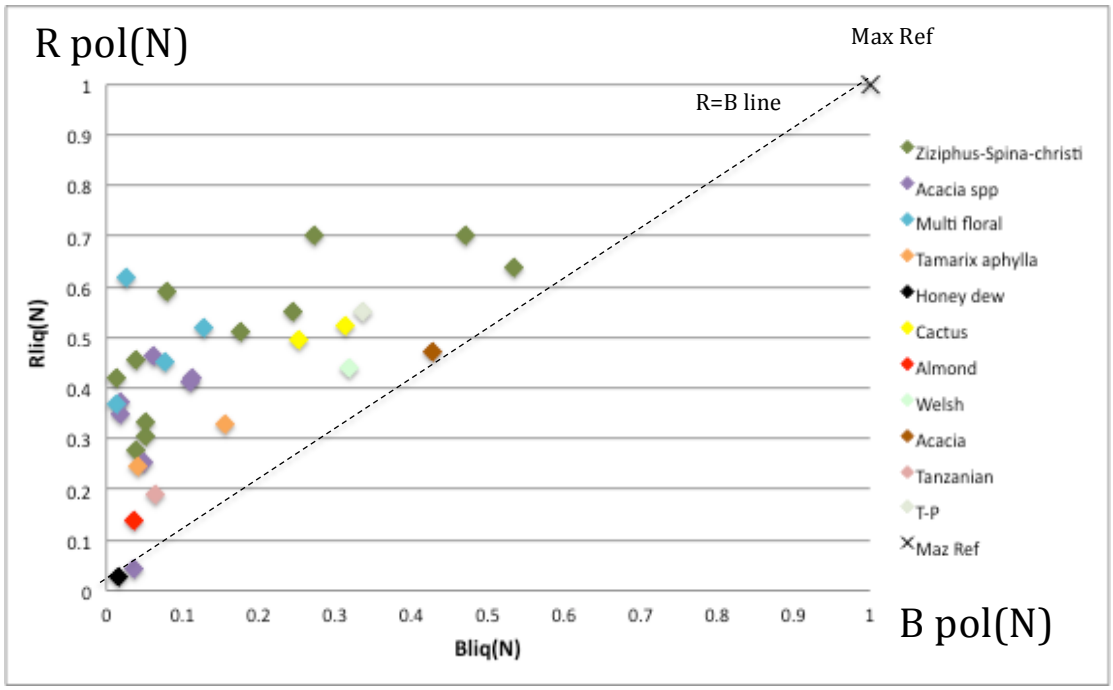

Figure 7.17(b): Cluster map of polarized light parameters Rpol(N):Bpol(N) at 45-degree polarizer angle

Figure 7.17: Processed polarized light chromatic parameters for various honey samples at 45-degree polarizing angle

(a) Calibration graph of RGB polarized light parameters against various honey samples

(b) Cluster map of polarized light parameters Rpol(N):Bpol(N)

7.5 Summary

This chapter has presented chromatically processed results from various calibration mixtures of (water-tea-milk) and (water-syrup-honey) and chromatically processed results from various types of honeys samples.

The various optical conditions used indicated:

- Light transmission from a VDU screen
- Ambient reflected/scattered light
- Fluorescent light
- Polarized light transmitted at 45-degree polarizing angle

Both the normalized results and chromatic cluster maps have been presented. The graphs form the basis of further discussion of the results.

A quantities assessment of the system performance and discrimination of honey test samples are discussed in Chapter 9.

Chapter 8

Chromatic Maps Of Test Data

8.1 Introduction

This chapter describes the application of the primary and secondary chromatic procedures described in Chapter 5 for analyzing the test data in Chapter 6 and 7 from the experiments considered in Chapter 4.

Firstly the primary chromatic procedures are first applied to the tea-water-milk and water-syrup-honey calibration mixtures (Section 7.3 and 7.4, Chapter 7), which provided a calibration measures for identifying the composition and condition of complex liquids. Thereafter the primary procedures are applied to real honey samples, which are divided into two groups – classified (i.e. known condition) and unclassified (i.e. unknown condition). This leads to the production of R:B or G:B maps for each type of optical signals used (transmission, polarization and fluorescence). Such maps are regrouped as primary chromatic maps.

Secondly the secondary chromatic procedures are applied to the outputs of the primary procedures to combine the outputs from the primary chromaticity to produce a simple secondary chromatic map. This combines together the chromaticities for the three apparent types of optical signals (transmission, polarization and fluorescence) on a single chromatic map.

Such secondary processing is first applied to the calibration results (water-syrup-honey) before being applied to the real classified and unclassified honeys. These maps form the basis upon which the condition/composition of various honeys may found.

8.2 Primary Chromatic Maps

8.2.1 Primary Calibration Maps

The form and features of the primary chromatic cluster maps were used address the issue of the effect of complex liquid mixtures on chromatic signatures.

8.2.1.1 Water, Tea, Milk Mixtures

Chromatic cluster maps were used to examine various trends produced by the physically different forms of liquid mixtures, two clear liquids with different transmission spectra, turbid component in an otherwise colorless mixture and a turbid component with two clear liquids of different concentrations. The chromatic cluster maps were based upon the camera outputs R (long wavelengths) and B (short wavelengths) corrected and normalized (0-1) with the water result and plotted against each other as shown on figure 8.1.
Ambient light was mathematically, rather then physically, excluded from the transmission by means of subtracting the reflected light from the combined result of VDU illumination plus reflected light (Section 7.3.2, Chapter 7).

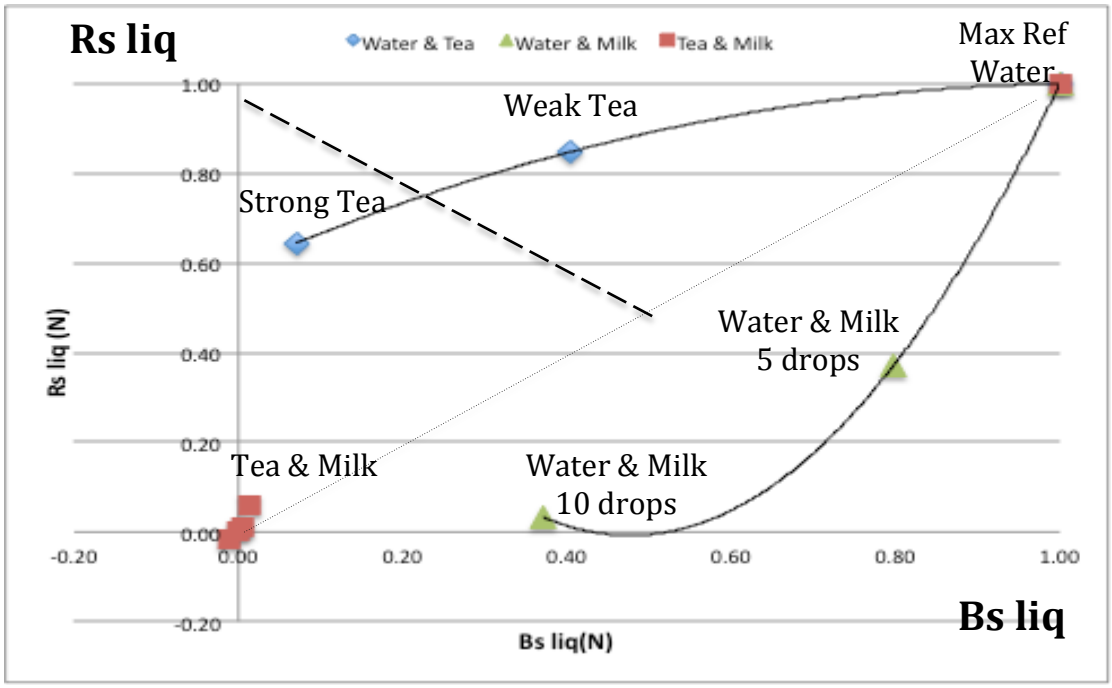

(a): Rs liq(N):Bs liq(N

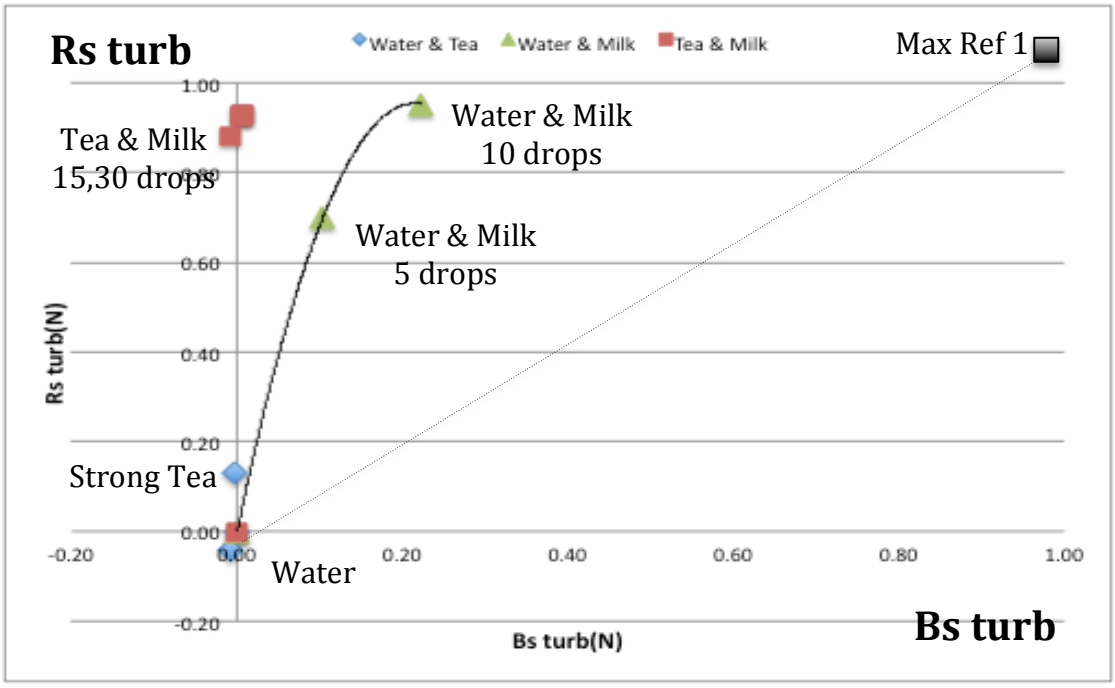

(b): Rs turb(N):Bs turb(N)

Figure 8.1: Chromatic cluster maps for water, tea diluted with water and milk mixtures

(c) Cluster map of transmitted light liquid parameter Rs liq(N):Bs liq(N)

(d) Cluster map of reflected light turbidity parameter Rs turb(N):Bs turb(N)

Figure 8.1(a) shows a (2-D) Rs liq(N) : Bs liq(N) chromatic map for optical transmission of the VDU illumination of tea diluted with water, water with a few drops (5,10) of milk and water-tea-milk mixtures (milk 5,10,15,30 drops).

The Rs liq(N) : Bs liq(N) results for the mixtures of water and tea (clear liquids mixtures) show that the short wavelengths (B) reduces in strength with increasing tea concentration more rapidly than the long wavelengths (R) consistent with changes expected from the different transmission spectra of the two liquids. As such the locus line Rs liq(N):Bs liq(N) lies above the equal strength locus line Rs liq(N)=Bs liq(N).

The Rs liq(N) : Bs liq(N) results for mixtures of water and milk (turbid mixtures) show that the long wavelengths (R) reduces in strength with increasing milk concentration more rapidly than the short wavelengths (B) and maybe associated with polychromatic light reflected/ scattered by the turbidity. The Rs liq(N):Bs liq(N) locus lies well below the equal strength locus line Rs liq(N)=Bs liq(N).

The result for the more complex mixtures of water, tea and milk show how the Rs liq(N) and Bs liq(N) strengths have both been substantially reduced from water and tea values by the same milk concentrations (5 and 10 drops) used for the water and milk tests. They lie close to the origin i.e. Rs liq(N) = Bs liq(N) = 0.

Figure 8.1(b) shows a (2-D) Rs turb(N) : Bs turb (N) chromatic map for the turbidity with ambient light only for the liquid mixtures in the absence of screen illumination (Section 7.3.2, Chapter 7), reflected/ scattered by various concentrations of milk in water (turbid mixture). The Rs turb(N) : Bs turb (N) results for the water and milk (turbid mixtures) shows that long wavelengths (R) increases in strength with increasing milk concentration more rapidly than the short wavelengths (B). The Rs turb(N): Bs turb(N) locus lies well above the equal strength locus Rs turb(N)=Bs turb(N).

The Rs turb(N) : Bs turb (N) result for the more complex mixtures of water, tea and milk show how that long wavelengths (R) increases in strength with high milk concentration (milk 15, 30 drops) and with no change in the short wavelengths (B). This shows that for complex mixtures, high levels of turbidity can still be monitored.

8.2.1.2 Water-Syrup-Honey Mixtures

Primary chromatic cluster maps were used to examine various trends produced by the different forms of viscous sugary liquid mixtures (honey, syrup) with pure liquid (water) and a viscous sugary component (honey) in an otherwise viscous sugar mixture (syrup) of different concentrations. The chromatic cluster maps were based upon the camera outputs R (long wavelengths), G (medium wavelengths) and B (short wavelengths) corrected and normalized (0-1) and plotted against each other as shown on figures 8.2, 8.3 and 8.4.

(a) Light Transmission R:B Map

Figure 8.2 shows a (2-D) Rliq(N) : Bliq(N) chromatic cluster map for the optical transmission of the VDU illumination of the syrup diluted with water, honey diluted with water and a further complex condition of honey and syrup (syrup 4g, 6g, 8g) mixture samples at different concentrations.

The Rliq(N) : Bliq(N) results for the mixtures of water-syrup and water-honey (viscous liquid mixture) show that the short wavelengths (B) reduces in strength with increasing sugar concentration more rapidly than the long wavelengths (R) consistent with changes expected from the different transmission spectra of the two liquids. As such the locus line Rs liq(N):Bs liq(N) lies above the equal strength locus line Rs liq(N)=Bs liq(N).

The result for the more complex condition of honey and syrup mixture (added invert sugar) shows that the short wavelengths (B) and the long wavelengths (R) increase in strength with increasing syrup concentration

The locus line Rliq(N)=Bliq(N) denotes equal strength of long wavelength (R) and short wavelength (B) components. The locus line Rliq(N)+Bliq(N) = 1 denotes the boundary between clear and turbid samples . The samples that lie above Rliq(N)+Bliq(N) > 1 are highly transmitted samples i.e. clear liquids. The samples that lie below Bliq(N) < 0.12 have only weak transmitted i.e. highly turbid samples.

The implications of these results are that highly water diluted honey and syrup-honey mixtures are distinguishable from normal honey according to their B, R coordinates values.

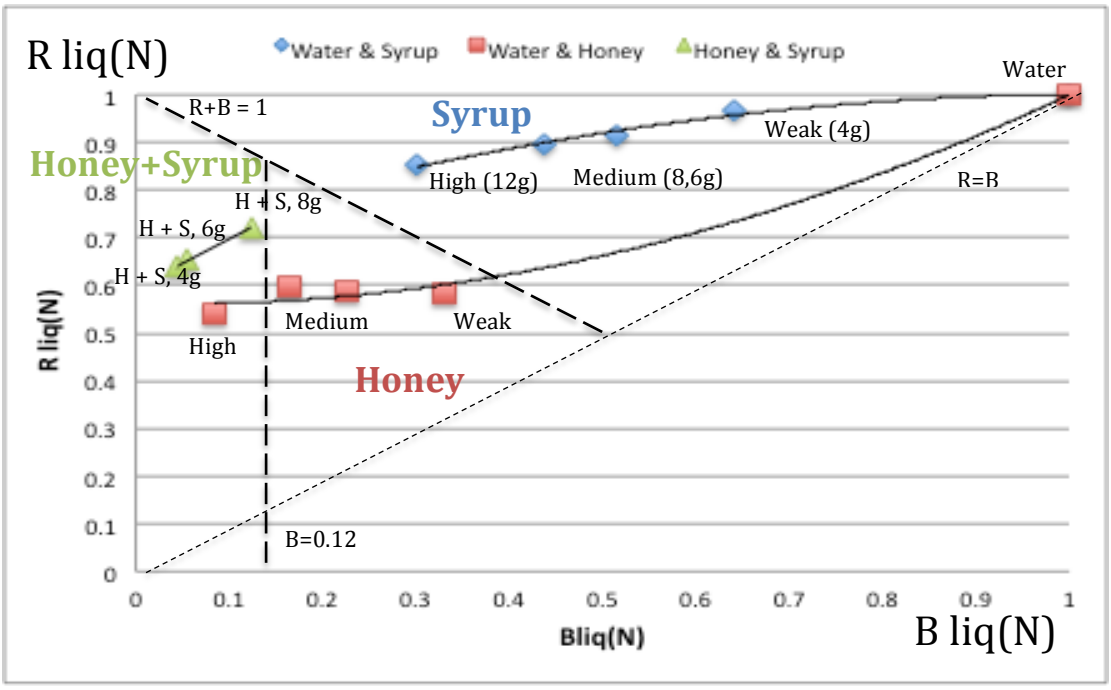

Figure 8.2: Chromatic cluster map of transmitted light parameter Rliq(N):B(liqN) for (water, syrup, honey) mixture samples

(b) Fluorescence G:B Map

Figure 8.3 shows a (2-D) Gflo(N) : B'flo(N) chromatic cluster map for the optical fluorescence when violet LED illumination excites the sample mixtures of syrup diluted with water, honey diluted with water and a further complex condition of honey and syrup (syrup 4g, 6g, 8g) mixture samples at different concentrations. For the fluorescence map the chromatic parameter chosen to yield clearer discrimination of components were Gflo(N) and B'flo(N) (B'flo(N) = 1- Bflo(N)).

In the fluorescence optical test, no filters were used to eliminate the excitation light, however the use of the normalization procedures for the fluorescent light (equation 7.4-7.6) discussed in (Section 7.4.3, Chapter 7) was an advantage because the noise resulted from the excitation light and ambient light were mathematically removed by comparing the results with water sample which was used as a reference sample.

The scattered light from water sample at the Green wavelengths (figure 6.26(a) and 6.26(b), Chapter 6) was low (≈ 0.32) compared to the calibration mixtures (≈0.4-0.7) and honey samples (≈0.6-0.9) (figure 6.27, Chapter 6) mainly due to noise resulted from the scattered light due to excitation light and ambient light, therefore, it was removed in the normalization procedure (equation 7.5, Chapter 7) giving as value of (G=0) as shown on figures (figure 7.12(a) and 7.12(b)) so it doesn't affect the results.

The scattered light from the water sample at the Blue wavelengths (figure 6.26(a) and (b), Chapter 6) was highly saturated (≈1) compared with the calibration mixtures and honey samples (figure 6.27, Chapter 6) mainly due to the scattered excited light and ambient light from the water sample. This was removed in the normalization procedure (equation 7.6, Chapter 7) to eliminate firstly the ambient light and later using the chromatic parameter B'flo(N) (B'flo(N)=1- Bflo(N)) to eliminate the effect of the excitation light so it doesn't affect the results.

The locus line Gflo(N)=B'flo(N) on figure 8.3 denotes equal strength of G and B and as such it's approximately a boundary for a fluorescence shift. The water sample (pure liquid) which was used as a bench mark in the dilutions has Gflo(N)=B'flo(N)= 0 i.e. no fluorescence shift.

The Gflo(N) : B'flo(N) results for the weak and medium mixtures of syrup and honey when diluted in water (low viscosity liquids) show that they lie below the Gflo(N)='Bflo(N) locus line i.e. Gflo(N) < B'flo(N). This indicates that at high water concentration (i.e. low strength of (glucose/fructose)/purities/etc.) in syrup and honey, the fluorescence light is emitted at the short wavelengths (B) part of the spectrum giving blue/cyan fluorescence.

For higher concentrations mixture of water-syrup and water-honey (high viscosity liquids), the Gflo(N) : B'flo(N) results show that higher concentrations of syrup in water, honey in water lie above Gflo(N)=B'flo(N) locus line i.e. Gflo(N)>B'flo(N). This indicates that at high strength of ((glucose/fructose)/purities/etc.) in syrup and honey the fluorescence light is emitted at the medium wavelengths (G) part of the spectrum giving green colour fluorescence.

The result for the more complex condition of honey and syrup mixture (added invert sugar) shows that as the syrup concentration increases in honey, the short wavelengths (B) increases in strength (B'flo(N) > 0.28) more rapidly than the medium wavelengths (G). This indicates that as the level of impurities (added invert sugar/ syrup/ water / etc.) increase in the honey, the emitted fluorescent light is shifted more towards the short wavelengths (B) part of the spectrum. The gradient of Gflo(N) : B'flo(N) show similar fluorescent spectra as the syrup liquid i.e. (Gflo(N) + B'flo(N) > 0.8).

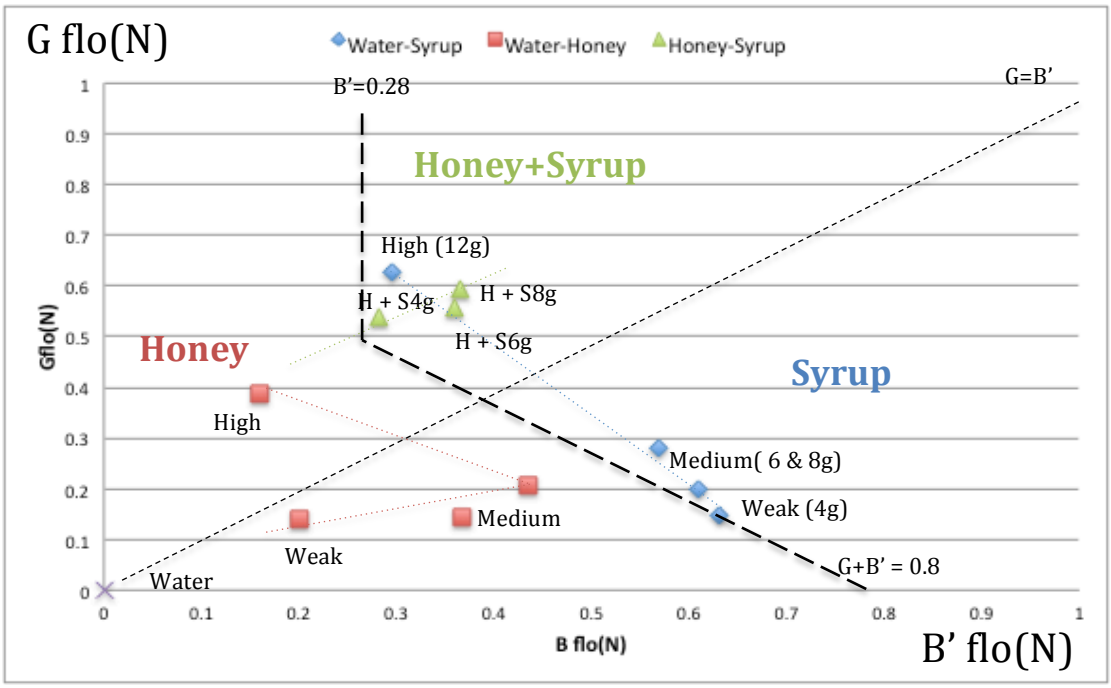

Figure 8.3: Chromatic cluster map of fluorescence parameter Gflo(N):B'flo(N) for (water, syrup, honey) mixture samples

(c) Polarization R:B Map

Figure 8.4 shows a (2-D) Rpol(N) : Bpol(N) chromatic cluster map for the polarized light when white VDU illumination is transmitted with polarization filters inclined at 45 degrees to each other through mixtures of syrup diluted with water, honey diluted with water and a further complex condition of honey and syrup (syrup 4g, 6g, 8g) mixtures of different concentrations.

The Rpol(N) : Bpol(N) results for the mixtures of water-syrup (viscous liquid mixture) show that the short wavelengths (B) reduce rapidly in strength with increasing syrup concentrations. However, the long wavelengths (R) approximately stay the same (Rpol(N)~0.6) for weak and medium concentrations but increases at high syrup concentration (Rpol(N) ~ 0.82). The water-syrup mixtures all lie above Bpol(N) > 0.3. This indicates highly polarized samples at the short (B) and the long (R) wavelengths i.e. clear liquids with invert sugar/ syrup content.

For the water-honey mixtures (viscos liquid mixtures), the short wavelengths (B) reduce in strength with increasing honey concentration more rapidly then the long wavelengths (R). However, the water-honey mixtures all lie below Bpol(N) < 0.3 which indicates low polarization.

The result for the more complex condition of honey and syrup mixtures (added invert sugar) shows that the short wavelengths (B) reduce in strength with increasing syrup concentration, which is expected as the mixtures become heavily turbid. However, the long wavelengths (R) increase more rapidly at high concentration of sugar (i.e. glucose/fructose) in honey and syrup (H +S, 8g). This shows that polarized long wavelengths (R) are sensitive to high levels of sugar (i.e. glucose/fructose) concentration in honey. The locus line Rliq(N)=Bliq(N) indicates equal strength of long wavelength (R) and short wavelength (B).

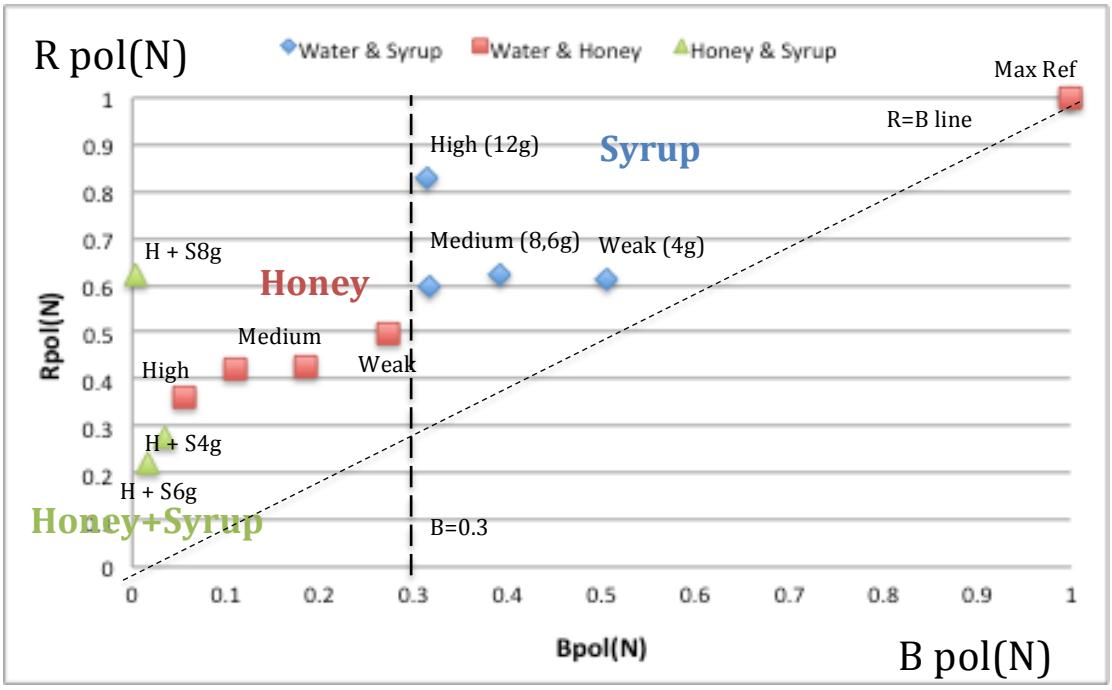

Figure 8.4: Cluster map of polarized light parameters Rpol(N):Bpol(N) at 45-degree polarizer angle

8.2.2 Primary Chromatic Maps Of Real Honey Samples

8.2.2.1 Introduction

Results of primary chromatic processing of various honey samples are presented. The samples have divided into tow groups, classified and unclassified honeys.

The classified honeys have a broad formal classification and therefore enable the chromatic processing to be assured. The unclassified honeys provide an opportunity to blind test the chromatic processing capability.

The classified and unclassified honey samples included samples from different sources (beehive farms, honey shops, supermarkets, etc.) from different international location. They include many samples from the Yemen for which details about geographical location, floral source, quality, authenticity, etc. was available.

For each of the honey groups, three sets of chromatic maps are presented corresponding to transmitted, fluorescent and polarized light. Each map has designated areas corresponding to various features of the honey and which are derived from (water-syrup-honey) and (water-tea-milk) calibration maps of Section 8.2.1.

Figures 8.5 (a), (b) and (c) show the features maps for transmitted, polarized and fluorescent light respectively.

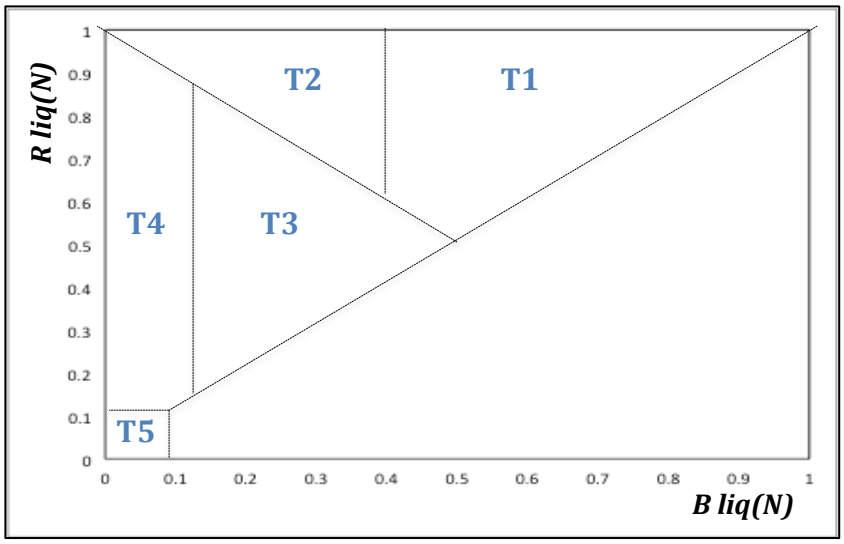

(a) Rliq(N) : Bliq(N) map

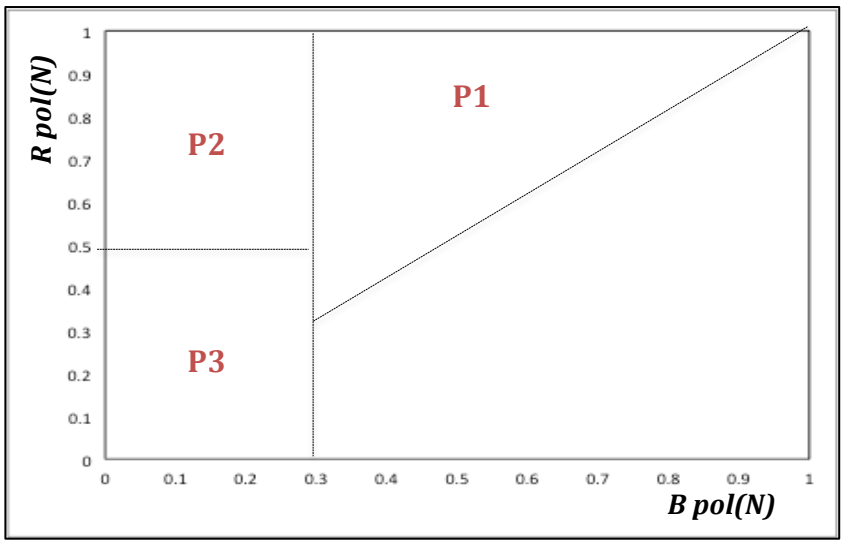

(b) Rpol(N) : Bpol(N) map

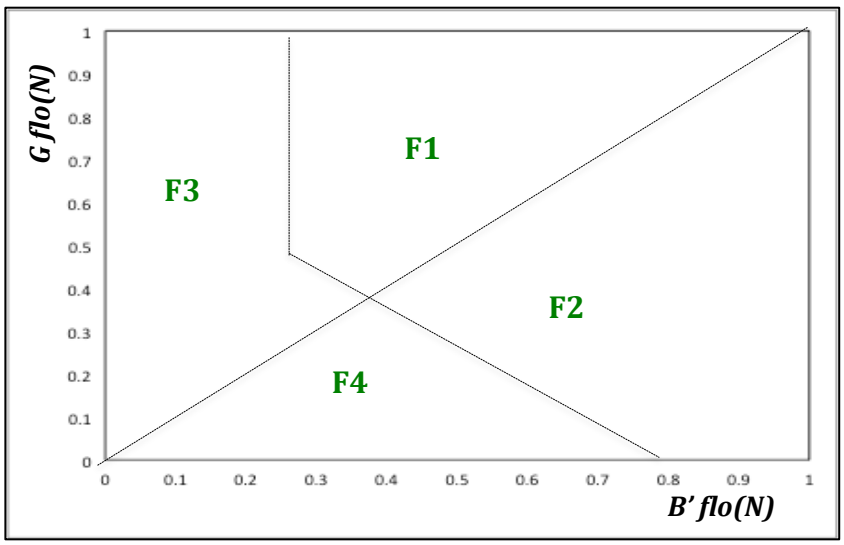

(c) Gflo(N) : B'flo(N) map

Figure 8.5: Chromatic features map for (a) Transmission, (b) polarization, (c) Fluorescence

The transmitted light map has five regions corresponding to:

- **T1**: B > 0.4, R > B ➔ High water dilution (very clear)
- **T2**: B < 0.4, R+B > 1 ➔ Low water dilution (moderate clear)
- **T3**: 0.12 < B > 0.4, R+B < 1 ➔ Low turbidity
- **T4**: B < 0.12 ➔ High turbidity
- **T5**: B ≈ R ≈ 0 ➔ Very dark

The polarized light map has three regions corresponding to:

- **P1**: B > 0.3, R > B ➔ High Glucose/ Fructose with water
- **P2**: B < 0.3, R > 0.5 ➔ High Glucose/ Fructose
- **P3**: B < 0.3, R < 0.5 ➔ Low Glucose/ Fructose

The fluorescent light map has four regions corresponding to:

- **F1**: B > 0.28, G > B' ➔ High Impurities
- **F2**: G + B; > 0.8, G < B' ➔ Low Impurities with water
- **F3**: B < 0.28, G > B' ➔ Honey with High Purities
- **F4**: G + B' < 0.8, G < B' ➔ Honey with Low Purities & water

8.2.2.2 Classified Honey Samples

Figure 8.6 (a), (b) and (c) show the primary chromatic maps of transmitted, polarized and fluorescent light respectively for 21 classified honey samples. The various classification areas are the same as for the features map discussed on figure 8.5.

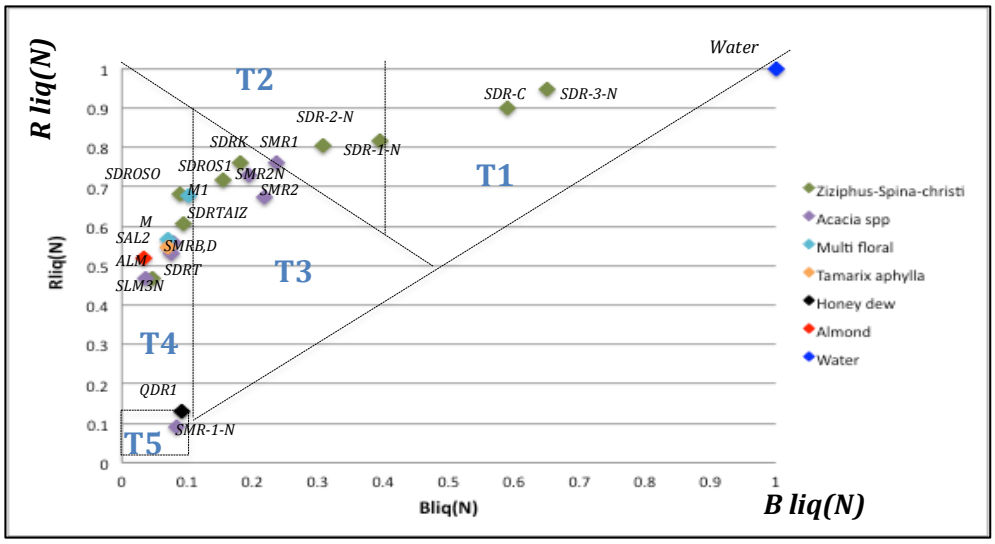

(a) Transmission Rliq(N) : Bliq(N) Map

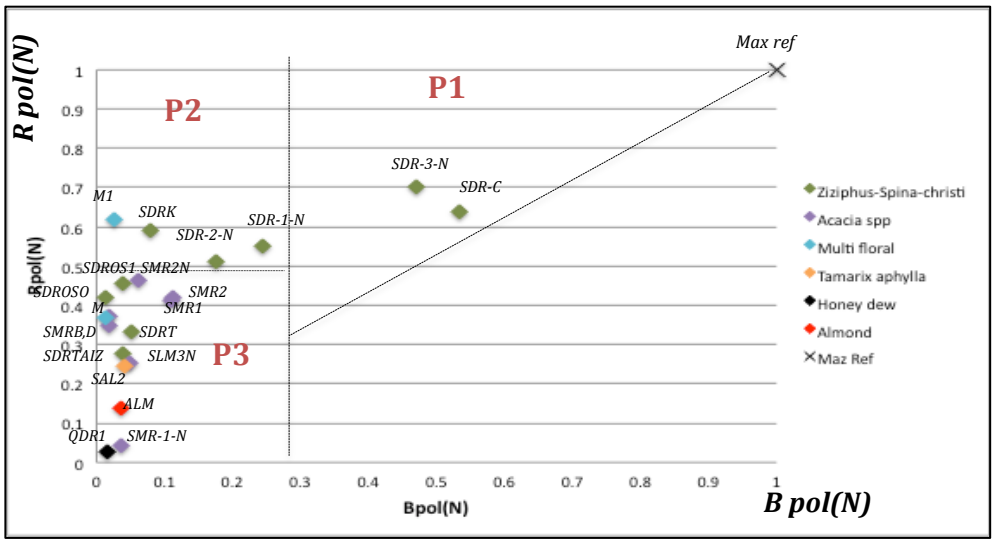

(b) Polarization Rpol(N) : Bpol(N) Map

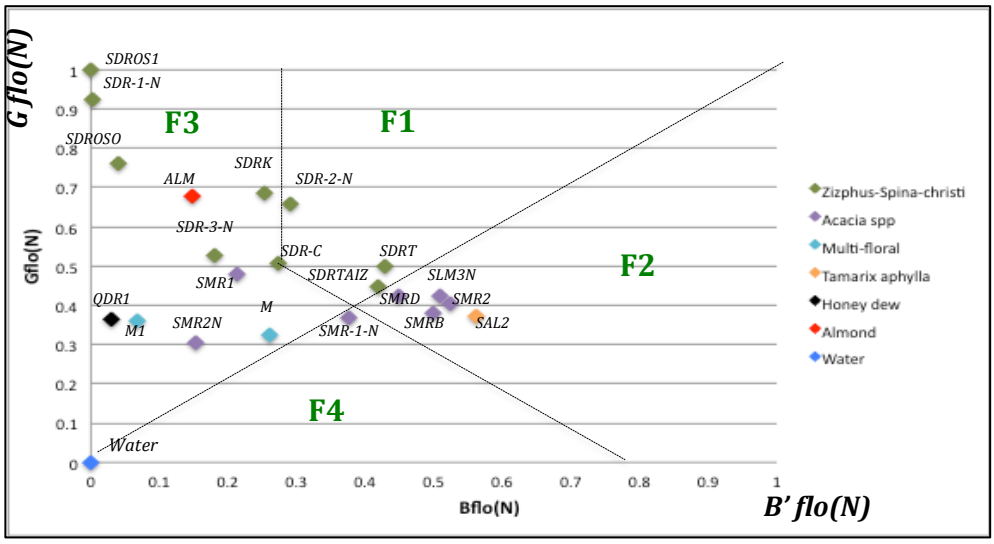

(b) Fluorescence Gflo(N) : B'flo(N) Map

Figure 8.6: Primary Chromatic Map for Classified honey: (a) Transmission, (b) Polarization, (c) Fluorescence. (……>> classification boundaries from figure 8.5)

(a) Transmission R:B Map

Figure 8.6(a) show a chromatic cluster map of R(liq)N : Bliq(N) for 21 classified honey samples. The locus line Rliq(N) = Bliq(N) represent samples with equal long and short wavelengths components. The locus line Rliq(N) + Bliq(N) = 1 is the approximate boundary between clear and turbid samples (as indicated by the water, tea, milk reults) . The samples for which Rliq(N) + Bliq(N) > 1 are clear liquids. Samples for which Bliq(N) < 0.12 are highly turbid samples. Samples close to the origin (Rliq(N) ≅ Bliq(N) ≅ 0) are samples with only little transmission or reflection i.e. black in colour.

The R:B transmission map allows the honeys to be classified in regions as follows:

- **T1**: High water concentration ➔ Samples (SDR-C, SDR-3-N)
- **T2**: Relatively pure (clear honey) ➔ Samples (SDR-1-N, SDR-2-N)
- **T3**: Moderately pure (Turbid honey) ➔ Samples (SMR1, SMR2, SMR-2-N, SDRK, SDROS1)
- **T4**: Highly turbid honey ➔ Samples (SDROSO, M1, M, SDRTAIZ, SDR-T, SMRB, SMRD, SAL2, ALM, SLM3N)
- **T5**: Very dark honey ➔ Samples (QDR1, SMR-1-N)

(b) Polarization R:B Map

Figure 8.6(b) shows a Rpol(N) : Bpol(N) chromatic cluster map for classified honey samples with polarized light when a white VDU illumination is transmitted through polarizing filters incident at 45 degrees to each other. The locus line Rpol(N) = Bpol(N) represent signals with equal short and long wavelengths components. The honey samples that lie above Bpol(N) > 0.3 represent samples with higher fraction of polarized blue light. Honey samples that lie above Rpol(N) > 0.5 represent samples with higher fraction of polarized red light. Most honey samples are located in the region Bpol(N) < 0.3.

The R:B polarization map allows the honeys to be classified in regions as follows:

- **P1**: High Glucose/ Fructose with water ➔ Samples (SDR-C, SDR-3-N)
- **P2**: High Glucose/ Fructose ➔ Samples (SDR-1-N, SDR-2-N, SDRK, M1)
- **P3**: Low Glucose/ Fructose ➔ Samples (SMR1, SMR2, SMR-2-N, SDR-OS1, SDR-OSO, M, SDRTAIZ, SDR-T, SLM3N, SMRB, SMRD, SAL2, ALM, SLM3N, QDR1, SMR-1-N)

(c) Fluorescence G:B' Map

Figure 8.6(c) shows a chromatic cluster map of Gflo(N) : B'flo(N) for classfied honey samples (where B'flo(N)=1-Bflo(N)). The locus line Gflo(N)=B'flo(N) represent the fluorescence spectrum for which Gflo(N)+B'flo(N) = 1 components. Samples located above Gflo(N)= B'flo(N) i.e. Gflo(N) > B'flo(N) are samples with fluorescence spectra shifted towards the medium wavelengths (G) giving a green colour fluorescence. Samples located below Gflo(N)=B'flo(N) i.e. Gflo(N) < B'flo(N) are samples with fluorescence spectra shifted towards the short wavelengths (B) giving a blue/cyan fluorescence.

The results given on figure 8.6(c) show that the Gflo(N), B'flo(N) signatures of the various honey samples can differ from each other. Which is expected from the different nature of composition in such honeys.

The G:B' fluorescence map allows the honeys to be classified in regions as follows:

- **F1**: High Impurities ➔ Samples (SDR-2-N, SDR-C, SDR-T, SDRTAIZ)
- **F2**: Low Impurities with water ➔ Samples (SMRD, SMRB, SMR2, SLM3N, SAL2)
- **F3**: High Purities➔ Samples (SDR0S1, SDR-1-N, SREOSO, ALM, SDRK, SDR-3-N, SMR1, SMR-2-N, M1, M, QDR1)
- **F4**: Low Purities with water ➔ Samples (SMR-1-N)

8.2.2.3 Unclassified Honey Samples

Figure 8.7 (a), (b) and (c) show the primary chromatic maps of transmitted, polarized and fluorescent light respectively for 11 unclassified honey samples. The various classification areas are the same as for classified honey samples.

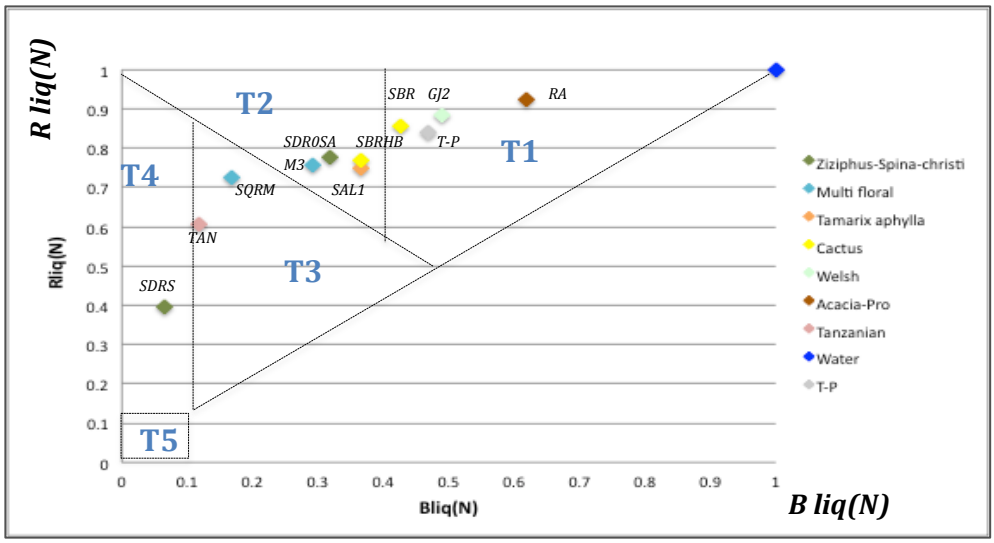

(a) Transmission Rliq(N) : Bliq(N) Map

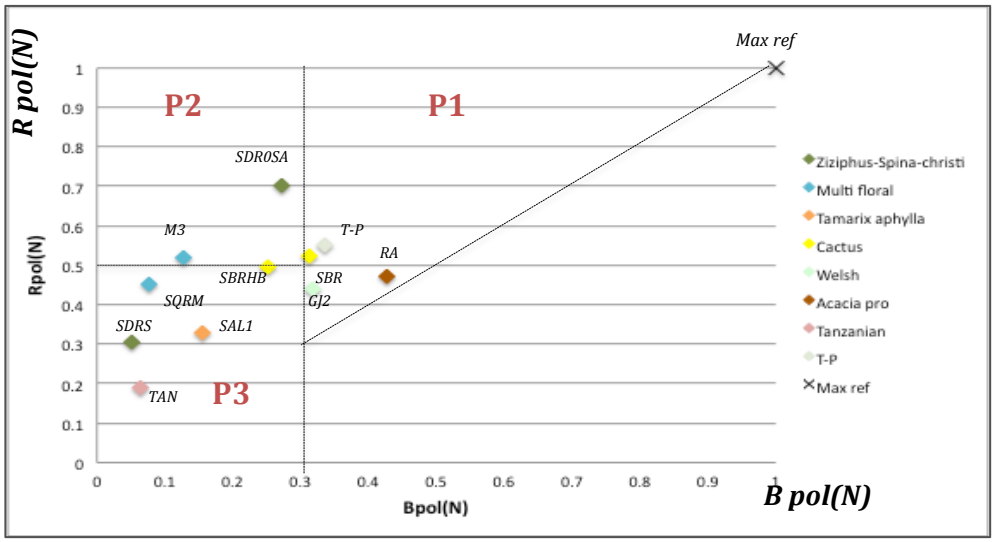

(b) Polarization Rpol(N) : Bpol(N) Map

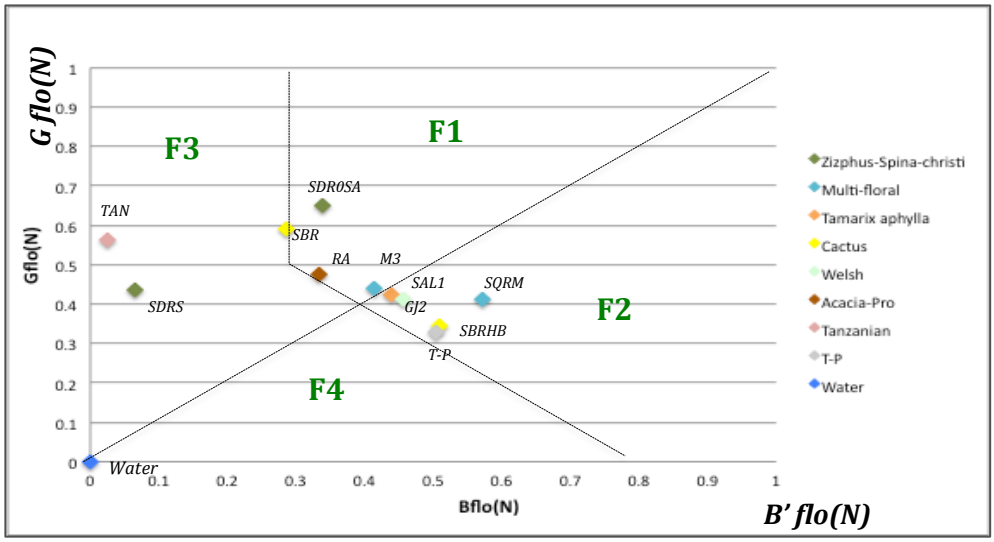

(c) Fluorescence Gflo(N) : B'flo(N) Map

Figure 8.7: Primary Chromatic Map for Unclassified honey: (a) Transmission, (b) Polarization, (c) Fluorescence. (……>> classification boundaries from figure 8.5)

(a) Transmission R:B Map

Figure 8.7(a) shows the R:B transmission map for 11 unclassified honey samples. This leads to the following classification of the honey samples as follows:

- **T1**: High water concentration ➔ Samples (RA, GJ2, T-P, SBR)
- **T2**: Relatively pure (clear honey) ➔ Samples (SBR-HB, SAL1, SDR-OSA, M3)
- **T3**: Moderately pure (Turbid honey) ➔ Samples (SQRM, TAN)
- **T4**: Highly turbid honey ➔ Samples (SDRS)

(b) Polarization R:B Map

Figure 8.7(b) shows the R:B polarization map for 11 unclassified honey samples. This leads to the following classification of the honey samples as follows:

- **P1**: High Glucose/ Fructose with water ➔ Samples (RA, GJ2, T-P, SBR)
- **P2**: High Glucose/ Fructose ➔ Samples (SDR-OSA, M3)
- **P3**: Low Glucose/ Fructose ➔ Samples (SQRM, TAN, SBR-HB, SAL1, SDRS)

(c) Fluorescence G:B' Map

Figure 8.7(c) shows the G:B' fluorescence map for 11 unclassified honey samples. This leads to the following classification of the honey samples as follows:

- **F1**: High Impurities ➔ Samples (SDR-OSA, SBR, RA, M3)
- **F2**: High Impurities with water ➔ Samples (SAL1, GJ2, T-P, SBR-HB, SQRM)
- **F3**: High Purities➔ Samples (TAN, SDRS)

8.3 Secondary Chromatic Maps

8.3.1 Water, Syrup, Honey Calibration Map (Secondary Chromaticity)

Figure 8.8 shows a Cartesian XYZ chromatic map of the water, syrup and honey mixtures. The regions dominated by transmission, polarization and fluorescence are distinguished on this figure so that samples dominated by each effect can be identified.

- The benchmark sample water is dominated by a high transmission parameter (Y(T) = 1) and no fluorescence (X(F)) and polarization (Z(P)) parameters.
- Mixtures of water-syrup samples have moderate transmission ($0.2 < Y(T) < 0.55$), moderate fluorescence ($X(F) \sim 0.3$) and low polarization ($Z(P) < 0.3$) parameters (blue diamonds).
- Mixtures of water-honey samples have moderate-low transmission ($0.1 < Y(T) < 0.5$), low fluorescence ($X(F) < 0.3$) and moderately high polarization ($0.4 < Z(P) < 0.6$) parameters (red squares).
- Mixtures of honey- syrup samples have very low transmission ($Y(T) < 0.1$), moderately high fluorescence ($X(F) \sim 0.5$) and polarization ($Z(P) \sim 0.5$) (green triangles).

Of course this map only indicates relative levels and not magnitude.

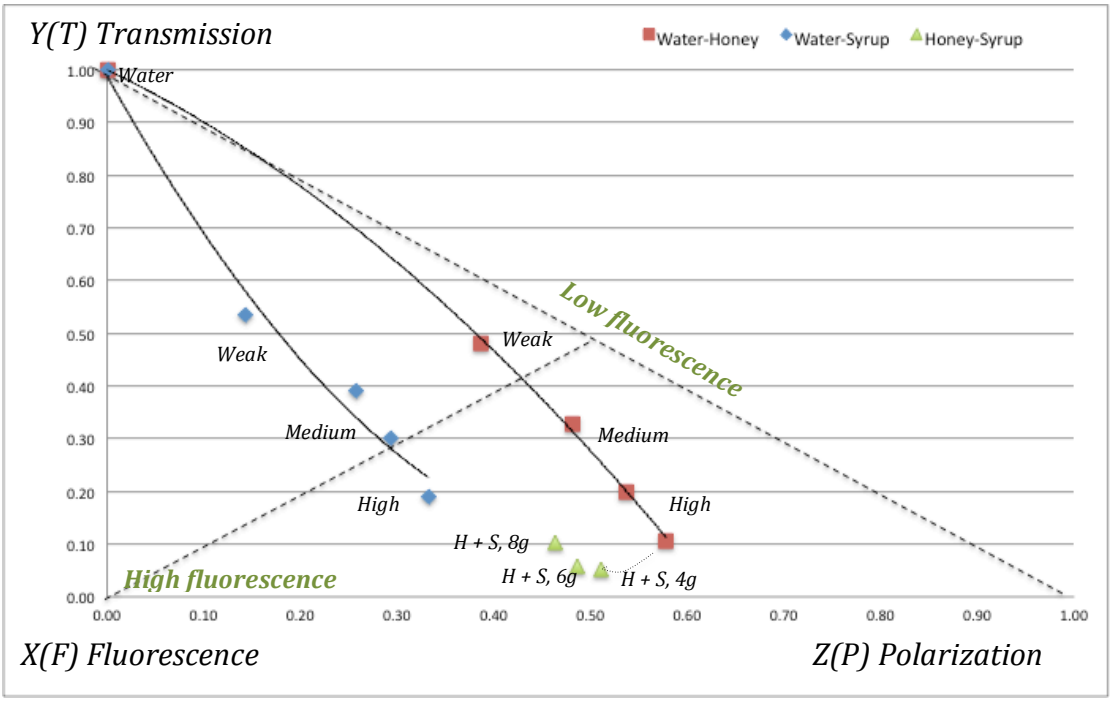

Figure 8.2: Chromatic Cartesian XYZ diagram of water, syrup and honey mixtures

8.3.2 Real Honey Secondary Chromatic Maps

(a) Distinguishing Regions

Figure 8.9 shows a Cartesian XYZ chromatic map with featured regions corresponding to the over all condition dominated by the honey sample, which are derived from (water-syrup-honey) secondary calibration maps.

The secondary chromatic map has three regions corresponding to:

- **Red region**: {Y(T) > Z(P)} ➔ Relatively high water concentration, high invert sugar, high Impurity with water ➔ **Processed honey (P)**
- **Orange region:** {Y(T) ≤ 0.09} & {Z(P) ~ 0.5} ➔ [highly turbid, highly viscous, crystalized, high impurity] ➔ **Adulterated or Long shelf life (A/L)**
- **Green region:** {Y(T) < Z(P)} ➔ – [moderate clear/turbid, moderate/high sugar levels, moderate/high purities] ➔ **Normal honey (N)**

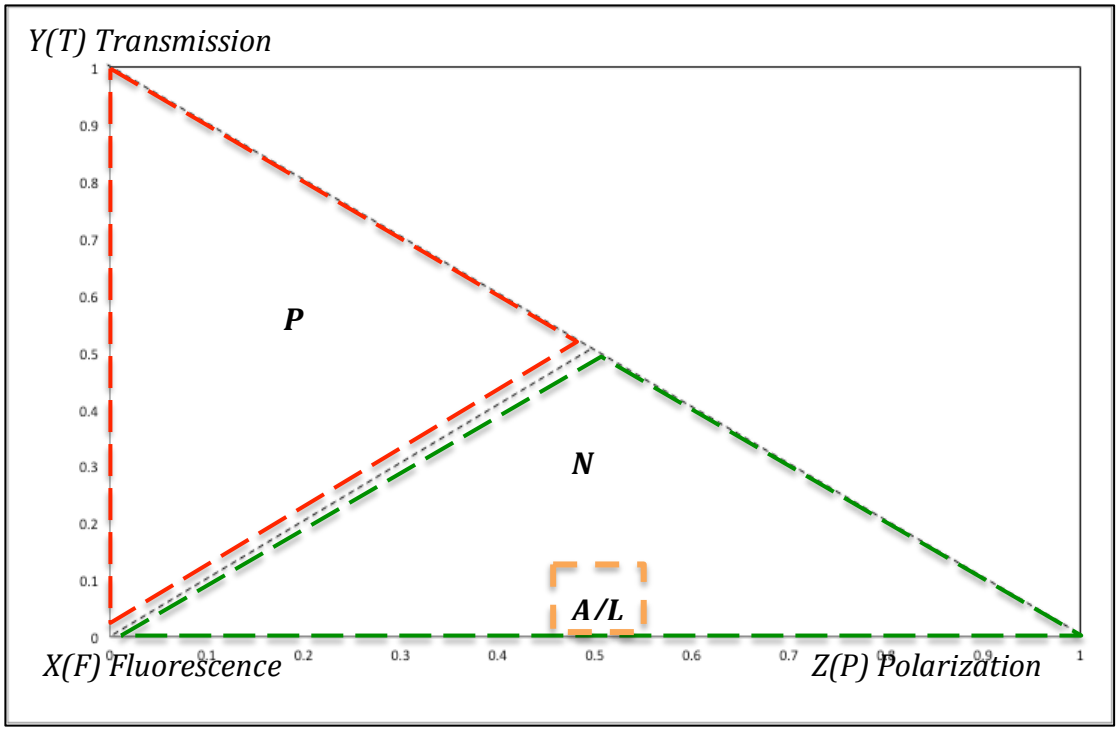

Figure 8.9: Chromatic Y:Z Map with over all condition region: (Red= P, Orange=A/L and Green=N)

(b) Classified Honeys

Figure 8.10 shows a Cartesian XYZ chromatic map of 21 classified honey samples. The various overall condition regions are the same as those in the features map discussed on figure 8.9. The honey samples points are coloured according to their conventionally classified grades.

The Y:Z chromatic map allows the honeys to be classified in regions as follows:

- Red Region (P) ➔[Grade 3 - poor adulterated honey]
- Orange Region (A/L) ➔[Grade 3 – poor adulterated honey] & [Good-Long shelf life honey]
- Green Region (N) ➔[Grade 1 - good honey] & [Grade 2 - moderate adulterated honey]

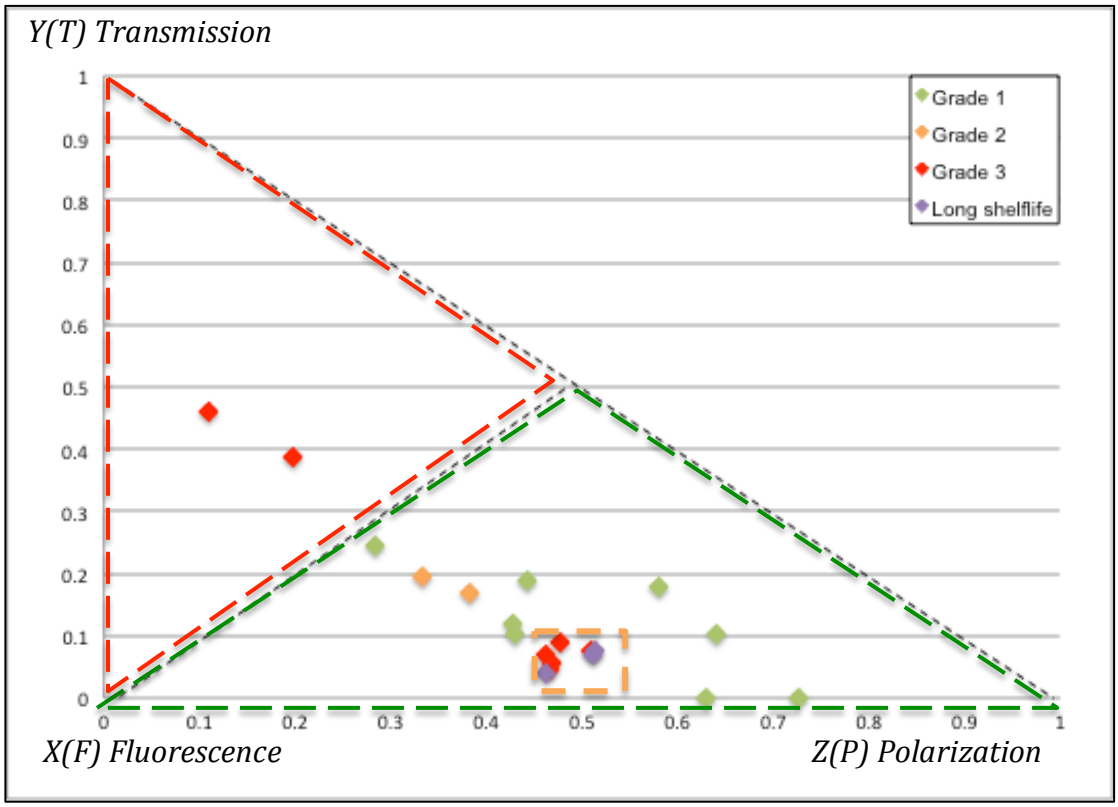

Figure 8.10: Chromatic Y:Z Map of classified honey samples.

(Red region = processed, Orange region = Adulterated/Long shelf life , Green region = Normal)

(c) Unclassified Honeys

Figure 8.11 shows a Cartesian XYZ chromatic map of 11 unclassified honey samples. The various overall condition regions are the same as for classified honeys. The honey samples points are coloured according to their source (similar to the primary chromatic map).

The Y:Z chromatic map allows the honeys to be classified in regions as follows:

- Red Region (P) ➔ Samples [RA, GJ2, T-P, SBR]
- Green Region (N) ➔ Samples [TAN, SDRS, SQRM, M3, SDR-OSA, SBR-HB, SAL1]

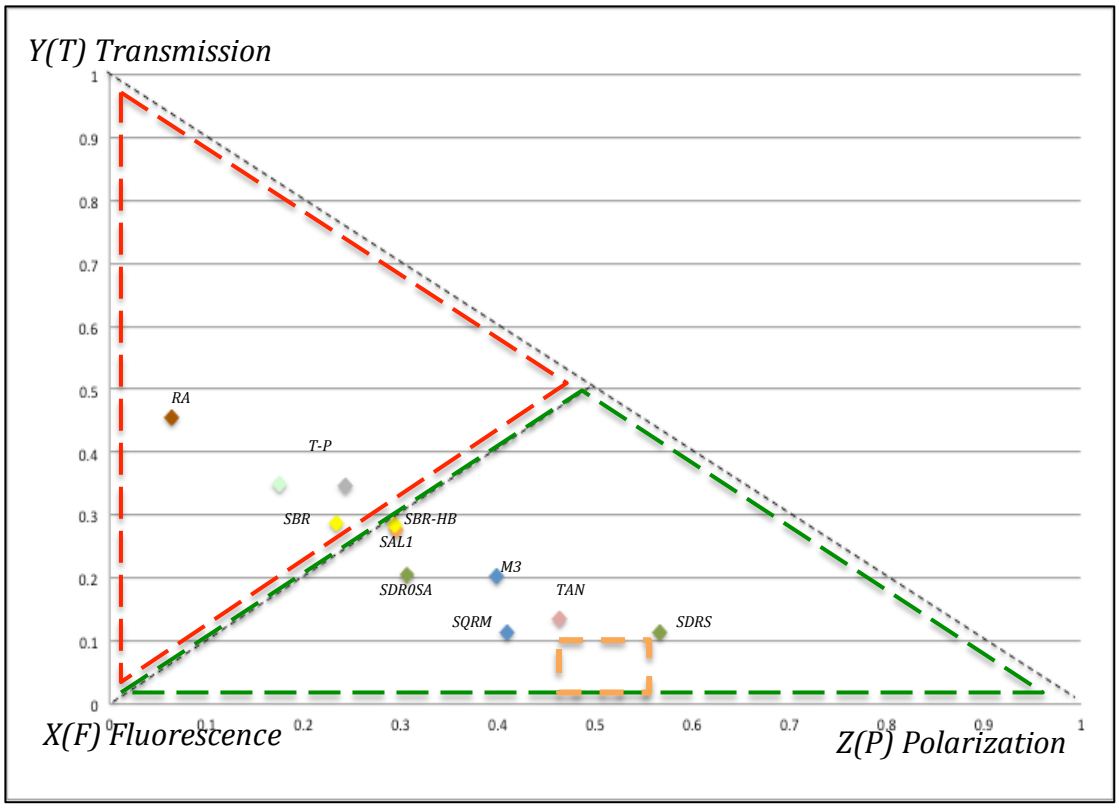

Figure 8.11: Chromatic Y:Z Map of unclassified honey samples.

(Red region = processed, Orange region = Adulterated/Long shelf life, Green region = Normal)

8.4 Summary

This chapter has presented both primary and secondary chromatic maps for calibration liquid mixtures and real honey samples (classified and unclassified).

The primary chromatic processing has yielded R:B maps for transmitted/reflected and polarised light plus a G:B map for the fluorescent emission, using calibration with controlled mixtures of liquid components (water-tea-milk) and (water-syrup-honey).
Such maps have been presented for:

a) Water-Tea-Milk calibration mixtures (transmitted /reflected light only for different concentrations of "colourless" (water), generally clear (tea) and highly turbid (milk) liquids.)
b) Water-Syrup-Honey calibration mixtures
c) Classified honey samples
d) Unclassified honey samples

The mixtures of (water-syrup-honey) of known concentrations were used to obtain broad calibration indications of liquid mixture samples and to establish classification regions for the primary chromatic maps. These regions were then deployed with classified real honey samples and unknown quality honey samples.

The secondary chromatic processing has enabled results for different optical signals (transmission, polarisation and fluorescence) to be mapped together on a single chromatic map. These maps were calibrated with the (water-syrup-honey) mixtures and applied to the real classified and unclassified honeys.

The classified honeys have a broad formal classification and therefore enable the chromatic processing to be assured. The unclassified honeys provide an opportunity to blind test the chromatic processing capability. The quantitative assessment and the analysis discrimination performance are discussed in Chapter 9.

Chapter 9

Assessment Procedures for Honey Samples

9.1 Introduction

This chapter summarizes the chromatic classification of the honey samples analyzed in Chapter 8 for comparison with conventional grading of the samples.

The results of the comparison have been used to produce a decision flow chart whose uses have been illustrated using the ungraded honey samples which was analyzed chromatically.

9.2 Comparison Of Chromatic Results With Conventional Classification

An interpretation of the primary and secondary chromatic results presented in Chapter 8 is made with the aid of an assessment table (Table 9.1). For detailed information on the conventional grading assessment of the honey samples are shown on Appendix III.

Table 9.1 shows the properties of a honey sample in terms of its classification according to it.

- Test samples are shown on column 1
- The secondary chromatic map (i.e. relative significance of optical transmission, polarization and fluorescence – column 2)
- Each of the primary chromatic maps – transmission (R:B), polarization (R:B) and fluorescence (G:B') (column 3,4,5).
- An assessment scale (0-4) from the primary chromatic maps (column 6).
- An overall chromatic assessment based upon this score (column 7)
- The chromatic assessment of column 7 is compared with the conventional grading shown column 8.
- A primary indication on the condition of the honey sample is based upon the area of the secondary chromatic map occupied by a honey sample (N, P, A/L) (Section 8.3.2, Chapter 8)
- The grading of the sample is based upon the area of the primary chromatic maps occupied by a honey sample along with classifications regions T1-T5, P1-P3, F1-F4 (Section 8.2.2, Chapter 8).
- Each coloured boxes (column 3,4,5) represent different features and scores based upon the area of the primary chromatic maps occupied by a honey sample (Table 9.2).

Table 9.1

Test Sample	*Secondary Chromatic Map*	*Primary Chromatic Map*				*Overall Chromatic Classification*	*Grade*
	Y(T): Z(P)	**Rliq(N):Bliq(N)**	**Rpol(N):Bpol(N)**	**Gflo(N):B'flo(N)**	**Overall Score**		
SDR-1-N	**N**	Clear	High G/F	High Purities	4	Good (R)	1
SDR-K	**N**	Turbid	High G/F	High Purities	4	Good (R)	1
SDR-OS1	**N**	Turbid	Low G/F	High Purities	3.5	Good (R)	1
SMR-2-N	**N**	Turbid	Low G/F	High Purities	3.5	Good (R)	1
SMR1	**N**	Turbid	Low G/F	High Purities	3.5	Good (R)	1
M1	**N**	High Turbid	High G/F	High Purities	3.5	Good (R)	1
QDR1	**N**	Very Dark	-	High Purities	2.5	Good (R)	1
M	**N**	High Turbid	-	High Purities	2.5	Good (R)	1
SDR-OSO	**A/L**	High Turbid	-	High Purities	2.5	Good (R)(L)	1
ALM	**A/L**	High Turbid	-	High Purities	2.5	Good (R)(L)	1
SMR-B	**A/L**	High Turbid	-	Low Impurities	0.5	Poor (A)	1
SMR-1-N	**N**	Very Dark	-	Low Purities	1.5	Moderate (A)	1
SDR-2-N	**N**	Clear	High G/F	High Impurities	2	Moderate (A)	2
SMR2	**N**	Turbid	Low G/F	Low Impurities	1.5	Moderate (A)	2
SAL2	**A/L**	High Turbid	-	Low Impurities	0.5	Poor (A)	3
SDR-T	**A/L**	High Turbid	-	High Impurities	0.5	Poor (A)	3
SDR-TAIZ	**A /L**	High Turbid	-	High Impurities	0.5	Poor (A)	3
SLM-3-N	**A/L**	High Turbid	-	Low Impurities	0.5	Poor (A)	3
SMR-D	**A/L**	High Turbid	-	Low Impurities	0.5	Poor (A)	3
SDR-C	**P**	High water	High G/F with water	High Impurities	0	Poor (A)(P)	3
SDR-3-N	**P**	High water	High G/F with water	High Purities	2	Moderate (A)(P)	3

Table 9.1: Primary and secondary chromatic results plus classification of the various classified honeys. (N= Normal honey, P= Processed honey, A= Adulterated, L= Long shelf life, R= Raw honey, Grade1=Raw honey/good quality, Grade2= moderately quality/ moderate adulteration, Grade3= Adulterated honey/ poor quality, Dark green box= Agree, Dark red box=Disagree).

Primary Map → Features ↓	*Rliq(N):Bliq(N)* (Score)	*Rpol(N):Bpol(N)* (Score)	*Gflo(N):B'flo(N)* (Score)	*Overall Score*
Good	(1)	(1)	(2)	2 > Good
Moderate	(0.5)	(0.5)	(1)	1> Moderate ≤2
Poor	(0)	(0)	(0)	Poor ≤ 1

Table 9.2: Primary chromatic map classification scores

9.2.1 Primary Chromatic Maps

(a) Transmission R:B Map (Figure 8.6(a), Chapter 8)

Honey samples lying in the region T1 are highly transparent, have a high liquid content and hence very low viscosity. Such conditions are honey samples being highly diluted with pure liquid (water) during processing or being exposed to overheating or over filtering process, i.e. the honey is regarded as processed/adulterated honey. Samples that are diluted with other pure liquid such as (SDR-C and SDR-3-N) lie in this region and classified as grade 3 according to the traditional assessment method (Table 9.1).

Honey samples lying in the regions T2 and T3 are moderately clear and low turbid liquids respectively. These conditions indicate the likelihood of the honey sample being raw with low pollens such as (SDR-1-N) or moderate pollens such as (SMR1, SMR-2-N) which vary according to the different types of floral source. Floral source of raw Accacia spp honey have higher level of water insoluble matter (mainly pollens) amongst other types of Yemeni honey according to (AL-Zoreky, Alza'aemy et al. 2001).

It also highlights the likelihood of the honey sample being slightly blended with other clear honey liquids but not processed such as (SDR-2-N, SMR2) due to moderate-low viscosity. The level of viscosity can vary according to the type and composition of (minerals, pollens, water, sugar etc) in the honey. Most of the honey samples classified as grade 1 and 2 according to the traditional assessment method (Table 9.1) lie on this region, therefore further checks is necessary to differentiate between both grades.

Honey samples lying in the region T4 are highly turbid liquids similar to strong honey and honey-syrup calibration mixtures. The honey samples that lie in this region normally have darker colour, this has been related to the long shelf life and storage temperature (Gonzales, Burin et al. 1999, White 1975). Samples such as (SDR-OSO, M) are raw honey samples but have a long shelf life before they were tested. It was also indicated that the cause of the darkening of the honey could be attributed to Caramelization and Maillard reaction due to the instability of the fructose and amino acids as a result of storage temperatures (Lynn, Englis et al. 1936). The dark colour appearance of honey also has been related to the botanical source and characteristics of the pollen grains, for example brown pollen grains yield the darkest honey (Terrab, Escudero et al. 2004).

Crystallization of honey can also affect the level of turbidity due to small crystals being formed over time when there is a high glucose ratio compared to other sugars in honey composition (Crane 1975). Factors like sugar and moisture content are possible reasons that there is an increase in the rate of crystallization causing the honey to be highly viscous. High pollen grains content or pieces of unfiltered beeswax in the honey are other possible factors leading to moderate crystallization of honey during a long shelf life (Davis 2007), causing the honey to be highly turbid.

Adulterated honey samples, i.e. honey samples with added invert sugar classified as grade 3 such as (SDR-T, SDR-TAIZ, SLM-3-N, SMRD, SAL2) lie in this region together with high pollen samples such as (M1) and long shelf life honey with a beeswax content (ALM). Slightly crystalized honey such as (SMRB) also lie on this region and classified as grade 1. Further checks are necessary to differentiate between adulterated honey and raw honey that have long shelf life or high pollens.

Honey samples lie in the region T5 are samples with only small transmission or reflection as do the tea and milk calibration mixture. Mineral content of honey have been also attributed to very darker honey (González-Miret, Heredia et al. 2005). The samples that lie on this region (QDR1, SMR-1-N) represent honeydew honeys grade 1 samples, because of their unique compound and mineral compositions, they have a very dark colour and they don't contain pollen grains such as those of blossom honey that are produced from nectar flowers. The honeydew honey is produced by honeybees collecting nectar from plant stems or exuded from another insect such as an aphid (Bentabol Manzanares, García et al. 2011).

(b) Polarization R:B Map (Figure 8.6(b), Chapter 8)

Honey samples that lie in the region P1 represent samples with higher fraction of polarized blue and red light as do the syrup calibration mixtures (Figure 8.4, Chapter 8). The honey samples that lie on this region represent high sugar (Glucose/Fructose) with water content. Honey samples that are highly diluted with other pure liquid such as (SDR-3-N and SDR-C) are classified as grade 3 according to the traditional assessment method (Table 9.1). Honey samples lie on this region indicates that syrup liquid mixture dominates.

The honey samples that lie in the region P2 represent samples with high fraction of polarized red light. Honey samples such those of Zizphus-Spina-christi botanical source (SDR-1-N, SDR-K, SDR-2-N) that lie on this region indicates that they have high levels of sugar (Glucose/Fructose) content. The physio-chemical analysis of the Yemeni honey investigated by (AL-Zoreky, Alza'aemy et al. 2001) shows that Yemeni honey of Zizphus-Spina-christi botanical source had glucose/fructose as a major constituent represented 71.6% (on average) of dry substance in honey, this was above the minimum level set for floral honeys. Also (Crane 1975) indicated that raw honey of the botanical source (ziziphus spina-christi) has higher fructose to glucose ratio, which allows it to stay liquid for several years without crystallisation.

The honey samples that lie in the region P3 represent samples with low fraction of polarized light as do the water-honey calibration mixture (moderate turbid) and honey-syrup mixture (highly turbid) (Figure 8.4, Chapter 8).

Honey samples in this region indicate that they have low sugar (Glucose/Fructose) content. However, because some samples in this region are highly turbid causing less transmission of light therefore less rotation. Further checks needs to be investigated to differentiate between turbid raw honey and turbid adulterated honey.

(c) Fluorescence G:B' Map (Figure 8.6(c), Chapter 8)

Honey samples that lie in the region F3, F4 are samples with fluorescence spectra shifted towards the medium wavelengths (G) represent honey samples with moderate-high purity as does the low/medium honey strength and the high honey strength calibration mixture (Figure 8.3, Chapter 8).

Honey samples that lie in region F3 such as those of the same botanical source (Zizphus-Spina-christi) (SDR-1-N, SDR-OS1 and SDR-OSO) which are moderate clear, turbid and highly turbid respectively represent samples with high-level of purities (flavins, fluorophore compounds) in honey, where $G > 0.5$ and $B \sim 0$. Other honey samples of different botanical source (Accacia Spp, Multi-floral and Honeydew) such as turbid samples (SMR1, SMR-2-N) and highly turbid samples (QDR1, M1, M) also lie on this region but have $G < 0.5$. Samples in this region were classified as grade 1 according to the traditional assessment method (Table 9.1).

It was pointed out by (AL-Zoreky, Alza'aemy et al. 2001) physo-chemical analysis of Yemeni honey that honey of botanical source Zizphus-Spina-christi had higher means of Ash content (mainly minerals) than those of *Acacia spp* and multi-floral honey. This can be seen by the high level of fluorescent intensity at the (G) wavelengths compared to other honeys from other botanical sources mainly because of high level of fluorescent compounds presents in such types of floral honeys.

High turbid honey samples such as (SDR-OSO, ALM, M1, M) lie in the same region as the above, although the transmission chromatic map indicated high turbidity signature which could have been due to long shelf storage, high pollen content and crystallization, these samples show that they have high level of purity and regarded to be raw honey samples.

Very dark sample such as (QDR1) also lie in same region and was classified to be a grade 1 honeydew honey with moderate-high levels of minerals and fluorescent compounds.

Honey samples that lie in the region F1 and F2 represent honey samples with high impurities and high impurities with water content respectively. These samples lie on the same region as the syrup and the honey+syrup calibration mixtures with similar fluorescence signature shifted towards the short wavelengths (B) (Figure 8.3, Chapter 8).

High turbid honey samples such as (SLM-3-N, SMR-D, SAL2, SDR-T and SDR-TAIZ) lie in this region represent honey samples with high level of impurities, mainly because of the high levels of HMF and phenolic compounds as a result of Maillard reaction caused by overheating of samples in processing (Karoui, Dufour et al. 2007) or due to other fluorescent compounds such as NADH (nicotimide adenine dinucleotide) as a result of the presence of invert sugar (cane sugar) in the honey (GHOSH, VERMA et al. 2005) which has fluorescent peaks at the blue wavelength (~ 425-440nm). These samples indicate that they are adulterated samples i.e. honey samples were blended with an invert sugar liquid such as (syrup, cane sugar, etc.). These samples were classified as grade 3 (Table 9.1).

High glucose/fructose honey sample such as (SDR-2-N) that lie in the same region represent honey that have been moderately blended with other less quality honey of high glucose/fructose level. This sample was classified as grade 2 (Table 9.1).

9.2.2 Secondary Chromatic Maps

The composition of honey differs depending on the water content, ratios of various sugars (Glucose/Fructose/Sucrose), minerals, pollens, etc. The transmission/absorption/ fluorescent and polarization properties of honey vary in a regular manner with its liquid / solid content, which can differ from those of an invert-sugar solution of the same water content. Measuring the liquid content of honey is a great value for the honey industry since it has a direct relationship to the likelihood of adulteration and undesired fermentation (White 1975).

A processed honey or unripen honey means that various methods have been used that could have affected and changed the nature of the original honey. For example, the original honey sample could have been highly diluted with water or honey has been taken out of the beeswax before it has been ripen. Other methods can be exposing the original honey sample to an overheating /over filtering during processing resulting the loss of nutrition and pollen grains from the honey. These kinds of behaviors affect the nature of such complex liquid resulting in a more clear liquid with and less nutrition (glucose/fructose/pollens, minerals, etc.) (Guo, Zhu et al. 2010, Havenhand 2010).

An adulterated honey means that various methods have been used to make fraudulent honey and many methods continue to evolve. For example, the original honey is blended with other less expensive components including inverted sugar (Martin, Bogdanov 2002). Alternatively, bees are intentionally fed sweeteners to increase its production in order to seek a quick profit (Pilizota V, Nedic Tiban N 2009).

Long shelf life and storage temperature of honey can have an effect on the colour shade of the honey, it eventually becomes darker and makes the honey highly turbid, this is due to progressive moisture loss during long storage (water contents of honey decreased to various extents), which causes crystallization. Factors like sugar, moisture and HMF content are possible factors that increase the rate of crystallization causing the honey to be highly viscous. High pollen content or unfiltered waxes left in the honey during bottling are other possible factors leading to crystallization of honey (Gonzales, Burin et al. 1999, Davis 2007).

Honeydew honey is a particular types of honey that has low levels of glucose levels and very dark in colour. According to (Bentabol Manzanares, García et al. 2011, Astwood, Lee et al. 1998), honeydew honeys are characterized by their dark color and lower values of glucose, sucrose, turanose and melezitose than those included as blossom honeys.

9.3 Summary Of Comparison Of Chromatic And Classified Honey

The sensitivity and specificity for detecting the good honey samples (with respect to moderate and poor samples) are shown on below:

- 10 good samples of grade 1 were correctly classified (TP)
- 8 poor samples of grade 2 and 3 were correctly classified (TN)
- 1 samples of grade 3 was wrongly classified (FN)
- 2 samples of grade 1 were wrongly classified (FP)

The sensitivity and specificity for detecting very poor honey samples (with respect to good and moderate samples) are shown on below:

- 6 poor samples of grade 3 were correctly classified (TP)
- 12 good samples of grade 1 and moderate samples of grade 2 were correctly classified (TN)
- 2 samples of grade 1 or 2 were wrongly classified (FN)
- 1 samples of grade 3 were wrongly classified (FP)

Overall correctly classified honey samples were 18 out of 21 samples and 3 were wrongly classified. A summary of the sensitivity and specificity is shown on table 9.3.

$$Senesivity = \frac{True\ Positive\ (TP)}{True\ Positive\ (TP)+Fales\ Negative\ (FN)} \quad (9.1)$$

$$Specificity = \frac{True\ Negative\ (TN)}{True\ Negative\ (TN)+Fales\ Positive\ (FP)} \quad (9.2)$$

$$Positive\ Predictive\ Value\ (PPV) = \frac{(TP)}{(TP)+(FP)} \quad (9.3)$$

$$Negative\ Predictive\ Value\ (NPV) = \frac{(TN)}{(TN)+(FN)} \quad (9.4)$$

%	High quality (Grade 1)	Poor quality (Grade 3)
Sensitivity	91	75
Specificity	80	92
PPV	83	86
NPV	89	86

Table 9.3: A summary of sensitivity and specificity for high quality honey (with respect to moderate and poor samples) and poor quality honey (with resect to good and moderate samples).

The two wrongly classified grade 1 samples were classified as poor/adulterated honey and moderate/adulterated honey because they had an overall assessment scale of (0.5) and (1.5) respectively which is below the minimum score for good samples according to the defined chromatic boundary's of primary chromatic maps. Samples (SMRB) and (SMR-1-N) appeared to be highly turbid and very dark samples respectively on the transmission map. Both samples also had low sensitivity on the polarization map because of the very low liquid content. The fluorescence map showed that sample (SMRB) has low impurities maybe due to the sample being crystallized as a result of Maillard reaction causing high levels of HMF content or possibility that the sample being blended with invert sugar mixture (e.g. syrup). The fluorescent map showed that the honey sample (SMR-1-N) has low purities maybe due to the long shelf life of the sample.

One honey sample of grade 3 (SDR-3-N) was classified as moderate/adulterated honey because it had an overall assessment score of 2. This is because the honey sample appeared to lie on the "high purity" region on the fluorescence map (possibly because due to some fluorescent compounds such as flavins presents in this particular type of floral honey (Zizphus-Spina-christi) causing it to fluoresce at the Green wavelengths although it was blended with other honey liquid with less quality (possibly invert sugar). The secondary chromatic map showed that the sample was in the "processed region" (i.e. high liquid content) which indicate that the sample have been blended with other liquid and the overall chromatic assessment classified the sample as being moderately adulterated honey.

The traditional assessment method for grading honey samples by experienced beekeepers can also sometimes be misleading because it lacks scientific evidence and is rather depends upon experience.

9.4 Honey chromatic Assessment Decision chart

A scheme for utilizing the chromatic information at various levels of detail and to give traceability of results is shown on figure 9.1. This based upon both the primary chromatic processing (Section 8.2, Chapter 8), secondary processing Section 8.3, Chapter 8), and the resulting chromatic maps as used in the comparison table 9.1

A first assessment is made via the secondary map XYZ (Figure 8.9, Chapter 8). This allows an overall dominated distinction to be made between processed, adulterated and normal honey samples. Thereafter each of the three primary maps (Figures 8.5), Chapter 8) is visited. The transmission map (Figure 8.5(a)) indicates the level of turbidity and liquid content. The polarization map (Figure 8.5(b)) indicates the level of sugar content (Glucose/Fructose) and sugar with high liquid content. The fluorescence map (Figure 8.5(c)) indicated the level of purity and impurity of such honey sample dominated by fluorescent compounds in the honey.

The honey sample (SDR-1-N) coloured in red font (Column 1, Table 9.1) is shown as an example. The first assessment of the overall condition of the honey from the secondary chromatic map indicate it's a normal (N). The primary chromatic maps are then checked starting with the transmission map where it indicates it's a clear liquid (T3), the polarization map indicates it has a high Glucose/Fructose content (P2) and the polarization map indicates it has high purities (F3), therefore the honey sample is regarded as a good honey sample.

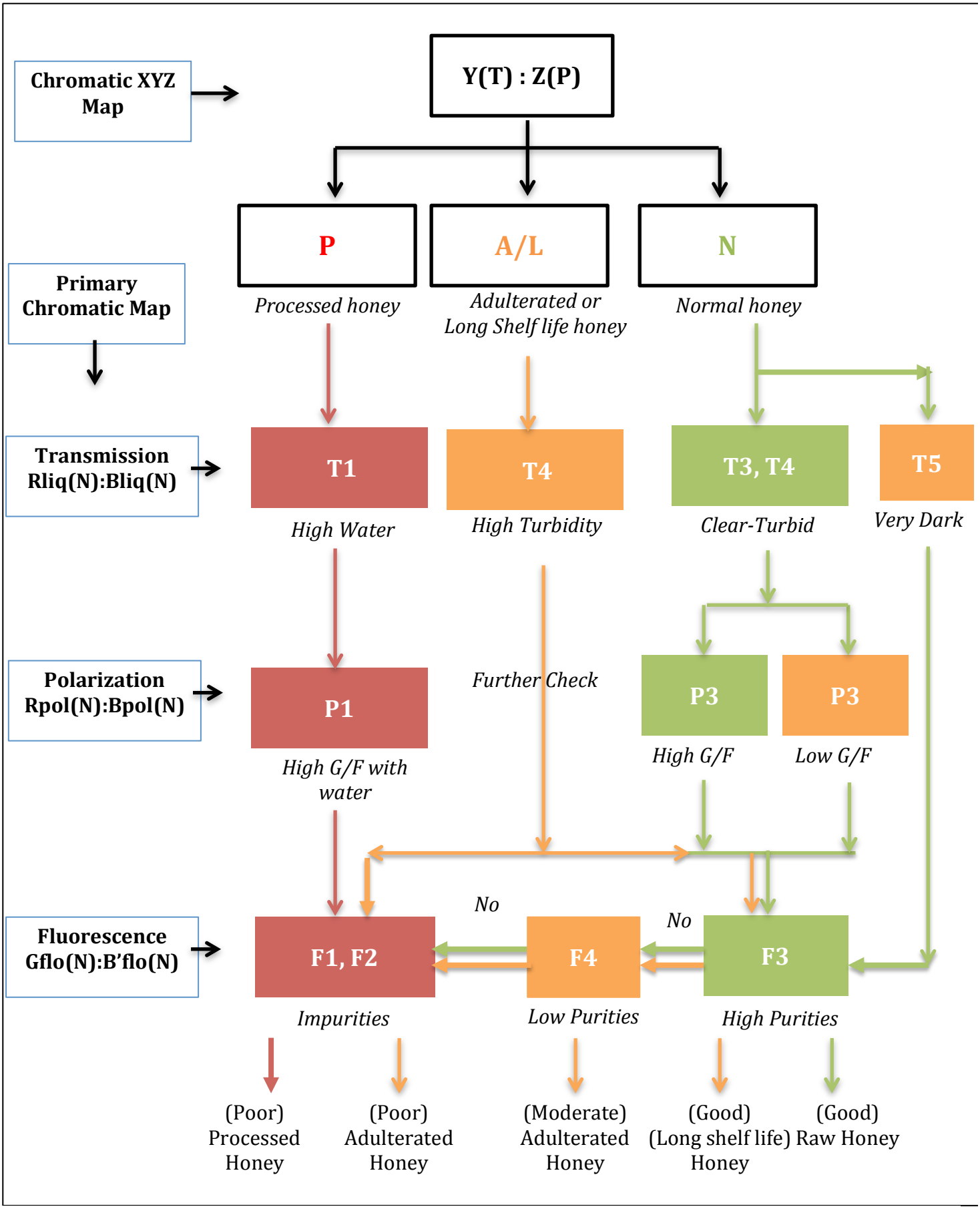

Figure 9.1: Honey Chromatic Assessment Decision Chart

9.5 Application of the Chromatic Decision Chart for Classifying the Unknown Honey samples

A summary of the primary and secondary chromatic results plus the chromatic classification of the 11 unclassified honeys is given on Table 9.4.

Test Sample	*Secondary Chromatic Map*	*Primary Chromatic Map*				*Overall Chromatic Classification*	*Comments*
	Y(T): Z(P)	**Rliq(N):Bliq(N)**	**Rpol(N):Bpol(N)**	**Gflo(N):B'flo(N)**	**Overall Score**		
TAN	**N**	Turbid	Low G/F	High Purities	3.5	Good (R)	
SDRS	**N**	High Turbid	-	High Purities	2.5	Good (R)(L)	Long shelf life honey
SDR-OS-A	**N**	Clear	High G/F	High Impurities	2	Moderate (A)	
ZHUR-M3	**N**	Clear	High G/F	High Impurities	2	Moderate (A)	
SQR-M	**N**	Turbid	Low G/F	Low impurities with water	1.5	Moderate (A)	
SAL1	**N**	Clear	Low G/F	Low impurities with water	1.5	Moderate (A)	
SBR-HB	**N**	Clear	Low G/F	Low impurities with water	1.5	Moderate (A)	
SBR	**N**	High water	High G/F with water	High Impurities	0	Poor (P)(A)	
RA	**P**	High water	High G/F with water	High Impurities	0	Poor (P)(A)	Market shelf honey
GJ2	**P**	High water	High G/F with water	Low impurities	0	Poor (P)(A)	Market shelf honey
T-P	**P**	High water	High G/F with water	Low impurities	0	Poor (P)(A)	Market shelf honey

Table 9.4: Primary and secondary chromatic results plus classification of the various unclassified honeys. (N = Normal honey, P = Processed honey, A = Adulterated, L = Long shelf life, Grade1=Raw honey/good quality, Grade2= moderately quality/ moderate adulteration, Grade3= Adulterated honey/ poor quality, Dark green box= Agree, Dark red box=Disagree)

The chromatic classification of the various unclassified honey samples given on Table 9.4 shows the following:

- 2 samples were classified as good /raw honey
- 5 samples were classified as moderate /adulterated honey
- 4 samples were classified as poor /processed /adulterated honey

The honey sample (TAN) lied in the normal region (N) on the secondary chromatic map. It was shown that the sample was turbid with low glucose/fructose content and has high purity on the primary chromatic maps. The overall score was 3.5, therefore it was classified as raw honey (good quality).

The honey sample (SDRS) lied on the boundary between (N) and (A/L) (Normal, Adulterated or Long shelf life honey) on the secondary chromatic map (Figure 8.11, Chapter 8). The primary chromatic maps showed that the liquid is highly turbid with high purity. The polarization map was not taken in to account here because the liquid might have lost sensitivity due to the high turbidity. However the sample overall chromatic score was 2.5 (above the boundary score 2), therefore it was classified as a good raw honey with long shelf life. The honey sample was in the shelf for long time before it was tested but the quality was not known then. The chromatic approach has relatively correctly classified such condition.

Samples (SDR-OSA, ZHUR-M3, SQR-M) were in the normal region (N) and (SAL1 and SBR-HB) were on the boundary region between (N) and (P) (processed) as shown by the secondary chromatic map (Figure 8.11, Chapter 8). However this map is just for primary quick indication and further investigations needed. All the samples showed to have impurities (Figure 8.7(c), Chapter 8) and low level of glucose/ fructose (Figure 8.7(b), Chapter 8) except for (ZHUR-M3) which was slightly above the boundary and (SDR-OSA) which had a high level glucose/fructose content, this might be due to the botanical source (Zizphus-Spina-christi) of the later which has characteristics of high fructose/glucose ratio (AL-Zoreky, Alza'aemy et al. 2001, Crane 1975).

Samples (SQR-M, SAL1 and SBR-HB) had low glucose/fructose content, low impurities and are clear/turbid samples scored an overall chromatic assessment grade of (1.5) and regarded as moderate quality honey sample.

Samples (RA, GJ2 and T-P) were all in the processed region (P) and (SBR) on the boundary region between (N) and (P) as shown on the secondary chromatic map (Figure 8.11, Chapter 8). The primary chromatic maps showed that the three samples had high water content (Figure 8.7(a), Chapter 8), high glucose/fructose content with water (Figure 8.7(b), Chapter 8) with impurity content (Figure 8.7(c), Chapter 8) (i.e. invert sugar). These conditions indicate the likelihood of the honey sample being highly diluted with pure liquid (water) or blended with invert sugar liquid (e.g. syrup) during processing or being exposed to over heating and over filtering process. The overall chromatic score was 0, which is the lowest score compared to other honey samples, therefore the samples were regarded as processed honey with poor quality. Samples (T-P, Gj2 and RA) were obtained from the market shelf, which are normally being processed for mass production. The chromatic approach has relatively correctly classified such condition.

9.6 Summary

A method for classifying the quality of honey samples has been described which is based on a table 9.1 showing different levels of chromatic parameters using the chromatic results of (Chapter 8, Section 8.2.2.2).

The results for the conventionally classified honey samples have been discussed in detail with the aid of this chart and compared with conventional graded conditions. The chromatic approach gave 91% correct classification of good quality honey samples and 75% correct classification of very poor quality honey samples.

These results have led to the production of an assessment decision chart. An illustration of the use of this chart has been made with the chromatically processed, unclassified honey samples (Chapter 8, Section 8.2.2.3)

Chapter 10

Evaluation Of Method For Field Testing

10.1 Introduction

The proposed honey monitoring system is suitable for use on site at honey beekeeping farms, shops etc. To examine the viability of such a deployment the system using a portable PC was based for monitoring honey quality at various beehive farms and shops at various locations across the Yemen (supported by a grant from the British Yemeni Society). The objective of the study was to confirm the robustness of the monitoring system for use in the field and to further validate the laboratory-based tests described in Chapter 8 and 9 and the use the decision chart (Figure 9.1, Chapter 9)

The raw results together with the normalised chromatic parameters are attached in Appendix II.

Figure 10.1 shows a map of Yemen where the field tests have been done at the three different geographical sites as indicated on the map:

1. Beehive farm located on the outskirts of Al-Mahweet Governorate – West Yemen (Green star)
2. Beehive farm located on Tubasha'a Village, Sabir mount, Taiz Governorate - Middlands Yemen (Red star)
3. Local honey shop located on Sana'a Capital city – North Yemen (Blue star)

Figure 10.1: Geographical map of Yemen with the field-tests sites

Figures 10.2 and 10.3 shows images of the beehive farm where the onsite test have been performed. Figures 10.4 and 10.5 shows an image of the portable system (portable PC and webcam) in ambient conditions including bright sunlight (figure 10.4) at a beehive farm and ambient room light (figure 10.5) at a local honey shop.

Figure 10.2: Honey beekeeping farm site on Almahwet Al-Mahweet governorate – West Yemen

Figure 10.3: Beekeeping at farm on Tubasha'a Village, Sabir mount, Taiz governorate - Middlands

Figure 10.4: Image of onsite test taken by a portable PC in Tubasha'a Village, Sabir mount, Taiz governorate – Middlands

Figure 10.5: Image of onsite test taken by a portable PC in alocal honey shop, Sanaa, North - Yemen

10.2 Chromatic Processing

The procedure shown on the decision chart (Figure 9.1, Chapter 9) was followed. The initial assessment was made with the secondary chromatic mapping before tracking a sample using the primary chromatic maps.

Figure 10.6 shows a Cartesian XYZ chromatic map of the various honey samples from the Yemen field tests. The various overall condition regions are the same as those in the features map discussed on (Figure 8.9, Chapter 8).

Figure 10.6(a) shows each sample represented by a diamond who's colour indicates the botanical source from which its was obtained. Figure 10.6(b) shows the samples coloured according to the conventional classification grades. The chromatic results from the secondary processing are shown on Table 10.1 along with a conventional classification of each sample.

All samples results were then inspected on primary chromatic maps for transmitted, polarized and fluorescent light (figure 10.7 (a), (b) and (c) respectively. The results from these maps are shown on Table 10.1.

10.2.1 Secondary Chromatic Map For Honey Field Tests

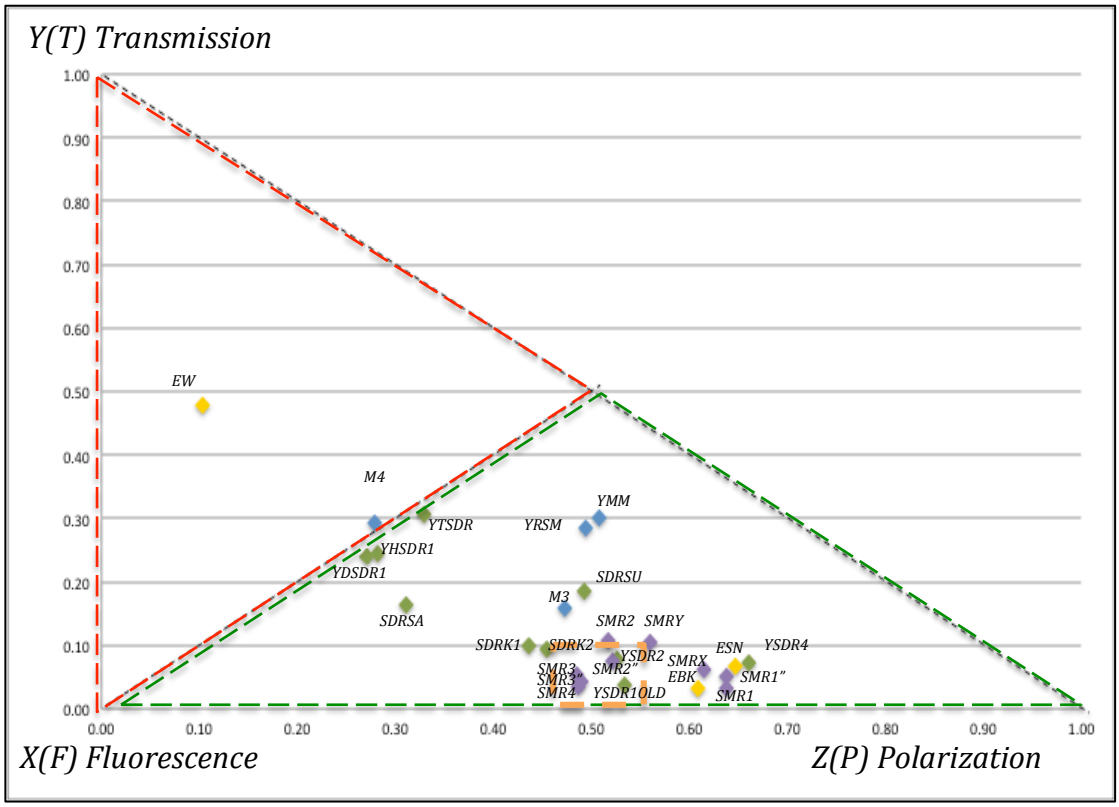

Figure 10.6 (a)

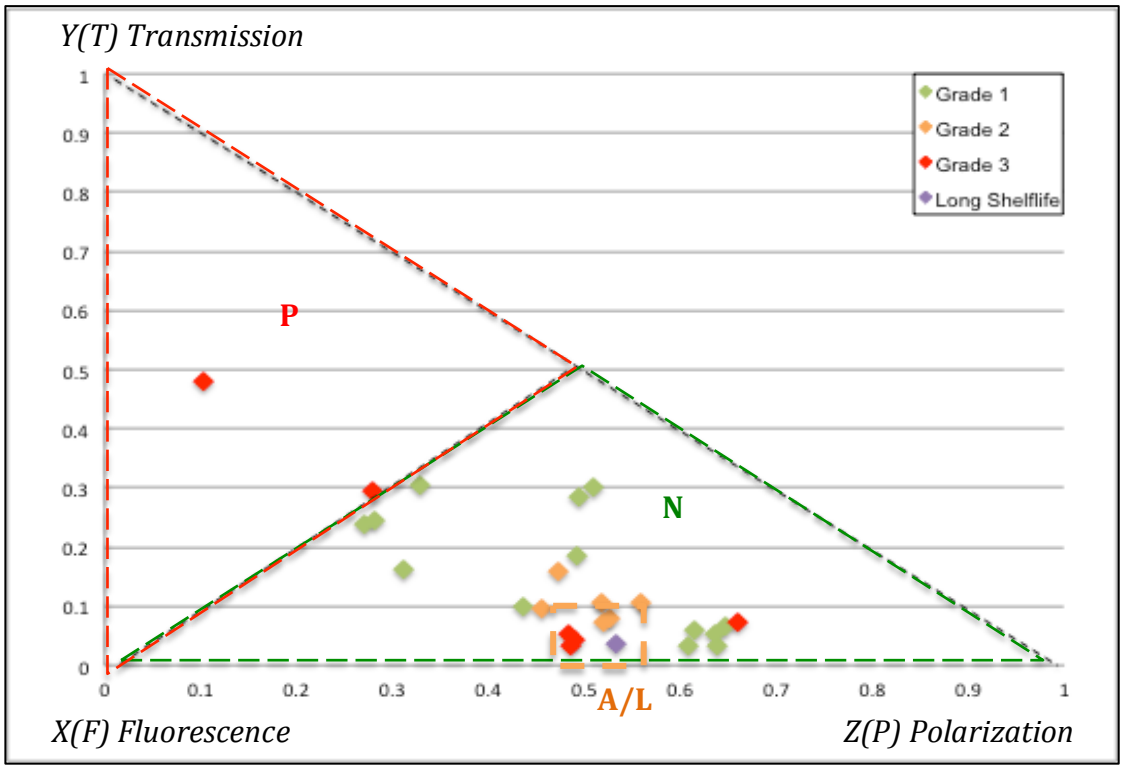

Figure 10.6(b)

Figure 10.6: Chromatic Cartesian XYZ diagram of various field test honey samples.
(Featured regions >>> Red =Processed, Orange=Adulterated/Long shelf life, Green=Normal)
(a):The type of botanical sources (Green=Zizphuz-Spina-chris, Purple=Acacia spp, Blue=Multi floral, Yellow=Ethiopian multi floral)
(b): Quality grade (Green= grade 1, Yellow=grade 2, Red=grade 3, Purple= grade1 long shelf life)

10.2.2 Primary Chromatic Maps For Honey Field Tests

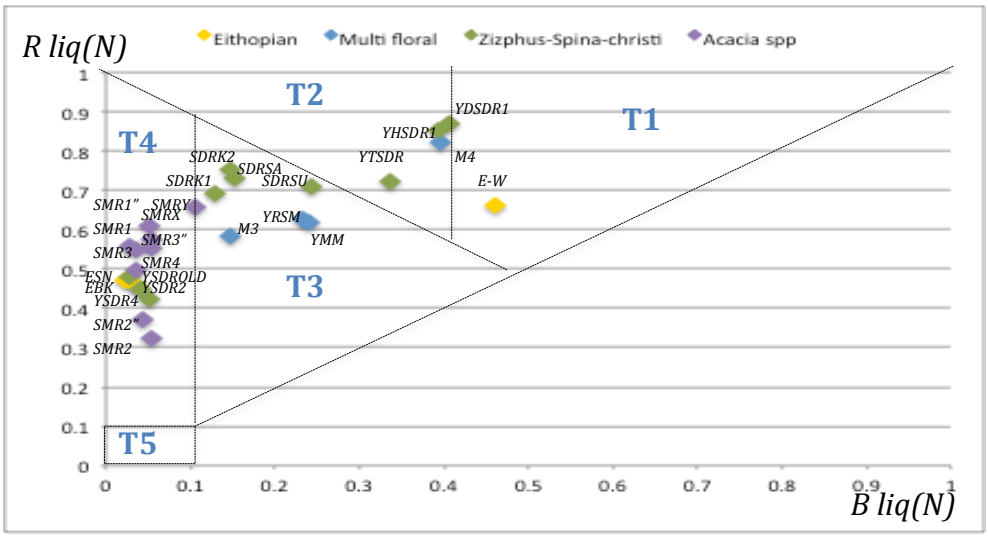

Figure 10.7 (a): Transmission Rliq(N) : Bliq(N) Map

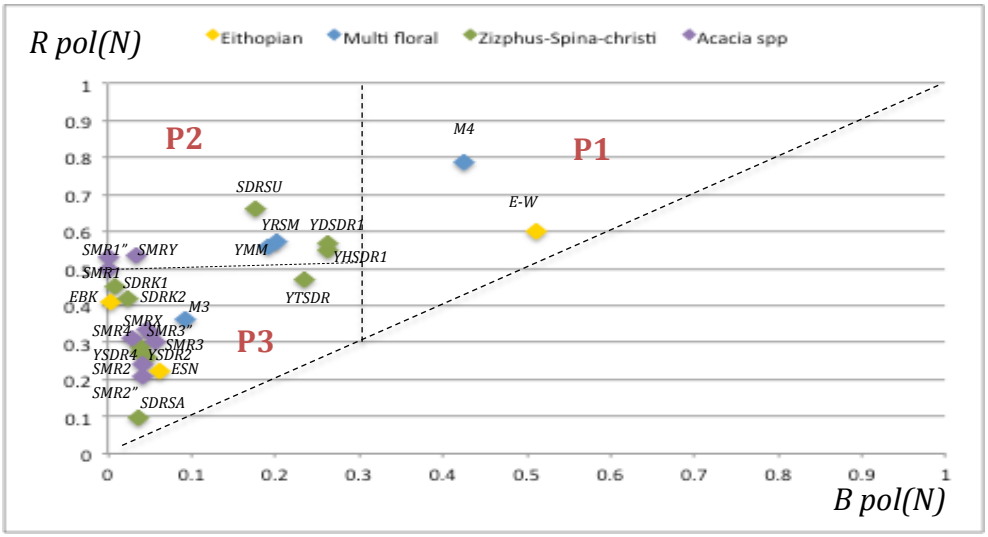

Figure 10.7(b): Polarization Rpol(N) : Bpol(N) Map

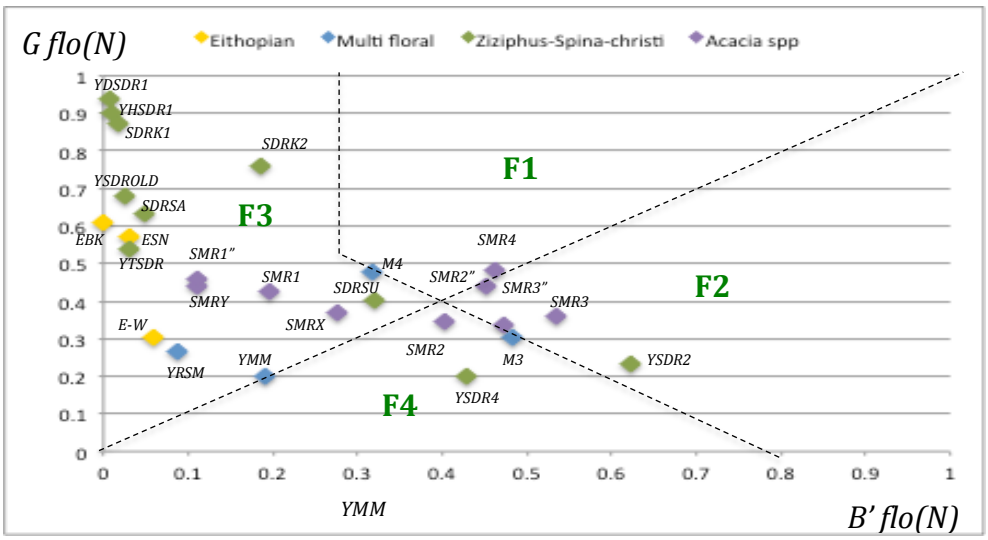

Figure 10.7(c): Fluorescence Gflo(N) : B'flo(N) Map

Figure 10.7: Primary Chromatic Maps for honey field samples: (a) Transmission, (b) Polarization, (c) Fluorescence. (……>> classification boundaries from ((Figure 8.5, Chapter 8))

10.2.3 Comparison Of Chromatic Results With Conventional Classification

Table 10.1

Test Sample	*Secondary Chromatic Map*	*Primary Chromatic Map*				*Overall Chromatic Classification*	*Grade*
	Y(T): Z(P)	**Rliq(N):Bliq(N)**	**Rpol(N):Bpol(N)**	**Gflo(N):B'flo(N)**	**Overall Score**		
Y-D-SDR1	N	Clear	High G/F	High Purities	4	Good (R)	1
SDR-SUM	N	Turbid	High G/F	High Purities	4	Good (R)	1
Y-M-M	N	Turbid	High G/F	High Purities	4	Good (R)	1
Y-R-SM	N	Turbid	High G/F	High Purities	4	Good (R)	1
SDR-K1	N	Turbid	High G/F	High Purities	4	Good (R)	1
Y-T-SDR	N	Clear	Low G/F	High Purities	3.5	Good (R)	1
Y-H-SDR1	N	Clear	Low G/F	High Purities	3.5	Good (R)	1
SDRSA	N	Turbid	Low G/F	High Purities	3.5	Good (R)	1
Y-SMR1	N	High Turbid	High G/F	High Purities	3.5	Good (R)	1
Y-SMR1"	N	High Turbid	High G/F	High Purities	3.5	Good (R)	1
SMR-X	N	High Turbid	Low G/F	High Purities	3	Good (R)	1
E-SN	N	High Turbid	-	High Purities	2.5	Good (R)	1
E-BK	N	High Turbid	-	High Purities	2.5	Good (R)	1
Y-D-SDR OLD	A/L	High Turbid	-	High Purities	2.5	Good (R)(L)	1
M3	N	Turbid	Low G/F	Low Impurities	1.5	Moderate (A)	2
Y-SMR2	A/L	High Turbid	-	Low Purities	1.5	Moderate (A)	2
E-W	P	High water	High G/F with water	High Purities	2	Moderate (A)(P)	2
Y-SMR2"	A/L	High Turbid	-	Low Impurities	0.5	Poor (A)	2
SMR-Y	A/L	Turbid	High G/F	High Purities	4	Good (R)	2
SDR-K2	A/L	Turbid	Low G/F	High Purities	3.5	Good (R)	2
M4	P	Clear	High G/F with water	High Impurities	1	Poor (A)(P)	3
Y-SMR3	A/L	High Turbid	-	Low Impurities	0.5	Poor (A)	3
Y-SMR3"	A/L	High Turbid	-	High Impurities	0.5	Poor (A)	3
Y-SMR4	A/L	High Turbid	-	High Impurities	0.5	Poor (A)	3
Y-SDR2	A/L	High Turbid	-	Low Impurities	0.5	Poor (A)	3
Y-SDR4	N	High Turbid	-	Low Purities	1.5	Moderate (A)	3

Table 10.1: Primary and secondary chromatic results plus classification of the various honey field tests. (N= Normal honey, P= Processed honey, A= Adulterated, L= Long shelf life, R= Raw honey, Grade1=Raw honey/good quality, Grade2= moderately quality/ moderate adulteration, Grade3= Adulterated honey/ poor quality, Dark green box= Agree, Dark red box=Disagree).

The results presented in Table 10.1 allow the following conclusions to be drawn:

The sensitivity and specificity for detecting the good honey samples (with respect to moderate and poor honey samples) are shown on below:

- 14 good samples of grade 1 were correctly classified (TP)
- 10 poor and moderate samples of grade 2 and grade 3 were correctly classified (TN)
- 2 samples of grade 2 and 3 were wrongly classified (FN)
- 0 samples of grade 1 were wrongly classified (FP)

The sensitivity and specificity for detecting the very poor honey samples (with respect to moderate and good honey samples) are shown on below:

- 5 poor samples of grade 3 were correctly classified (TP)
- 17 good and moderate honey samples of grade 1 and 2 were correctly classified (TN)
- 3 samples of grade 2 were wrongly classified (FN)
- 1 samples of grade 3 was wrongly classified (FP)

Overall correctly classified honey samples were 22 out of 26 samples and 4 were wrongly classified. A summary of the sensitivity and specificity is shown on table 10.2.

%	High quality (Grade 1)	Very Poor quality (Grade 3)
Sensitivity	88	63
Specificity	100	94
PPV	100	83
NPV	83	85

Table 10.2: A summary of sensitivity and specificity for high quality honey (with respect to moderate and poor samples) and poor quality honey samples (with resect to good and moderate samples).

The two wrongly classified grade 2 samples were classified as good raw honey because they had an overall assessment scale of 4 and 3.5 which is above the defined boundary for the primary chromatic maps. The secondary map showed both samples to lie on the boundary of the Adulterated (poor) honey and normal honey region.

Samples (SMRY) and (SDRK2) both appeared to be turbid on the transmission map. (SMRY) sample lied on the region of high glucose/fructose while (SDRK2) lies on the region low glucose/fructose but it was nor far from the boundary (P2) on the polarization map. The fluorescence map showed that both samples had high purities. The primary chromatic evaluation for both samples didn't show ambiguity for the wrongly classified samples. However, there is a possibility for a misleading grading being made by the beekeepers.

The primary chromatic evaluation helped to resolve the ambiguity for the good long shelf life honey sample (Y-D-SDR OLD) where it lied on the Adulterated /Long shelf life (A/L) region, this is because the high turbidity was more dominated by the transmission parameter in the secondary chromatic map. Another examples (M3) and (Y-SDR4)) where they lied on the Normal honey region but after the primary chromatic evaluation they showed to be poor samples with adulteration behaviors. Sample (M4) also lied on the boundary between two regions, Processed (P) and Normal (N), but the primary chromatic evaluation confirmed it was a poor sample. Sample (Y-SMR2) also lied on the boundary between two regions, Adulterated (A/L) and Normal (N), but the primary chromatic evaluation confirmed it was a poor sample.

The secondary chromatic map showed correct initial assessment for the following:

- 13 good honey samples were in the Normal honey region
- 6 poor and moderate honey samples were in the Adulterated honey region
- 2 poor and moderate honey samples were in the Processed honey region

The primary chromatic maps successfully resolved the ambiguity for the following:

- 1 good honey sample with long shelf life that was in the A/L region
- 2 poor and moderate honey samples that were in the (N) region
- 1 poor honey sample that lied on the (P- N) boundary
- 3 good honey samples that lied on the boundary of (P-N)
- 1 poor honey samples that lied on the (N-A/L) boundary

10.3 Summary

The portable system performance has been tested in the field trial in ambient conditions including bright sunlight.

Primary and Secondary chromatic processing have been applied to honey samples from the field test results.

The results have been presented in a classification chart of the form derived in Chapter 9, Section 9.1. This allowed the chromatic results to be compared with the conventional grading of the honey samples.

The results show that the chromatic approach gave 88% sensitivity of correct classification of the very good quality honey samples and 63% sensitivity of correct classification of the very poor quality honey samples.

Chapter 11

Conclusion and Future Work

11.1 Conclusions

It has been shown how complex liquids such as honey can be tested for classification according to quality attributes with optical chromaticity approach using readily available, cost effective and portable instrumentation based upon a personal computer whose VDU provides a tunable illumination source.

Procedures for chromatically analyzing test data with three different optical methods simultaneously (transmission, polarization and fluorescence) have been developed suitable for use as chromatic calibration charts, primary and secondary cluster maps which are original aspect of this work and a new contribution to knowledge in order to quantify complex composition of honey samples and alert for deviations from the required quality/ authenticity and to give early warning indications of adulteration rather than precise analysis.

Secondary chromatic maps used to combine relevant data from the three optical signals (transmission, polarisation and fluorescence) on a single graph to provide an initial judgment on the condition of the honey sample.

Primary chromatic processing has yielded three primary chromatic maps (transmitted and polarised light plus fluorescent emission) to provide detailed classification boundaries for honey samples (i.e. level of liquid content, turbidity, sugar and purity).

The classification boundaries obtained using calibration with controlled mixtures of liquid components (water-tea-milk) and (water-syrup-honey) to enable broad calibration indications of liquid mixture samples and to establish classification regions for the primary chromatic maps. These regions were then deployed with real honey samples.

Calibration, normalization and ambient light rejection procedures have been developed to allow operation in a range of lightening conditions such as in the field (sunlight) and factory. Methods for compensating for variation in the ambient light, varying illumination conditions in the field and variations in the VDU illumination or camera characteristics from the supplier or time have also been developed which are also original.

A chromatic classification table have been developed based upon 21 classified honey results and compared with conventional grading conditions. These honey samples have been tested with non-blind tests to provide a calibration means for chromatic approach.

The chromatic approach sensitivity for identifying the correct classification of high quality honey samples was 91% and the sensitivity for identifying very poor quality samples was 75%.

The classified honeys enable the chromatic processing method to be validated. As a result a honey assessment decision chart has been produced which is original and a new contribution to knowledge which shows the philosophy for relating optical properties of light and visually observed properties of honey to decision making and honey quality in one single graph analysis.

An illustration of the use of this chart has been made with the chromatically processed, unclassified honey samples.

Field tests were undertaken at three different remote locations in Yemen using readily available, cost effective and portable system (webcam-personal computer as VDU screen illumination source and simple LED circuitry)

Other methods available for honey quality testing (e.g. using different chemical procedures and optical spectroscopy) are expensive (cost of equipment, laboratory infrastructure) and time consuming (samples need to be sent to labs for testing) because of the complexity of the composition of such liquid.

Honey samples were tested in field trials using the chromatic approach, the sensitivity for correct classifications of the high quality honey sample samples were 88% and the very poor quality honey samples were 63%. Chromatic methodology provided robustness for field use.

11.2 Further applications

The developed chromatic approach can be used for honey monitoring in remote sites such as (beekeeping farms, honey shops, etc.) for making a quick decision on the conditions of the honey. As such it can provide insight into conditions important to the food industry.

Future applications of this academic research can open doors to honey monitoring in Yemen using simple, portable and cost effective methods that could also be incorporated within a mobile phone. It will also encourage the government, non-government organisations and private laboratories to form a national honey monitoring and quality control hub or even implementing a quality certification system that guarantees the integrity and traceability in order to help maintain the reputation of the famous Yemeni honey (Ministry of Agriculture and Irrigation 2012). It will also open doors in the future for more

research interactions between the United Kingdom and Yemen that will promote good relations between the two nations.

Other applications of the developed chromatic approach can also be explored for monitoring honey in the UK and Europe to give early indications of conditions evolving affecting the honeybee population to decline i.e. (loosing valuable pollination service for many crops). Such evolving conditions can be viruses spreading in the beehive due to toxic pesticides used to control pests on crops (Glover, Adams et al. 2011, Williamson, Wright 2013, Morelle 2013) or sudden changes in the honeybee nutrition (which affects honey colour), influences the mortality rate and low honey production in honeybees (Andries 2012).

The primary calibration chromatic mapping described for (Water-Tea-Milk) mixtures has been applied for analyzing laboratory results with mixtures of urine and E. coli samples for calibration purposes. Based on this chromatic technique, an approach for monitoring urine samples using a portable system (webcam-computer and combination of VDU screen illumination source) was developed and shown to operate in a robust manner with potential for use as a point of care test in primary care (Deakin, Jones et al. 2014).

Chromatic analysis has the advantage of providing quantifiable measurements of turbidity, which could potentially give a finer scale of turbidity than the broad categories of human visual assessment as well as quantifying additional chromatic parameters that could indicate other conditions of the urine sample (Deakin, Jones et al. 2014).

11.3 Recommendations and Future Work

The developed system is capable of further evaluation through the acquisition of additional test data and empirical knowledge regarding honey authenticity.

For example the current chromatic system has the potential for further development to improve sample identification level through tuning the classification boundaries on the primary and secondary chromatic maps. Also the optical light used for (transmission, polarization and fluorescent) has the capability for further refinement and development.

Transmission of light:

Preliminary investigation using different colour background light from the VDU screen (cyan, magenta) indicates the capability to enhance the sensitivity of the liquid content in the honey. Further sensitivity for discriminating highly turbid samples can be achieved by increasing the intensity of light from the VDU screen.

Polarization of light:

Preliminary investigation using different angle of rotation (30, 70 deg) for the analysing filter indicated the capability of the system to be improved for better discrimination. However, tuning the rotational angle can be further investigated in order to improve the discrimination of sugar levels in the honey.

Fluorescent of light:

Using LED's with different wavelengths of light can be explored, for example, using LED's at the short wavelengths (i.e. in the UV spectrum) in order to enhance the fluorescent emission from complex fluorescent compounds found in the honey for better discrimination. Or perhaps using two different excitation wavelengths to further enhance the fluorescence emission detection.

A great degree of automation would be advantageous- for example producing automated software for the current chromatic analysis and the development of user-friendly data visualization.

The chromatic analysis approach can be incorporated for use with mobile phone technology using daylight or artificial illumination with the mobile phone camera and cost effective materials. Preliminary tests have been investigated using the optical transmission and polarization of light from a daylight source (e.g. sunlight) with a transparent intelligent chart (for calibration) and a sample holder. However further investigation to accommodate the optical fluorescence test into the developed scheme is still to be done.

The chromatic analysis approach can also be incorporated within a simple handled device using simple circuitry, LED's as the source of illumination and display screen for use in remote sites.

References

ABDUL-GHANI, R., AL-MEKHLAFI, A.M. and KARANIS, P., 2012. Loop-mediated isothermal amplification (LAMP) for malarial parasites of humans: Would it come to clinical reality as a point-of-care test *Acta Tropica,* **122**(3), pp. 233-240.

AL-MUBARAKPURI, S.R., 2003. The Tafsir of Surat An-Nahl. *Tafsir Ibn Kathir*. 5 edn. King Fahd national Library: Darussalam, pp. 488-490.

AL-MURAQAB, A., 2012, 13 December 2012. LIQUID POT OF GOLD, YEMEN'S HONEY TRADE. *Yemen Times* **Business**. [online]. Available:http://www.yementimes.com/en/1633/business/1736/Liquid-pot-of-gold-Yemen's-honey-trade.htm.

ALQARNI, A.S., OWAYSS, A.A., MAHMOUD, A.A. and HANNAN, M.A., Mineral content and physical properties of local and imported honeys in Saudi Arabia. *Journal of Saudi Chemical Society*, (0),.

AL-ZOREKY, N., ALZA'AEMY, A. and ALHUMIARI, A., 2001. Quality Spectrum of Yemeni Honey. *Journal of Agricultural Science, Damascus University*, **17**(2), pp. 110.

ANDRIES, K., October 11, 2012, 2012-last update, Colorful Honey [Homepage of Nationalgeographic], [Online]. Available: http://news.nationalgeographic.co.uk/news/2012/10/pictures/121011-blue-honey-honeybees-animals-science/ [February/20, 2014].

ANKLAM, E., 1998. A review of the analytical methods to determine the geographical and botanical origin of honey. *Food Chemistry*, **63**(4), pp. 549-562.

ASTWOOD, K., LEE, B. and MANLEY-HARRIS, M., 1998. Oligosaccharides in New Zealand Honeydew Honey. *Journal of Agricultural and Food Chemistry*, **46**(12), pp. 4958-4962.

ATAGO CO, , Hand-held Refractometers [Homepage of www.kocintok.com.tr], [Online]. Available: http://www.kocintok.com.tr/katalog/kul/atago.pdf [February/6, 2014].

BALL, D.W., 2006. Concentration scales for sugar solutions. *Journal of chemical education*, **83**(10), pp. 1489.

BENTABOL MANZANARES, A., GARCÍA, Z.H., GALDÓN, B.R., RODRÍGUEZ, E.R. and ROMERO, C.D., 2011. Differentiation of blossom and honeydew honeys using multivariate analysis on the physicochemical parameters and sugar composition. *Food Chemistry*, **126**(2), pp. 664-672.

BERTELLI, D., PLESSI, M., SABATINI, A.G., LOLLI, M. and GRILLENZONI, F., 2007. Classification of Italian honeys by mid-infrared diffuse reflectance spectroscopy (DRIFTS). *Food Chemistry*, **101**(4), pp. 1565-1570.

BERTONCELJ, J., DOBERŠEK, U., JAMNIK, M. and GOLOB, T., 2007. Evaluation of the phenolic content, antioxidant activity and colour of Slovenian honey. *Food Chemistry,* **105**(2), pp. 822-828.

BOGDANOV, S., 2002. HARMONISED METHODS OF THE INTERNATIONAL HONEY COMMISSION. *IHC responsible for the methods: Swiss Bee Research CentreFAM, Liebefeld, CH-3003 Bern, Switzerland,* **International Honey Commission**.

BOGDANOV, S., LÜLLMANN, C., MARTIN, P., VON DER OHE, W., RUSSMANN, H., VORWOHL, G., PERSANO ODDO, L., SABATINI, A., MARCAZZAN, G.L. and PIRO, R., 1999. Honey quality and international regulatory standards: review by the international honey commission. *Bee World,* **80**(2), pp. 61-69.

BOGDANOV, S., JURENDIC, T., SIEBER, R. and GALLMANN, P., 2008. Honey for nutrition and health: a review. *Journal of the American College of Nutrition,* **27**(6), pp. 677-689.

BOUATRA, S., AZIAT, F., MANDAL, R., GUO, A.C., WILSON, M.R., KNOX, C., BJORNDAHL, T.C., KRISHNAMURTHY, R., SALEEM, F. and LIU, P., 2013. The human urine metabolome. *PloS one,* **8**(9), pp. e73076.

BRETEAU, J., October 2007, 2007-last update, Colorimetry and instrumentation [Homepage of Optics 4 Engineers online courses], [Online]. Available: http://www.optique-ingenieur.org/en/courses/OPI_ang_M07_C02/co/Grain_OPI_ang_M07_C02_6.html [January/06, 2014].

CLAYDEN, J., GREEVES, N. and WARREN, S.G., 2012. *Organic chemistry*. Oxford : Oxford University Press, 2012; 2nd ed. / Jonathan Clayden, Nick Greeves, Stuart Warren.

CODEX ALIMENTARIUS COMMISSION, 1981. Revised Codex Standard for Honey Codex Stan 12-1981, Rev. 1 (1987), Rev. 2 (2001). *Codex Standard,* **12**, pp. 1-7.

CORTES, M.E., VIGIL, P. and MONTENEGRO, G., 2011. *The medicinal value of honey: a review on its benefits to human health, with a special focus on its effects on glycemic regulation*.

COUNCIL DIRECTIVE, 2001/110/EC. Official Journal of the European Communities, COUNCIL DIRECTIVE 2001/110/EC of 20 December 2001 relating to honey, pp. L 10/47: L 10/52.

CRANE, E., 1975. Honey. A comprehensive survey. *Honey.A comprehensive survey.,* .

DAVIES, A.M.C., RADOVIC, B., FEARN, T. and ANKLAM, E., 2002. A preliminary study on the characterisation of honey by near infrared spectroscopy. *Journal of Near Infrared Spectroscopy,* **10**(2), pp. 121-135.

DAVIS, C.F., 2007. *The Honey Bee Around and About*. 1 edn. Bee Craft Ltd.

DEAKIN, A.G., JONES, G.R., SPENCER, J.W., BONGARD, E.J., GAL, M., SUFIAN, A.T. and BUTLER, C.C., 2014. A portable system for identifyig urinary tract infection in primary care using a PC-based chromatic technique. *Physiological Measurement, Institute of Physics,*.

DELFINO, I.(.1.)., CAMERLINGO, C.(.2.)., PORTACCIO, M.(.3.)., VENTURA, B.D.(.3.)., MITA, L.(.3.)., MITA, D.G.(.3.). and LEPORE, M.(.3.)., 2011. Visible micro-Raman spectroscopy for determining glucose content in beverage industry. *Food Chemistry,* **127**(2), pp. 735-742.

DERVOS, C.T., PARASKEVAS, C.D., SKAFIDAS, P.D. and VASSILIOU, P., 2005. *A complex permittivity based sensor for the electrical characterization of high-voltage transformer oils*.

DESHPANDE, A., Y., MURALI KRISHNAN, J. and SUNIL KUMAR, P.B., 2010. *Rheology of complex fluids [electronic book] / Abhijit P. Deshpande, J. Murali Krishnan, P.B. Sunil Kumar, editors*. New York ; Springer, c2010.

DOWNEY, G., FOURATIER, V. and KELLY, J.D., 2003. Detection of honey adulteration by addition of fructose and glucose using near infrared transflectance spectroscopy. *Journal of Near Infrared Spectroscopy,* **11**(6), pp. 447-456.

EGAN, C.A., 2006. *Monitoring of optically active chemicals using chromatic modulation techniques*. Liverpool : Thesis Ph.D., 2006.

ELZAGZOUG, E., JONES, G.R., DEAKIN, A.G. and SPENCER, J.W., 2014. *Condition monitoring of hjgh voltage transformer oil using optical chromaticity*. Journal paper edn. Measurement In Action: Institute of physics.

ELZAGZOUG, E., 2013. *Chromatic Monitoring Of Transformer Oil Condition Using CCD Camera Technology*, Electrical and Electronics Engineering Department, University of Liverpool.

EREJUWA, O.O., SULAIMAN, S.A. and AB WAHAB, M.S., 2012. Honey - a novel antidiabetic agent. *International Journal of Biological Sciences,* **8**(6), pp. 913-934.

FLEXIM GMBH, , Transmitted Light Process Refractometer / Technical Specification PIOX® R400 [Homepage of http://www.flexim.com/], [Online]. Available: http://www.flexim.com/en/piox-r [February/6, 2014].

FOOD ENGLAND, 2003-last update, The Honey (England) Regulations 2003, (SI **2003**/2243) [Homepage of Secretary of State, Department of Health], [Online]. Available: http://www.legislation.gov.uk/uksi/2003/2243/made [January/8, 2012].

FREY, L., PARREIN, P., RABY, J., PELLÉ, C., HÉRAULT, D., MARTY, M., MICHAILOS, J., FREY, L., PARREIN, P., RABY, J., PELLÉ, C., HÉRAULT, D., MARTY, M. and MICHAILOS, J., 2011. Color filters including infrared cut-off integrated on CMOS image sensor. *Optics Express,* **19**(14), pp. 13073.

FUJITA, I., 2013. A study of sugars in honey. *Agricultural Journal,* **8**(2), pp. 113-114.

GELBART, W.M. and BEN-SHAUL, A., 1996. The "new" science of "complex fluids". *The Journal of physical chemistry,* **100**(31), pp. 13169-13189.

GHOSH, N., VERMA, Y., MAJUMDER, S.K. and GUPTA, P.K., 2005. A Fluorescence Spectroscopic Study of Honey and Cane Sugar Syrup. *Food Science and Technology Research,* **11**(1), pp. 59.

GISPERT, J.R., 2008. *Coordination Chemistry*. Wiley.

GLOVER, R.H., ADAMS, I.P., BOONHAM, N., BUDGE, G. and WILKINS, S., 2011. Detection of honey bee (Apis mellifera) viruses with an oligonucleotide microarray. *Journal of invertebrate pathology,* **107**(3), pp. 216-219.

GOLDEN, S.W., CRAFT, S. and VILLALANTI, D.C., 1995. Refinery analytical techniques optimize unit performance. *Hydrocarbon Processing,* (11), pp. 85.

GONZALES, A.P., BURIN, L. and BUERA, M.D.P., 1999. Color changes during storage of honeys in relation to their composition and initial color. *Food Research International,* **32**(3), pp. 185-191.

GONZÁLEZ-MIRET, M.L., HEREDIA, F.J., TERRAB, A., HERNANZ, D. and FERNÁNDEZ-RECAMALES, M.A., 2005. Multivariate correlation between color and mineral composition of honeys and by their botanical origin. *Journal of Agricultural and Food Chemistry,* **53**(7), pp. 2574-2580.

GRAVES, P., GARDINER, D. and GRAVES, P., 1989. Practical Raman Spectroscopy.

GULER, A.(.1.)., BEK, Y.(.2.). and KEMENT, V.(.3.)., 2008. Verification test of sensory analyses of comb and strained honeys produced as pure and feeding intensively with sucrose (Saccharum officinarum L.) syrup. *Food Chemistry,* **109**(4), pp. 891-898.

GUO, W., ZHU, X., LIU, Y. and ZHUANG, H., 2010. Sugar and water contents of honey with dielectric property sensing. *Journal of Food Engineering,* **97**(2), pp. 275-281.

HART, H., CRAINE, L.E. and HART, D.J., 1999. *Organic chemistry : a short course*. Boston : Houghton Mifflin Co, c1999; 10th ed. / Harold Hart, Leslie E. Craine, David J. Hart.

HASSAN, S., 2012. Yemeni honey's reputation faces risk of fraud.

HAVENHAND, G., 2010. *Honey: Nature's Golden Healer*. 1 edn. Kyle Cathie.

HEALTH PROTECTION AGENCY, 2002. *Diagnosis of UTI quick reference guide for primary care*. http://www.hpa.org.uk/Topics/InfectiousDiseases/InfectionsAZ/PrimaryCareGuidance/: Health Protection Agency.

ISEKI, H., TAKAHASHI, N., YOKOYAMA, N., IGARASHI, I., KAWAI, S., HIRAI, M. and TANABE, K., 2010. Evaluation of a loop-mediated isothermal amplification method as a tool for diagnosis of infection by the zoonotic simian malaria parasite Plasmodium knowlesi. *Journal of clinical microbiology,* **48**(7), pp. 2509-2514.

ISENGARD, H.D., SCHULTHEI, D., RADOVIC, B., ANKLAM, E., ISENGARD, H., SCHULTHEISS, D., RADOVIĆ, B. and ANKLAM, E., 2001. Alternatives to official analytical methods used for the water determination in honey. *Food Control,* **12**(7), pp. 459.

JONES G. R, DEAKIN A. G and SPENCER J. W, 2008. *Chromatic Monitoring of Complex Conditions*. Boca Raton, Florida, USA: Taylor and Francis.

JONES, G.R., DEAKIN, A.G. and SPENCER, J.W., 2009. Chromatic signatures of broadband optical spectra for liquor discrimination. *Measurement Science and Technology,* **20**(2),.

KAROUI, R., DUFOUR, E., BOSSET, J.-. and DE BAERDEMAEKER, J., 2007. The use of front face fluorescence spectroscopy to classify the botanical origin of honey samples produced in Switzerland. *Food Chemistry,* **101**(1), pp. 314-323.

KNECHT, R., 1990. Properties of sugar. *Sugar,* , pp. 46.

LAKOWICZ, J.R., 2006. *Principles of fluorescence spectroscopy [electronic book]*. Boston, MA : Springer Science+Business Media, LLC, 2006; Third Edition.

LORIN, P., 2005. Forever young [longer-lasting transformers]. *Power Engineer,* **19**(2), pp. 18-21.

LOSCHENOV, M.V., PARFENOV, A.S., KISSELEV, G.L., STRATONNIKOV, A.A., ERSHOVA, K. and STEINER, R.W., 2001. Flourescence method for monitoring of glucose in interstitial fluids, *Proceedings of SPIE - The International Society for Optical Engineering* 2001, pp. 34-39.

LYNN, E.G., ENGLIS, D.T. and MILUM, V.G., 1936. Effect of Processing and Storage on Composition and Color of Honey. *Journal of Food Science,* **1**(3), pp. 255.

MARTIN, P. and BOGDANOV, S., 2002. Honey Authenticity: a Review. *Swiss Bee Research Centre, Dairy Research Station, Liebefeld ; Q. P. Services, Hayes, Great Britain,* .

MCNICHOLS, R.J. and COTÉ, G.L., 2000. Optical glucose sensing in biological fluids: An overview. *Journal of Biomedical Optics,* **5**(1), pp. 5-16.

MINISTRY OF AGRICULTURE AND IRRIGATION, 2012. *A Promising sector for Diversified Economy in Yemen*. Cabinet Decree No. (37 – 2012). National Agriculture Sector Strategy 2012-2016-Republic of Yemen: Ministry of Agriculture and Irrigation.

MORELLE, R., March 23, 2013, 2013-last update, Neonicotinoid pesticides "damage brains of bees" [Homepage of BBC News, Science and Environment], [Online]. Available: http://www.bbc.co.uk/news/science-environment-21958547 [May/4, 2013].

NANDA, V.(.1.)., SARKAR, B.C.(.1.)., SHARMA, H.K.(.1.). and BAWA, A.S.(.2.)., 2003. Physico-chemical properties and estimation of mineral content in honey produced from different plants in Northern India. *Journal of Food Composition and Analysis,* **16**(5), pp. 613-619.

NAREDO, J.L., FUERTE, C.R., GUARDADO, J.L. and MORENO, P., 2001. A comparative study of neural network efficiency in power transformers diagnosis using dissolved gas analysis. *IEEE Transactions on Power Delivery,* **16**(4), pp. 643-647.

NATIONAL HONEY BOARD, 2013-last update, About Honey [Homepage of National Honey Board], [Online]. Available: http://www.honey.com/honey-at-home/learn-about-honey/2013].

NORDSTROM, L., LIU, C.M. and PRICE, L.B., 2013. Foodborne urinary tract infections: a new paradigm for antimicrobial-resistant foodborne illness. *Frontiers in Microbiology,* **4**, pp. 29-29.

OTHMAN, S., YOOK, C.C. and CHIRK, J.N., 2003. Accuracy of urinalysis in detection of urinary tract infection in a primary care setting. *Asia Pacific Family Medicine,* **2**, pp. 206-212.

ÖZBALCI, B., BOYACI, I.H., TOPCU, A., KADILAR, C. and TAMER, U., 2013. Rapid analysis of sugars in honey by processing Raman spectrum using chemometric methods and artificial neural networks. *Food Chemistry,* **136**(3-4), pp. 1444-1452.

PERFECTOR SCIENTIFIC, 2014-last update, Plastic disposable cuvettes
 [Homepage of Perfector Scientific, Inc], [Online]. Available: http://www.perf-sci.com/d_cuvettes/cuvette.html [January/11, 2014].

PILIZOTA V and NEDIC TIBAN N, 2009. Advances in Honey Adulteration Detection. (August/September),.

POPEK, S., 2002. A procedure to identify a honey type. *Food Chemistry,* **79**(3), pp. 401-406.

PRERANA, SHENOY, M.R. and PAL, B.P., 2008. *Method to determine the optical properties of turbid media*.

PRIDAL, A. and VORLOVA, L., 2002. Honey and its physical parameters. *Czech J. Anim. Sci., 47, 2002 (10): 439–444,* (10), pp. 439-44.

ROITHNER LASERTECHNIK, 19/4/2012, 2012-last update, Violet LED (405nm) [Homepage of Roithner LaserTechnik GmbH], [Online]. Available: http://www.roithner-laser.com/led_diverse.html#violet [February/ 20, 2014].

ROSHAN, A.-.A., GAD, H.A., EL-AHMADY, S., AL-AZIZI, M., ABOU-SHOER, M. and KHANBASH, M.S., 2013. Authentication of monofloral yemeni sidr honey using ultraviolet spectroscopy and chemometric analysis. *Journal of Agricultural and Food Chemistry,* **61**(32), pp. 7722-7729.

RYER, A., 1997. *Light measurement handbook*. 2 edn. International Light, NEWBURYPORT, MA: Citeseer.

SANZ, M.L., DEL CASTILLO, M.D., CORZO, N. and OLANO, A., 2003. 2- Furoylmethyl amino acids and hydroymethylfurfural as indicators of Money quality. *Journal of Agricultural and Food Chemistry,* (51), pp. 4278-4283.

SANZ, M.L., SANZ, J., MARTÍNEZ-CASTRO, I., GONZALEZ, M. and DE LORENZO, C., 2005. A contribution to the differentiation between nectar honey and honeydew honey. *Food Chemistry,* **91**(2), pp. 313-317.

SCHANDA, J., EPPELDAUER, G. and SAUTER, G., 2007. Tristimulus Color Measurement of Self-Luminous Sources. *Colorimetry: Understanding the CIE system,* , pp. 135-157.

SERRANO, S., VILLAREJO, M., ESPEJO, R. and JODRAL, M., 2004. Chemical and physical parameters of Andalusian honey: classification of Citrus and Eucalyptus honeys by discriminant analysis. *Food Chemistry,* **87**(4), pp. 619-625.

SEVERINGHAUS, J.W. and KELLEHER, J.F., 1992. Recent developments in pulse oximetry. *Anesthesiology,* **76**(6), pp. 1018-1038.

SMITH, E. and DENT, G., 2005. *Modern Raman Spectroscopy [electronic book] : A Practical Approach*. Hoboken : Wiley, 2005.

SOMMER, L., 2012. *Analytical absorption spectrophotometry in the visible and ultraviolet: the principles*. Elsevier.

STEVENSON, A., ed, 2010. *Oxford Dictionary of English*. 3 edn. Oxford University Press.

STOCKLEY, C., OXLADE, C. and WERTHEIM, J., 2007. *The Usborne illustrated dictionary of Science*. London: Usborne, 2007.

STOROZHUK, A.I., 2010. *Color [electronic book] : ontological status and epistemic role / Anna Storozhuk*. New York. : Nova Science Publishers, 2010.

TERRAB, A., ESCUDERO, M.L., GONZÁLEZ-MIRET, M.L. and HEREDIA, F.J., 2004. Colour characteristics of honeys as influenced by pollen grain content: A multivariate study. *Journal of the science of food and agriculture,* **84**(4), pp. 380-386.

The Qur'an. Trans. by ALI, A. Y., ELIYASEE, M. A. H., TAHA, O., 2007. TTQ, INC.

TISSUE, B.M., June,2003, 2003-last update, Schematic of a wavelength-selectable, single-beam UV-Vis spectrophotometer [Homepage of www.chem.vt.edu/chem-ed/index.html], [Online]. Available: http://www.files.chem.vt.edu/chem-ed/spec/uv-vis/singlebeam.html [January/6, 2014].

TOMITA, N., MORI, Y., KANDA, H. and NOTOMI, T., 2008. Loop-mediated isothermal amplification (LAMP) of gene sequences and simple visual detection of products. *Nature Protocols,* **3**(5), pp. 877-882.

TOPAC INC, , Quartz Wedge Saccharimeter [Homepage of Topac Inc], [Online]. Available: http://www.topac.com/saccharomat.pdf [January/6, 2014].

TORRE, R., 2007. *Time-resolved spectroscopy in complex liquids [electronic book] : an experimental perspective*. New York : Springer Science+Business Media,LLC, 2007.

TOSUN, M., 2013. *Detection of adulteration in honey samples added various sugar syrups with isotope ratio analysis method [electronic resource]*. Elsevier Ltd.

TRONTECH, , Visible Spectrophotometer [Homepage of www.torontech.com], [Online]. Available: http://www.torontech.com/materials-testing/spectroscopy/other-analyzer/vis1000nm [January/6, 2014].

TUBEROSO, C.I.G., JERKOVIĆ, I., SARAIS, G., CONGIU, F., MARIJANOVIĆ, Z. and KUŠ, P.M., 2014. Color evaluation of seventeen European unifloral honey types by means of spectrophotometrically determined CIE chromaticity coordinates. *Food Chemistry,* **145**(0), pp. 284-291.

UNITED STATES DEPARTMENT OF AGRICULTURE, 1985. *United States Standards for Grades of Extracted Honey*. FEDERAL REGISTER (50 FR 15861): .

USAID, September 2012, 2012-last update, Capacity to Improve Agriculture and Food Security (CIAFS). The World Market For Honey - Market Survey 1 [Homepage of http://www.fintrac.com/], [Online]. Available: http://www.fintrac.com/cpanelx_pu/Ethiopia%20CIAFS/12_06_4949_CIAFS%20_1%20Honey%20Final%20Oct%2011.pdf2014].

WHITE, J.W., 1975. Composition of honey. *Honey: A Comprehensive Survey*. Heinemann: London, UK, pp. 157-206.

WHITE, J.W., 1975. Physical characteristics of honey. *Honey: A Comprehensive Survey*.. Heinemann: London, UK, pp. 207-239.

WHITE, J. and JONATHAN, W., 1978. Honey. *Advances in Food Research,* **24**, pp. 287-374.

WILLIAMSON, S.M. and WRIGHT, G.A., 2013. Exposure to multiple cholinergic pesticides impairs olfactory learning and memory in honeybees. *Journal of Experimental Biology,* **216**(10), pp. 1799-1807.

WYSZECKI, G. and STILES, W.S., 1982. *Color science*. Wiley New York.

Appendix I

I.1 LED Data Sheet

LED405-series

TECHNICAL DATA

Violet LED	**InGaN**

LED405-series are InGaN LEDs mounted on a lead frame and encapsulated in various types of clear silicone lens, which offers different design settings.
On forward bias, it emits a radiation of typical 15 mW at a peak wavelength at 405 nm.

Specifications

- Structure: InGaN
- Peak Wavelength: typ. 405 nm
- Optical Ouput Power: typ. 15 mW
- Resin Material: Clear silicone resin
- Solder: Lead free

Absolute Maximum Ratings (T_a=25°C)

Type	Symbol	Value	Unit
Power Dissipation	P_D	200	mW
Forward Current	I_F	50	mA
Reverse Voltage	V_R	5	V
Operating Temperature	T_{OP}	-30 ... +85	°C
Storage Temperature	T_{STG}	-40 ... +100	°C
Soldering Temperature (for 5 sec.)	T_{SOL}	265	°C

Electro-Optical Characteristics (T_a=25°C)

Item	Symbol	Condition	Min.	Typ.	Max.	Unit
Forward Voltage	V_F	I_F = 20 mA	-	3.5	4.0	V
Reverse Current	I_R	V_R = 5 V	-	-	10	µA
Radiated Power	P_O	I_F = 20 mA	-	15	-	mW
Peak Wavelength	λ_P	I_F = 20 mA	400	405	410	nm
Half Width	$\Delta\lambda$	I_F = 20 mA	-	15	-	nm

Figure I.2: Data Sheet for Violet LED

!.2 Constant Current Source Circuit

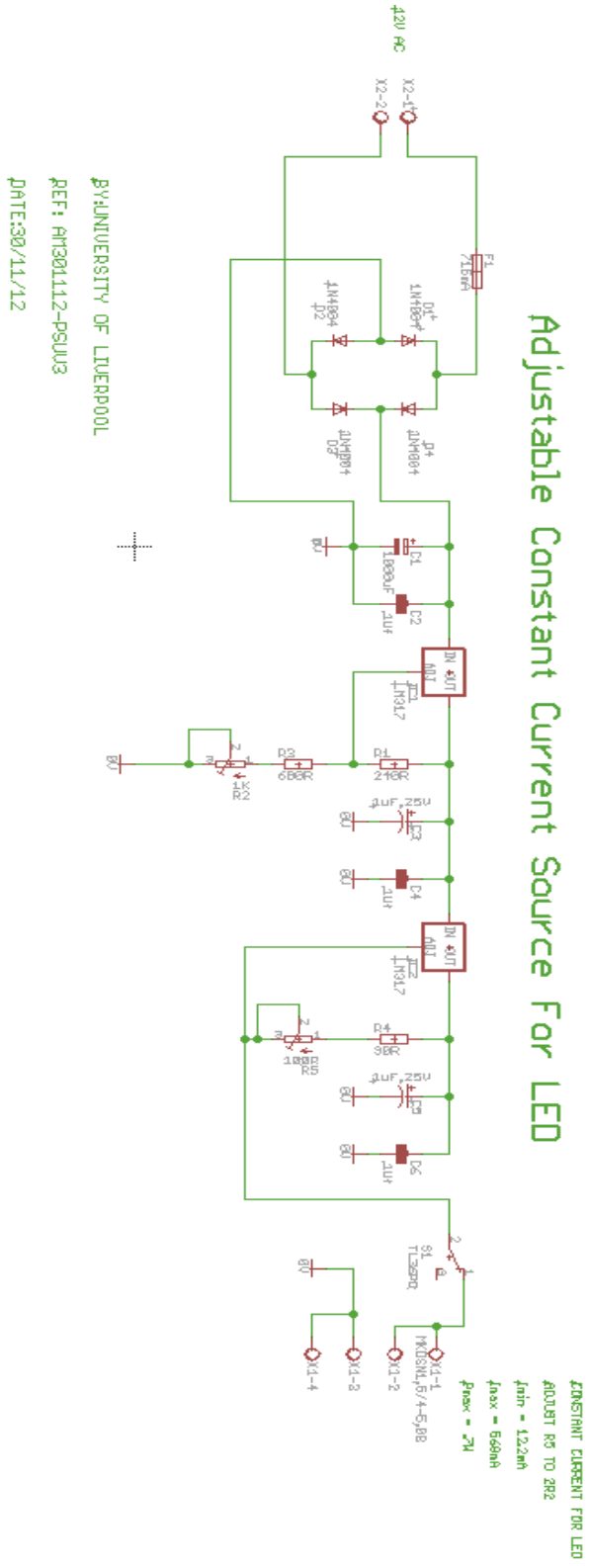

Figure I.2: Constant current source circuit diagram

I.3 Capsoft Software

The primary function of Capsoft chromatic software figure I.1, alongside many additional functions, specially developed at CIMS by Anthony Deakin for use in numerous applications, enables R, G and B values from an images pixel regions selected by the user to be obtained and logged together with their chromatic transformations into, for example, hue, lightness and saturation. The log file serves as input for further chromatic analyses and graphing outputs, for example transformation and graphing of r, g, b in terms of X, Y, Z. The text file (figure I.2) contains the raw values of RGB and HLS extracted from the analysed areas highlighted in squares (figure I.1).

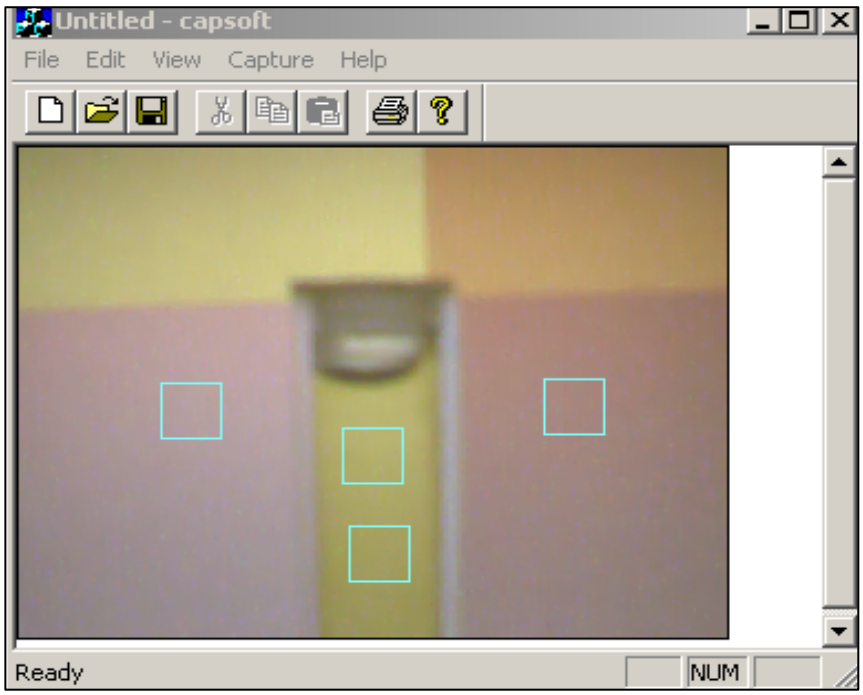

Figure I.3: Capsoft analysis window

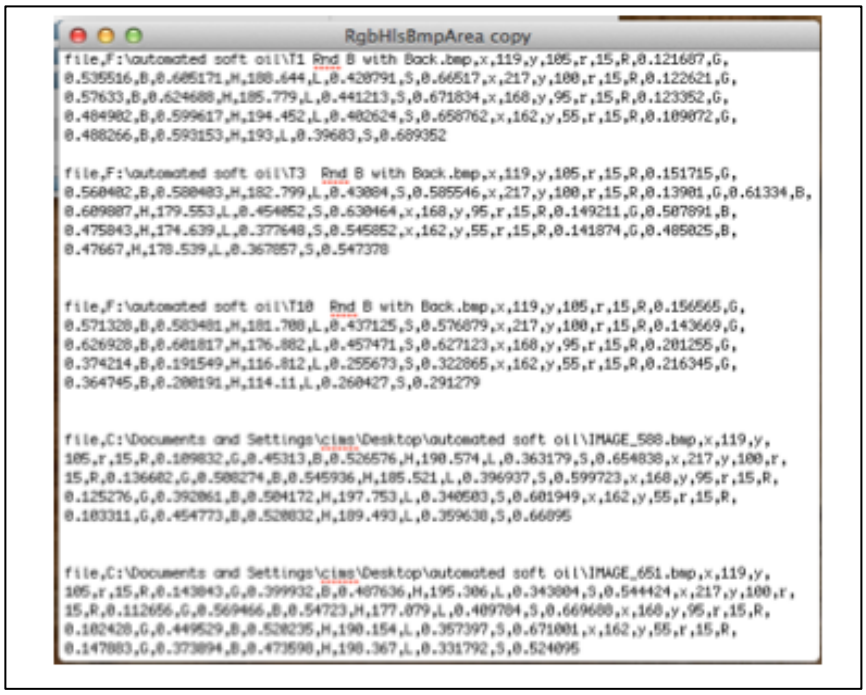

Figure I.4: RGB extracted text file from the Capsoft analysis points.

I.4 Webcam Settings

Brightness: 54/100
Contrast: 23/100
Gama: 54/100
Hue: 53/360
Saturation: 39/100
Sharpness: 46/100
Image quality: 3/3
USB Bandwidth: 8
Exposure: 0/100
Red: 35/100
Blue: 35/100
Green: 35/100
White balance: Indoor
Display: LCD, 60Hz

Appendix II

II.1 Experimental Results

II.1.1 Raw RGB Outputs Of The Optical Polarization System At Different Rotational Angles

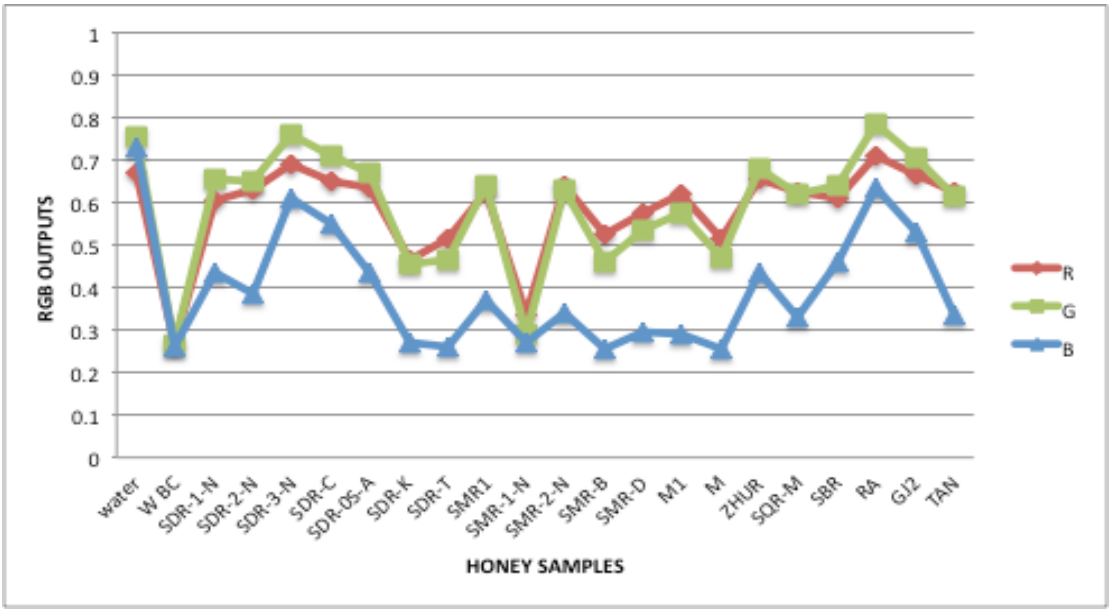

Figure II.2: Raw RGB outputs vs. water and honey samples with white VDU illumination and polarizing filter angle at 0 degrees

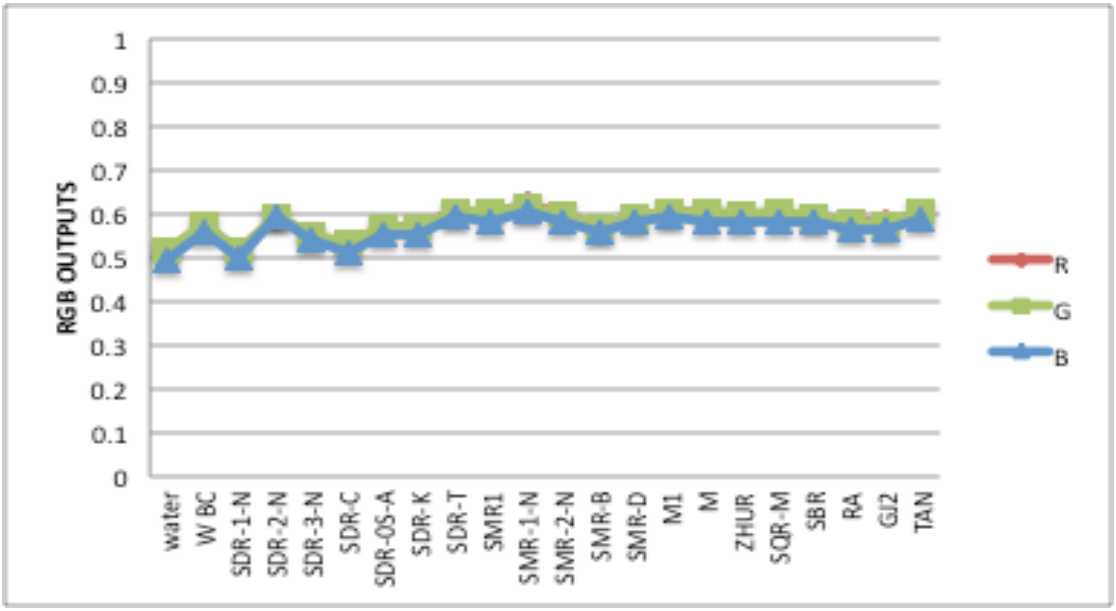

Figure II.3: RGB output of the L (left) reference area with water and 28 different honey tests white VDU illumination and polarizing filter angle at 0 degrees

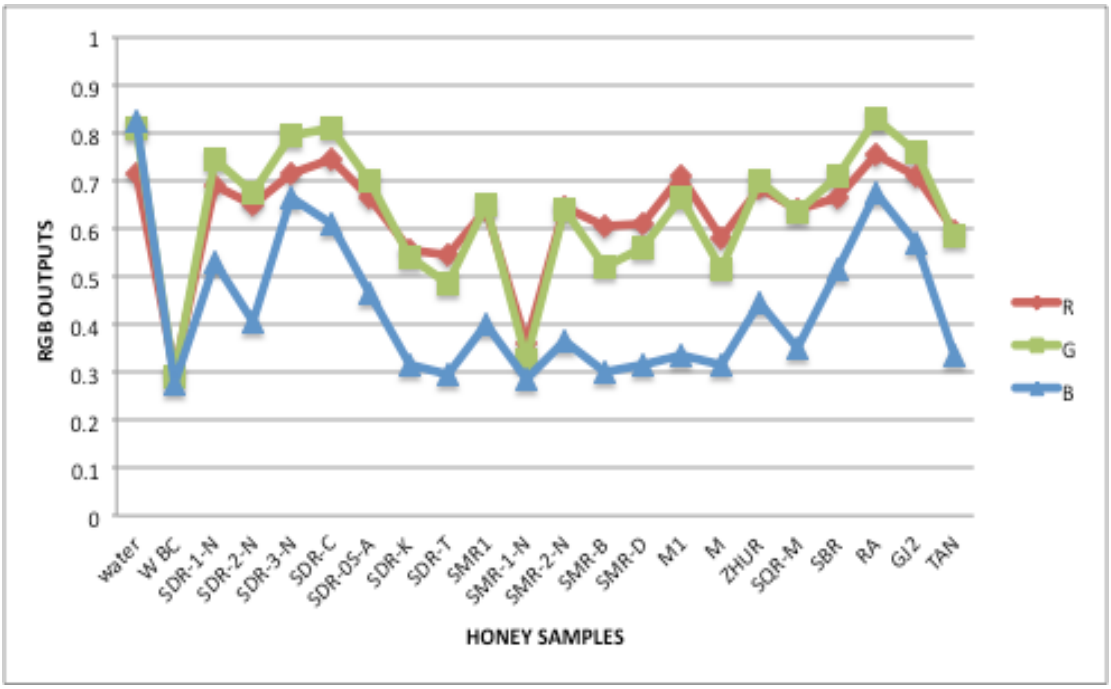

Figure II.3: Raw RGB outputs vs. water and honey samples with white VDU illumination and polarizing filter angle at 30 degrees

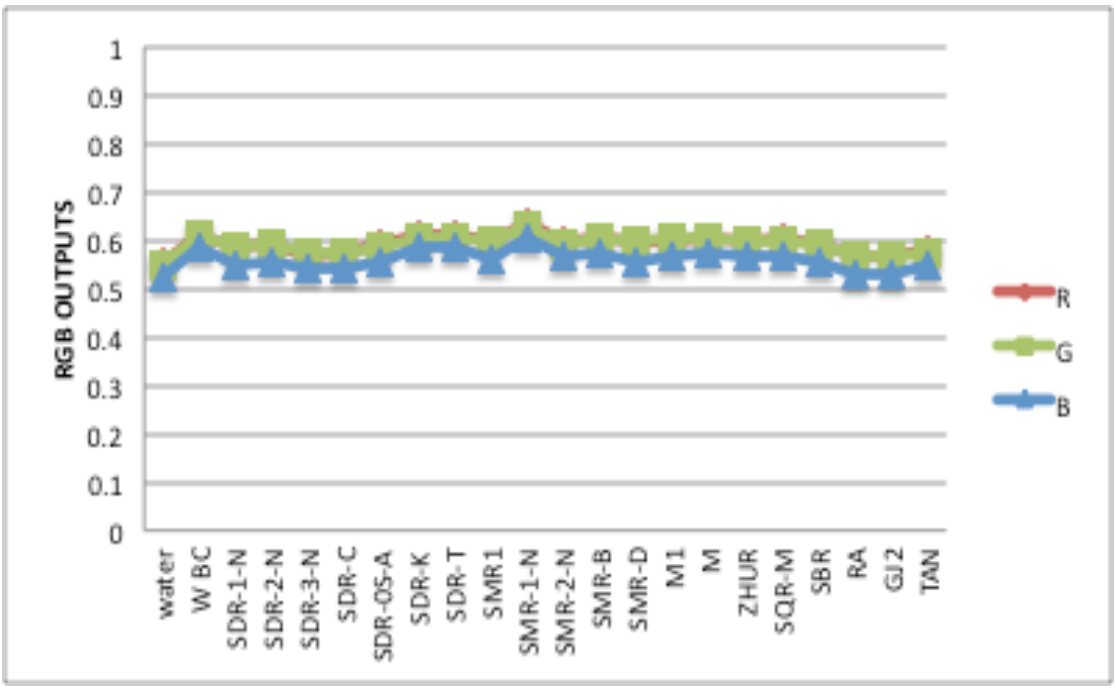

Figure II.4: RGB output of the L (left) reference area with water and 28 different honey tests white VDU illumination and polarizing filter angle at 30 degrees

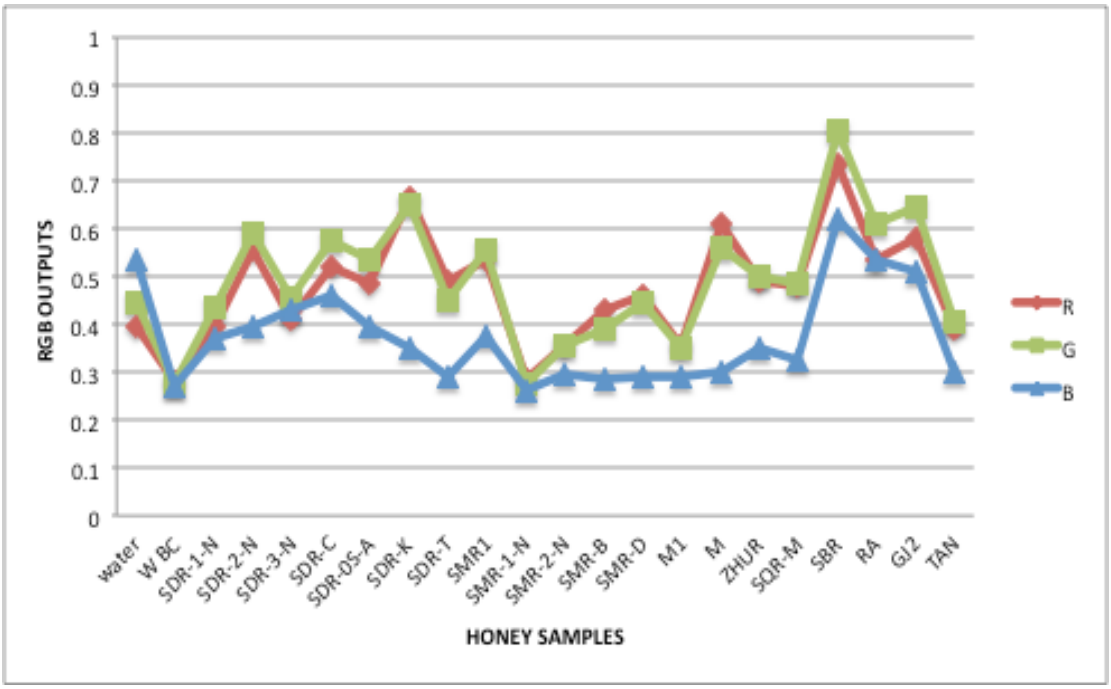

Figure II.5: Raw RGB outputs vs. water and honey samples with white VDU illumination and polarizing filter angle at 70 degrees

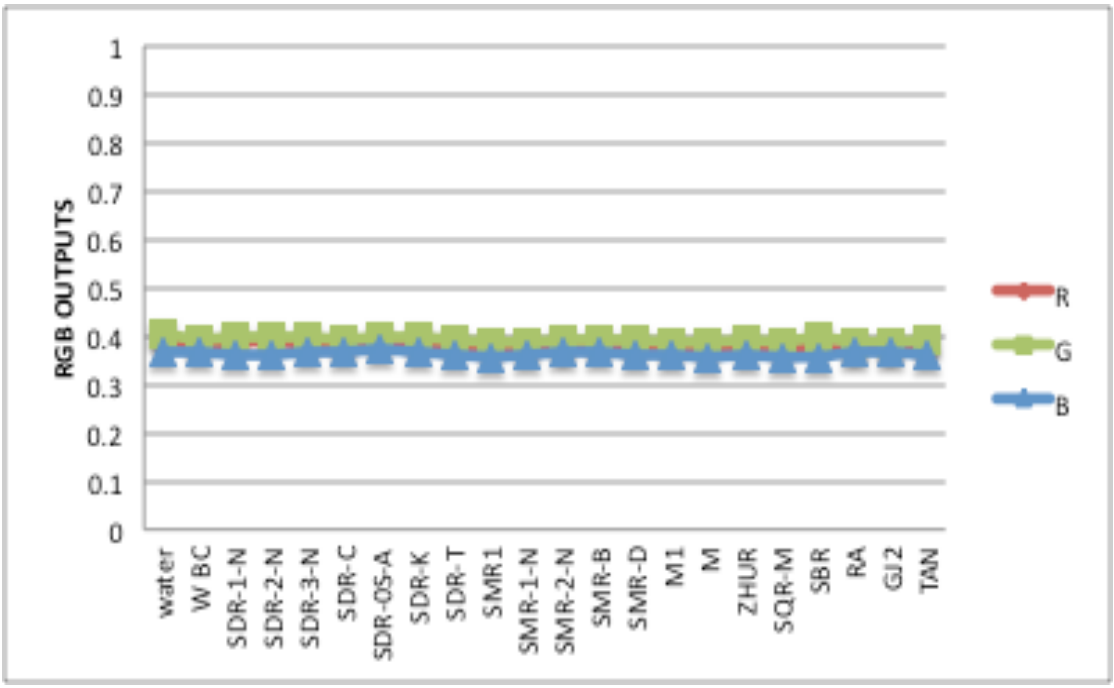

Figure II.6: RGB output of the L (left) reference area with water and 28 different honey tests white VDU illumination and polarizing filter angle at 70 degrees

II.2 Analysis Of Results

II.2.1 Transmitted Blue Illumination Through Honey Samples

Figure II.7 shows the normalized results for the blue light illumination through water and various honey samples. Figure II.7(a) shows calibration curves for each of the three chromatic parameters, R(liq)N, G(liq)N, B(liq)N as a function of water and various honey samples. Figure II.7(b) shows a chromatic cluster map Rliq(N) against Bliq(N)for various honey samples. There is little variation in Bliq(N) for Rliq(N) ≤ 0.6.

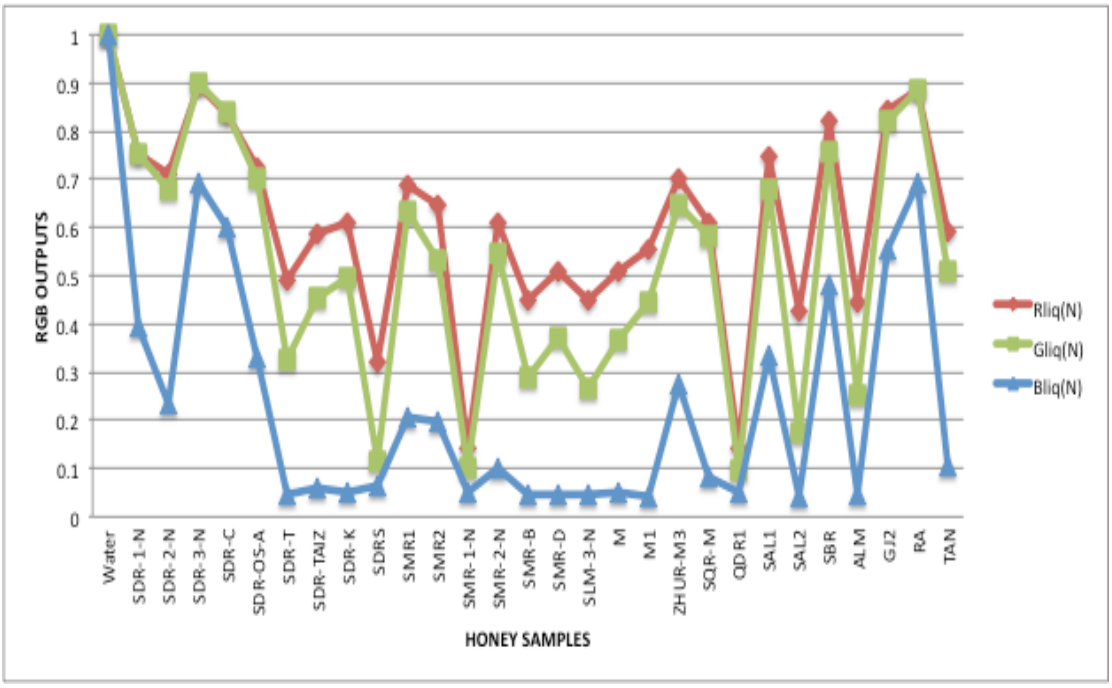

Figure II.7 (a): Calibration graph of RGB transmitted light parameters against water and various honey samples

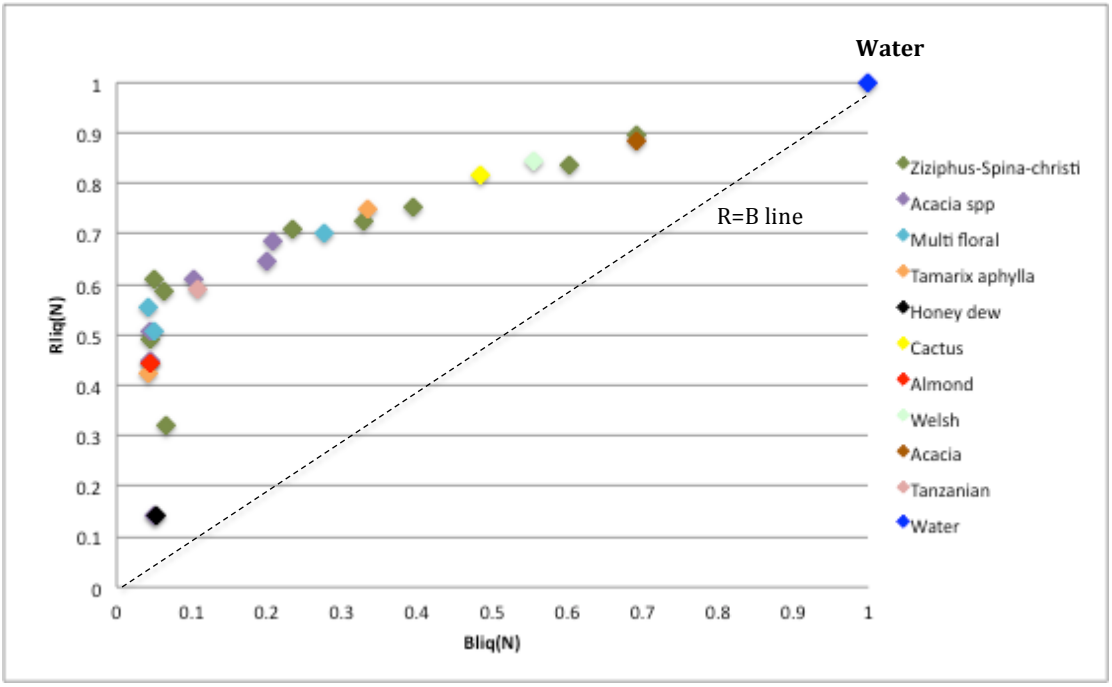

Figure II.7 (b): Chromatic cluster map of transmitted light parameter Rliq(N):B(liqN) for water and various honey samples

Figure II.7: Processed Transmitted light result for various honey samples and water with blue illumination screen

(a) Calibration graph of RGB transmitted light parameter against water and various honey samples

(b) Chromatic cluster map of transmitted light parameter Rliq(N):B(liqN)

II.2.2 Transmitted Polarized light Through Honey Samples At Different Polarizing Angles

Figures II.8, II.9 and II.10 shows R(pol)N, G(pol)N and B(pol)N results for the polarized light parameters through various honey samples at different polarizing angles (0, 30 and 70 degrees), the values were obtained from (Equation 7.3, Chapter 7).

Figure II.8(a) shows calibration curves for each of the three chromatic parameters R(pol)N, G(pol)N and B(pol)N as a function of water and various honey samples with the polarizing filters indirection at 0 degrees to each other.

Figure II.8(b) shows a chromatic cluster map Rpol(N) against Bpol(N) of various honey samples and water corresponding to this 0 degree relative indirection of the polarizing filters.

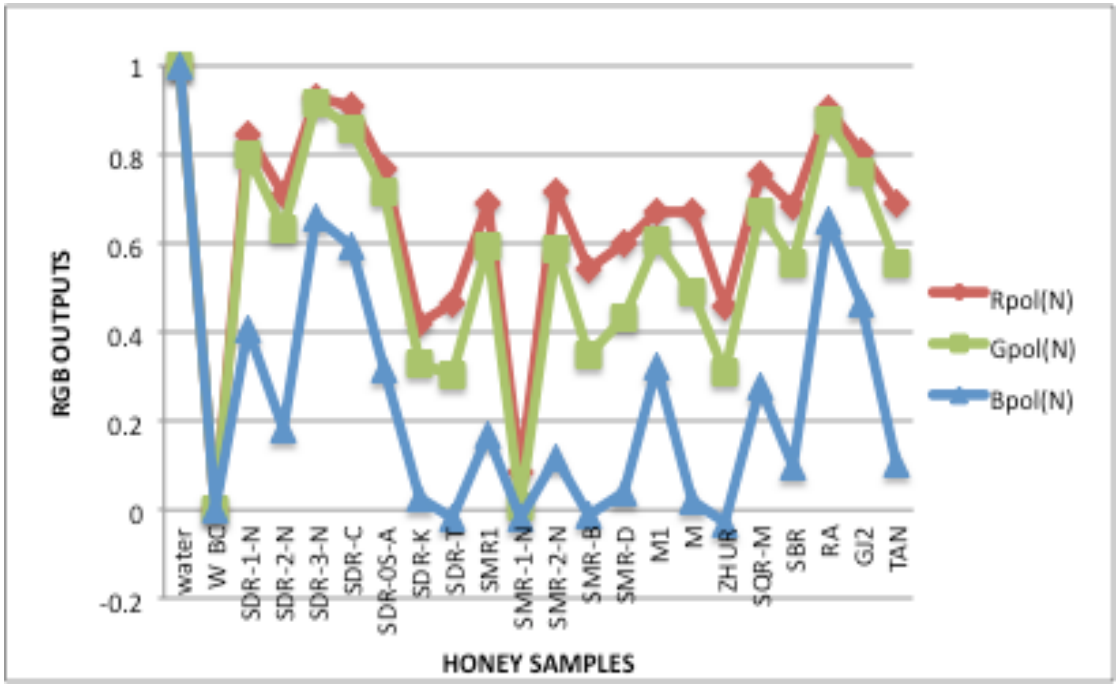

Figure II.8 (a): Calibration graph of RGB polarized light parameters against water and various honey samples at 0-degree polarizer angle

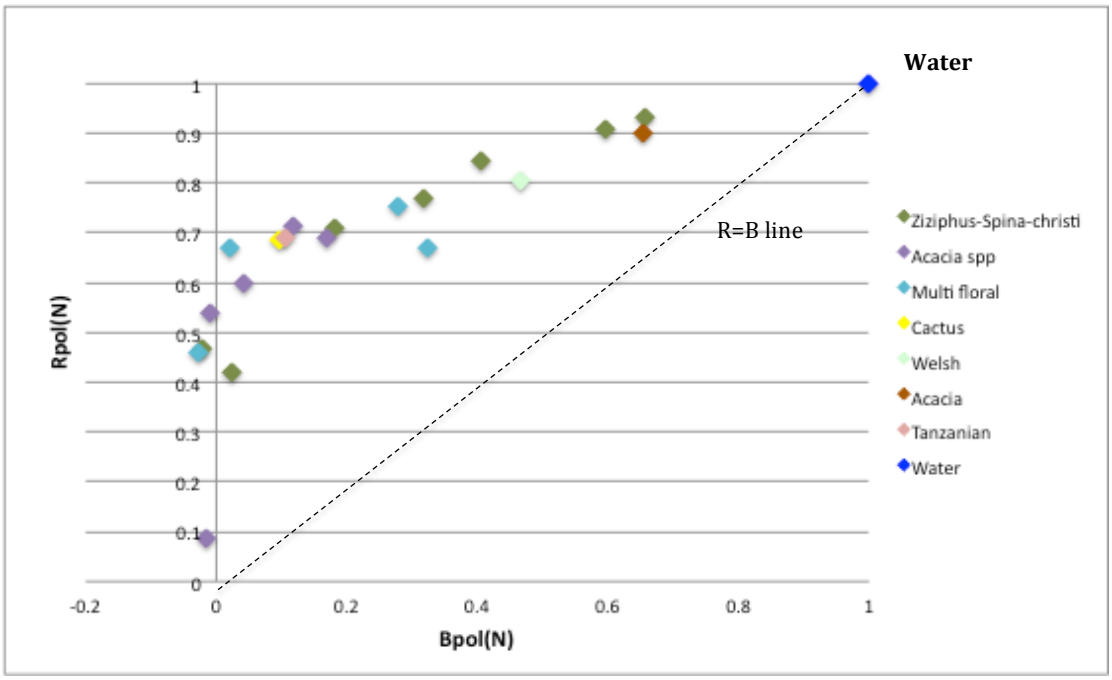

Figure II.8(b): Cluster map of polarized light parameters Rpol(N):Bpol(N) at 0-degree polarizer angle

Figure II.8: Processed polarized light chromatic parameters for various honey samples at 0-degree polarizer angle

(a) Calibration graph of RGB polarized light parameters against water and various honey samples

(b) Cluster map of polarized light parameters Rpol(N):Bpol(N)

Figure II.9(a) shows calibration curves for each of the three chromatic parameters R(pol)N, G(pol)N and B(pol)N as a function of water and for various honey samples with an angle of 30 degree between the polarizing angles of the polarizing filters.

Figure II.9(b) shows a chromatic cluster map Rpol(N) against Bpol(N) of various honey samples and water corresponding to this 30 degree relative direction of the polarizing filters.

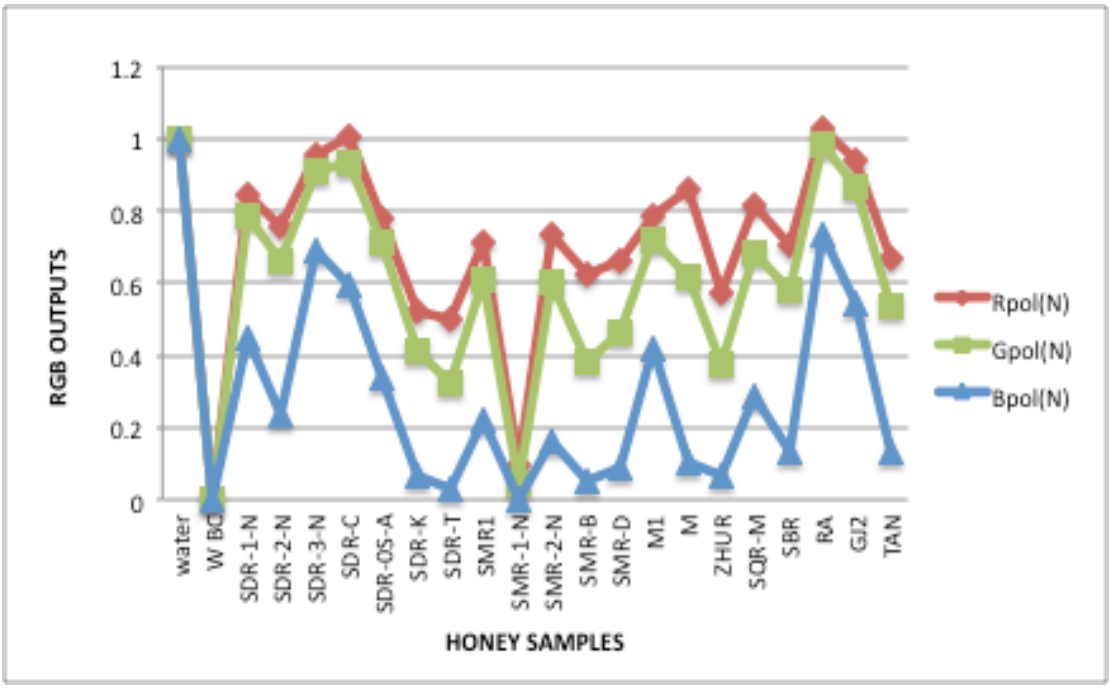

Figure II.9 (a):Calibration graph of RGB polarized light parameters against water and various honey samples at 30-degree polarizer angle

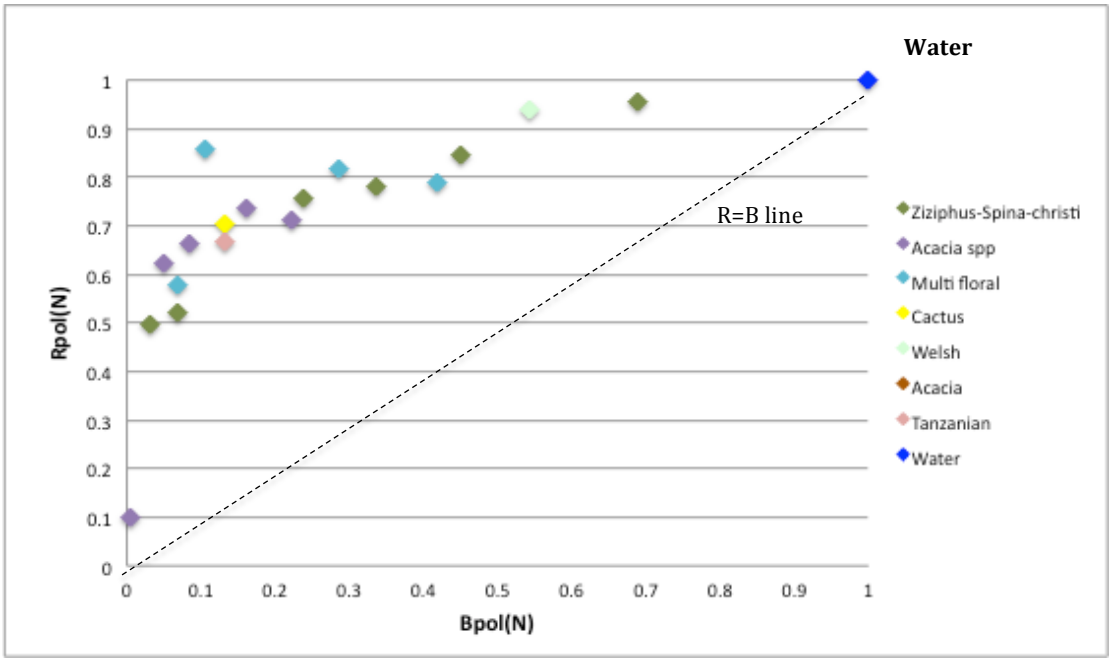

Figure II.9(b): Cluster map of polarized light parameters Rpol(N):Bpol(N) at 30-degree polarizer angle

Figure II.9: Processed polarized light chromatic parameters for various honey samples at 30-degree polarizer angle

(a) Calibration graph of RGB polarized light parameters against water and various honey samples

(b) Cluster map of polarized light parameters Rpol(N):Bpol(N)

Figure II.10(a) shows calibration curves for each of the three chromatic parameters R(pol)N, G(pol)N and B(pol)N as a function of water and various honey samples with an angle of 70 degree between the polarizing angles of the polarizing filters.

Figure II.10(b) shows a chromatic cluster map Rpol(N) against Bpol(N) of various honey samples and water corresponding to this 70 degree relative direction of the polarizing filters.

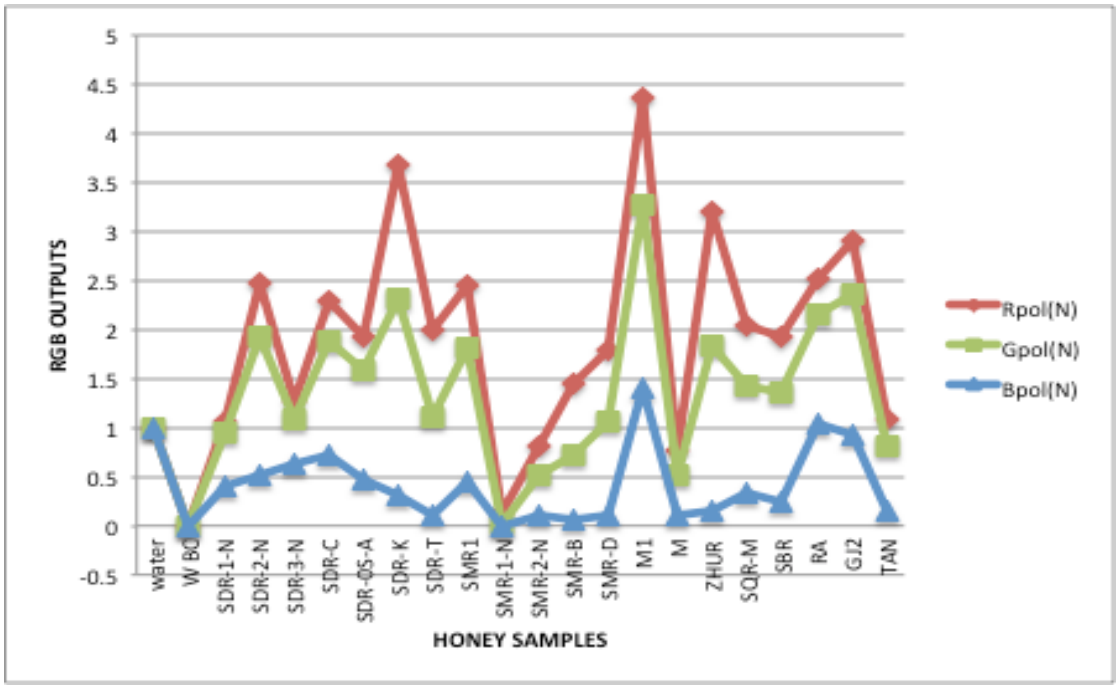

Figure II.10 (a):Calibration graph of RGB polarized light parameters against water and various honey samples at 70-degree polarizer angle

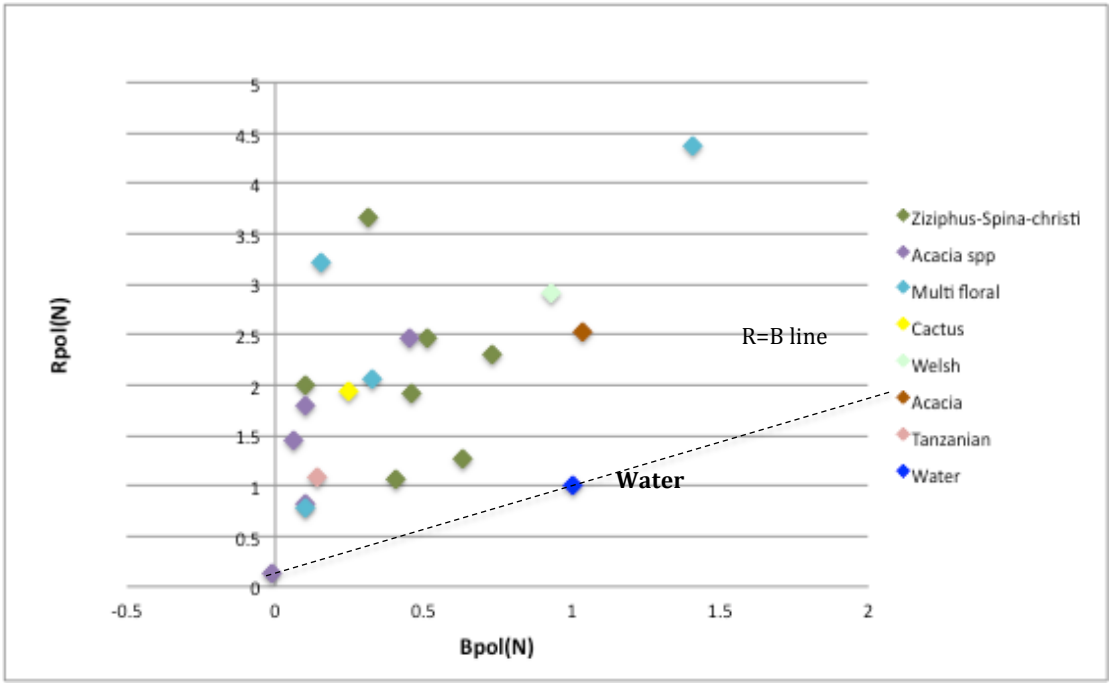

Figure II.10(b): Cluster map of polarized light parameters Rpol(N):Bpol(N) at 70-degree polarizer angle

Figure II.10: Processed polarized light chromatic parameters for various honey samples at 70-degree polarizer angle

(a) Calibration graph of RGB polarized light parameters against water and various honey samples

(b) Cluster map of polarized light parameters Rpol(N):Bpol(N)

II.3 Evaluation Of Method For Field Testing

II.3.1 Raw RGB Results for Honey Field Test

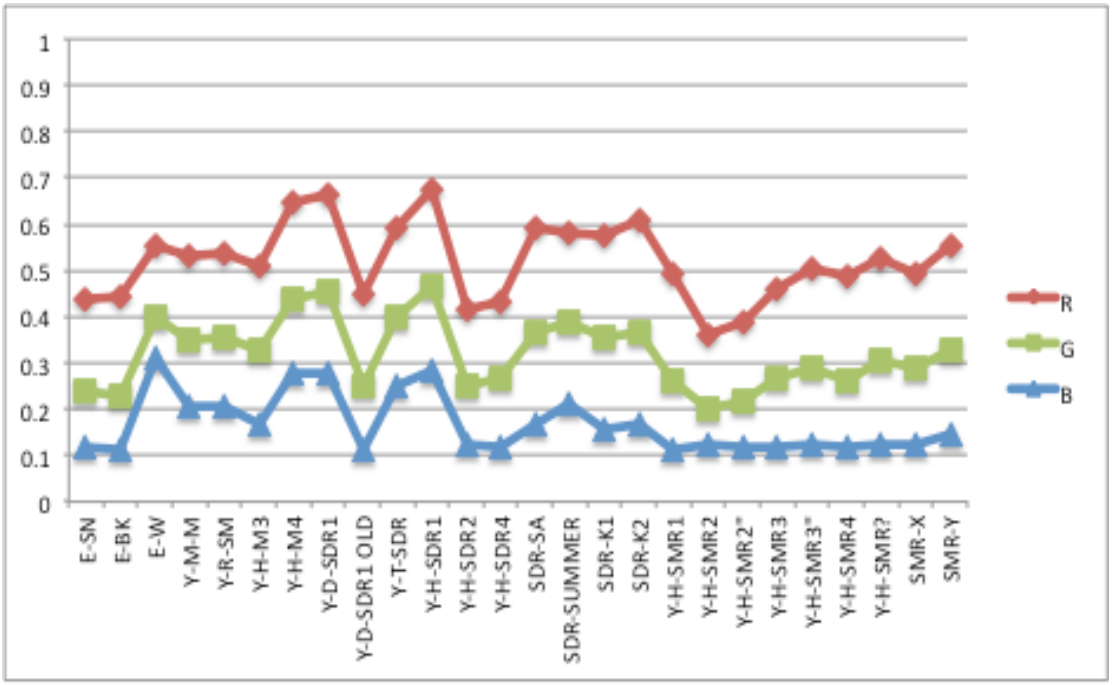

Figure II.11: Raw RGB outputs vs various honey samples with white VDU illumination

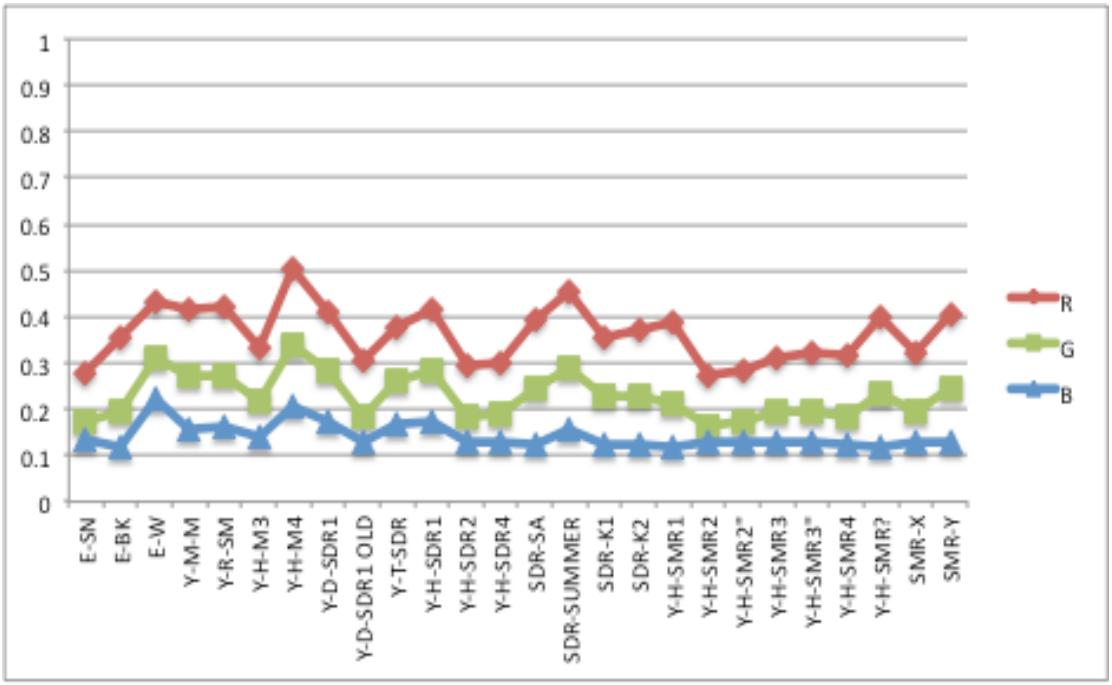

Figure II.12: Raw RGB outputs vs. various honey samples with white VDU illumination and polarizing filter angle at 45 degrees

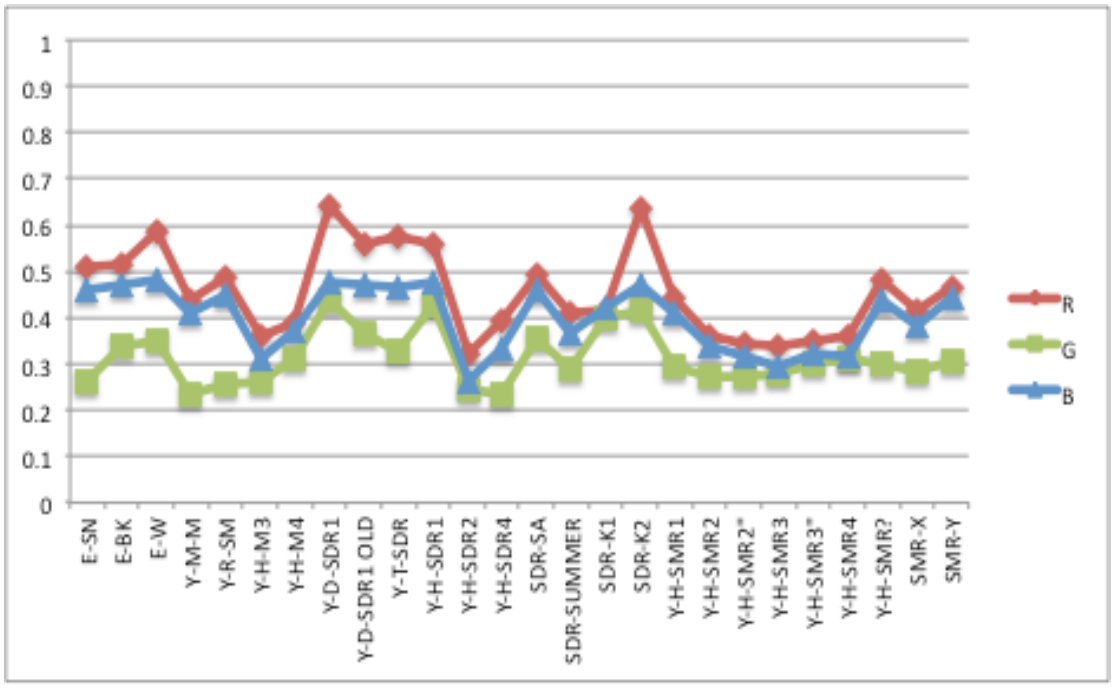

Figure II.13: Raw RGB outputs vs. various honey samples with Violet LED illumination

II.3.2 Normalized RGB Results for Honey Field Test

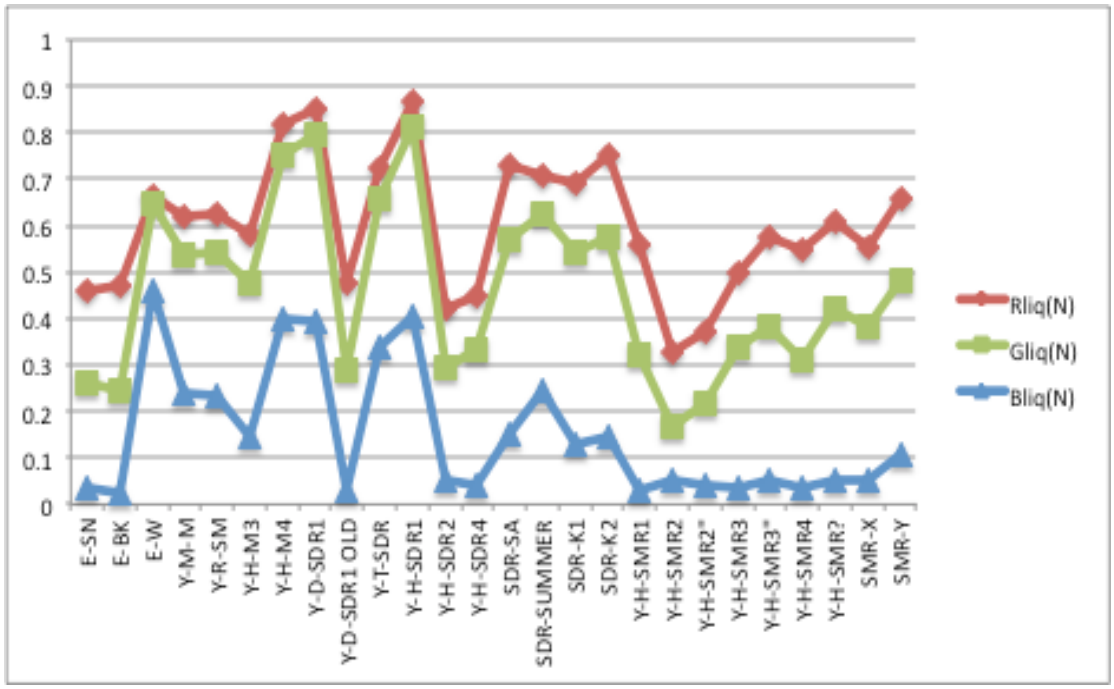

Figure II.14: Calibration graph of RGB transmitted light parameters against various honey samples

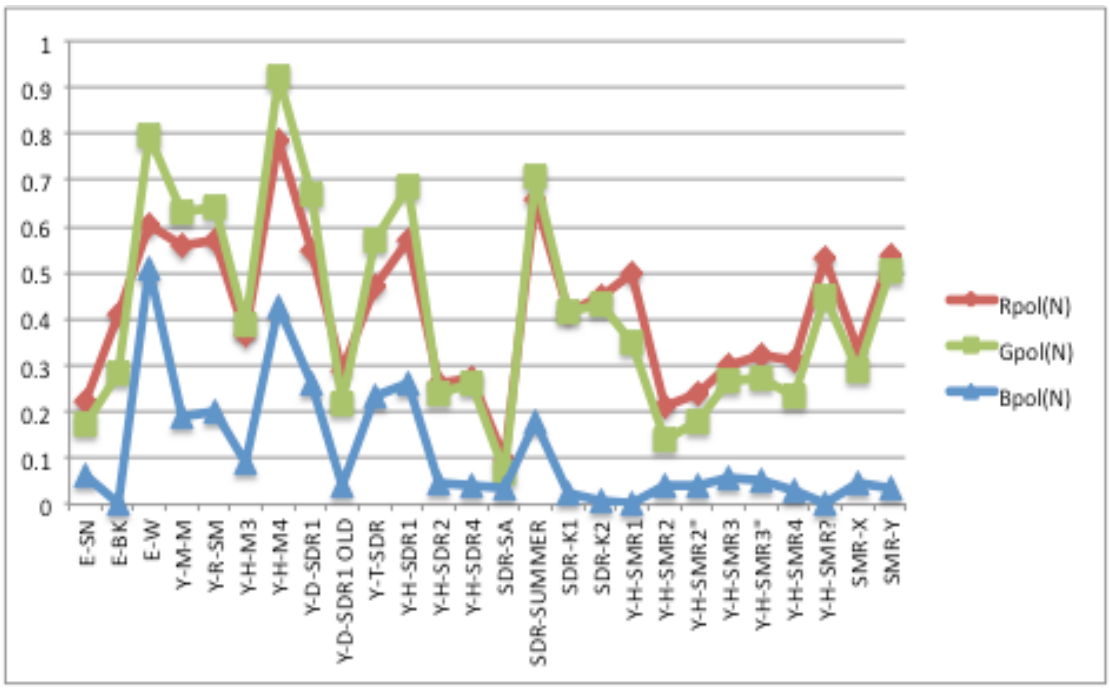

Figure II.15: Calibration graph of RGB polarized light parameters against various honey samples at 45-degree polarizing angle

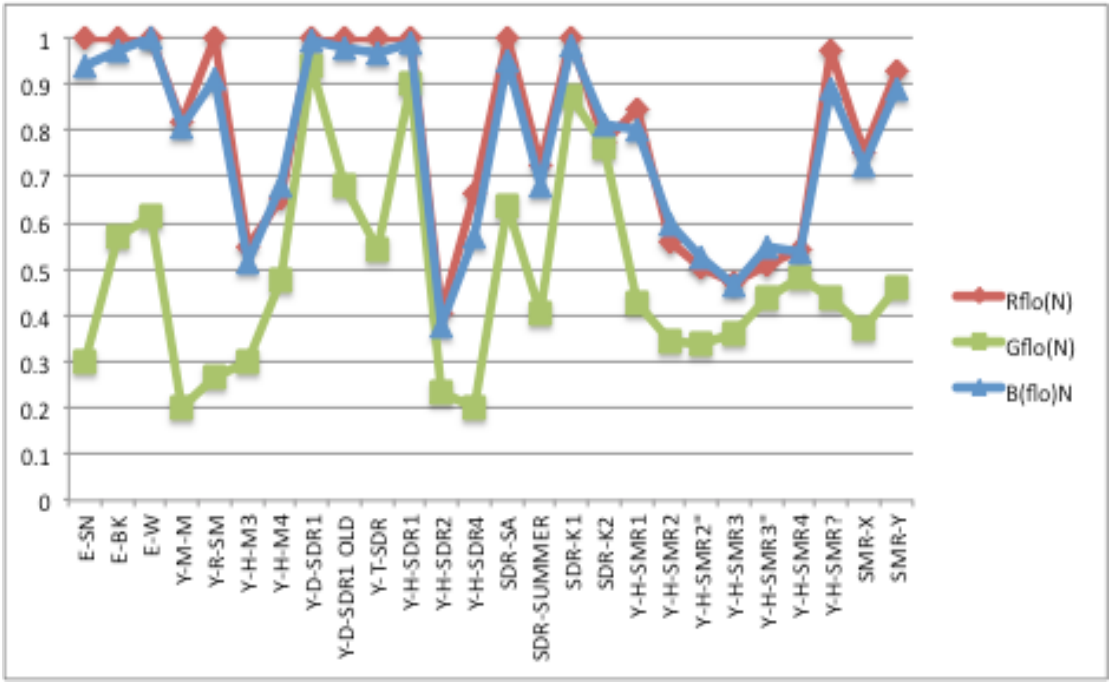

Figure II.16: Calibration graph of RGB fluorescent light parameters against various honey samples

II.3.3 Example of Images obtained From The Optical Chromatic System

II.3.3.1 Optical Chromatic Transmission System

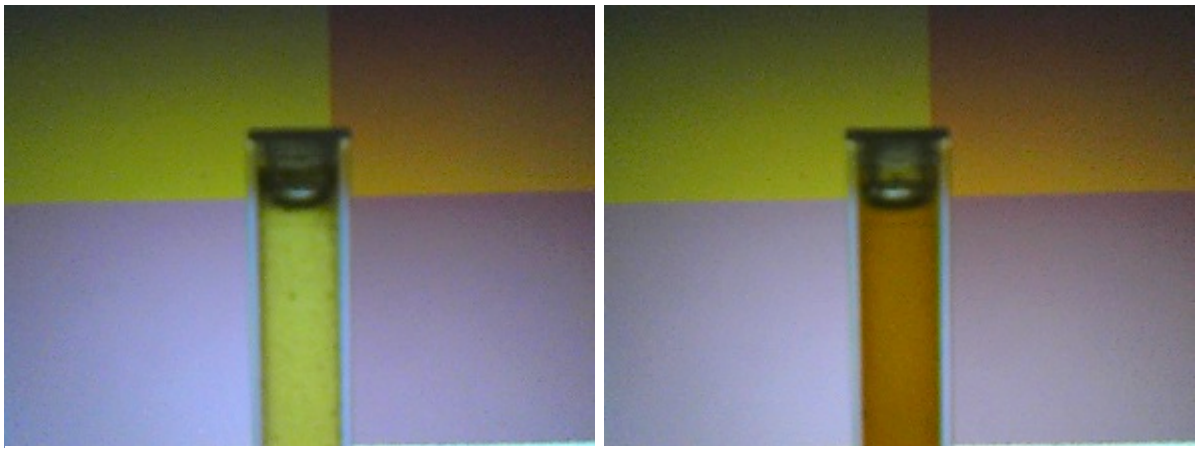

Figure II.17: Example images obtained with the optical chromatic transmission system

II.3.3.2 Optical Chromatic Polarization System

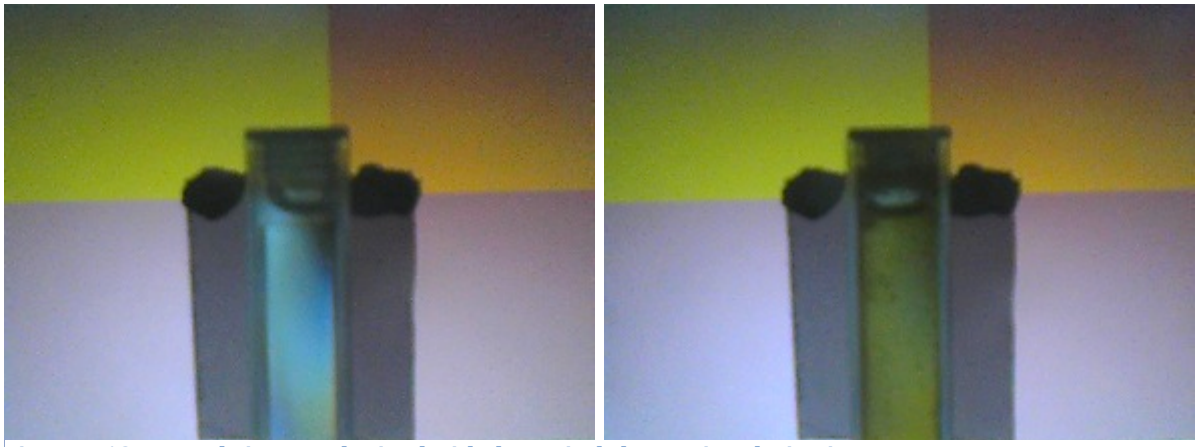

Figure II.18: Example images obtained with the optical chromatic polarization system

II.3.3.3 Optical Chromatic Polarization System

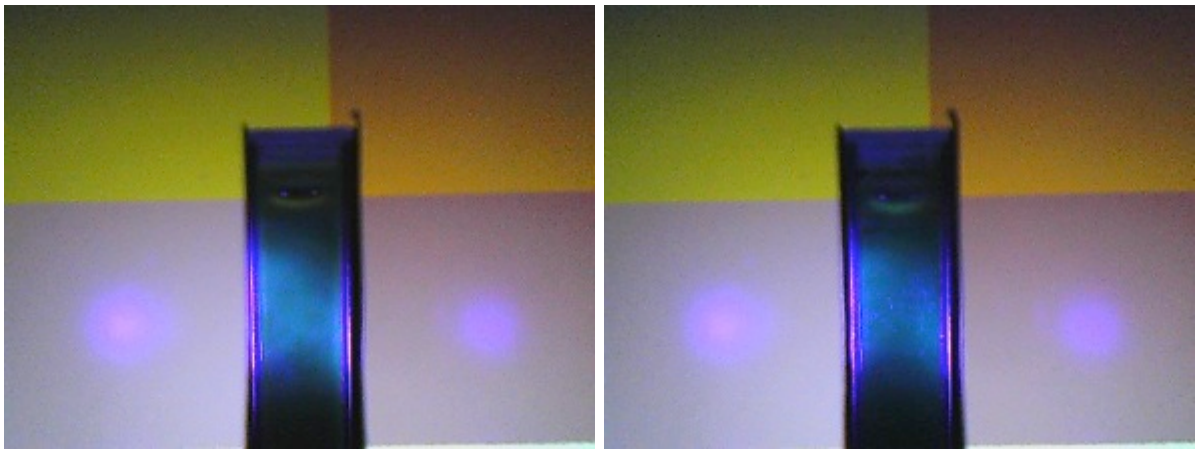

Figure II.19: Example images obtained with the optical chromatic fluorescence system

II.3.3 Example of picture Taken at Field Tests

Honey Beekeeping Farm site - Almahweet – North Yemen

Tubasha'a Village, Sabir Mount, Midlands - Yemen
Beekeeping at roof tops

Honey Shop - Sana'a -Yemen

Appendix III

III.1 Classified Honey

III.1.1 Grade 1 Honey Samples

Sample	Type	Botanical source	Location	Condition	Date obtained
SDR-1-N	Mono-floral	Ziziphus spina-christi	South East Yemen-Hadramout	Raw honey, high levels of minerals, high levels of (fructose/glucose)	January 2013
SDR-OS-1	Mono-floral	Ziziphus spina-christi	North Yemen-Osimat	Raw honey, high levels of minerals, high levels of (fructose/glucose)	January 2013
SMR1	Mono-floral	Acacia spp	South East Yemen-Hadramout	Raw honey, high pollens	July 2012
SMR-1-N	Honeydew	Acacia spp	South East Yemen-Hadramout	Raw honey, very dark colour, low levels of glucose/fructose	January 2013
QDR1	Honeydew	Acacia spp	South East Yemen-Hadramout	Raw honey, very dark colour, low levels of glucose/fructose	July 2011
M1	Multi-floral	Multi source	South East Yemen-Hadramout	Raw honey , High pollens	January 2012
M	Multi-floral	Multi source	South East Yemen-Hadramout	Raw honey	January 2012
SDR-K	Mono-floral	Ziziphus spina-christi	Pakistan-Kashmir	Raw honey, moderate levels of minerals	May 2013
SMR-2-N	Mono-floral	Acacia spp	South East Yemen-Hadramout	Raw honey, moderate pollens	January 2013

ALM	Mono-floral	Almond	North-Yemen-khawlan	Raw honey, highly turbid, low levels of crystallizatio n, high wax, long shelf life	January 2013
SDR-OS-2-OLD	Mono-floral	Ziziphus spina-christi	North Yemen-Osimat	Raw honey, was left in shelf for long periods	January 2013
SMR-B	Mono-floral	Acacia spp	South East Yemen-Hadramout	Raw honey, moderate levels of pollens, moderate crystalized and long shelf life	January 2012

Table III.1: Grade 1 honey samples (Classified Honey)

III.1.2 Grade 2 Honey Samples

Sample	Floral type	Botanical source	Location	Condition	Date obtained
SDR-2-N	Mono-floral	Ziziphus spina-christi	South East Yemen-Hadramout	Raw honey, moderate levels of minerals, high levels of (fructose/glu cose) Blended with other honey liquid,	January 2013
SMR2	Multi floral	Acacia spp + Other sources	South East Yemen-Hadramout	Blended with other honey liquid,	January 2012

Table III.2: Grade 2 honey samples (Classified Honey)

III.1.3 Grade 3 Honey Samples

Sample	Floral type	Botanical source	Location	Condition	Date obtained
SDR-T	Mono-floral	Ziziphus spina-christi	Middlands-Yemen-Tahama	Moderate levels of (syrup sugars)	January 2013
SDR-TAIZ	Mono-floral	Ziziphus spina-christi	Middlands-Yemen-Taiz	Sugar fed bees	January 2013
SMR-D	Multi floral	Acacia spp + Other sources	South East Yemen-Hadramout	Blended with other honey liquid, moderate crystalized was left in shelf for long periods	January 2012
SLM-3-N	Mono-floral	Ziziphus spina-christi	Middlands-Yemen-Tahama	Sugar fed bees	January 2013
SAL2	Mono-floral	Tamarix aphylla	Middlands-Yemen-Ibb	Thick Brown cream honey, high turbid, high acidic	January 2013
SDR-3-N	Mono-floral	Ziziphus spina-christi	South East Yemen-Hadramout	Bended with other honey liquid, high levels of (syrup sugars)	January 2013
SDR-C	Mono-floral	Ziziphus spina-christi	South East Yemen-Hadramout	Bended with other honey liquid, high levels of (syrup sugars)	January 2012

Table III.3: Grade 3 honey samples (Classified Honey)

III.2 Unclassified Honey

Sample	Floral type	Botanical source	Location	Condition	Date obtained
ZHUR-M3	Multi-floral	-	Middlands-Yemen-Tahama	Clear honey	January 2012
SBR-HB	Mono-floral	Cactus	Ethiopia	Moderate levels of Crystallization	January 2013
SQR-M	Multi-floral	-	Socatra Island-yemen	Clear honey	January 2013
TAN	-	-	Tanzania	-	July 2012
SDR-OS-A	Mono-floral	Ziziphus spina-christi	North Yemen-Osimat	Clear honey	January 2013
SDRS	Multi floral	Ziziphus spina-christi + Other sources	North East Yemen-Shabwa	Moderate crystallized honey, long shelf life	July 2011
SBR	Mono-floral	Cactus	Middlands-Yemen-Ibb	Clear honey	January 2012
SAL1	Mono-floral	Tamarix aphylla	Middlands-Yemen-Ibb	Cream thick honey	January 2013
RA	-	Acacia	UK	Processed honey obtained from local market	July 2012
GJ2	-	-	Wales-UK	Processed honey obtained from local honey shop	July 2012
TP	Unknown	-	UK	Processed honey obtained from local market	January 2013

Table III.4: Unclassified honey samples

III.3 Classified Honey (Field Tests)

III.3.1 Grade 1 Honey Samples

Sample	Floral type	Botanical source	Location	Condition
Y-D-SDR1	Mono-floral	Ziziphus spina-christi	South East Yemen-Hadramout	Raw honey, high levels of minerals, high levels of (fructose/glucose)
Y-D-SDR1 old	Mono-floral	Ziziphus spina-christi	South East Yemen-Hadramout	high levels of minerals , was left in shelf for long periods
Y-T-SDR	Mono-floral	Ziziphus spina-christi	Middlands-Yemen-Taiz-Sabir mawadim(Tubashia)	Raw honey, high moisture, moderate wax bits inside honey,
Y-H-SDR1	Mono-floral	Ziziphus spina-christi	South East Yemen-Hadramout	Raw honey high levels of minerals, high levels of (fructose/glucose)
SDR-K1	Mono-floral	Ziziphus spina-christi	Pakistan-Kashmir	Raw honey, moderate levels of minerals,
Y-H-SMR1	Mono-floral	Acacia spp	South East Yemen-Hadramout	Raw honey, high pollens
SMR-X	Mono-floral	Acacia spp	South East Yemen-Hadramout	Raw honey, high pollens
Y-M-M	Multi-floral		West highlands-Yemen-Al-Mahweet	Raw honey, high moisture, moderate wax bits inside honey,
Y-R-SM	Mono/multi	Ziziphus spina-christi/ other	West highlands-Yemen-Raymah	Raw honey, High moisture, moderate wax bits inside honey,
E-SN	Multi-floral		Ethiopian	Raw honey, dark colour
E-BK	Multi-floral		Ethiopian	Raw honey, Moderate crystalized, highly turbid
SDR-SUM	Mono-floral	Ziziphus spina-christi	South East Yemen-Hadramout	Raw honey only available in summer season, high moisture, high levels of minerals

Table III.5: Grade 1 honey samples (Field tests)

III.3.2 Grade 2 Honey Samples

Sample	Floral type	Botanical source	Location	Condition
SDR-K2	Multi-floral	Ziziphus spina-christi + other	Pakistan-Kashmir	Raw honey, Low levels of minerals/
Y-H-SMR2	Mono-floral	Acacia spp	South East Yemen-Hadramout	Raw honey, moderate levels of pollens/low minerals
Y-H-SMR2"	Mono-floral	Acacia spp + other	South East Yemen-Hadramout	Raw honey, moderate levels of pollens//minerals/blended
SMR-Y	Mono/multi - floral	Acacia spp/other	South East Yemen-Hadramout	Raw honey, moderate levels of pollens/minerals/ blended
Y-H-M3	Multi-floral		South East Yemen-Hadramout	Blended with other honey liquid, high pollens
E-W	Multi-floral		Ethiopian	White cream honey, moderate level of pollens

Table III.6: Grade 2 honey samples (Field tests)

III.3.3 Grade 3 Honey Samples

Sample	Floral type	Botanical source	Location	Condition
Y-H-M4	Multi-floral		South East Yemen-Hadramout	Sugar fed bees, high levels of (syrup sugars)
Y-H-SDR2	Mono-floral	Ziziphus spina-christi	South East Yemen-Hadramout	Blended with other honey liquid,
Y-H-SDR4	Mono/multi floral	Ziziphus spina-christi + Other	South East Yemen-Hadramout	Added (Syrup Sugar), high pollens
Y-H-SMR3	Mono/multi - floral	Acacia spp + other	South East Yemen-Hadramout	Blended with other honey liquid, added syrup sugar
Y-H-SMR3"	Mono/multi- floral	Acacia spp + other	South East Yemen-Hadramout	Blended with other honey liquid, added syrup sugar
Y-H-SMR4	Mono/multi – floral	Acacia spp + other	South East Yemen-Hadramout	Blended with other honey liquid, high levels of added (syrup sugar), moderate pollens

Table III.7: Grade 3 honey samples (Field tests)